Aus der Poliklinik für Kieferorthopädie
der Ludwig-Maximilians-Universität München

Direktorin: Prof. Dr. med. dent. A. Wichelhaus

Individualisierung und klinische Prozessoptimierung in der kieferorthopädischen Diagnostik und Therapie durch digitale Technologien und biomechanische Simulationssysteme

Habilitationsschrift
zur Erlangung der Venia Legendi
im Fach Kieferorthopädie

vorgelegt von

Dr. med. dent. Hisham Sabbagh

München 2024

Mit Genehmigung der Medizinischen Fakultät

der Ludwig-Maximilians-Universität München

Vorsitzende des Fachmentorats:	Prof. Dr. med. dent. A. Wichelhaus
Fachmentorat:	Prof. Dr. med. dent. Daniel Edelhoff
	Prof. Dr. med. Dr. med. dent. Sven Otto
Dekan:	Prof. Dr. med. Thomas Gudermann

Dieser kumulativen Habilitationsarbeit liegen folgende Arbeiten zugrunde:

Sabbagh, H.; Heger, S.M.; Stocker, T.; Baumert, U.; Wichelhaus, A.; Hoffmann, L.
Accuracy of 3D Tooth Movements in the Fabrication of Manual Setup Models for Aligner Therapy.
Materials 2022, 15, 3853.

Popova, T.; Stocker, T.; Khazaei, Y.; Malenova, Y.; Wichelhaus, A.; **Sabbagh, H.**
Influence of growth structures and fixed appliances on automated cephalometric landmark recognition with a customized convolutional neural network.
BMC Oral Health 2023, 23, 274, doi:10.1186/s12903-023-02984-2.

Sabbagh, H.; Khazaei, Y.; Baumert, U.; Hoffmann, L.; Wichelhaus, A.; Janjic Rankovic, M.
Bracket Transfer Accuracy with the Indirect Bonding Technique: A Systematic Review and Meta-Analysis.
Journal of Clinical Medicine 2022, 11, 2568.

Hoffmann, L.; **Sabbagh, H.**; Wichelhaus, A.; Kessler, A.
Bracket transfer accuracy with two different three-dimensional printed transfer trays vs silicone transfer trays.
The Angle Orthodontist 2022, 92, 364-371, doi:10.2319/040821-283.1.

Hegele, J.; Seitz, L.; Claussen, C.; Baumert, U.; **Sabbagh, H.**; Wichelhaus, A.
Clinical effects with customized brackets and CAD/CAM technology: a prospective controlled study.
Progress in Orthodontics 2021, 22, 40, doi:10.1186/s40510-021-00386-0.

Malenova, Y.; Ortner, F.; Liokatis, P.; Haidari, S.; Tröltzsch, M.; Fegg, F.; Obermeier, K.T.; Hartung, J.T.; Kakoschke, T.K.; Burian, E.; Otto, S.; **Sabbagh, H.**; Probst, F.
Accuracy of maxillary positioning using computer-designed and manufactured occlusal splints or patient-specific implants in orthognathic surgery.
Clin Oral Investig 2023, doi:10.1007/s00784-023-05125-9.

Dotzer, B.; Stocker, T.; Wichelhaus, A.; Janjic Rankovic, M.; **Sabbagh, H.**
Biomechanical simulation of forces and moments of initial orthodontic tooth movement in dependence on the used archwire system by ROSS (Robot Orthodontic Measurement & Simulation System).
J Mech Behav Biomed Mater 2023, 144, 105960, doi:10.1016/j.jmbbm.2023.105960.

Haas, E.; Schmid, A.; Stocker, T.; Wichelhaus, A.; **Sabbagh, H.**
Force-Controlled Biomechanical Simulation of Orthodontic Tooth Movement with Torque Archwires using HOSEA (Hexapod for Orthodontic Simulation, Evaluation and Analysis).
Bioengineering 2023; 10(9):1055

Inhaltsverzeichnis

1. Einleitung

Die Wissenschaft und die Medizin befinden sich durch das Aufkommen digitaler Technologien und künstlicher Intelligenz im Wandel. Die Digitalisierung schafft neue diagnostische und therapeutische Möglichkeiten und erleichtert die Kommunikation sowie den Datenaustausch im Gesundheitswesen. Neben der Standardisierung und der Erhöhung der Präzision und Effizienz von Prozessen strebt die datengetriebene Medizin auch eine Individualisierung der Patientenversorgung an.

In der Kieferorthopädie haben insbesondere die Möglichkeiten zur digitalen Erfassung von Zähnen und Kiefern, sowie die Einführung der CAD/CAM Technologie (computer-aided-design/computer-aided-manufacturing) zu bedeutenden Veränderungen geführt [1].
Behandlungen von Zahn- und Kieferfehlstellungen können virtuell simuliert, geplant und die Behandlungsapparaturen individuell gestaltet und automatisiert hergestellt werden. Die computergestützte Fertigung erlaubt dabei die Verarbeitung neuer Materialgruppen und die Fertigung komplexer Geometrien [2]. Die Anwendungen digitaler Technologien im Bereich der kieferorthopädischen Diagnostik und Therapie sind inzwischen vielfältig und bringen teilweise weitreichende Neuerungen in der Arbeitsweise mit sich [3].

Im Bereich der kieferorthopädischen Diagnostik und Behandlungsplanung ermöglichen digitale Technologien beispielsweise das Zusammenführen und die Verarbeitung von Daten verschiedener diagnostischer Verfahren. So können Gesichtsscans und Intraoralscans mit Daten dreidimensionaler Bildgebung virtuell in Computerprogrammen überlagert und dargestellt werden [4]. Dies ermöglicht die gleichzeitige Visualisierung und Analyse der oberflächlichen und tieferliegenden Gewebe von Gesicht, Zähnen und Kiefern. Neben diagnostischen Analysen können sowohl kieferorthopädische Zahn- und Wurzelbewegungen als auch Osteotomien der Kiefer im Rahmen kombiniert kieferorthopädisch-kieferchirurgischer Therapien präzise simuliert werden. Messungen und Analysen an digitalen Modellen bzw. Datensätzen sind dabei nicht nur ausreichend präzise, sondern steigern die Effizienz und übertreffen die Reliabilität manueller Messungen [5-8]. Durch den Einsatz von Algorithmen und künstlicher Intelligenz (KI) kann dabei ein hoher Automatisierungsgrad und damit eine Effizienzsteigerung erreicht werden. Darüber hinaus können KI-Modelle Muster in medizinischen Bildern oder Datensätzen erkennen, die für das menschliche Auge

möglicherweise nicht offensichtlich sind und den diagnostischen Prozess und die Entscheidungsfindung unterstützen [9-15]. Ein Beispiel ist die automatisierte Analyse von Fernröntgenseitenbildern im Rahmen der kieferorthopädischen Kephalometrie, die eine effizientere und reproduzierbarere Musteranalyse ermöglicht als die manuelle Beurteilung durch einen erfahrenen Behandler oder eine erfahrene Behandlerin [11,12,14].

Im Bereich der kieferorthopädischen Therapie können Behandlungsapparaturen anhand virtueller Daten digital gestaltet und computergestützt gefertigt werden [2,16,17]. Die digitale Arbeitsweise führt dabei zu Veränderungen im Herstellungsprozess von Behandlungsapparaturen sowie im klinischen Arbeitsablauf. Im Vergleich mit konventionellen Verfahren können durch die Anwendung computergestützter Technologien mögliche Fehlerquellen in der manuellen Fertigung und die Anzahl erforderlicher Laborprozessschritte reduziert werden [18]. Des Weiteren zeichnet sich durch die verbesserte Planbarkeit und Reproduzierbarkeit in der Apparaturherstellung ein möglicher Paradigmenwechsel ab. Bei ausreichender Präzision wird ein optimierter klinischer Behandlungsablauf möglich, der mit weniger Behandlungsschritten und einer reduzierten Gesamtbehandlungsdauer einhergehen kann [19-23].
So können beispielsweise kieferorthopädische Brackets können anhand eines simulierten Behandlungsziels virtuell positioniert und mit Hilfe additiv gefertigter Brackettransferschienen entsprechend dieser Planung klinisch übertragen werden (Backward Planning). Da das Behandlungsergebnis maßgeblich von der Präzision der Bracketplatzierung abhängt, könnte mit Hilfe einer individuellen Bracketpositionierung die Anzahl der notwendigen Ausgleichsbiegungen, Bracket-Neupositionierungen und damit der benötigten Behandlungstermine reduziert werden [23,24]. Auch andere Elemente der festsitzenden Behandlung, die bisher konfektioniert waren und auf Mittelwertsystemen basierten, können auf diese Weise individualisiert werden, wie beispielsweise kieferorthopädische Bögen, Bracketbasen und Bracketgeometrien [25-27].

Neben der gestiegerten Effizienz ist ein weiteres Ziel Behandlungen durch Individualisierung biologischer zu gestalten. In der kieferorthopädischen Therapie stellen Apparaturen die Schnittstelle zwischen Biologie und Technologie durch die Applikation von Kraft- und Momentsystemen auf die Zähne und die umliegenden Gewebe dar [28]. Die Kenntnis der durch die eingesetzten Mechaniken erzeugten Kräfte und Drehmomente ist daher von wesentlicher Bedeutung, jedoch klinisch in vielen Fällen nicht ermittelbar oder ausreichend präzise abschätzbar [29]. In diesem Bereich tragen digitale Technologien, insbesondere

robotergestützte biomechanische Simulationssysteme und computergestützte numerische Verfahren wie die Finite-Elemente-Methode, dazu bei, klinische Prozesse in vitro bzw. in silico zu simulieren [30-33]. Basierend auf den Ergebnissen dieser Untersuchungen können mechanische Behandlungsapparaturen hinsichtlich ihres physikalischen Verhaltens für die Anwendung in verschiedenen klinischen Ausgangssituationen charakterisiert und für den klinischen Einsatz zu individualisiert werden [34].

Im Sinne einer patientenorientierten Medizin müssen neue Ansätze in der Diagnostik und Therapie evidenzbasiert beurteilt werden und einen medizinischen Mehrwert schaffen.
Die vorliegende Habilitationsschrift umfasst experimentelle und klinische Forschungsarbeiten zu digitalen Technologien in der kieferorthopädischen Diagnostik und Therapie mit dem Fokus auf die vorgestellten Themenbereiche additive Fertigung, virtuelle Behandlungsplanung, künstliche Intelligenz und biomechanische Simulationssysteme hinsichtlich Individualisierung und klinischer Prozessoptimierung.

2. Forschungsarbeiten und deren Bedeutung für das Fachgebiet

Im folgenden Abschnitt werden die dieser Habilitationschrift zugrundeliegenden Originalarbeiten, die in englischsprachigen Peer-begutachteten Fachjournalen veröffentlicht wurden, mit ihren übersetzten Zusammenfassungen vorgestellt.

Vorangestellt ist jeweils eine Einführung in die spezifischen Themenbereiche.

2.1 Digitale Technologien in der Kieferorthopädischen Diagnostik und Behandlungplanung

In der Kieferorthopädie basiert die Diagnosestellung auf einer Vielzahl spezifischer Untersuchungsmethoden, wobei die einzelnen diagnostischen Befunde im Rahmen der sogenannten Summationsdiagnostik zusammengeführt und hinsichtlich ihrer Relevanz gewichtet werden. Die Behandlungsplanung erfolgt auf Grundlage der Diagnosen mithilfe technischer Analysen, Prognosemodellen und Simulationen.

Digitale Technologien finden bereits in den meisten Teilbereichen der kieferorthopädischen Diagnostik Anwendung, unter anderem zur Anamnese und Befunderhebung [1,4,5,35], Fotoanalyse [36-38], Modellanalyse [5,7,8,39-41], Röntgenanalyse [42] und kephalometrischen Analyse [12,13]. Desweiteren werden sie in der Behandlungsplanung, unter anderem zur Wachstumsprognose [43-47], zur Simulation von Behandlungszielen und Abwägung von Therapiealternativen [48] sowie zur klinischen Entscheidungsfindung eingesetzt [11,14,49].

Der Einsatz digitaler Technologien in der Diagnostik und Behandlungsplanung verfolgt vielfältige Ziele. Neben der Steigerung der Effizienz steht dabei häufig auch eine Steigerung der Reliabilität und Reproduzierbarkeit im Fokus des Interesses. Insbesondere manuell durchgeführte diagnostische Analysen sind zeitaufwendig und mit potentiellen Fehlerquellen verbunden [8].

Eine häufige Maßnahme zur diagnostischen Visualisierung des Behandlungsziels und Abwägung verschiedener Therapiealternativen sowie zur Behandlungsplanung einer herausnehmbaren oder festsitzenden Behandlung ist die Anfertigung kieferorthopädischer Setups [25,48]. Dabei werden die Zähnen am phyischen oder virtuellen Modell dreidimensional

bewegt und indikationsabhängig die Reduktion von Zahnmaterial im Sinne einer approximalen Schmerzreduktion (ASR) oder die Entfernung von Zähnen im Sinne einer geplanten Extraktionstherapie simuliert [50]. Bei der Planung festsitzender Behandlungen können Setups verwendet werden um individuelle Bracketpositionen zu bestimmen und individuelle Bracketbasen sowie individuelle orthodontische Bögen herzustellen [23,25,51]. Während die Anfertigung eines Setups zur Planung einer festsitzenden Behandlung nicht obligatorisch ist, können herausnehmbare Behandlungen mit Alignern ausschließlich auf Grundlage eines Setups geplant werden [48]. Obwohl die Erstellung von Setups zunehmend virtuell durchgeführt wird, erfolgt diese häufig noch manuell, nicht zuletzt weil die notwendige digitale Infrastruktur (Intraoralscanner und 3D Drucker) nicht überall verfügbar ist [39]. Insbesondere in der Alignertherapie ist die Genauigkeit des Setups jedoch entscheidend, um einerseits den Platzbedarf korrekt zu diagnostizieren und andererseits über geeignete Bewegungsgrößen im Setup angemessene Kräfte und Drehmomente mit der Alignerschiene erzeugen zu können. Bereits Abweichungen im Bereich von 0.1 mm können die Vorhersagbarkeit geplanter Zahnbewegungen nachteilig beeinflussen [52]. Lediglich eine Studie verglich manuelle und digitale Setups mit Hinblick auf die Erhebung eines Index zur Bewertung der Qualität von kieferorthopädischer Behandlungsergebnisse (American Board of Orthodontics Objective Grading System/ABO OGS) und stellte keine statistisch signifikanten Unterschiede zwischen der Verwendung manueller und digitaler Setups fest [50]. Jedoch wurde die Genauigkeit der einzelnen Zahnbewegungen im Setup nicht untersucht, was keine Rückschlüsse hinsichtlich der Diagnostik des Platzbedarfs, der Genauigkeit der Zahnumstellungen und der Eignung für die Anwendung in der Alignertherapie zulässt. Daher wurde eine experimentelle Studie zur Präzision manueller Setups durchgeführt (Originalarbeit 2.1.1.).

Ein weiterer Bereich in dem digitale Technologien im Bereich der kieferorthopädischen Diagnostik eingesetzt werden ist die kephalometrische Analyse. Diese beinhaltet die Identifizierung von Referenzpunkten am Fernröntgenseitenbild und die Beschreibung der kraniofazialen Morphologie anhand deren Beziehungen. Traditionell erfolgte die kephalometrische Analyse anhand einer manuellen Durchzeichnung auf Acetatpapier und einer nachfolgenden Vermessung [53]. Diese Methode ist jedoch zeitintensiv und weist zahlreiche potentielle Fehlerquellen bei der Identifikation der Referenzpunkte und bei dem Prozess des Durchzeichnens und Vermessens auf [53]. Die diagnostische Aussagekraft der kephalometrischen Auswertungen ist darüber hinaus durch eine eingeschränkte Intra-Beobachter-Reliabilität und Inter-Beobachter-Reliabilität limitiert. Um die Effizienz, die Genauigkeit und die Reproduzierbarkeit zu verbessern, wurden Computerprogramme entwickelt, die eine digitale Lokalisation der Referenzpunkte am Fernröntgenseitenbild samt

rechnerischer Auswertung ermöglichen [53]. Während die Effizienz durch die digitale Auswertung gestiegert werden konnte, blieben die Genauigkeit und Reproduzierbarkeit jedoch vergleichbar mit der konventionellen Auswertungsmethode [54,55].

In jüngster Zeit gab es daher Bestrebungen, den Prozess der Referenzpunkterkennung zu automatisieren. Hierbei wurde der Einsatz von künstlicher Intelligenz (KI), speziell in Form von Convolutional Neural Networks (CNNs) propagiert. CNNs sind eine Art von neuronalen Netzwerken, die insbesondere für die Verarbeitung und Analyse von Bilddaten geeignet sind. Ein zentrales Element dieser Automatisierung ist die Erkennung von Grauwerten im Fernröntgenseitenbild, die eine entscheidende Rolle bei der Differenzierung und Identifikation von anatomischen Strukturen spielen. Ein Hauptvorteil von CNNs gegenüber herkömmlichen neuronalen Netzwerken besteht darin, dass sie weniger vortrainierte Merkmale benötigen, da sie automatisch räumliche Hierarchien von Merkmalen erlernen können. Dies ermöglicht es, durch die Verarbeitung großer Datenmengen Muster präzise zu erkennen, die für das menschliche Auge nicht wahrzunehmen sind. Erste Studien zeigten vielversprechende Ergebnisse bei der automatisierten Identifikation von Referenzpunkten mithilfe von KI [56]. Die Leistung der Systeme ist jedoch unter anderem abhängig von der Qualität der verwendeten Daten und der verwendeten Architektur der Algorithmen. In vorangegangenen Untersuchungen wurden primär Röntgenaufnahmen von Patienten mit permanentem Gebiss evaluiert [57,58], während andere Studien diese spezifische Charakteristik der Datensätze nicht explizit erwähnten [59]. Trotz des erkennbaren Potenzials automatisierter Verfahren zur Identifikation kephalometrischer Orientierungspunkte, fehlen Erkenntnisse hinsichtlich der Reliabilität KI-basierter Systeme bei verschiedene klinisch relevante Charakteristika der verwendeten Datensätze. Vor diesem Hintergrund wurde daher eine Untersuchung durchgeführt (Originalarbeit 2.1.2), um den Einfluss von Wachstumsstrukturen, insbesondere von Zahnkeimen im Wechselgebiss sowie von Bildartefakten durch festsitzende Apparaturen und zahnärztlichen Restautrationen auf die automatische Erkennung kephalometrischer Orientierungspunkte zu analysieren.

2.1.1 Originalarbeit: Accuracy of 3D Tooth Movements in the Fabrication of Manual Setup Models for Aligner Therapy

Sabbagh, H.; Heger, S.M.; Stocker, T.; Baumert, U.; Wichelhaus, A.; Hoffmann, L.
Accuracy of 3D Tooth Movements in the Fabrication of Manual Setup Models for Aligner Therapy.
Materials 2022, 15, 3853.

Zusammenfassung:

Zielsetzung: Das klinische Ergebnis einer Aligner-Therapie hängt eng mit der Präzision des Setups zusammen, das manuell oder digital hergestellt werden kann. Ziel der Studie ist es, die Eignung manueller Setups für die Aligner-Therapie im Hinblick auf die Präzision der Zahnbewegungen zu untersuchen.

Methoden: Sechs Zahntechniker wurden angewiesen, jedes der elf Gipsduplikate eines Patientenmodells wie folgt umzustellen: eine reine vestibuläre Translation von 1 mm an Zahn 11 und eine reine mesiale Rotation von 15° an Zahn 23. Die bearbeiteten Aufstellungsmodelle wurden 3D-gescannt und mit dem Referenzmodell abgeglichen. Zur Auswertung wurde der Wilcoxon-Signed-Rank-Test ($p < 0,05$) mit einer Stichprobe verwendet.

Ergebnisse: Die Gesamtpräzision der translatorischen Bewegung umfasste einen weiten Wertebereich von 0,25 bis 2,26 mm (Median: 1,09 mm). Der Zielwert für die Rotation von Zahn 23 wurde mit einer medianen Rotation von 9,76° in apikal-okklusaler Richtung erreicht. Unerwünschte Bewegungen in den anderen Ebenen begleiteten die Rotation ebenfalls.

Schlussfolgerungen: Ein manuelles Setup kann nur mit begrenzter Präzision hergestellt werden. Neben der sehr hohen Variabilität zwischen den Technikern traten zusätzliche unerwünschte Bewegungen in anderen räumlichen Ebenen auf. Manuell hergestellte Setups sollten aufgrund der begrenzten Präzision nicht für die Aligner-Therapie bevorzugt werden.

2.1.2 Originalarbeit: Influence of growth structures and fixed appliances on automated cephalometric landmark recognition with a customized convolutional neural network

Popova, T.; Stocker, T.; Khazaei, Y.; Malenova, Y.; Wichelhaus, A.; **Sabbagh, H.**
Influence of growth structures and fixed appliances on automated cephalometric landmark recognition with a customized convolutional neural network.
BMC Oral Health 2023, 23, 274, doi:10.1186/s12903-023-02984-2.

Zusammenfassung:

Zielsetzung: Eine der wichtigsten Anwendungen der künstlichen Intelligenz im Bereich der Kieferorthopädie ist die automatische kephalometrische Analyse. Ziel der vorliegenden Studie war es, zu untersuchen, ob verschiedene Entwicklungsstadien des Gebisses oder festsitzende kieferorthopädische Apparaturen die Erkennung kephalometrischer Landmarken beeinflussen.
Methoden: Für diese Studie wurde ein neuronales Netzwerk (Convolutional Neural Network, CNN) zur automatischen Erkennung von kephalometrischen Landmarken entwickelt. Das Modell wurde an 430 kephalometrischen Röntgenbildern trainiert und seine Leistung anschließend an 460 neuen Röntgenbildern getestet. Die Genauigkeit der Erkennung von Orientierungspunkten bei Patienten mit bleibendem Gebiss wurde mit der bei Patienten mit Wechselgebiss verglichen. Außerdem wurde der Einfluss von festsitzenden kieferorthopädischen Apparaturen und kieferorthopädischen Brackets und/oder Bändern nur bei Patienten mit bleibendem Gebiss untersucht. Es wurde ein t-Test durchgeführt, um die mittleren radialen Fehler (MREs) gegen die entsprechenden SDs für jede Landmarke in den beiden Kategorien zu bewerten, wobei die Signifikanz auf $p < 0,05$ festgelegt wurde.
Ergebnisse: Die Studie zeigte signifikante Unterschiede in der Erkennungsgenauigkeit des Ap-Inferior-Punktes und des Is-Superior-Punktes zwischen Patienten mit bleibendem Gebiss und Wechselgebiss und keine signifikanten Unterschiede im Erkennungsprozess zwischen Patienten ohne festsitzende kieferorthopädische Apparaturen und Patienten mit kieferorthopädischen Brackets und/oder Bändern und anderen festsitzenden kieferorthopädischen Apparaturen.
Schlussfolgerungen: Die Ergebnisse deuten darauf hin, dass Wachstumsstrukturen und Entwicklungsstadien eines Gebisses einen Einfluss auf die Leistung des individuellen CNN-Modells anhand von kephalometrischen Orientierungspunkten haben. Festsitzende kieferorthopädische Apparaturen wie Brackets, Bänder und andere festsitzende kieferorthopädische Elemente hatten keine signifikanten Auswirkungen auf die Leistung des CNN-Modells.

2.2 Digitale Technologien in der Kieferorthopädischen Therapie

In der kieferorthopädischen Therapie können digitale Technologien zur individuellen Gestaltung und computergestützten Herstellung von Apparaturen auf der Grundlage virtueller Daten und Behandlungsplanungen eingesetzt werden.

Um computergestützte Systeme zu diesem Zweck einsetzen zu können, müssen relevante Strukturen wie Zähne, Kiefer und Weichgewebe digital erfasst werden. Die Erfassung von Oberflächen von Zähnen und Kiefern sowie der fazialen Weichgewebe kann mithilfe von optischen Scansystemen erfolgen. Bei intraoralen Oberflächen können Intraoralscanner zur direkten Erfassung oder Modellscanner zur indirekten Erfassung über eine Abformung und ein konventionelles Modell eingesetzt werden [60]. Solche Scansysteme arbeiten nach verschiedenen optischen Prinzipien unter anderem Triangulation, konfokale Mikroskopie, Streifenlichttopometrie oder optischer Kohärenztomographie (OTC) [61]. Bei der Erfassung fazialer Oberflächen wird vorwiegend das Verfahren der Stereophotogrammetrie eingesetzt. Dabei zeichnen mehrere Digitalkameras Bilder aus verschiedenen Winkel auf, die sekundär zu einer dreidimensionalen Datei zusammengefügt werden [62]. Die digitale Beschreibung der Oberflächen erfolgt in standardisierten Datenformaten wie STL (Standard Tesselation Language), DICOM (Digital Imaging and Communications in Medicine), PLY (Polygon File Format) oder OBJ (Object File Format), wobei STL zu den geläufigsten verwendeten Dateiformat zählt [63,64]. Im STL Format werden die dreidimensionalen Oberflächen durch dreieckige, verknüpfte Facetten repräsentiert, wobei jeder Facette ein Normalvektor zur Determinierung der Ausrichtung im dreidimensionalen kartesischen Koordinatensystem zugeordnet ist [65]. Die digitale Darstellung von Knochengewebe sowie von Zahnwurzeln erfolgt hingegen mithilfe dreidimensionaler röntgenologischer Verfahren wie der digitalen Volumentomographie (DVT) oder Computertomographie (CT), wobei die Datenverarbeitung üblicherweise im DICOM Format erfolgt. Die digitalen Datensätze können anschließend in Softwareprogrammen weiterverarbeitet und konvertiert werden, um sie für virtuelle Behandlungsplanungen zu verwenwenden. Indikationsabhängig erfolgt dabei eine Verknüpfung verschiedener Datensätze, um beispielsweise Daten aus Oberflächenscans von Zähnen, Kiefern und Gesicht mit Datensätzen radiologischer Untersuchungen zur Darstellung von Knochengewebe und Zahnwurzeln zu kombinieren (Abb. 1) [66,67].

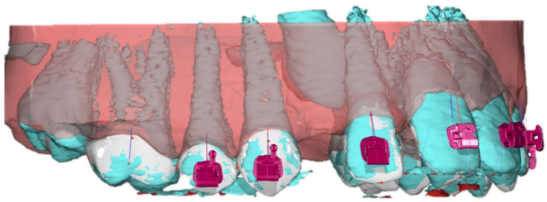

Abb. 1 (links): Kombination von dreidimensionalen Röntgendatensätzen (DVT) mit einem Intraoralscan zur gleichzeitigen Darstellung von Zahnoberflächen und Zahnwurzeln zur virtuellen Bracketplatzierung und Behandlungsplanung (eigene Aufnahme aus dem Softwareprogramm OnyxCeph^{3TM}, Image Instruments GmbH, Chemnitz, Deutschland).
Abb. 1 (rechts): Kombination von dreidimensionalen Röntgendatensätzen (DVT) mit einem Gesichtsscan zur gleichzeitigen Darstellung von Zähnen und Kiefern sowie der fazialen Weichgewebe zur Planung einer kombiniert kieferorthopädisch-kieferchirurgischen Therapie (eigene Aufnahme aus dem Softwareprogramm OnyxCeph^{3TM}, Image Instruments GmbH, Chemnitz, Deutschland).

Die Fusion verschiedener Datensätze erfolgt anhand einem Registrierungsprozess, bei dem die Datensätze in einem gemeinsamen Koordinatensystem ausgerichtet und anschließend zusammengefügt werden. Häufig erfolgt die initale Vorausrichtung anhand manuell festgelegter anatomischer Landmarken, bevor die Oberflächen computergestützt beispielsweise mithilfe von Iterative Closest Point (ICP) Algorithmen überlagert werden [68]. Neuerdings wurden auch Ansätze für auf künstlicher Intelligenz basierende Systeme zur automatischen Überlagerung beschrieben [69].
Je nach klinischer Indikation können auf der Grundlage dieser registrierten Daten verschiedene therapeutische Hilfsmittel, zum Beispiel Apparaturen für die festsitzende oder herausnehmbare kieferorthopädische Therapie, hergestellt werden.

In der festsitzenden Behandlung mit Multibracketapparaturen ist die Positionierung kieferorthopädischer Brackets maßgeblich für das Ergebnis der Behandlung [70,71]. Eine Fehlpositionierung von Brackets kann die Gesamtbehandlungsdauer und die Anzahl notwendiger Biegungen in orthodontischen Bögen sowie das Repositionieren von Brackets erforderlich machen [71-77]. Bereits geringfügige Abweichungen der Bracketpositionen können zu klinisch signifikanten Abweichungen von der angestrebten Zahnstellung führen [70,78].
Die Bracketplatzierung kann klinisch entweder direkt mithilfe von Bracketsetzpinzetten oder indirekt mithilfe von Brackettransferschienen erfolgen. Jedoch wurden für keine direkte oder konventionell indirekte Bracketplatzierungsmethode ideale klinische Ergebnisse beschrieben, sodass kompensatorische Biegungen und Bracketrepositionierungen erforderlich bleiben [79]. Dies ist vorwiegend auf die Verwendung konfektionierter, auf Populationsmittelwerten

basierenden Bracketsystemen bei einer interindividuell hohen Variabilität der Zahnmorphologien zurückzuführen [80]. Desweiteren ist eine Berücksichtigung der Wurzelmorphologie und -achse mit konventionellen Methoden nicht möglich, obgleich die Erreichung einer Wurzelparallellität eines der vorrangigen Ziele der kieferorthopädischen Behandlung ist [42,75]. Behandlungsplanungssoftwares hingegen ermöglichen eine individuelle Bracketpositionierung anhand einer Behandlungszielsimulation durchzuführen. Dabei können dreidimensionale Daten zur Darstellung der Zahnwurzeln integriert und die Auswirkungen verschiedener Bracketpostionen auf die erwartete Zahnstellung verglichen und entsprechend angepasst werden, um individuelle anatomische Gegebenheiten zu berücksichtigen [75]. Um diese virtuell geplanten, individuellen Bracketpositionen klinisch zu übertragen müssen Brackettransferschienen für die Bracketplatzierung hergestellt werden. Dabei stehen verschiedene Prozesse zur sogenannten digitalen indirekten Bracketplatzierung zur Verfügung [81,82]. Einerseits können Modelle mit Hilfsstrukturen zur Platzierung der klinisch verwendeten Brackets additiv im 3D Druckverfahren erstellt werden [82]. Andererseits ist es auch möglich, Modelle mit Kunststoffbrackets als Platzhalter für die spätere Integration der klinisch zu verwendenden Brackets in die Tranfersschiene herzustellen. Bei beiden Methoden werden anschließend Brackettransferschienen aus Silikon oder Tiefziehfolien labortechnisch konventionell hergestellt [80,81]. Alternativ ist auch die virtuelle Gestaltung der Brackettransferschiene und direkte additive Fertigung im 3D Druckverfahren möglich [81]. Die additive Fertigung von Brackettransferschienen kann im Digital Light Processing Verfahren (DLP), Sterolithographie Verfahren (SLA) oder im Poly-Jet Modeling Verfahren (PJM) erfolgen [81,83]. Häufig basieren die dafür verwendeten Materialien auf einer Mischung aus Methacrylaten und Acrylaten, sowie Photoinitiatoren und weiteren Additiven [83].

Das Erreichen des virtuell geplanten Behandlungsziels ist abhängig von der Genauigkeit der Brackettransferschienen und der Genauigkeit der indirekten Bracketplatzierung. In der Literatur lagen jedoch teilweise widersprüchliche Daten zur Genauigkeit der verschiedenen Verfahren vor, sodass eine evidenzbasierte Beurteilung der am geeignetsten Methoden nicht möglich war. Um die relevantesten Methoden hinsichtlich ihrer zu erwartenden Genauigkeit zu bewerten wurde eine Systematische Übersichtsarbeit einschließlich Meta-Analyse durchgeführt (Originalarbeit 2.2.1). Ziel war es dabei neben der allgemeinen Übertragunsgenauigkeit auch Untergruppenanalysen zu zahnbezogenen und kieferbezogenen Faktoren zu bewerten. Darüber hinaus wurde in einer experimentellen Studie die Umsetzungsgenauigkeit verschiedener additiv gefertigter Bracketübertragungsschienen im DLP-Verfahren und einer Silikon-Bracketübertragungsschiene auf der Basis eines im SLA-

Verfahren hergestellten Modells mit Hilfsstrukturen für die digitale indirekte Bracketplatzierung verglichen (Originalarbeit 2.2.2).

Neben der Determinierung und Übertragung individueller Bracketpositionen ermöglicht die virtuelle Behandlungsplanung auch die Fertigung individueller Bracketbasen und individueller orthodontischer Bögen [23,84]. Abhängig davon ob lediglich die Bracketpositionen oder zusätzlich auch andere Komponenten individualisiert sind, werden solche Systeme als teilindividuelle oder vollindividuelle CAD-CAM Bracketsysteme bezeichnet [25,84-86]. Klinisch relevante Fragestellung bei der Bewertung der Effektivität dieser Systeme sind die Gesamtbehandlungsdauer, die Anzahl notwendiger Termine, die Anzahl notwendiger Bracketrepositionierungen, die Bracketverlustraten und die Qualität des Behandlungsergebnisses. Nur wenige Autorengruppen haben konventionelle Bracketsysteme mit teilindividuellen und vollindividuellen CAD-CAM Bracketsystemen hinsichtlich dieser Aspekte klinisch verglichen. Brown et al. stellten eine verkürzte Behandlungsdauer von fünf Monaten für teilindividuelle Systeme sowie eine verkürzte Behandlungsdauer von acht Monaten für vollindividuelle Systeme gegenüber konventionellen Systemen fest [23]. Die digitale indirekte Bracketplatzierung hatte somit einen stärkeren Einfluss auf die Effizienz der Behandlung als die Individualisierung der Bracketbasen. Desweiteren konnte auch die Anzahl der notwendigen Termine reduziert werden, bei gleichem Behandlungsergebnis gemäß dem ABO-OGS. Diese Ergebnisse wurden im Allgemeinen durch andere klinische Studien bestätigt, obwohl aufgrund der verwendeten Methodiken ein hohes Verzerrungsrisiko besteht [87-89]. Zusätzlich zu den genannten klinischen Fragestellungen ist auch von Interesse, inwiefern die virtuell geplanten Zahnbewegungen erreicht werden, beziehungsweise inwiefern das erreichte klinische Ergebnis der Planung entspricht. Zu diesem Ziel wurde eine randomisierte, klinische Studie durchgeführt, bei der ein vollindividuelles Bracketsystem mit einem konventionellen Bracketsystem verglichen wurde (Originalarbeit 2.2.3).

Im Bereich der kombiniert kieferorthopädisch-kieferchirurgischen Therapie basierte die Operationsplanung über mehrere Jahrzehnte hinweg auf konventionellen Methoden unter Verwendung von Fotografien, Gipsmodellen, einer Gesichtsbogenübertragung, einem Zenrikregistrat und einem Fernröntgenseitenbild [90,91].

Initial erfolgte bei dieser Methode die kephalometrische Operationsplanung am seitlichen Fernröntgenseitenbil, um die chirurgisch notwendigen Bewegungen zur Harmonisierung der Kieferbasen und kraniofazialen Morphologie zu bestimmen, wobei individuelle sagittale und vertikale Befunde berücksichtigt werden konnten [90]. Anschließend wurden die Ergebnisse

der kephalometrischen Planung im Rahmen einer Modelloperation im Artikulator übertragen und zur Einstellung der Okklusion modifiziert. Auf Grundlage der Modelloperation erfolgte die Herstellung eines Operationssplintes, der intraoperativ zur Umsetzung der festgelegten Kieferrelation eingesetzt wurde [90].

Die konventionelle Planungsmethode weist zahlreiche Einschränkungen auf. Zunächst ist die kephalometrische Planung am seitlichen Fernröntgenseitenbild lediglich im zweidimensionalen Raum möglich, sodass die Transversalebene nicht berücksichtigt werden kann. Im Prinzip kann bei Vorliegen von Laterognathien beziehungsweise Anomalien in der Transversalebene auch ein frontales Fernröntgenseitenbild zur chirurgischen Planung verwendet werden. Jedoch existieren keine Bewertungsschemata für eine individualisierte Kephalometrie, sodass die synoptische Berücksichtigung der Ergebnisse der beiden Aufnahmen (laterales und frontales Fernröntgenseitenbild) nur eingeschränkt möglich ist. Desweiteren stellt auch die Modelloperation eine starke Vereinfachung dar, da knöcherne Strukturen des Ober- und Unterkiefers nicht dargestellt sind. Ebenso ist eine reliable Vorhersage der für die Ästhetik relevanten Weichgewebestrukturen und der Lachlinie nicht möglich. Zudem bestehen zahlreiche potentielle Quellen für Ungenauigkeiten im labortechnischen Prozess der Modellerstellung, Zentrikregistrierung und Gesichtsbogenübertragung [91-94]. Letztlich kann ein Operationssplint lediglich die Umsetzung der geplanten Relation der Kiefer zueinander über die interokklusale Referenz gewährleisten. Jedoch bietet er keine Kontrollmöglichkeit über das Ausmaß und die Richtung der durchgeführten chirurgischen Bewegungen und die erreichte Positionierung in Bezug auf die kraniofaziale Morphologie.

Im letzten Jahrzehnt wurden daher zunehmend digitale Planungsysteme eingesetzt, um die Limitationen konventioneller Verfahren zu überwinden. Behandlungsplanungssoftwares ermöglichen die virtuelle Okklusionseinstellung sowie eine Planung der chirurgischen Osteotomien am dreidimensionalen Modell. Dabei werden Daten aus dreidimensionaler Bildgebung (Digitale Volumentomographie/DVT oder Computertomographie/CT) mit Daten eines Modellscans oder Intraoralscans kombiniert [67]. Dieses Verfahren ermöglicht die Beurteilung der Dysgnathie in allen drei Raumebenen und die simultane Darstellung der Hart- und Weichgewebe im Rahmen der virtuellen Operationsplanung. So können auch Risikosituationen berücksichtigt werden, zum Beispiel die Nähe zu Zahnwurzeln oder Nerven, insbesondere zum Nervus alveolaris inferior bei geplanten Umstellungsosteotomien im Unterkiefer (Abb. 2).

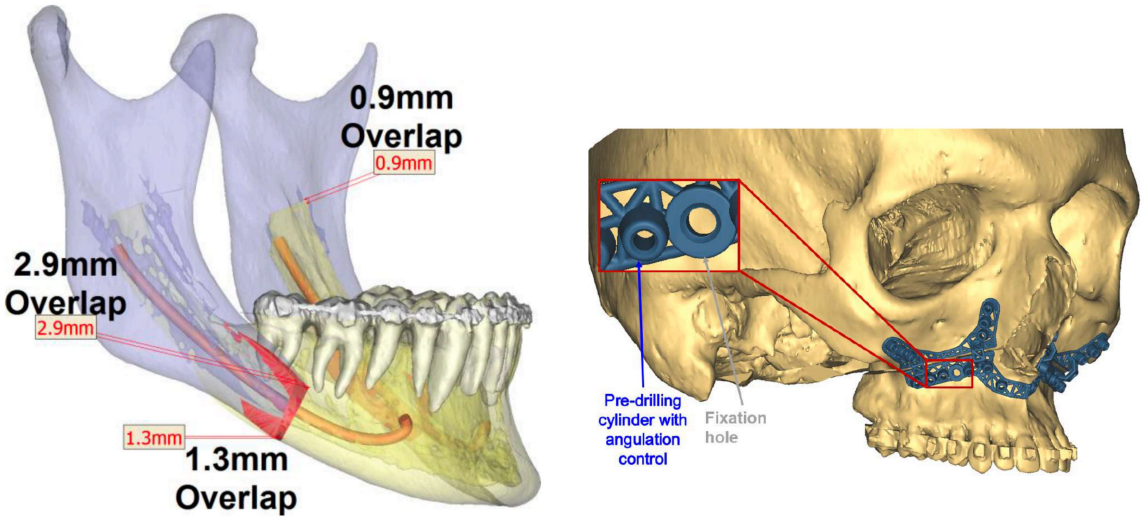

Abb. 2 (links): Darstellung von Zähnen einschließlich der Zahnwurzeln, des Nervus alveolaris inferior (orange) und Überlappungsbereichen (rot) bei einer geplanten Umstellungsosteotomie des Unterkiefers (eigene Aufnahme aus dem Softwareprogramm ProPlan CMF™, Materialise, Neuven, Belgien)
Abb. 2 (rechts): Virtuell gestaltete Schablone zur navigierten Osteotomie und navigierten Vorbohrung für die Verwendung eines patientenspezifischen Implantats zur Positionierung des Oberkiefer bei einer geplanten Umstellungsosteotomie (Screenshot aus einem CaseReport des Softwareprogramms ProPlan CMF™, Materialise, Neuven, Belgien)

Klinische Studien und systematische Übersichtsarbeiten belegen die vergleichsweise hohe Umsetzungsgenauigkeit 3D geplanter Operationen [95-100]. Desweiteren ist es möglich anhand der dreidimensionalen Planungen Schablonen für die navigierte Durchführung von Osteotomien und patientenspezifische Implantate im Sinne von individuellen Ostesyntheseplatten vorzufertigen [101]. Bei Verwendung von Navigationsschablonen kann auch die Vorbohrung für individuelle Osteosyntheplattensysteme, sogenannte patientenspezifische Implantate (PSI), integriert werden, so dass die Positionierung der Kieferbasen auch ohne Operationssplinte erfolgen kann (Abb. 2) [101]. Insbesondere bei Umstellungsosteotomien des Oberkiefers könnte dieses Verfahren signifikante Vorteile aufweisen. Die Positionierung kann dadurch über unbeweglichen Mittelgesichtstrukturen erfolgen und ist somit nicht von der interokklusalen Referenz sowie der Mobilität des Unterkiefers bei einem anästhesierten Patienten abhängig [101]. Zu diesem Verfahren liegen nur wenige, jedoch hinsichtlich der Erreichten Positionierung vielversprechende Ergebnisse vor [102]. Daher wurde eine Studie durchgeführt, um die Genauigkeit von 3D geplanten splintbasierten und splintfreien Umstellungsosteotomien zu untersuchen (Originalarbeit 2.2.4).

2.2.1 Originalarbeit: Bracket Transfer Accuracy with the Indirect Bonding Technique: A Systematic Review and Meta-Analysis

Sabbagh, H.; Khazaei, Y.; Baumert, U.; Hoffmann, L.; Wichelhaus, A.; Janjic Rankovic, M. Bracket Transfer Accuracy with the Indirect Bonding Technique: A Systematic Review and Meta-Analysis.
Journal of Clinical Medicine 2022, 11, 2568. DOI: 10.3390/jcm11092568

Zusammenfassung:

Zielsetzung: Untersuchung der Bracketübertragungsgenauigkeit bei der indirekten Klebetechnik (IDB).

Methoden: Bis November 2021 wurde eine systematische Literatursuche in PubMed MEDLINE, Web of Science, Embase und Scopus durchgeführt.

Auswahlkriterien: Berücksichtigt wurden In-vivo- und Ex-vivo-Studien, in denen die Genauigkeit der Bracketübertragung durch Vergleich der geplanten und der erreichten Bracketpositionen mit der IDB-Technik untersucht wurde. Es wurden Informationen zu Patienten, Proben und angewandter Methodik gesammelt. Gemessene mittlere Übertragungsfehler (MTE) für anguläre und lineare Richtungen wurden extrahiert. Das Risiko für systematische Verzerrungen (RoB) in den Studien wurde mithilfe eines RoB-Tools bewertet. Eine Meta-Analyse der Ex-vivo-Studien wurde für die gesamte lineare und anguläre Bracket-Übertragungsgenauigkeit sowie für Untergruppenanalysen nach Art der Bracketübertragung, Zahngruppen, Kiefern und nach Bewertungsmethode durchgeführt.

Ergebnisse: Insgesamt 16 Studien erfüllten die Einschlusskriterien für diese systematische Überprüfung. Die linearen mittleren Übertragungsfehler (MTE) in mesiodistaler, vertikaler und bukkolingualer Richtung betrugen 0,08 mm (95 % CI 0,05; 0,10), 0,09 mm (0,06; 0,11) bzw. 0,14 mm (0,10; 0,17). Die mittleren angulären Übertragungsfehler (MTE) für Angulation, Rotation und Drehmoment betrugen 1,13° (0,75; 1,52), 0,93° (0,49; 1,37) bzw. 1,11° (0,68; 1,53). Silikontrays zeigten die höchste Genauigkeit, gefolgt von vakuumgeformten Trays und 3D-gedruckten Trays. Untergruppenanalysen zwischen Zahngruppen, rechter und linker Seite sowie Ober- und Unterkiefer zeigten geringe Unterschiede.

Schlussfolgerungen und Implikationen: Die Gesamtgenauigkeit der indirekten Klebetechnik kann als klinisch akzeptabel angesehen werden. Zukünftige Studien sollten sich mit der Validierung der verwendeten Methoden zur Beurteilung der Genauigkeit befassen.

2.2.2 Originalarbeit: Bracket transfer accuracy with two different three-dimensional printed transfer trays vs silicone transfer trays

Hoffmann, L.; **Sabbagh, H.**; Wichelhaus, A.; Kessler, A.
Bracket transfer accuracy with two different three-dimensional printed transfer trays vs silicone transfer trays.
The Angle Orthodontist 2022, 92, 364-371, doi:10.2319/040821-283.1.

Zusammenfassung:

Zielsetzung: Vergleich der Übertragungsgenauigkeit von zwei verschiedenen additiv gefertigten Bracketübertragungsschienen mit Bracketübertragungsschienen aus Polyvinylsiloxan (PVS) für die indirekte Bracketplatzierung.

Material und Methoden: Für jedes untersuchte Material wurden insgesamt 10 Zahnmodelle angefertigt. Die virtuelle Bracketplatzierung wurde auf einem gescannten Zahnmodell mit OnyxCeph (OnyxCeph 3D Lab, Chemnitz, Deutschland) durchgeführt. Es wurden dreidimensional gedruckte Transferschienen und Silikon-Transferschienen hergestellt. Die Bracketpositionen wurden nach dem indirekten Klebeverfahren gescannt. Es wurden lineare und anguläre Übertragungsfehler gemessen. Signifikante Unterschiede zwischen den mittleren Übertragungsfehlern und der Häufigkeit der klinisch akzeptablen Fehler (<0,25 mm/1°) wurden mit dem Kruskal-Wallis- bzw. dem $\chi 2$-Test analysiert.

Ergebnisse: Alle Bracketübertragungsschienen zeigten eine vergleichbare Genauigkeit bei der Platzierung der Brackets. NextDent wies eine signifikant höhere Häufigkeit von Rotationsfehlern innerhalb der 1°-Grenze auf (P = 0.01) als das PVS-Tray. Während PVS in allen linearen Dimensionen signifikante Unterschiede zwischen den Zahngruppen zeigte, wies Dreve nur in bukkolingualer Richtung einen signifikanten Unterschied auf. Alle Gruppen zeigten eine ähnliche Verteilung der Richtungsabweichung.

Schlussfolgerungen: Dreidimensional gedruckte Bracketübertragungsschienen erzielten vergleichbare Ergebnisse mit den PVS-Bracketübertragungsschienen in Bezug auf die Genauigkeit der Bracketpositionierung. NextDent scheint im Vergleich zu PVS hinsichtlich der Häufigkeit von klinisch akzeptablen Fehlern unterlegen zu sein, während Dreve als gleichwertig eingestuft wurde. Der Einfluss von Zahngruppen auf die Genauigkeit der Bracketpositionierung kann durch die Verwendung einer geeigneten dreidimensionalen gedruckten Bracketübertragungsschienen (Dreve) reduziert werden.

2.2.3 Originalarbeit: Clinical effects with customized brackets and CAD/CAM technology: a prospective controlled study

Hegele, J.; Seitz, L.; Claussen, C.; Baumert, U.; **Sabbagh, H.**; Wichelhaus, A.
Clinical effects with customized brackets and CAD/CAM technology: a prospective controlled study.
Progress in Orthodontics 2021, 22, 40, doi:10.1186/s40510-021-00386-0.

Zusammenfassung:

Zielsetzung: Ziel dieser prospektiven, kontrollierten Studie war es, die klinische Effizienz eines vollindividualisierten CAD-CAM Bracketsystems im Vergleich mit einem konventionellen Bracketsystem zu untersuchen.

Material und Methoden: Insgesamt wurden 38 Patienten in zwei Gruppen aufgeteilt, die entweder mit einem direkt geklebten konventionellen Bracketsystem (Damon, Ormco, USA) oder mit einem indirekt geklebten vollindividuellem CAD-CAM Bracketsystem (Insignia™, Ormco, USA) behandelt wurden. Verglichen wurden die Gesamtbehandlungszeit, die Anzahl der Behandlungstermine, die Anzahl der verlorenen oder neu positionierten Brackets, die Anzahl der Bögen und Biegungen, der Little Irregularity Index, kephalometrische Analysen und ABO-Scores. Um die klinische Umsetzung der Behandlungsplanung zu bewerten, wurden Überlagerungen der virtuellen Aufstellungen und der Behandlungsergebnisse der CAD/CAM-Gruppe durchgeführt.

Ergebnisse: Es wurden keine Unterschiede zwischen den beiden Behandlungsgruppen in Bezug auf die Gesamtbehandlungszeit, die Anzahl der Termine und die Anzahl der Biegungen festgestellt. Mit dem CAD/CAM-System traten häufiger Bracketverluste auf. Indirekt geklebte Brackets mussten nicht so oft neu positioniert werden wie direkt geklebte Brackets. Die Behandlungsergebnisse mit beiden Systemen waren hinsichtlich ihrer Auswirkungen auf die Verringerung der ABO-Scores vergleichbar. Beim Vergleich der Behandlungsergebnisse mit den virtuellen Aufstellungen wurden die mesio-distalen Positionen am besten erreicht, gefolgt von den vertikalen Positionen. Transversale Positionen wiesen die größten Diskrepanzen auf. Bei den Winkeln stimmten die Angulationswerte am besten mit dem virtuellen Set-up überein, während bei den Inklinationswerten die größten Diskrepanzen auftraten.

Schlussfolgerung: Im Vergleich zu einem direkt geklebten selbstligierenden Bracketsystem hatte die Verwendung von indirekt geklebten individuellen CAD/CAM-Brackets nur einen geringen Einfluss auf die Behandlungseffizienz und die Behandlungsergebnisse.

2.2.4 Originalarbeit: Accuracy of maxillary positioning using computer-designed and manufactured occlusal splints or patient-specific implants in orthognathic surgery.

Malenova, Y.; Ortner, F.; Liokatis, P.; Haidari, S.; Tröltzsch, M.; Fegg, F.; Obermeier, K.T.; Hartung, J.T.; Kakoschke, T.K.; Burian, E.; Otto, S.; **Sabbagh, H.**; Probst, F.
Accuracy of maxillary positioning using computer-designed and manufactured occlusal splints or patient-specific implants in orthognathic surgery.
Clin Oral Investig 2023, doi:10.1007/s00784-023-05125-9.

Zusammenfassung:

Zielsetzung: Bestimmung der Genauigkeit der Oberkieferpositionierung unter Verwendung von am Computer entworfenen und hergestellten Positionierungsschablonen oder patientenspezifischen Implantaten in der orthognathen Chirurgie.

Material und Methoden: Es wurde eine retrospektive Analyse von 28 Patienten durchgeführt, die sich einer virtuell geplanten orthognathen Operation mit Le-Fort-I-Osteotomie des Oberkiefers unterzogen, wobei entweder VSP-generierte Schablonen (n = 13) oder patientenspezifische Implantate (PSI) (n = 15) verwendet wurden. Die Genauigkeit und das chirurgische Ergebnis beider Techniken wurden durch Überlagerung der präoperativen chirurgischen Planung mit postoperativen CT-Scans und Messung der Translations- und Rotationsabweichung für jeden Patienten verglichen.

Ergebnisse: Die globale geometrische 3D-Abweichung zwischen der geplanten Position und dem postoperativen Ergebnis betrug 0,60 mm (95%-CI 0,46-0,74, Bereich 0,32-1,11 mm) für Patienten mit PSI und 0,86 mm (95%-CI 0,44-1,28, Bereich 0,09-2,60 mm) für Patienten mit chirurgischen Schablonen. Die postoperativen Unterschiede bei den einzelnen linearen Abweichungen zwischen der geplanten und der postoperativen Position waren bei der PSI im Vergleich zu den chirurgischen Schablonen etwas größer in Bezug auf die x-Achse und die Neigung, aber geringer in Bezug auf die y- und z-Achse. Hinsichtlich der globalen geometrischen Abweichung, den linearen Abweichungen in der x-, y- und z-Achse sowie der Rotationen gab es keine signifikanten Unterschiede zwischen beiden Gruppen.

Schlussfolgerungen: Hinsichtlich der Genauigkeit bei der Positionierung von Oberkiefersegmenten nach Le Fort I Osteotomie in der orthognathen Chirurgie bieten patientenspezifische Implantate und chirurgische Schablonen eine gleich hohe Genauigkeit.

2.3 Digitale Technologien und biomechanische Simulationssysteme

Die kieferorthopädische Zahnbewegung ist ein komplexer biologischer Prozess, der durch die therapeutische Applikation von Kräften und Drehmomenten auf die Zähne und damit auf das Parodontale Ligament (PDL) und den Alveolarfortsatzknochen induziert wird [103,104]. Dabei führen mehrere zelluläre und molekulare Signalwege in Folge der mechanischen Belastung zu einem Knochenremodeling über Knochenresorption durch Osteoklasten und Knochenapposition durch Osteoblasten (Mechanotransduktion) [105].

Die Größe und Richtung der kieferorthopädisch verwendeten Kräfte ist von entscheidender Bedeutung, um einerseits eine effiziente Zahnbewegung zu erreichen und andererseits unerwünschte Nebenwirkungen wie Schmerzen, ausgeprägte Hyalinisation und apikale Wurzelresorptionen zu vermeiden [28,106].

Während die Kraftgrößen für einige Komponenten, die bei festsitzenden Apparaturen verwendet werden, wie z.B. elastische Ketten, Nickel-Titan-Federn, Kragarme und intermaxilläre Gummizüge, relativ genau bestimmt werden können, sind die resultierenden Kräfte komplexerer Bogenaktivierungen oder -biegungen klinisch nicht zu bestimmen [29]. Daher sind in der Kieferorthopädie biomechanische Untersuchungen zur Bestimmung dieser Kenngrößen und des Materialverhaltens etabliert [107]. Digitale Technologien ermöglichen heutzutage eine detaillierte Modellierung und Quantifizierung des biomechanischen Verhaltens kieferorthopädischer Apparaturen. Durch den Einsatz von computergesetützten Finite-Elemente-Simulationen (FES) und robotergestützten biomechanischen Versuchsständen können spezifische Kraftvektoren und Stressverteilungen innerhalb der kieferorthopädischen Systeme präzise analysiert werden [107].

Die Finite-Elemente-Methode ist ein rechnerisches Verfahren, das komplexe biologische Systeme und deren Reaktionen auf mechanische Belastungen in silico simulieren kann [30,108,109]. Ein signifikanter Vorteil dieser Methode, insbesondere im Kontext kieferorthopädischer biomechanischer Untersuchungen, besteht in der Möglichkeit, das Verhalten des Alveolarknochens und des Parodontalligaments zu berücksichtigen. Die Übertragbarkeit dieser Simulationsmodelle ist jedoch abhängig von der Qualität und Richtigkeit der verwendeten Versuchsbedingungen [108,109]. Insbesondere die Darstellung der Morphologie der Gewebe und die Determinierung deren Eigenschaften sowie der mechanischen Interaktionen der Behandlungsapparaturen sind komplex [110]. Aus diesem Grund korrelieren die Ergebnisse solcher Untersuchungen nur eingeschränkt mit dem tatsächlichen Materialverhalten und der biologischen Reaktion. Die Ergebnisse von FES sollten daher unabhängig von der Art des verwendeten Modells mit experimentellen Daten verglichen werden um ihre Gültigkeit zu prüfen [111].

Biomechanische Versuchsstände hingegen ermöglichen die Untersuchung von Behandlungsmechaniken, die in der untersuchten Form auch klinisch eingesetzt werden. Insbesondere die mechanische Interaktion der verschiedenen eingesetzten Komponenten entsprechen dabei weitestgehend dem zu erwartenden Verhalten in der therapeutischen Anwendung. Eine Schwierigkeit bei der Durchführung solcher Untersuchungen sind die dynamischen Kraft-Drehmoment-Systeme, die sich aufgrund der fortlaufenden

kieferorthopädischen Zahnbewegungen kontinuierlich ändern. Trotz des Einsatzes von computer- und robotergestützten Systemen zur Überwindung dieser Limitation existieren bislang nur eine begrenzte Anzahl an biomechanischen Prüfständen, die spezifisch für die Untersuchung dynamischer kieferorthopädischer Zahnbewegungen konzipiert und validiert wurden [33,112]. Im Jahr 1992 wurde mit dem "Orthodontic Measurement und Simulation System, OMSS" erstmals ein computergesteuerter Versuchsstand vorgestellt, der Kräfte und Momente anhand eines simplifizierten Zwei-Zahn-Systems untersuchen kann [113]. Die Bewegung des Versuchsstands erfolgte dabei statisch über einen 6-Achs-Positionierungstisch. Im Jahr 2006 wurde mit dem "Robotic Measurement System, RMS" ein Versuchsstand vorgestellt, der einen Roboter zur Bewegungskontrolle des Versuchsstands einsetzt [114]. Obwohl dieses System einen größeren Steuerungsspielraum und damit die Simulation umfangreicherer und komplexerer Zahnbewegungen ermöglicht, erfolgte die Steuerung weiterhin statisch.

In den dieser Habilitationsschrift zugrundeliegenden biomechanischen Untersuchungen (Originalarbeit 2.3.1 und 2.3.2) wurde zur automatisierten Bewegungssteuerung ein Feedback-Mechanismus zwischen den gemessenen Kräften und Drehmomenten und den von den Systemen ausgeführten Bewegungen entwickelt (Kraftsteuerung). Die Kraftsteuerung basiert auf computerberechnungen und übersetzt die gemessenen Kräfte und Drehmomente am Ort des Sensors über eine Transformationsmatrix in den Kraftansatzpunkt (center of force, CoF) und das Widerstandszentrum (center of resistance, CoR). Diese Punkte und deren Beziehung determinieren auch klinisch das Rotationszentrum (center of rotation, CRot) und die Art und die Richtung der Zahnbewegung (Abb. 3)

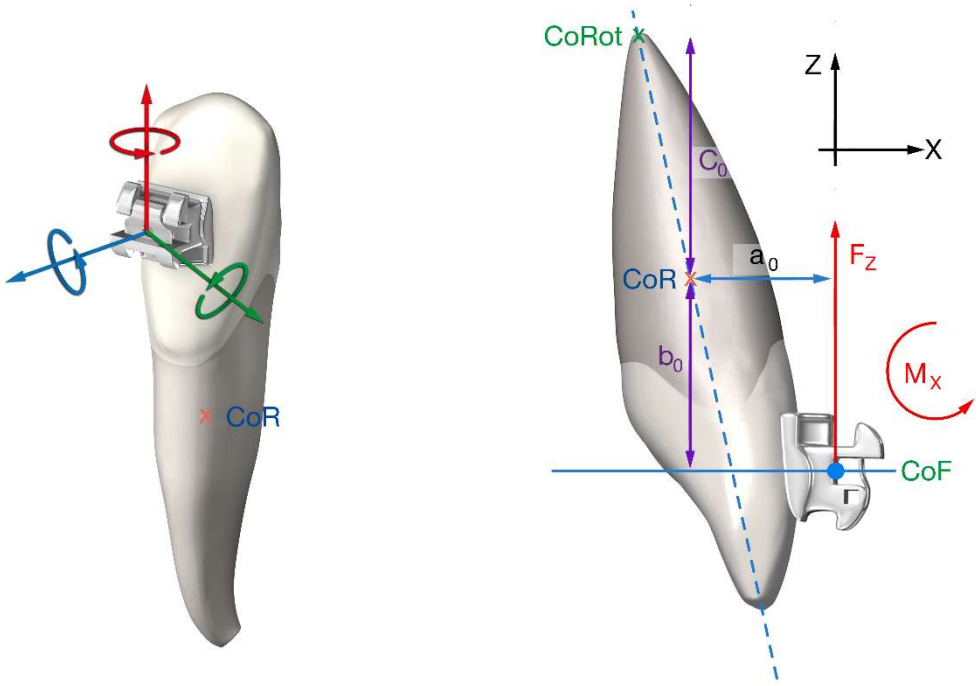

Abb. 3 links: Grafik eines Zahns mit im Bracket/CoF eingeblendeten Koordinatensystem der Messungen.

Abb. 3 rechts: Schematische Darstellung eines Zahns mit den determinierenden Parametern der kieferorthopädischen Zahnbewegung (CoF, CoR, CoRot) in abhängigkeit einer Intrusiven Beispielkraft.

Das entwickelte Kontrollprogramm steuert basierend auf diesen Berechnungen den Roboter, der automatisiert in die Richtung der sich ergebenden Zahnbewegung verfährt, wobei sich die anliegenden Kräfte und Drehmomente abbauen. Die Erfassung dieser Größen erfolgt simultan und wird iterativ fortgesetzt, bis beide Parameter gegen null konvergieren. Das Prinzip der Kraftsteuerung wurde im Rahmen der zugrundeliegenden Originalarbeiten (2.3.1 und 2.3.2) für die Untersuchung verschiedener Zahnbewegungsszenarien in unterschiedliche Versuchsstände implementiert.

Der Versuchsstand ROSS (Robotic Orthodontic Measurement & Simulation System) verwendet zur Steuerung einen Industrieroboter (KUKA KR 5-sixx R650, KUKA Roboter GmbH, Deutschland) und wurde zur Simulation von Einzelzahnbewegungen konzipiert, wobei der Sensor direkt mit dem zu bewegenden Zahn verbunden ist (Abb. A)

Der Versuchsstand HOSEA (Hexpod for Orthodontic Simulation Evaluation and Analysis) verwendet zur Steuerung eine Stewart-Plattform (HP-550, PPI GmbH, Karlsruhe, Deutschland) und wurde zur Simulation von Bewegungen von Zahngruppen konzipiert, wobei der Sensor und die Zahngruppe am Gehäuse befestigt sind und die Plattform den statischen Teil bewegt (Abb. B).

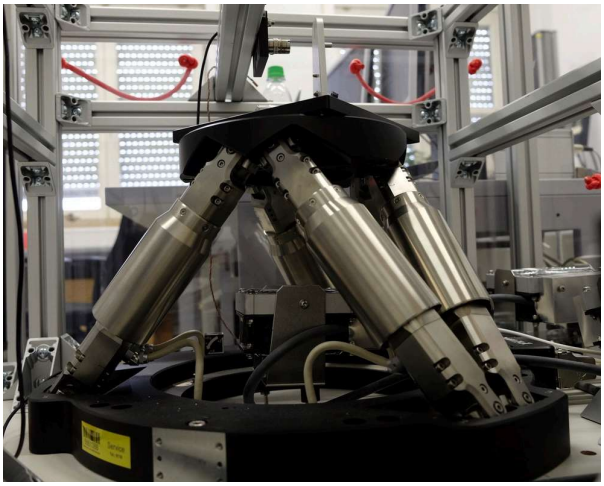

Abb. 4 links: Kraftgesteuerter biomechanischer Versuchsstand ROSS. Der 6-Achs-Roboter mit Kraft-Moment-Sensor und Prüfzahn verfährt zum statisch fixiertem experimentellen Modell.
Abb. 4 rechts: Kraftgesteuerter biomechanischer Versuchsstand HOSEA. Die 6-Achs Stewart Plattform verfährt das Versuchsmodell zum statisch fixierten Kraft-Moment-Sensor.

Ziel der Studien war es, Einzelzahnbewegungen der kieferorthopädischen Nivellierungsphase (Originalarbeit 2.3.1), und Bewegungen von Zahngruppen in der kieferorthopädischen Kontraktions- und Justierungsphase (Originalarbeit 2.3.2) kraftgesteuert zu simulieren. Dabei wurden kieferorthopädische Mechaniken anhand von Literaturempfehlungen ausgewählt und verwendet um die resultierenden Kraft- und Drehmomentwerte dynamisch zu quantifizieren und die Literaturempfehlungen hinsichtlich der Mechaniken für die klinische Anwendung zu bewerten.

2.3.1 Originalarbeit: Biomechanical simulation of forces and moments of initial orthodontic tooth movement in dependence on the used archwire system by ROSS (Robot Orthodontic Measurement & Simulation System)

Dotzer, B.; Stocker, T.; Wichelhaus, A.; Janjic Rankovic, M.; **Sabbagh, H.**
Biomechanical simulation of forces and moments of initial orthodontic tooth movement in dependence on the used archwire system by ROSS (Robot Orthodontic Measurement & Simulation System).
J Mech Behav Biomed Mater 2023, 144, 105960, doi:10.1016/j.jmbbm.2023.105960.

Zusammenfassung:

Zielsetzung: Ziel dieser Studie war es, die Kräfte und Momente während simulierter initialer kieferorthopädischer Zahnbewegungen mit Hilfe eines neuartigen biomechanischen Versuchsstands zu bestimmen.

Material und Methoden: Der Versuchsaufbau bestand aus einem industriellen Präzisionsroboter mit einem Kraft-Drehmoment-Sensor, einem Oberkiefermodell und einem Steuercomputer mit Software. Kräfte und Drehmomente, die während der Bewegungssimulationen auf den entsprechenden Versuchszahn wirkten, wurden für zwei 0,016" NiTi-Rundbögen (Sentalloy Light/Sentalloy Medium) dynamisch gemessen. Intrusive (#1), rotatorische (#2) und anguläre (#3) Zahnbewegungen wurden durch ein Steuerprogramm simuliert, das auf dem Prinzip der Kraftkontrolle basiert und vom Roboter ausgeführt wurde. Die Ergebnisse wurden mittels K-S-Test und Mann-Whitney-U-Test mit einem Signifikanzniveau von $\alpha = 5$ % statistisch ausgewertet.

Ergebnisse: Die Sentalloy Medium Bögen erzeugten in allen Simulationen höhere Kräfte und Momente als die Sentalloy Light Bögen. In Simulation #1 erreichten die mittleren Anfangskräfte/Momente 1,442 N/6,781 Nmm für die Light-Bögen und 1,637 N/9,609 Nmm für die Medium-Bögen. Bei der Bewegung Nr. 2 erzeugten leichte Bögen mittlere Anfangskräfte/Momente von 0,302 N/-8,271 Nmm, während mittlere Bögen 0,432 N/-9,653 Nmm erzeugten. Simulation #3 zeigte mittlere Anfangskräfte/Momente von -0,122 N/8,477 Nmm für die leichten Bögen im Vergleich zu -0,300 N/11,486 Nmm für die mittleren Bögen.

Schlussfolgerungen: Die gemessenen Kräfte und Momente waren für die anfängliche kieferorthopädische Zahnbewegung in den Simulationen Nr. 2 und Nr. 3 geeignet, in Simulation Nr. 1 jedoch unzureichend. Für die initiale Nivellierung von vertikalen Malokklusionen sollten reduzierte Bogendrahtdimensionen (<0,016″) gewählt werden.

2.3.2 Originalarbeit: Force-controlled biomechanical simulation of orthodontic tooth movement with torque archwires using HOSEA (hexapod orthodontic simulation, evaluation and measurement system)

Haas, E.; Schmid, A.; Stocker, T.; Wichelhaus, A.; **Sabbagh, H.**
Force-Controlled Biomechanical Simulation of Orthodontic Tooth Movement with Torque Archwires using HOSEA (Hexapod for Orthodontic Simulation, Evaluation and Analysis). Bioengineering 2023

Zusammenfassung:

Zielsetzung: Ziel dieser Studie war es, das dynamische Verhalten verschiedener Torquebögen für die festsitzende kieferorthopädische Behandlung mit Hilfe eines automatisierten, kraftgesteuerten biomechanischen Simulationssystems zu untersuchen.

Material und Methode: Ein neuartiges biomechanisches Simulationssystem (HOSEA) wurde verwendet, um dynamische Zahnbewegungen zu simulieren und die Drehmomententwicklung von vier verschiedenen Bogengruppen zu untersuchen: 0. 017 x 0,025 Torque-Segmentierte Bögen (TSA) mit 30 Drehmomenten, 0,018 x 0,025 TSA mit 45° Torque, 0,017 x 0,025 Stahlbögen (SS) mit 30° Torque und 0,018 x 0,025 SS mit 30° Torque (n = 10/Gruppe. Für die statistische Analyse wurde der Kruskal-Wallis-Test verwendet ($p < 0,050$).

Ergebnisse: Die 0,018 x 0,025 SS-Bögen erzeugten das höchste initiale Rotationsmoment (My) von 9,835 Nmm. Die Reduzierung des Drehmoments pro Grad (My/Ry) war bei TSA im Vergleich zu SS-Bögen signifikant geringer ($p < 0,001$). TSA 0,018 x 0,025 war die einzige Gruppe, in der alle Bögen in der Simulation eine Rotation von mindestens 10° induzierten. Kollateralkräfte und Momente, insbesondere Fx, Fz und Mx, traten während der Drehmomententwicklung auf.

Schlussfolgerungen: Die gemessenen Kräfte und Momente lagen bei den 0,018 x 0,025 Bögen in einem geeigneten Bereich für die Übertragung eines palatinalen Wurzeldrehmoments auf die Schneidezähne. Der 0,018 x 0,025 TSA erreichte zuverlässig mindestens 10° Rotation ohne Reaktivierung.

3. Zusammenfassung und Ausblick

Digitale Technologien erfahren immer mehr Anwendungen in der Kieferorthopädie und beeinflussen zunehmend die alltägliche Arbeitsweise. Unabhängige wissenschaftliche Untersuchungen ermöglichen es, diese Technologien evidenzbasiert zu bewerten und im Sinne einer patientenorientierten Medizin differenziert einzusetzen und weiterzuentwickeln.

Ziel dieser kumulativen Habiliationsschrift war es, verschiedene Aspekte digitaler Technologien einschließlich biomechanischer Simulationssysteme im Hinblick auf die kieferorthopädische Diagnostik und Therapie zu untersuchen. Dabei standen insbesondere auch Fragestellungen zu Möglichkeiten der klinischen Prozessoptimierung und Individualisierung im Vordergrund.

Im ersten Teil dieser Habilitationsschrift lag der Schwerpunkt auf Untersuchungen zu Applikationen digitaler Technologien in der kieferorthopädischen Diagnostik und Behandlungsplanung.
Im Rahmen der ersten Untersuchung konnte gezeigt werden, dass die manuelle Herstellung von Setupmodellen eine hohe Variabilität bei manuell durchgeführten Zahnbewegungen aufweist und die Genauigkeit nicht für eine Behandlungsplanung in der Alignertherapie ausreichend ist (Originalarbeit 2.1.1). Auf diesem Gebiet bietet die virtuelle Durchführung von Zahnbewegungen und anschließende additive Fertigung von Setupmodellen eine wesentlich höhere Genauigkeit [115-117]. Desweiteren ist die rein digitale Arbeitsweise klinisch effektiver, da Alignerserien über viele Zwischenschritte hinweg anhand eines Intraoralscans hergestellt werden können, wohingegen die manuelle Arbeitsweise Abformungen nach drei manuell erstellten Zwischenschritten erfordert [118]. In diesem Bereich ist in Zukunft ein vollständiger Wechsel zur rein digitalen Arbeitsweise zu erwarten, wobei inzwischen modellfreie Verfahren und die direkte Herstellung von Alignern basierend auf virtuellen Setups Gegenstand aktueller Untersuchungen sind [119]. Dies könnte auch bestehende Limitationen der Tiefziehtechnik bei der Alignerherstellung überwinden und eine individuelle Gestaltung der Schichtstärken in verschiedenen Bereichen der Alignerschienen ermöglichen, um Kräfte und Drehmomente gezielt zu applizieren [120].
In der zweiten Untersuchung wurde die Reliabilität und Performance eines neuronalen Netzwerks zur automatisierten Erkennung kephalometrischer Landmarken evaluiert (Originalarbeit 2.2.2). Dabei wurde der Einfluss verschiedener Entwicklungsstadien des Gebisses und kieferorthopädischer Apparaturen sowie zahnärztlicher Restaurationen berücksichtigt. Während das Vorhandensein von Behandlungsapparaturen und zähnärztlicher Restaurationen keinen

statistisch signifikanten Einfluss auf die Erkennung kephalometrischer Landmarken hatte, zeigte sich im Wechselgebiss eine reduzierte Detektionsgenauigkeit bezüglich dentaler Landmarken. Im Wechselgebiss ergab sich bei dem verwendeten Framework eine Erhöhung des mean radial error (MRE) um 0.5 mm für den kephalometrischen Referenzpunkt Apicale inferior und eine Erhöhung des MRE um 0.34 mm für den Referenzpunkt Incisale Superior. Dieses Ergebnis zeigt die Notwendigkeit auf, diagnostische Anwendungen künstlicher Intelligenz gezielt für den Einsatz bei verschiedenen klinischen Situationen zu optimieren. Dabei ist als Mindestanforderung für einen routinemäßigen Einsatz eine Detektionsgenauigkeit zu fordern, die der eines erfahrenen Behandlers oder einer erfahrenen Behandlerin entspricht. KI-Modelle sollten darüber hinaus sowohl validierbar als auch verifizierbar sein und ihre Funktionsweise sollte transparent und nachvollziehbar dargelegt werden, insbesondere wenn sie bei kritischen medizinischen Diagnosestellungen eingesetzt werden soll [121]. Desweiteren sollten automatisiert generierte diagnostische Analysen ärztlich überprüft werden, um Fehldiagnosen und Fehlinterpretationen zu vermeiden.
In Zukunft ist eine zunehmende Integration KI-basierter Systeme über Schnittstellen in diagnostische Softwares oder Patientenverwaltungssysteme zu erwarten, was zu einer signifikanten Zeitersparnis im Rahmen des diagnostischen Prozesses führen dürfte. Weiterhin zeigen aktuelle Forschungsarbeiten auch vielversprechende Ergebnisse in der Anwendung bei der dreidimensionalen Kephalometrie unter Verwendung der Digitalen Volumenttomographie und der Computertomographie [122]. In diesem Zusammenhang trägt auch die Forschung an strahlenfreien Methoden zur Hartgewebedarstellung mithilfe von Dental-MRT Systemen dazu bei, den Indikationsbereich der dreidimensionalen Bildgebung und Diagnostik in der Kieferorthpädie zu erweitern [123].

Im zweiten Teil der Habilitationsschrift lag der Schwerpunkt auf Untersuchungen zu Applikationen digitaler Technologien in der kieferorthopädischen Therapie. Die Ergebnise der durchgeführten systematischen Übersichtsarbeit zur indirekten Klebetechnik zeigten, dass die modellfreie Arbeitsweise und die Anwendung additiv gefertigter Bracketübertragungsschienen eine vergleichbare Genauigkeit aufweisen wie modellbasierte konventionelle Verfahren (Originalarbeit 2.2.1). Die digitale, modellfreie Arbeitsweise unter Nutzung additiv gefertigter Brackettransferschienen kann daher als effektiver angesehen werden, da sie mit weniger potentiellen Fehlerquellen behaftet ist und weniger labortechnische Zwischenschritte erfordert. Die anhand der Meta-Analyse ermittelten mittleren linearen und angulären Abweichungen der erreichten Bracketpositionen stimmten mit den Ergebnissen der durchgeführten Ex-vivo Studie zur digitalen indirekten Bracketplatzierung überein (Originalarbeit 2.2.2). In dieser zeigten die aus

verschiedenen Materialien additiv gefertigten Bracketübertragungsschienen vergleichbare Ergebnisse mit Bracketübertragungsschienen aus Silikon, die als Goldstandardmethode angesehen werden. Insgesamt ist auch in diesem Bereich eine deutliche Tendenz zur Anwendung modellfreier Verfahren zu erwarten. Aktuelle Forschungsarbeiten untersuchen den Einfluss verschiedener Materialien und Druckverfahren in der additiven Fertigung sowie verschiedene Gestaltungsweisen der additiv gefertigten Brackettransferschienen [24].
Im Rahmen der durchgeführten prospektiven, kontrollierten klinischen Studie wurde der Einfluss eines vollindividualiserten CAD-CAM Bracketsystems auf die Effektivität und Effizienz der Behandlung untersucht (Originalarbeit 2.2.3). Dabei wurden lediglich geringfügige Unterschiede im Vergleich zu dem konventionellen Bracketsystem festgestellt. Dies war möglicherweise auf die signifikant höhere Bracketverlustrate bei der CAD-CAM Gruppe zurückzuführen, die insbesondere die Effizienz der Behandlung negativ beeinträchtigt haben könnte. Höhere Bracketverlustraten sind für die indirekte Klebetechnik in der Literatur beschrieben [124,125]. Klinisch ist daher insbesondere bei Anwendung der indirekten Klebetechnik die sorgfältige Einhaltung eines geeigneten Klebeprotokolls zu berücksichtigen um die Behandlungseffizienz nicht nachteilig zu beeinflussen [126]. Nach wie vor fehlen prospektive klinische Studien hoher methodischer Qualität, die eine Überlegenheit von CAD-CAM Bracketsystemen in Bezug auf die Behandlungseffizienz und -effektivität belegen. Künftige Studien müssen daher diesen Nachweis führen, um den erhöhten Material- und Kostenaufwand dieser Methode zu rechtfertigen.

Im Bereich der kieferorthopädisch-kieferchirurgischen Therapie konnte im Rahmen der durchgeführten klinischen Studie gezeigt werden, dass die Genauigkeit virtuell geplanter und navigierter Umstellungsosteotomien eine hohe Umsetzungsgenauigkeit aufweisen (Originalarbeit 2.2.4). Dabei zeigten sowohl splintbasierte als auch das splintfreie Verfahren vergleichbare Ergebnisse und übertrafen vergleichbare Werte in der Literatur für konventionelle Planungsverfahren [99,100]. Tendenziell war die Positionierung des Oberkiefers über ein patientenspezifisches Implantat (PSI) genauer als die splintbasierte Positionierung, auch wenn bei der gegebenen Stichprobengröße keine statistische Signifikanz erreicht wurde. Die Anwendung von Navigationsschablonen und PSIs bietet dabei den zusätzlichen Vorteil unabhängig von einer interokklusalen Referenz zu sein [127].
Insgesamt ist in Zukunft auch in diesem Bereich von einer zunehmenden Implementierung digitaler Verfahren auszugehen, da diese neben einer hohen Umsetzungsgenauigkeit zahlreiche weitere Vorteile bieten. Dazu gehören unter anderem verbesserte Möglichkeiten in der Vorhersage des Verhaltens der Weichgewebe einschließlich der Atemwege, verbesserte Kommunikationsmöglichkeiten mit Patientinnen und Patienten, eine Verkürzung des

intraoperativen Zeitbedarfs und die Möglichkeit Risikosituationen zu antizipieren und intraoperative Komplikationen zu vermeiden [100]. Aktuelle Forschungsarbeiten zeigen vielversprechende Fortschritte hinsichtlich der Reliabilität von Weichgewebsvorhersagen im Rahmen virtueller dysgnathiechirurgischer Operationsplanungen [128,129]. Diese erfolgen häufig zumeist noch anhand von Oberflächensegmentierungen der computertomographischen Daten [128]. Weiterentwicklungen von Systemen zur fazialen Oberflächenerfassung lassen eine zunehmende Integration dieser Daten im Rahmen virtueller Planungen erwarten [4,130-133].

Im dritten Teil dieser Habilitationsschrift lag der Schwerpunkt auf Applikationen digitaler Technologien bei biomechanischen Simulationssystemen. Biomechanische Untersuchungen können Erkenntnisse über das Verhalten kieferorthopädischer Materialien und Mechaniken liefern, um diese in der klinischen Anwendung differenziert einzusetzen. Das Verständnis über entstehende Kraft-Drehmomentsysteme kieferorthopädischer Behandlungsmechaniken und die Verwendung geeigneter Kraftgrößen ist von entscheidender Bedeutung, um unerwünschte Nebenwirkungen wie ausgeprägte Hyalinisationen und kieferorthopädisch induzierte externe apikale Wurzelresorptionen (EARR) zu vermeiden [134,135]. Aus mechanobiologischer Sicht ist vor allem die entstehende Spannung im parodontalen Ligament (PDL) für die zellulären und molekularen Mechanismen im Rahmen der Mechanotransduktion für die biologische Gewebereaktion und damit auch Zahnbewegung entscheidend [136]. Klinisch können die entstehenden Spannungen jedoch nicht direkt gemessen werden, sodass stattdessen die Kontrolle der applizierten Kräfte im Vordergrund steht [136]. In diesem Zusammenhang hat in der biomechanischen Forschung im letzten Jahrzehnt insbesondere die Finite-Elemente-Methode (FEM) an Bedeutung gewonnen, da zumindest näherungsweise das Verhaltens des Alveolarknochens und des PDL simuliert und mit den applizierten Kräften in Zusammenhang gebracht werden kann [30,109]. Dennoch kann die Frage nach idealen Kraftgrößen für die kieferorthopädische Zahnbewegung auch nach mehreren Jahrzehnten experimenteller und klinischer Forschung noch nicht evidenzbasiert beantwortet werden [136]. Neben nur eingeschränkt auf den Menschen übertragbaren Erkenntnissen aus Tiermodellen, liegen gesichterte Erkenntnisse aus klinisch-histologischen Studien vor, die vorwiegend den Zusammenhang zwischen der Kraftgröße und dem Ausmaß der Wurzelresorptionen belegen [137-141]. Aus einer systematischen Übersichtsarbeit, die zwölf Humanstudien berücksichtigte, geht hervor, dass für translatorische Zahnbewegungen Kräfte im Bereich zwischen 50cN und 100cN empfohlen werden können [136]. Das PDL erfährt bei translatorischen Zahnbewegungen eine verhältnismäßig günstige Belastung. Bei Zahnbewegungen, die weniger Parodontalfasern

beanspruchen, wie z.B. der kieferorthopädischen Intrusion, sind reduzierte Kraftgrößen zu verwenden.

Um die durch orthodontische Bögen induzierten Kräfte zu bestimmen, werden häufig Dreipunkt-Biegeversuche oder modifizierte Biegeversuche durchgeführt und die aus dem resultierenden Entlastungsplaeus ermittelte mittlere Kraft angegeben [142]. Dies stellt jedoch eine starke Vereinfachung dar, da weder Aussagen über die im Bracket wirkenden Kräfte noch über Kräfte im Widerstandszentrum des Zahns oder Spannungen im PDL möglich sind. Computergestützte, apparative biomechanische Simulationssysteme erlauben in dieser Hinsicht eine exakte Bestimmung der im Bracket wirksamen Kräfte sowie eine näherungsweise Bestimmung der im Widerstandszentrum wirkenden Kräfte. Die Implementierung einer algorithmusbasierten Kraftsteuerung ermöglicht darüber hinaus, die zu erwartenden Zahnbewegungen zu simulieren und durchzuführen um den dynamischen Verlauf dieser Kenngrößen zu ermitteln.

In der ersten durchgeführten Studie wurden die dynamischen Kraft-Drehmoment-Systeme bei der initialen kieferorthopädischen Zahnbewegung für verschiedene Zahnfehlstellungen untersucht (Originalarbeit 2.3.1). Dabei konnte gezeigt werden, dass in der Literatur empfohlene Bogendimensionen für die initiale Zahnbewegung bei vertikalen Abweichungen deutlich zu hohe Kräfte generierten [143-145]. Um eine Überlastung des Parodonts zu vermeiden, sollten daher in der Nivellierungsphase bei vertikalen Abweichungen kleinere Bogendimensionen, z.B. 0,014" Nickel-Titan (NiTi) oder kleiner, verwendet werden. In der zweiten Untersuchung wurden die dynamischen Kraft-Drehmoment-Systeme von Torquebögen zur therapeutischen Korrektur der Frontzahninklination untersucht (Originalarbeit 2.3.2). Dabei konnte gezeigt werden, dass der Einsatz von orthodontischen Bögen der Dimensionen 0.017" x 0.025" in den untersuchten Konfigurationen nicht für eine kontrollierte und effiziente Drehmomentübertragung geeignet sind. Hingegen lieferte der untersuchte Bogen 0,018" x 0,025" TSA geeignete Drehmomente über einen Bereich von 10° Inklinationsänderung, ohne die Notwendigkeit von Reaktivierungen. Die Daten der durchgeführten Studien können als Grundlage für Finite-Elemente Simulationen verwendet werden, um zu erwartende Spannungen im PDL näherungsweise zu bestimmen.

Während im Rahmen der durchgeführten biomechanischen Studien lediglich verschiedene klinische Ausgangsbedingungen und verschiedene Mechaniken in Simulationen untersucht werden konnten, ist in Zukunft ein integrierter Ansatz denkbar, der Erkenntnisse aus biomechanischen Simulationssystemen, Finite-Element-Simulationen und künstlicher Intelligenz zusammenführt. Dadurch könnten Behandlungsapparaturen nicht nur nach verschiedenen Dysgnathiegruppen und Kategorien biomechanisch gezielt eingesetzt und individualisiert werden, sondern nach dem Konzept der stratifizierten Medizin auf Grundlage der individuell vorliegenden Dysagnathie, parodontaler Faktoren und der genetischen Konstitution.

4. Abkürzungsverzeichnis

CAD	Computer Aided Design
CAM	Computer Aided Manufacturing
CNN	Convolutional Neural Network
PDL	Parodontales Ligament
FEM	Finite Elemente Methode
ASR	Approximale Schmelzreduktion
KI	Künstliche Intelligenz
DVT	Digitale Volumentomographie
CT	Computertomographie
MRT	Magnetresonanztomographie
SLA	Stereolithographie
DLP	Digital Light Processing
PJM	Poly-Jet Modeling
FFF	Fused Filament Fabrication
TSA	Torque Segmented Archwire
STL	Standard Tesselation Language
DICOM	Digital Imaging and Communications in Medicine
PLY	Polygon File Format
OBJ	Object File Format
OTC	Optische Kohärenztomographie
MRE	Mean Radial Error
PSI	Patientenspezifisches Implantat
EARR	Externe apikale Wurzelresorptionen
NiTi	Nickel-Titan

5. Literaturverzeichnis

1. Kong, L.; Li, Y.; Liu, Z. Digital versus conventional full-arch impressions in linear and 3D accuracy: a systematic review and meta-analysis of in vivo studies. *Clin Oral Investig* **2022**, *26*, 5625-5642, doi:10.1007/s00784-022-04607-6.
2. Balhaddad, A.A.; Garcia, I.M.; Mokeem, L.; Alsahafi, R.; Majeed-Saidan, A.; Albagami, H.H.; Khan, A.S.; Ahmad, S.; Collares, F.M.; Della Bona, A.; et al. Three-dimensional (3D) printing in dental practice: Applications, areas of interest, and level of evidence. *Clin Oral Investig* **2023**, *27*, 2465-2481, doi:10.1007/s00784-023-04983-7.
3. Leonardi, R.M. 3D Imaging Advancements and New Technologies in Clinical and Scientific Dental and Orthodontic Fields. *J Clin Med* **2022**, *11*, doi:10.3390/jcm11082200.
4. Park, J.H.; Lee, G.H.; Moon, D.N.; Yun, K.D.; Kim, J.C.; Lee, K.C. Creation of Digital Virtual Patient by Integrating CBCT, Intraoral Scan, 3D Facial Scan: An Approach to Methodology for Integration Accuracy. *J Craniofac Surg* **2022**, *33*, e396-e398, doi:10.1097/scs.0000000000008275.
5. Aragón, M.L.; Pontes, L.F.; Bichara, L.M.; Flores-Mir, C.; Normando, D. Validity and reliability of intraoral scanners compared to conventional gypsum models measurements: a systematic review. *Eur J Orthod* **2016**, *38*, 429-434, doi:10.1093/ejo/cjw033.
6. Sabbagh, H.; Heger, S.M.; Stocker, T.; Baumert, U.; Wichelhaus, A.; Hoffmann, L. Accuracy of 3D Tooth Movements in the Fabrication of Manual Setup Models for Aligner Therapy. *Materials* **2022**, *15*, 3853.
7. Kiviahde, H.; Bukovac, L.; Jussila, P.; Pesonen, P.; Sipilä, K.; Raustia, A.; Pirttiniemi, P. Inter-arch digital model vs. manual cast measurements: Accuracy and reliability. *Cranio* **2018**, *36*, 222-227, doi:10.1080/08869634.2017.1344811.
8. Koretsi, V.; Tingelhoff, L.; Proff, P.; Kirschneck, C. Intra-observer reliability and agreement of manual and digital orthodontic model analysis. *Eur J Orthod* **2018**, *40*, 52-57, doi:10.1093/ejo/cjx040.
9. Wong, K.F.; Lam, X.Y.; Jiang, Y.; Yeung, A.W.K.; Lin, Y. Artificial intelligence in orthodontics and orthognathic surgery: a bibliometric analysis of the 100 most-cited articles. *Head Face Med* **2023**, *19*, 38, doi:10.1186/s13005-023-00383-0.
10. Bichu, Y.M.; Hansa, I.; Bichu, A.Y.; Premjani, P.; Flores-Mir, C.; Vaid, N.R. Applications of artificial intelligence and machine learning in orthodontics: a scoping review. *Prog Orthod* **2021**, *22*, 18, doi:10.1186/s40510-021-00361-9.
11. Evangelista, K.; de Freitas Silva, B.S.; Yamamoto-Silva, F.P.; Valladares-Neto, J.; Silva, M.A.G.; Cevidanes, L.H.S.; de Luca Canto, G.; Massignan, C. Accuracy of artificial intelligence for tooth extraction decision-making in orthodontics: a systematic review and meta-analysis. *Clin Oral Investig* **2022**, *26*, 6893-6905, doi:10.1007/s00784-022-04742-0.

12. Rauniyar, S.; Jena, S.; Sahoo, N.; Mohanty, P.; Dash, B.P. Artificial Intelligence and Machine Learning for Automated Cephalometric Landmark Identification: A Meta-Analysis Previewed by a Systematic Review. *Cureus* **2023**, *15*, e40934, doi:10.7759/cureus.40934.
13. Subramanian, A.K.; Chen, Y.; Almalki, A.; Sivamurthy, G.; Kafle, D. Cephalometric Analysis in Orthodontics Using Artificial Intelligence-A Comprehensive Review. *Biomed Res Int* **2022**, *2022*, 1880113, doi:10.1155/2022/1880113.
14. Khanagar, S.B.; Al-Ehaideb, A.; Vishwanathaiah, S.; Maganur, P.C.; Patil, S.; Naik, S.; Baeshen, H.A.; Sarode, S.S. Scope and performance of artificial intelligence technology in orthodontic diagnosis, treatment planning, and clinical decision-making - A systematic review. *J Dent Sci* **2021**, *16*, 482-492, doi:10.1016/j.jds.2020.05.022.
15. Polizzi, A.; Quinzi, V.; Ronsivalle, V.; Venezia, P.; Santonocito, S.; Lo Giudice, A.; Leonardi, R.; Isola, G. Tooth automatic segmentation from CBCT images: a systematic review. *Clinical Oral Investigations* **2023**, *27*, 3363-3378, doi:10.1007/s00784-023-05048-5.
16. Graf, S.; Tarraf, N.E. Advantages and disadvantages of the three-dimensional metal printed orthodontic appliances. *J World Fed Orthod* **2022**, *11*, 197-201, doi:10.1016/j.ejwf.2022.10.003.
17. Graf, S.; Vasudavan, S.; Wilmes, B. CAD-CAM design and 3-dimensional printing of mini-implant retained orthodontic appliances. *Am J Orthod Dentofacial Orthop* **2018**, *154*, 877-882, doi:10.1016/j.ajodo.2018.07.013.
18. Cunha, T.; Barbosa, I.D.S.; Palma, K.K. Orthodontic digital workflow: devices and clinical applications. *Dental Press J Orthod* **2021**, *26*, e21spe26, doi:10.1590/2177-6709.26.6.e21spe6.
19. Wilmes, B.; Tarraf, N.E.; de Gabriele, R.; Dallatana, G.; Drescher, D. Procedure using CAD/CAM-manufactured insertion guides for purely mini-implant-borne rapid maxillary expanders. *J Orofac Orthop* **2022**, *83*, 277-284, doi:10.1007/s00056-022-00375-w.
20. Wilmes, B.; Vasudavan, S.; Drescher, D. CAD-CAM-fabricated mini-implant insertion guides for the delivery of a distalization appliance in a single appointment. *Am J Orthod Dentofacial Orthop* **2019**, *156*, 148-156, doi:10.1016/j.ajodo.2018.12.017.
21. De Gabriele, O.; Dallatana, G.; Riva, R.; Vasudavan, S.; Wilmes, B. The easy driver for placement of palatal mini-implants and a maxillary expander in a single appointment. *J Clin Orthod* **2017**, *51*, 728-737.
22. Wilhelmy, L.; Willmann, J.H.; Tarraf, N.E.; Wilmes, B.; Drescher, D. Maxillary space closure using a digital manufactured Mesialslider in a single appointment workflow. *Korean J Orthod* **2022**, *52*, 236-245, doi:10.4041/kjod21.203.

23. Brown, M.W.; Koroluk, L.; Ko, C.C.; Zhang, K.; Chen, M.; Nguyen, T. Effectiveness and efficiency of a CAD/CAM orthodontic bracket system. *Am J Orthod Dentofacial Orthop* **2015**, *148*, 1067-1074, doi:10.1016/j.ajodo.2015.07.029.
24. Palone, M.; Koch, P.J.; Jost-Brinkmann, P.G.; Spedicato, G.A.; Verducci, A.; Pieralli, P.; Lombardo, L. Accuracy of indirect bracket placement with medium-soft, transparent, broad-coverage transfer trays fabricated using computer-aided design and manufacturing: An in-vivo study. *Am J Orthod Dentofacial Orthop* **2023**, *163*, 33-46, doi:10.1016/j.ajodo.2021.08.023.
25. Müller-Hartwich, R.; Jost-Brinkmann, P.G.; Schubert, K. Precision of implementing virtual setups for orthodontic treatment using CAD/CAM-fabricated custom archwires. *J Orofac Orthop* **2016**, *77*, 1-8, doi:10.1007/s00056-015-0001-5.
26. Hodecker, L.D.; Scheurer, M.; Scharf, S.; Roser, C.J.; Fouda, A.M.; Bourauel, C.; Lux, C.J.; Bauer, C.A.J. Influence of Individual Bracket Base Design on the Shear Bond Strength of In-Office 3D Printed Brackets-An In Vitro Study. *J Funct Biomater* **2023**, *14*, doi:10.3390/jfb14060289.
27. Bauer, C.A.J.; Scheurer, M.; Bourauel, C.; Kretzer, J.P.; Roser, C.J.; Lux, C.J.; Hodecker, L.D. Precision of slot widths and torque transmission of in-office 3D printed brackets : An in vitro study. *J Orofac Orthop* **2023**, doi:10.1007/s00056-023-00460-8.
28. Wichelhaus, A. *Kieferorthopädie: Therapie Band 1; Grundlegende Behandlungskonzepte; Farbatlanten der Zahnmedizin*; Georg Thieme Verlag KG: 2013.
29. Koenig, H.A.; Vanderby, R.; Solonche, D.J.; Burstone, C.J. Force systems from orthodontic appliances: an analytical and experimental comparison. *J Biomech Eng* **1980**, *102*, 294-300, doi:10.1115/1.3138226.
30. Singh, J.R.; Kambalyal, P.; Jain, M.; Khandelwal, P. Revolution in Orthodontics: Finite element analysis. *J Int Soc Prev Community Dent* **2016**, *6*, 110-114, doi:10.4103/2231-0762.178743.
31. Geramy, A.; Mahmoudi, R.; Geranmayeh, A.R.; Borujeni, E.S.; Farhadifard, H.; Darvishpour, H. A comparison of mechanical characteristics of four common orthodontic loops in different ranges of activation and angular bends: The concordance between experiment and finite element analysis. *Int Orthod* **2018**, *16*, 42-59, doi:10.1016/j.ortho.2018.01.011.
32. Simon, M.; Keilig, L.; Schwarze, J.; Jung, B.A.; Bourauel, C. Forces and moments generated by removable thermoplastic aligners: incisor torque, premolar derotation, and molar distalization. *Am J Orthod Dentofacial Orthop* **2014**, *145*, 728-736, doi:10.1016/j.ajodo.2014.03.015.

33. Badawi, H.M.; Toogood, R.W.; Carey, J.P.; Heo, G.; Major, P.W. Three-dimensional orthodontic force measurements. *Am J Orthod Dentofacial Orthop* **2009**, *136*, 518-528, doi:10.1016/j.ajodo.2009.02.025.
34. Dotzer, B.; Stocker, T.; Wichelhaus, A.; Janjic Rankovic, M.; Sabbagh, H. Biomechanical simulation of forces and moments of initial orthodontic tooth movement in dependence on the used archwire system by ROSS (Robot Orthodontic Measurement & Simulation System). *J Mech Behav Biomed Mater* **2023**, *144*, 105960, doi:10.1016/j.jmbbm.2023.105960.
35. Baser, B.; Gulnar, B.; Tuhan Kutlu, E. Comparison of conventionally and digitally completed patient consent-anamnesis forms in terms of surface contamination. *Technol Health Care* **2023**, *31*, 1737-1746, doi:10.3233/thc-220600.
36. Alhammadi, M.S.; Al-Mashraqi, A.A.; Alnami, R.H.; Ashqar, N.M.; Alamir, O.H.; Halboub, E.; Reda, R.; Testarelli, L.; Patil, S. Accuracy and Reproducibility of Facial Measurements of Digital Photographs and Wrapped Cone Beam Computed Tomography (CBCT) Photographs. *Diagnostics (Basel)* **2021**, *11*, doi:10.3390/diagnostics11050757.
37. Manosudprasit, A.; Haghi, A.; Allareddy, V.; Masoud, M.I. Diagnosis and treatment planning of orthodontic patients with 3-dimensional dentofacial records. *Am J Orthod Dentofacial Orthop* **2017**, *151*, 1083-1091, doi:10.1016/j.ajodo.2016.10.037.
38. Dindaroğlu, F.; Kutlu, P.; Duran, G.S.; Görgülü, S.; Aslan, E. Accuracy and reliability of 3D stereophotogrammetry: A comparison to direct anthropometry and 2D photogrammetry. *Angle Orthod* **2016**, *86*, 487-494, doi:10.2319/041415-244.1.
39. Fleming, P.S.; Marinho, V.; Johal, A. Orthodontic measurements on digital study models compared with plaster models: a systematic review. *Orthod Craniofac Res* **2011**, *14*, 1-16, doi:10.1111/j.1601-6343.2010.01503.x.
40. Lippold, C.; Kirschneck, C.; Schreiber, K.; Abukiress, S.; Tahvildari, A.; Moiseenko, T.; Danesh, G. Methodological accuracy of digital and manual model analysis in orthodontics - A retrospective clinical study. *Comput Biol Med* **2015**, *62*, 103-109, doi:10.1016/j.compbiomed.2015.04.012.
41. Schieffer, L.; Latzko, L.; Ulmer, H.; Schenz-Spisic, N.; Lepperdinger, U.; Paulus, M.; Crismani, A.G. Comparison between stone and digital cast measurements in mixed dentition : Validity, reliability, reproducibility, and objectivity. *J Orofac Orthop* **2022**, *83*, 75-84, doi:10.1007/s00056-022-00376-9.
42. Yilmaz, H.; Eglenen, M.N. Comparison of the effect of using panoramic and cone-beam computed tomography on the accuracy of root position in indirect digital bracket placement: A retrospective study. *Orthod Craniofac Res* **2022**, *25*, 401-408, doi:10.1111/ocr.12549.

43. Zakhar, G.; Hazime, S.; Eckert, G.; Wong, A.; Badirli, S.; Turkkahraman, H. Prediction of Pubertal Mandibular Growth in Males with Class II Malocclusion by Utilizing Machine Learning. *Diagnostics (Basel)* **2023**, *13*, doi:10.3390/diagnostics13162713.
44. Zhou, J.; Zhou, H.; Pu, L.; Gao, Y.; Tang, Z.; Yang, Y.; You, M.; Yang, Z.; Lai, W.; Long, H. Development of an Artificial Intelligence System for the Automatic Evaluation of Cervical Vertebral Maturation Status. *Diagnostics (Basel)* **2021**, *11*, doi:10.3390/diagnostics11122200.
45. Akay, G.; Akcayol, M.A.; Özdem, K.; Güngör, K. Deep convolutional neural network-the evaluation of cervical vertebrae maturation. *Oral Radiol* **2023**, *39*, 629-638, doi:10.1007/s11282-023-00678-7.
46. Li, H.; Chen, Y.; Wang, Q.; Gong, X.; Lei, Y.; Tian, J.; Gao, X. Convolutional neural network-based automatic cervical vertebral maturation classification method. *Dentomaxillofac Radiol* **2022**, *51*, 20220070, doi:10.1259/dmfr.20220070.
47. Khazaei, M.; Mollabashi, V.; Khotanlou, H.; Farhadian, M. Automatic determination of pubertal growth spurts based on the cervical vertebral maturation staging using deep convolutional neural networks. *J World Fed Orthod* **2023**, *12*, 56-63, doi:10.1016/j.ejwf.2023.02.003.
48. Sereewisai, B.; Chintavalakorn, R.; Santiwong, P.; Nakornnoi, T.; Neoh, S.P.; Sipiyaruk, K. The accuracy of virtual setup in simulating treatment outcomes in orthodontic practice: a systematic review. *BDJ Open* **2023**, *9*, 41, doi:10.1038/s41405-023-00167-3.
49. Ryu, J.; Kim, Y.H.; Kim, T.W.; Jung, S.K. Evaluation of artificial intelligence model for crowding categorization and extraction diagnosis using intraoral photographs. *Sci Rep* **2023**, *13*, 5177, doi:10.1038/s41598-023-32514-7.
50. Im, J.; Cha, J.Y.; Lee, K.J.; Yu, H.S.; Hwang, C.J. Comparison of virtual and manual tooth setups with digital and plaster models in extraction cases. *Am J Orthod Dentofacial Orthop* **2014**, *145*, 434-442, doi:10.1016/j.ajodo.2013.12.014.
51. Wiechmann, D. Lingual orthodontics (part 2): archwire fabrication. *J Orofac Orthop* **1999**, *60*, 416-426, doi:10.1007/bf01388194.
52. Palone, M.; Longo, M.; Arveda, N.; Nacucchi, M.; Pascalis, F.; Spedicato, G.A.; Siciliani, G.; Lombardo, L. Micro-computed tomography evaluation of general trends in aligner thickness and gap width after thermoforming procedures involving six commercial clear aligners: An in vitro study. *Korean J Orthod* **2021**, *51*, 135-141, doi:10.4041/kjod.2021.51.2.135.
53. Polat-Ozsoy, O.; Gokcelik, A.; Toygar Memikoglu, T.U. Differences in cephalometric measurements: a comparison of digital versus hand-tracing methods. *Eur J Orthod* **2009**, *31*, 254-259, doi:10.1093/ejo/cjn121.

54. Sayinsu, K.; Isik, F.; Trakyali, G.; Arun, T. An evaluation of the errors in cephalometric measurements on scanned cephalometric images and conventional tracings. *Eur J Orthod* **2007**, *29*, 105-108, doi:10.1093/ejo/cjl065.
55. Tsorovas, G.; Karsten, A.L. A comparison of hand-tracing and cephalometric analysis computer programs with and without advanced features--accuracy and time demands. *Eur J Orthod* **2010**, *32*, 721-728, doi:10.1093/ejo/cjq009.
56. Schwendicke, F.; Chaurasia, A.; Arsiwala, L.; Lee, J.H.; Elhennawy, K.; Jost-Brinkmann, P.G.; Demarco, F.; Krois, J. Deep learning for cephalometric landmark detection: systematic review and meta-analysis. *Clin Oral Investig* **2021**, *25*, 4299-4309, doi:10.1007/s00784-021-03990-w.
57. Li, H.; Xu, Y.; Lei, Y.; Wang, Q.; Gao, X. Automatic Classification for Sagittal Craniofacial Patterns Based on Different Convolutional Neural Networks. *Diagnostics (Basel)* **2022**, *12*, doi:10.3390/diagnostics12061359.
58. Mohan, A.; Sivakumar, A.; Nalabothu, P. Evaluation of accuracy and reliability of OneCeph digital cephalometric analysis in comparison with manual cephalometric analysis-a cross-sectional study. *BDJ Open* **2021**, *7*, 22, doi:10.1038/s41405-021-00077-2.
59. Popova, T.; Stocker, T.; Khazaei, Y.; Malenova, Y.; Wichelhaus, A.; Sabbagh, H. Influence of growth structures and fixed appliances on automated cephalometric landmark recognition with a customized convolutional neural network. *BMC Oral Health* **2023**, *23*, 274, doi:10.1186/s12903-023-02984-2.
60. Kirschneck, C.; Kamuf, B.; Putsch, C.; Chhatwani, S.; Bizhang, M.; Danesh, G. Conformity, reliability and validity of digital dental models created by clinical intraoral scanning and extraoral plaster model digitization workflows. *Comput Biol Med* **2018**, *100*, 114-122, doi:10.1016/j.compbiomed.2018.06.035.
61. Kim, R.J.; Park, J.M.; Shim, J.S. Accuracy of 9 intraoral scanners for complete-arch image acquisition: A qualitative and quantitative evaluation. *J Prosthet Dent* **2018**, *120*, 895-903.e891, doi:10.1016/j.prosdent.2018.01.035.
62. Heike, C.L.; Upson, K.; Stuhaug, E.; Weinberg, S.M. 3D digital stereophotogrammetry: a practical guide to facial image acquisition. *Head Face Med* **2010**, *6*, 18, doi:10.1186/1746-160x-6-18.
63. Cevidanes, L.H.; Ruellas, A.C.; Jomier, J.; Nguyen, T.; Pieper, S.; Budin, F.; Styner, M.; Paniagua, B. Incorporating 3-dimensional models in online articles. *Am J Orthod Dentofacial Orthop* **2015**, *147*, S195-204, doi:10.1016/j.ajodo.2015.02.002.
64. Turkyilmaz, I.; Wilkins, G.N.; Benli, M. Relationship between the data quality of digital scans from intraoral scanners and surface topography of prepared teeth. *J Dent Sci* **2022**, *17*, 592-594, doi:10.1016/j.jds.2021.06.003.

65. Elbashti, M.; Molinero-Mourelle, P.; Aswehlee, A.; Bornstein, M.M.; Abou-Ayash, S.; Schimmel, M.; Ella, B.; Naveau, A. Effect of triangular mesh resolution on the geometrical trueness of segmented CBCT maxillofacial data into STL format. *J Dent* **2023**, *138*, 104722, doi:10.1016/j.jdent.2023.104722.
66. Baan, F.; Bruggink, R.; Nijsink, J.; Maal, T.J.J.; Ongkosuwito, E.M. Fusion of intra-oral scans in cone-beam computed tomography scans. *Clin Oral Investig* **2021**, *25*, 77-85, doi:10.1007/s00784-020-03336-y.
67. Mangano, C.; Luongo, F.; Migliario, M.; Mortellaro, C.; Mangano, F.G. Combining Intraoral Scans, Cone Beam Computed Tomography and Face Scans: The Virtual Patient. *J Craniofac Surg* **2018**, *29*, 2241-2246, doi:10.1097/scs.0000000000004485.
68. Becker, K.; Wilmes, B.; Grandjean, C.; Drescher, D. Impact of manual control point selection accuracy on automated surface matching of digital dental models. *Clin Oral Investig* **2018**, *22*, 801-810, doi:10.1007/s00784-017-2155-6.
69. Lee, S.C.; Hwang, H.S.; Lee, K.C. Accuracy of deep learning-based integrated tooth models by merging intraoral scans and CBCT scans for 3D evaluation of root position during orthodontic treatment. *Prog Orthod* **2022**, *23*, 15, doi:10.1186/s40510-022-00410-x.
70. Grunheid, T.; Lee, M.S.; Larson, B.E. Transfer accuracy of vinyl polysiloxane trays for indirect bonding. *Angle Orthod* **2016**, *86*, 468-474, doi:10.2319/042415-279.1.
71. Carlson, S.K.; Johnson, E. Bracket positioning and resets: five steps to align crowns and roots consistently. *Am J Orthod Dentofacial Orthop* **2001**, *119*, 76-80, doi:10.1067/mod.2001.111220.
72. Aguirre, M.J.; King, G.J.; Waldron, J.M. Assessment of bracket placement and bond strength when comparing direct bonding to indirect bonding techniques. *Am J Orthod* **1982**, *82*, 269-276, doi:10.1016/0002-9416(82)90461-4.
73. Birdsall, J.; Hunt, N.P.; Sabbah, W.; Moseley, H.C. Accuracy of positioning three types of self-ligating brackets compared with a conventionally ligating bracket. *J Orthod* **2012**, *39*, 34-42, doi:10.1179/14653121226806.
74. Castilla, A.E.; Crowe, J.J.; Moses, J.R.; Wang, M.; Ferracane, J.L.; Covell, D.A., Jr. Measurement and comparison of bracket transfer accuracy of five indirect bonding techniques. *Angle Orthod* **2014**, *84*, 607-614, doi:10.2319/070113-484.1.
75. El-Timamy, A.M.; El-Sharaby, F.A.; Eid, F.H.; Mostafa, Y.A. Three-dimensional imaging for indirect-direct bonding. *Am J Orthod Dentofacial Orthop* **2016**, *149*, 928-931, doi:10.1016/j.ajodo.2015.12.009.
76. Guenthner TA, L.B. Indirect bonding: A technique for precision and efficiency. *Seminars in Orthodontics* **2007**, 58-63.

77. Suarez, C.; Vilar, T. The effect of constant height bracket placement on marginal ridge levelling using digitized models. *Eur J Orthod* **2010**, *32*, 100-105, doi:10.1093/ejo/cjp029.
78. Germane, N.; Bentley, B.E., Jr.; Isaacson, R.J. Three biologic variables modifying faciolingual tooth angulation by straight-wire appliances. *Am J Orthod Dentofacial Orthop* **1989**, *96*, 312-319, doi:10.1016/0889-5406(89)90350-8.
79. Fukuyo K., N.Y., Nojima K., Yamaguchi H. A comparative study in three methods of bracket placement. *Orthod Waves* **2004**, *63*, 63-70.
80. Sabbagh, H. Ex-vivo-Studie zur Umsetzungsgenauigkeit virtuell geplanter Bracketpositionen-Ein Vergleich additiv gefertigter Bracketübertragungsschienen mit Polyvinyl-Siloxan Trays. Imu, 2021.
81. Hofmann, E.C.; Süpple, J.; von Glasenapp, J.; Jost-Brinkmann, P.G.; Koch, P.J. Indirect bonding: an in-vitro comparison of a Polyjet printed versus a conventional silicone transfer tray. *Angle Orthod* **2022**, *92*, 728-737, doi:10.2319/122021-925.1.
82. Süpple, J.; von Glasenapp, J.; Hofmann, E.; Jost-Brinkmann, P.G.; Koch, P.J. Accurate Bracket Placement with an Indirect Bonding Method Using Digitally Designed Transfer Models Printed in Different Orientations-An In Vitro Study. *J Clin Med* **2021**, *10*, doi:10.3390/jcm10092002.
83. von Glasenapp, J.; Hofmann, E.; Süpple, J.; Jost-Brinkmann, P.G.; Koch, P.J. Comparison of Two 3D-Printed Indirect Bonding (IDB) Tray Design Versions and Their Influence on the Transfer Accuracy. *J Clin Med* **2022**, *11*, doi:10.3390/jcm11051295.
84. Gracco, A.; Stellini, E.; Parenti, S.I.; Bonetti, G.A. Individualized orthodontic treatment: The Insignia system. *Orthodontics (Chic.)* **2013**, *14*, e88-94, doi:10.11607/ortho.929.
85. Müller-Hartwich, R.; Präger, T.M.; Jost-Brinkmann, P.G. SureSmile--CAD/CAM system for orthodontic treatment planning, simulation and fabrication of customized archwires. *Int J Comput Dent* **2007**, *10*, 53-62.
86. Jheon, A.H.; Oberoi, S.; Solem, R.C.; Kapila, S. Moving towards precision orthodontics: An evolving paradigm shift in the planning and delivery of customized orthodontic therapy. *Orthod Craniofac Res* **2017**, *20 Suppl 1*, 106-113, doi:10.1111/ocr.12171.
87. Jackers, N.; Maes, N.; Lambert, F.; Albert, A.; Charavet, C. Standard vs computer-aided design/computer-aided manufacturing customized self-ligating systems using indirect bonding with both. *Angle Orthod* **2021**, *91*, 74-80, doi:10.2319/012920-59.1.
88. Alford, T.J.; Roberts, W.E.; Hartsfield, J.K., Jr.; Eckert, G.J.; Snyder, R.J. Clinical outcomes for patients finished with the SureSmile™ method compared with conventional fixed orthodontic therapy. *Angle Orthod* **2011**, *81*, 383-388, doi:10.2319/071810-413.1.
89. Weber, D.J., 2nd; Koroluk, L.D.; Phillips, C.; Nguyen, T.; Proffit, W.R. Clinical effectiveness and efficiency of customized vs. conventional preadjusted bracket systems. *J Clin Orthod* **2013**, *47*, 261-266; quiz 268.

90. Steinhäuser, E.W.; Rudzki-Janson, I.M. *Kieferorthopädische Chirurgie: eine interdisziplinäre Aufgabe. 1. Grundlagen zur Behandlungsplanung und Behandlungsdurchführung*; Quintessenz-Verlag: 1988.
91. Zizelmann, C.; Hammer, B.; Gellrich, N.C.; Schwestka-Polly, R.; Rana, M.; Bucher, P. An evaluation of face-bow transfer for the planning of orthognathic surgery. *J Oral Maxillofac Surg* **2012**, *70*, 1944-1950, doi:10.1016/j.joms.2011.08.025.
92. Paul, P.E.; Barbenel, J.C.; Walker, F.S.; Khambay, B.S.; Moos, K.F.; Ayoub, A.F. Evaluation of an improved orthognathic articulator system: 1. Accuracy of cast orientation. *Int J Oral Maxillofac Surg* **2012**, *41*, 150-154, doi:10.1016/j.ijom.2011.09.019.
93. Paul, P.E.; Barbenel, J.C.; Walker, F.S.; Khambay, B.S.; Moos, K.F.; Ayoub, A.F. Evaluation of an improved orthognathic articulator system. 2. Accuracy of occlusal wafers. *Int J Oral Maxillofac Surg* **2012**, *41*, 155-159, doi:10.1016/j.ijom.2011.09.020.
94. Sharifi, A.; Jones, R.; Ayoub, A.; Moos, K.; Walker, F.; Khambay, B.; McHugh, S. How accurate is model planning for orthognathic surgery? *Int J Oral Maxillofac Surg* **2008**, *37*, 1089-1093, doi:10.1016/j.ijom.2008.06.011.
95. Tucker, S.; Cevidanes, L.H.; Styner, M.; Kim, H.; Reyes, M.; Proffit, W.; Turvey, T. Comparison of actual surgical outcomes and 3-dimensional surgical simulations. *J Oral Maxillofac Surg* **2010**, *68*, 2412-2421, doi:10.1016/j.joms.2009.09.058.
96. Bengtsson, M.; Wall, G.; Greiff, L.; Rasmusson, L. Treatment outcome in orthognathic surgery-A prospective randomized blinded case-controlled comparison of planning accuracy in computer-assisted two- and three-dimensional planning techniques (part II). *J Craniomaxillofac Surg* **2017**, *45*, 1419-1424, doi:10.1016/j.jcms.2017.07.001.
97. Alkaabi, S.; Maningky, M.; Helder, M.N.; Alsabri, G. Virtual and traditional surgical planning in orthognathic surgery - systematic review and meta-analysis. *Br J Oral Maxillofac Surg* **2022**, *60*, 1184-1191, doi:10.1016/j.bjoms.2022.07.007.
98. Alkhayer, A.; Piffkó, J.; Lippold, C.; Segatto, E. Accuracy of virtual planning in orthognathic surgery: a systematic review. *Head Face Med* **2020**, *16*, 34, doi:10.1186/s13005-020-00250-2.
99. Chen, Z.; Mo, S.; Fan, X.; You, Y.; Ye, G.; Zhou, N. A Meta-analysis and Systematic Review Comparing the Effectiveness of Traditional and Virtual Surgical Planning for Orthognathic Surgery: Based on Randomized Clinical Trials. *J Oral Maxillofac Surg* **2021**, *79*, 471.e471-471.e419, doi:10.1016/j.joms.2020.09.005.
100. Starch-Jensen, T.; Hernández-Alfaro, F.; Kesmez, Ö.; Gorgis, R.; Valls-Ontañón, A. Accuracy of Orthognathic Surgical Planning using Three-dimensional Virtual Techniques compared with Conventional Two-dimensional Techniques: a Systematic Review. *J Oral Maxillofac Res* **2023**, *14*, e1, doi:10.5037/jomr.2023.14101.

101. Heufelder, M.; Wilde, F.; Pietzka, S.; Mascha, F.; Winter, K.; Schramm, A.; Rana, M. Clinical accuracy of waferless maxillary positioning using customized surgical guides and patient specific osteosynthesis in bimaxillary orthognathic surgery. *J Craniomaxillofac Surg* **2017**, *45*, 1578-1585, doi:10.1016/j.jcms.2017.06.027.
102. Williams, A.; Walker, K.; Hughes, D.; Goodson, A.M.C.; Mustafa, S.F. Accuracy and cost effectiveness of a waferless osteotomy approach, using patient specific guides and plates in orthognathic surgery: a systematic review. *Br J Oral Maxillofac Surg* **2022**, *60*, 537-546, doi:10.1016/j.bjoms.2021.05.005.
103. Meikle, M.C. The tissue, cellular, and molecular regulation of orthodontic tooth movement: 100 years after Carl Sandstedt. *Eur J Orthod* **2006**, *28*, 221-240, doi:10.1093/ejo/cjl001.
104. Jeon, H.H.; Teixeira, H.; Tsai, A. Mechanistic Insight into Orthodontic Tooth Movement Based on Animal Studies: A Critical Review. *J Clin Med* **2021**, *10*, doi:10.3390/jcm10081733.
105. Li, Y.; Zhan, Q.; Bao, M.; Yi, J.; Li, Y. Biomechanical and biological responses of periodontium in orthodontic tooth movement: up-date in a new decade. *Int J Oral Sci* **2021**, *13*, 20, doi:10.1038/s41368-021-00125-5.
106. Wichelhaus, A.; Dulla, M.; Sabbagh, H.; Baumert, U.; Stocker, T. Stainless steel and NiTi torque archwires and apical root resorption. *Journal of Orofacial Orthopedics / Fortschritte der Kieferorthopädie* **2021**, *82*, 1-12, doi:10.1007/s00056-020-00244-4.
107. Adel, S.; Zaher, A.; El Harouni, N.; Venugopal, A.; Premjani, P.; Vaid, N. Robotic Applications in Orthodontics: Changing the Face of Contemporary Clinical Care. *Biomed Res Int* **2021**, *2021*, 9954615, doi:10.1155/2021/9954615.
108. Cicciù, M. Bioengineering Methods of Analysis and Medical Devices: A Current Trends and State of the Art. *Materials (Basel)* **2020**, *13*, doi:10.3390/ma13030797.
109. Cervino, G.; Fiorillo, L.; Arzukanyan, A.V.; Spagnuolo, G.; Campagna, P.; Cicciù, M. Application of bioengineering devices for stress evaluation in dentistry: the last 10 years FEM parametric analysis of outcomes and current trends. *Minerva Stomatol* **2020**, *69*, 55-62, doi:10.23736/s0026-4970.19.04263-8.
110. Fill, T.S.; Carey, J.P.; Toogood, R.W.; Major, P.W. Experimentally determined mechanical properties of, and models for, the periodontal ligament: critical review of current literature. *J Dent Biomech* **2011**, *2011*, 312980, doi:10.4061/2011/312980.
111. Cattaneo, P.M.; Cornelis, M.A. Orthodontic Tooth Movement Studied by Finite Element Analysis: an Update. What Can We Learn from These Simulations? *Curr Osteoporos Rep* **2021**, *19*, 175-181, doi:10.1007/s11914-021-00664-0.
112. Liu, Y.F.; Zhang, P.Y.; Zhang, Q.F.; Zhang, J.X.; Chen, J. Digital design and fabrication of simulation model for measuring orthodontic force. *Biomed Mater Eng* **2014**, *24*, 2265-2271, doi:10.3233/bme-141039.

113. Drescher, D.; Bourauel, C.; Thier, M. Application of the orthodontic measurement and simulation system (OMSS) in orthodontics. *Eur J Orthod* **1991**, *13*, 169-178, doi:10.1093/ejo/13.3.169.
114. Fuck, L.M.; Drescher, D. Force systems in the initial phase of orthodontic treatment -- a comparison of different leveling arch wires. *J Orofac Orthop* **2006**, *67*, 6-18, doi:10.1007/s00056-006-0521-0.
115. Etemad-Shahidi, Y.; Qallandar, O.B.; Evenden, J.; Alifui-Segbaya, F.; Ahmed, K.E. Accuracy of 3-Dimensionally Printed Full-Arch Dental Models: A Systematic Review. *J Clin Med* **2020**, *9*, doi:10.3390/jcm9103357.
116. Grassia, V.; Ronsivalle, V.; Isola, G.; Nucci, L.; Leonardi, R.; Lo Giudice, A. Accuracy (trueness and precision) of 3D printed orthodontic models finalized to clear aligners production, testing crowded and spaced dentition. *BMC Oral Health* **2023**, *23*, 352, doi:10.1186/s12903-023-03025-8.
117. Im, J.; Kim, J.Y.; Yu, H.S.; Lee, K.J.; Choi, S.H.; Kim, J.H.; Ahn, H.K.; Cha, J.Y. Accuracy and efficiency of automatic tooth segmentation in digital dental models using deep learning. *Sci Rep* **2022**, *12*, 9429, doi:10.1038/s41598-022-13595-2.
118. Echarri, P. *Clear-Aligner*; Ed. Ripano: 2013.
119. Tartaglia, G.M.; Mapelli, A.; Maspero, C.; Santaniello, T.; Serafin, M.; Farronato, M.; Caprioglio, A. Direct 3D Printing of Clear Orthodontic Aligners: Current State and Future Possibilities. *Materials (Basel)* **2021**, *14*, doi:10.3390/ma14071799.
120. Kim, K.B.; Graf, S. Direct printing of clear aligners. *J Clin Orthod* **2023**, *57*, 450-458.
121. Čartolovni, A.; Tomičić, A.; Lazić Mosler, E. Ethical, legal, and social considerations of AI-based medical decision-support tools: A scoping review. *Int J Med Inform* **2022**, *161*, 104738, doi:10.1016/j.ijmedinf.2022.104738.
122. Serafin, M.; Baldini, B.; Cabitza, F.; Carrafiello, G.; Baselli, G.; Del Fabbro, M.; Sforza, C.; Caprioglio, A.; Tartaglia, G.M. Accuracy of automated 3D cephalometric landmarks by deep learning algorithms: systematic review and meta-analysis. *Radiol Med* **2023**, *128*, 544-555, doi:10.1007/s11547-023-01629-2.
123. Flügge, T.; Gross, C.; Ludwig, U.; Schmitz, J.; Nahles, S.; Heiland, M.; Nelson, K. Dental MRI-only a future vision or standard of care? A literature review on current indications and applications of MRI in dentistry. *Dentomaxillofac Radiol* **2023**, *52*, 20220333, doi:10.1259/dmfr.20220333.
124. Dos Santos, A.L.; Wambier, L.M.; Wambier, D.S.; Moreira, K.M.; Imparato, J.C.; Chibinski, A.C. Orthodontic bracket bonding techniques and adhesion failures: A systematic review and meta-analysis. *J Clin Exp Dent* **2022**, *14*, e746-e755, doi:10.4317/jced.59768.
125. Czolgosz, I.; Cattaneo, P.M.; Cornelis, M.A. Computer-aided indirect bonding versus traditional direct bonding of orthodontic brackets: bonding time, immediate bonding

failures, and cost-minimization. A randomized controlled trial. *Eur J Orthod* **2021**, *43*, 144-151, doi:10.1093/ejo/cjaa045.

126. Dudás, C.; Czumbel, L.M.; Kiss, S.; Gede, N.; Hegyi, P.; Mártha, K.; Varga, G. Clinical bracket failure rates between different bonding techniques: a systematic review and meta-analysis. *Eur J Orthod* **2023**, *45*, 175-185, doi:10.1093/ejo/cjac050.
127. Gander, T.; Bredell, M.; Eliades, T.; Rücker, M.; Essig, H. Splintless orthognathic surgery: a novel technique using patient-specific implants (PSI). *J Craniomaxillofac Surg* **2015**, *43*, 319-322, doi:10.1016/j.jcms.2014.12.003.
128. Awad, D.; Reinert, S.; Kluba, S. Accuracy of Three-Dimensional Soft-Tissue Prediction Considering the Facial Aesthetic Units Using a Virtual Planning System in Orthognathic Surgery. *J Pers Med* **2022**, *12*, doi:10.3390/jpm12091379.
129. Yamashita, A.L.; Iwaki Filho, L.; Ferraz, F.; Ramos, A.L.; Previdelli, I.; Pereira, O.C.N.; Tolentino, E.S.; Chicarelli, M.; Iwaki, L.C.V. Accuracy of three-dimensional soft tissue profile prediction in orthognathic surgery. *Oral Maxillofac Surg* **2022**, *26*, 271-279, doi:10.1007/s10006-021-00988-2.
130. Conejo, J.; Dayo, A.F.; Syed, A.Z.; Mupparapu, M. The Digital Clone: Intraoral Scanning, Face Scans and Cone Beam Computed Tomography Integration for Diagnosis and Treatment Planning. *Dent Clin North Am* **2021**, *65*, 529-553, doi:10.1016/j.cden.2021.02.011.
131. Revilla-León, M.; Zandinejad, A.; Nair, M.K.; Barmak, A.B.; Feilzer, A.J.; Özcan, M. Accuracy of a patient 3-dimensional virtual representation obtained from the superimposition of facial and intraoral scans guided by extraoral and intraoral scan body systems. *J Prosthet Dent* **2022**, *128*, 984-993, doi:10.1016/j.prosdent.2021.02.023.
132. Revilla-León, M.; Zeitler, J.M.; Barmak, A.B.; Kois, J.C. Accuracy of the 3-dimensional virtual patient representation obtained by using 4 different techniques: An in vitro study. *J Prosthet Dent* **2022**, doi:10.1016/j.prosdent.2022.05.016.
133. Amezua, X.; Iturrate, M.; Garikano, X.; Solaberrieta, E. Analysis of the influence of the facial scanning method on the transfer accuracy of a maxillary digital scan to a 3D face scan for a virtual facebow technique: An in vitro study. *J Prosthet Dent* **2022**, *128*, 1024-1031, doi:10.1016/j.prosdent.2021.02.007.
134. Sabbagh, H.; Bamidis, E.P.; Keller, A.; Stocker, T.; Baumert, U.; Hoffmann, L.; Wichelhaus, A. Force behaviour of elastic chains during a simulated gap closure in extraction therapy cases. *Orthod Craniofac Res* **2022**, doi:10.1111/ocr.12626.
135. Villaman-Santacruz, H.; Torres-Rosas, R.; Acevedo-Mascarúa, A.E.; Argueta-Figueroa, L. Root resorption factors associated with orthodontic treatment with fixed appliances: A systematic review and meta-analysis. *Dent Med Probl* **2022**, *59*, 437-450, doi:10.17219/dmp/145369.

136. Theodorou, C.I.; Kuijpers-Jagtman, A.M.; Bronkhorst, E.M.; Wagener, F. Optimal force magnitude for bodily orthodontic tooth movement with fixed appliances: A systematic review. *Am J Orthod Dentofacial Orthop* **2019**, *156*, 582-592, doi:10.1016/j.ajodo.2019.05.011.
137. Ren, Y.; Maltha, J.C.; Kuijpers-Jagtman, A.M. Optimum force magnitude for orthodontic tooth movement: a systematic literature review. *Angle Orthod* **2003**, *73*, 86-92, doi:10.1043/0003-3219(2003)073<0086:Ofmfot>2.0.Co;2.
138. Casa, M.A.; Faltin, R.M.; Faltin, K.; Sander, F.G.; Arana-Chavez, V.E. Root resorptions in upper first premolars after application of continuous torque moment. Intra-individual study. *J Orofac Orthop* **2001**, *62*, 285-295, doi:10.1007/pl00001936.
139. Owman-Moll, P.; Kurol, J.; Lundgren, D. Effects of a doubled orthodontic force magnitude on tooth movement and root resorptions. An inter-individual study in adolescents. *Eur J Orthod* **1996**, *18*, 141-150, doi:10.1093/ejo/18.2.141.
140. Owman-Moll, P.; Kurol, J.; Lundgren, D. The effects of a four-fold increased orthodontic force magnitude on tooth movement and root resorptions. An intra-individual study in adolescents. *Eur J Orthod* **1996**, *18*, 287-294, doi:10.1093/ejo/18.3.287.
141. Owman-Moll, P. Orthodontic tooth movement and root resorption with special reference to force magnitude and duration. A clinical and histological investigation in adolescents. *Swed Dent J Suppl* **1995**, *105*, 1-45.
142. Lombardo, L.; Ceci, M.; Mollica, F.; Mazzanti, V.; Palone, M.; Siciliani, G. Mechanical properties of multi-force vs. conventional NiTi archwires. *Journal of Orofacial Orthopedics / Fortschritte der Kieferorthopädie* **2019**, *80*, 57-67, doi:10.1007/s00056-018-00164-4.
143. Jain, S.; Sharma, P.; Shetty, D. Comparison of two different initial archwires for tooth alignment during fixed orthodontic treatment-A randomized clinical trial. *J Orthod Sci* **2021**, *10*, 13, doi:10.4103/jos.JOS_17_20.
144. Wang, Y.; Jian, F.; Lai, W.; Zhao, Z.; Yang, Z.; Liao, Z.; Shi, Z.; Wu, T.; Millett, D.T.; McIntyre, G.T.; et al. Initial arch wires for alignment of crooked teeth with fixed orthodontic braces. *Cochrane Database Syst Rev* **2010**, Cd007859, doi:10.1002/14651858.CD007859.pub2.
145. Mandall, N.; Lowe, C.; Worthington, H.; Sandler, J.; Derwent, S.; Abdi-Oskouei, M.; Ward, S. Which orthodontic archwire sequence? A randomized clinical trial. *Eur J Orthod* **2006**, *28*, 561-566, doi:10.1093/ejo/cjl030.

6. Originalarbeiten

materials

MDPI

Article

Accuracy of 3D Tooth Movements in the Fabrication of Manual Setup Models for Aligner Therapy

Hisham Sabbagh [1], Sebastian Marcus Heger [2], Thomas Stocker [1], Uwe Baumert [1], Andrea Wichelhaus [1] and Lea Hoffmann [1,*]

[1] Department of Orthodontics and Dentofacial Orthopedics, University Hospital, LMU Munich, Goethestrasse 70, 80336 Munich, Germany; hisham.sabbagh@med.uni-meunchen.de (H.S.); thomas.stocker@med.uni-meunchen.de (T.S.); uwe.baumert@med.uni-muenchen.de (U.B.); andrea.wichelhaus@med.uni-meunchen.de (A.W.)

[2] Private Practice "Dr. Heger", Fürther Strasse 2, 90429 Nürnberg, Germany; info@zahnarzt-drheger.de

* Correspondence: lea.hoffmann@med.uni-muenchen.de; Tel.: +49-89-4400-53223

Abstract: Background: The clinical outcome of aligner therapy is closely related to the precision of its setup, which can be manually or digitally fabricated. The aim of the study is to investigate the suitability of manual setups made for aligner therapy in terms of the precision of tooth movements. Methods: Six dental technicians were instructed to adjust each of eleven duplicate plaster casts of a patient models as follows: a 1 mm pure vestibular translation of tooth 11 and a 15° pure mesial rotation of tooth 23. The processed setup models were 3D scanned and matched with the reference model. The one-sample Wilcoxon signed-rank test ($p < 0.05$) was used for evaluation. Results: The overall precision of the translational movement covers a wide range of values from 0.25 to 2.26 mm (median: 1.09 mm). The target value for the rotation of tooth 23 was achieved with a median rotation of 9.76° in the apical-occlusal direction. Unwanted movements in the other planes also accompanied the rotation. Conclusions: A manual setup can only be fabricated with limited precision. Besides the very high variability between technicians, additional unwanted movements in other spatial planes occurred. Manually fabricated setups should not be favored for aligner therapy due to limited precision.

Keywords: clear aligner; aligner; orthodontic appliance; dental casts

check for updates

Citation: Sabbagh, H.; Heger, S.M.; Stocker, T.; Baumert, U.; Wichelhaus, A.; Hoffmann, L. Accuracy of 3D Tooth Movements in the Fabrication of Manual Setup Models for Aligner Therapy. *Materials* **2022**, *15*, 3853. https://doi.org/10.3390/ma15113853

Academic Editor: Enrico Marchetti

Received: 2 May 2022
Accepted: 25 May 2022
Published: 28 May 2022

Publisher's Note: MDPI stays neutral with regard to jurisdictional claims in published maps and institutional affiliations.

Copyright: © 2022 by the authors. Licensee MDPI, Basel, Switzerland. This article is an open access article distributed under the terms and conditions of the Creative Commons Attribution (CC BY) license (https://creativecommons.org/licenses/by/4.0/).

1. Introduction

Treatment with aligners is an integral part of orthodontic therapy. Aligners are mainly used for the treatment of moderate crowding and spacing [1–4], for protrusion and retrusion, and minor intrusion and extrusion movements of teeth [4–6]. The therapeutic outcome closely correlates with the type and direction of the planned tooth movements. Tooth movements are achieved in increments, starting from the initial malocclusion to achieve the final setup [3,7]. The number of intermediate steps depends on the system used and the extent and type of tooth movements, e.g., Invisalign® (Align Technology, San Jose, CA, USA) usually employs movement increments of 0.25–0.33 mm [8], CA® (Scheu-Dental, Iserlohn, Germany) 0.5–1 mm [9], Essix® (Dentsply, Charlotte, NC, USA) 1 mm [10], and ClearSmile® 0.5 mm [11]. A corresponding number of setup models is therefore required for the fabrication of the aligners. Setup models can be created manually or with the aid of a CAD/CAM system. Today, the manual fabrication of aligner setups on plaster casts is increasingly being replaced by digital setups and 3D-printed models [12]. However, manual setup fabrication remains a common method for in-house aligner fabrication, as the necessary hardware (scanners and 3D printers) and software are not ubiquitously available.

The accuracy of setup models is essential owing to the small movement increments in aligner systems. The inaccurate implementation of tooth movements in the setup is a possible reason for the difference between setup and patient outcome [13]. An investigation

comparing digital and manual setups according to the ABO objective grading system (ABO OGS) showed only small differences [14]. However, the ABO OGS does not take into account the precision of each individual movement step's implementation. While translational and rotational tooth movements can be precisely executed in a digital setup (with 1/10 mm and/or 1/10° precision, depending on the software used), the precision and suitability of manual setups for aligner therapy has not yet been investigated. Therefore, the aim of this study was to investigate the precision of a defined translational tooth movement and a defined rotational tooth movement in a manual setup.

2. Materials and Methods

A plaster cast of an upper jaw with anterior crowding served as the reference model, from which a total of 72 identical casts were duplicated. Six dental technicians (A–F) experienced in the fabrication of manual setups agreed to participate in this study. Participating technicians had at least five years of experience and received training in the form of a hands-on course prior to the start of the study to ensure consistency. Each of them was instructed as follows: from the occlusal aspect, tooth 11 should be moved purely translationally 1 mm in the vestibular direction and tooth 23 should be rotated 15° in the mesial direction. To avoid familiarization effects, the technicians were instructed to process only one model per day. The work was to be completed within three months. Each technician was provided with standardized working instructions and twelve casts, of which eleven should be processed by the technician. The twelfth served as an unchanged reference cast. All setup casts were provided with vestibular and palatal silicone keys (Tresident 2000K, Schütz dental GmbH, Roßbach, Germany). The silicone keys served to reproduce the initial positions of teeth 11 and 23 at any time. An axial marking on the teeth being moved served as a rotation and reset guide.

After completion, the reference casts and processed setup models were digitized using a desktop scanner (KaVo Everest, KaVo Dental GmbH, Biberach/Riß, Germany). The scans were reviewed for scan artifacts (Everest Scan Control program, KaVo Dental GmbH), corrected if necessary, and then saved as STL files. From each STL file, teeth 11 and 23 were isolated using the program GOM Inspect (GOM GmbH, Braunschweig, Germany) and individually saved as STL files. Thus, virtual models of the entire dental arch and of the two exposed teeth were available for a software-assisted analysis using MeshLab v.1.3.2 (CNR-ISTI; Pisa, Italy) [15].

Using MeshLab, a coordinate system was placed in each STL file. Its system's origin ($x = 0$, $y = 0$, $z = 0$) was positioned in the crown of teeth 11 or 23, respectively (Figure 1), in such a way that its x-axis pointed in the mesio-distal direction, its y-axis in the apical-occlusal direction, and its z-axis in the orovestibular direction.

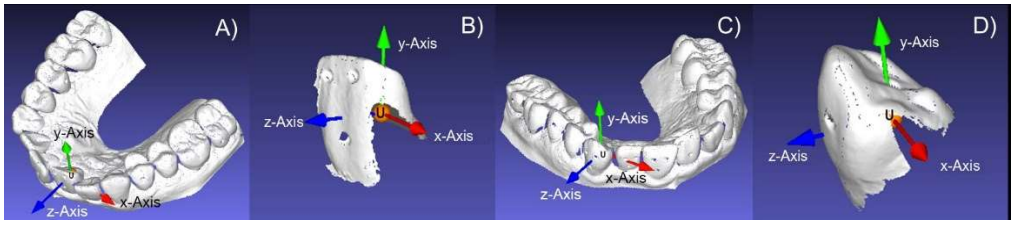

Figure 1. Orientation of the coordinate systems relative to the crown: tooth 11 in the dental arch (**A**) and the separated tooth (**B**); tooth 23 in the dental arch (**C**) and the separated tooth (**D**).

Afterwards, the scans of a processed model and the initial situation of each setup were congruently superimposed using an iterative closest point algorithm (ICP) as implemented in MeshLab's "Align Tool" [15] with the following settings: 1000 samples, target distance was set to "0", and 100 iterations were carried out (Figure 2).

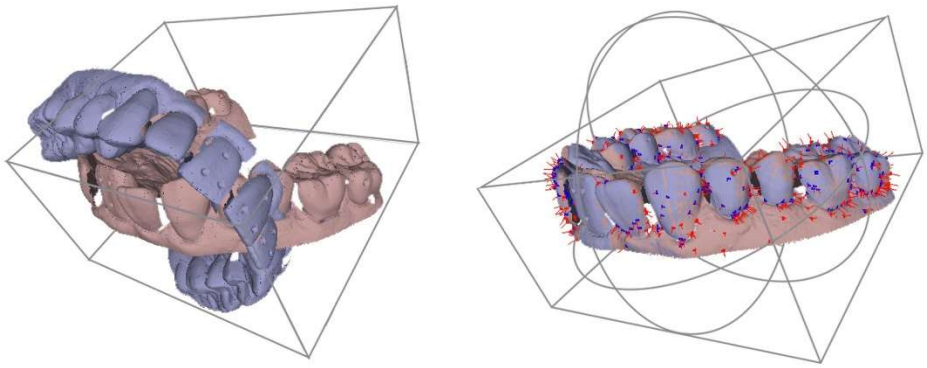

Figure 2. Software-based superimposition of comparison model (orange) and setup model (blue) using MeshLab's "Align Tool" and reference points.

In order to use this algorithm, an initial approximate alignment of the scans was necessary, which was acquired by matching the single coordinate systems of both scans (Figure 3).

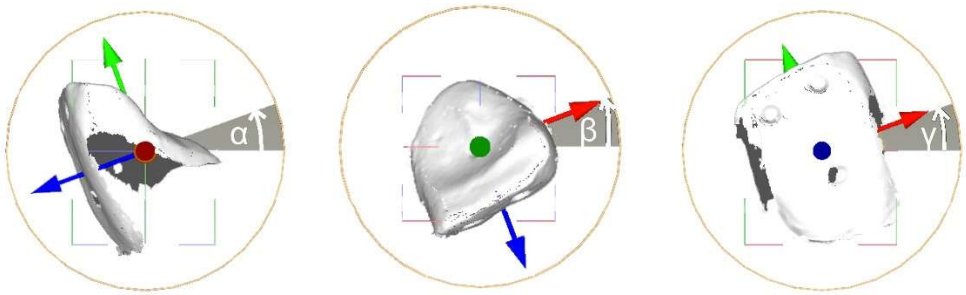

Figure 3. Tooth movement calculation using MeshLab's roto-translation matrix. The rotation angle was calculated with a rotation matrix according to "the roll, pitch and yaw convention" (accuracy ± 0.2 mm).

Based on the inaccuracies of the scanner (±20 µm, according to the manufacturer) and potential errors arising during the superimposition, we estimated the accuracy of the calculated values to be ±0.2 mm.

Descriptive and inferential statistical analyses were conducted using IBM SPSS Statistics 25 (IBM Corp., Armonk, NY, USA). For each combination of tooth, axis of movement, and direction of movement, descriptive statistics were reported as median and interquartile range (IQR). Additionally, mean, standard deviation, range, median, and IQR were tabulated. Due to the sample size (n = 66) and violation of the assumption of a normal distribution, a one-sample Wilcoxon signed-rank test ($p < 0.05$) was used to test whether the median of the samples was equal to the target values (Table 1). Post hoc power analysis was performed using the absolute values of means and standard deviations and a two-tailed Wilcoxon signed-rank test (one-sample case) with $\alpha = 0.05$ and $n = 66$ (G*Power version 3.1.9.6 for Mac) [16]. For rotational movements, the absolute mean difference between prescribed and actual rotation was 5.49 ± 3.28°, and for linear movements, the absolute mean difference was 0.34 ± 0.25 mm. In both cases, the achieved power was >0.99.

Table 1. Descriptive and inferential statistics of 1 mm translational vestibular (Z-axis) movement of tooth 11 and 15° mesial rotation (Y-axis) of tooth 23.

Tooth	Type of Movement	Axis of Movement	Expected Movement	Mean (SD)	Median (IQR)	Range	One-Sample Wilcoxon Signed Rank Test	
							Z	P
11	Rotation (°)	X	0	3.32 (2.17)	2.62 [1.77; 4.35]	−0.08 to 10.10	7.056	<0.001
		Y	0	−1.26 (1.51)	−0.91 [−2.15; 0.05]	−5.16 to 1.64	−5.350	<0.001
		Z	0	−1.39 (1.43)	−1.38 [−2.39; −0.81]	−5.63 to 2.57	−5.810	<0.001
	Translation (mm)	X	0	0.20 (0.13)	0.18 [0.09; 0.28]	−0.01 to 0.58	7.043	<0.001
		Y	0	−0.16 (0.26)	−0.13 [−0.33; 0.02]	−1.02 to 0.37	−4.532	<0.001
		Z	1	1.09 (0.42)	1.04 [0.79; 1.39]	0.25 to 2.26	1.434	0.152
23	Rotation (°)	X	0	−1.13 (4.03)	−0.52 [−3.57; 1.70]	−10.38 to 7.58	−1.607	0.108
		Y	15	9.61 (3.46)	9.76 [7.58; 12.19]	2.58 to 18.04	−6.915	<0.001
		Z	0	5.27 (2.99)	4.47 [2.99; 7.02]	−0.32 to 13.21	7.056	<0.001
	Translation (mm)	X	0	−0.26 (0.19)	−0.26 [−0.37; −0.14]	−0.77 to 0.08	−6.749	<0.001
		Y	0	0.16 (0.27)	0.14 [−0.02; 0.33]	−0.34 to 0.77	4.124	<0.001
		Z	0	−0.88 (0.40)	−1.01 [−1.16; −0.75]	−1.47 to 0.02	−7.024	<0.001

Translational movements in the directions x (mesio-distal), y (apical-occlusal), and z (orovestibular) and rotations around the same axes were analyzed. Values are presented as mean, standard deviation (SD), range, median, and interquartile range (IQR). Statistical significances were determined using the one-sample Wilcoxon signed-rank test with Z statistics and *p*-value reported.

3. Results

3.1. Orovestibular Translation of Tooth 11, 1 mm Vestibular

The overall measured precision of the translational movement covers a very wide range of values from 0.25 mm to 2.26 mm (Table 1). However, the median (and 95% interquartile range) translational movement of tooth 11 was 1.04 mm [0.79 mm; 1.39 mm] in the orovestibular direction, which was close to the proposed value of 1 mm (Z = 1.434; $p = 0.152$) (Table 1, Figure 4).

In addition to the proposed orovestibular translational movement, tooth 11 was also moved 0.18 mm [0.09 mm; 0.28 mm] mesio-distally (*x*-axis) and 0.13 mm [−0.33 mm; 0.02 mm] vertically (*y*-axis) (Table 1). Both unintentional movements were significantly different ($p < 0.001$) from the proposed value (0 mm) and showed a wide range of variation: in the mesio-distal direction between 0.01 mm and 0.58 mm and along the vertical axis between 1.02 mm and 0.37 mm (Table 1).

Additionally, unwanted rotations were introduced into the setup (Table 1). The median rotation around the *x*-axis was 2.62° [1.77; 4.35], around the *y*-axis −0.91° [2.15°; 0.05°], and around the *z*-axis 1.38° [2.39°; −0.81°]. All unintentional rotations were different in statistical significance ($p < 0.001$) from the proposed rotation.

Inter- and intra-technician comparisons revealed large deviations (Figure 4). Some technicians worked with good precision but less trueness. Others worked with good trueness but less precision. While dental technician E exhibited only a slight variation in the proposed setup, dental technician D showed a wider range of variation in the setup.

3.2. Mesio-Rotation Tooth 23, 15°

A median vertical rotational movement around the *y*-axis of 9.76° [7.58°; 12.19°] was applied to tooth 23 (Table 1, Figure 5).

Although only a 15° mesial rotational movement was requested, additional rotational and translational movements of the crown along the *x*-, *y*- and *z*-axes were applied (Table 1). Tooth 23 was moved −0.26 mm [−0.37 mm; −0.14 mm] along the *x*-axis (mesio-distal), 0.14 mm [0.02 mm; 0.33 mm] vertically along the *y*-axis, and −1.01 mm [1.16 mm; −0.75 mm] along the *z*-axis (orovestibular). Most movements significantly deviated ($p < 0.001$) from the proposed setup (Table 1). Additional rotational movements along the *x*-axis (−0.52° [−3.57°; 1.70°]; Z = −1.607, $p = 0.108$) and the *z*-axis (4.47° [2.99°; 7.02°]; Z = 7.056; $p < 0.001$) also occurred.

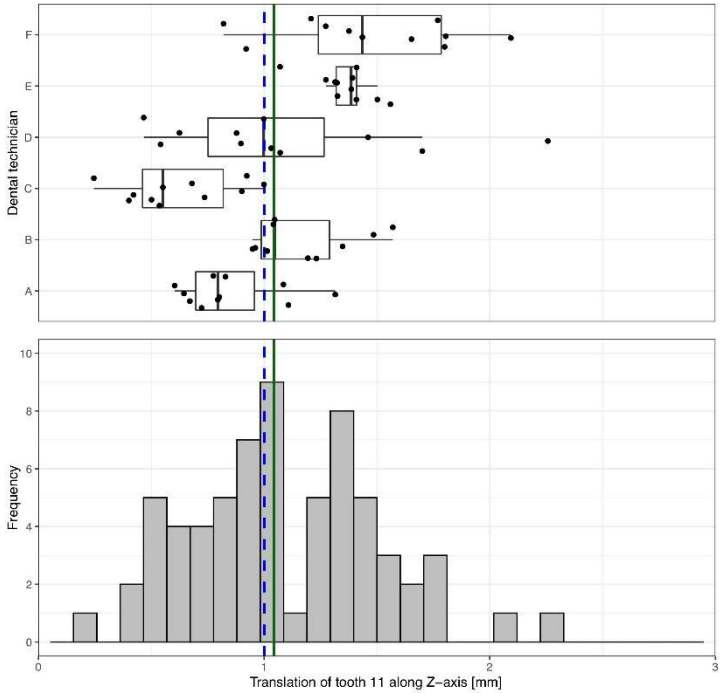

Figure 4. Determined orovestibular (*z*-axis) translational movement of tooth 11. A movement of 1 mm (blue dashed line) was specified. Across all technicians, a median movement of 1.04 mm (green solid line) was achieved. The box-and-whisker plot in the upper panel shows the measured movements of each individual dental technician. The histogram in the lower panel depicts the overall distribution of the measurements.

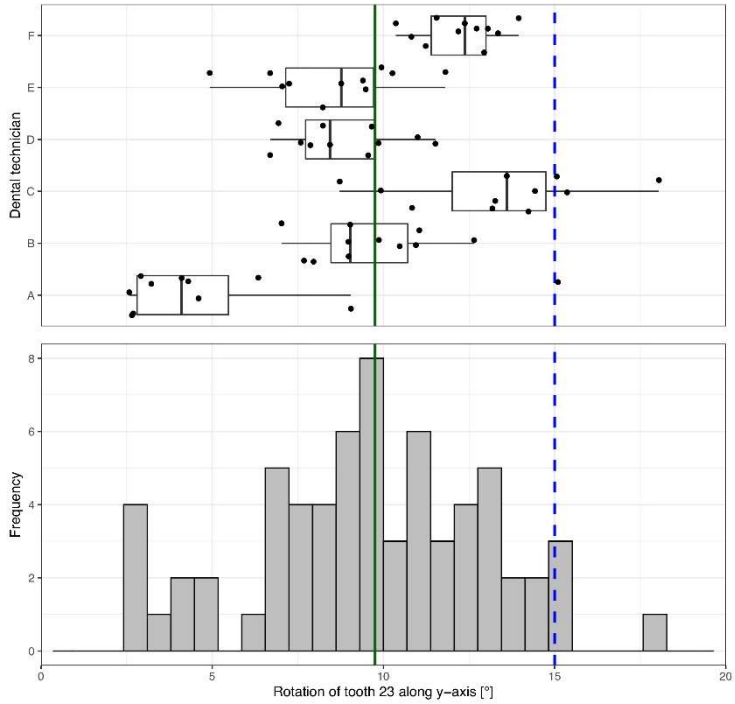

Figure 5. Rotation of tooth 23 around the *y*-axis (apical-occlusal). A rotation of 15° in the mesial direction was specified (blue dashed line); the median achieved across all technicians was 9.76° (green solid line). The box-and-whisker plot in the upper panel shows the measured movements of each individual dental technician. The histogram in the lower panel depicts the overall distribution of the measurements.

Results showed a wide intra- and inter-technician variation of the derotation accomplished (Figure 5). Some technicians worked with precision but less trueness. Others worked with high trueness but less precision. Only two of the dental technicians (A, C) achieved the proposed mesial derotation of 15° for tooth 23 (Figure 5). On average, the tooth was derotated less than specified.

4. Discussion

The results of this study illustrate the different perceptions of each individual dental technician concerning the position of a tooth and the requested movement in the setup. Although the exact final positions of each tooth were defined by the practitioner, the implemented movements of the teeth showed a very high inter- and intra-technician variability.

The consideration of six experienced operators in this study may not be representative of dental technicians as a whole; however, the implementation of planned tooth movements during manual fabrication of aligner setups does not appear to be possible with sufficient precision and reproducibility, as the specified simple tooth movements were not achieved even under study conditions involving training and detailed instructions.

In aligner therapy, the precision of tooth movements in the setup is of utmost importance, as the fit between the aligner and the tooth surface affects the transmission of orthodontic force and the onset of tooth movement [17–19]. Inaccuracies in the setup must be considered in addition to other critically discussed inaccuracies in aligner fabrication, such as model manufacturing [20,21] and thermoforming [22]. In 3D-printed models for aligner therapy, deviations of less than 0.25 mm compared to the virtual models are necessary [23]. After thermoforming, the resulting gap width between tooth surfaces and aligners was found to range between 0.10 mm and 0.35 mm, depending on the intraoral region and aligner material [19]. Since deviations as small as 0.10 mm may be sufficient to affect the predictability of tooth movement [17], the introduction of additional variability through manual setups seems impossible. Rather, variations due to aligner fabrication should be reflected and accounted for in the setup, for example, by adjusting movement staging in specific regions [17].

Nevertheless, the precision of the individual tooth movements should not be confounded with the overall quality of the setup. While individual tooth movements (translation, rotation) can be precisely and reproducibly executed in digital setups [24], the overall quality of the setup depends on the total tooth movements performed and relies on the operator for both manual and digital setup fabrication. For example, significant differences in the ABO OGS scores between two digital setups of the same original models made by one clinician were found [25].

The precision of the tooth movements is also relevant with regard to the forces occurring during aligner therapy. Experimental studies show that, even with small movement steps in the setup, forces of varying degrees occur. These forces vary depending on the individual malocclusion, step size, material, and aligner extension [26,27]. It may therefore be assumed, that the deviations from the desired movement described in this study are likely to result in undesirable or uncontrolled forces and moments due to the imprecision of the manual setup. The rotation of tooth 23 (15° rotation around *y*-axis) was accomplished with a median rotation of 9.76° (range: 2.58° to 18.04°). The results for the translational, orovestibular movement of tooth 11 show a wide range of 0.25–2.26 mm (i.e., a difference of 2.01 mm), which is also not acceptable. It is out of the question that smaller steps are clinically advisable and more effective in aligner therapy [28,29]. In order to reflect the maximum range of translational tooth movement within the manual setup, this study applied a target step of 1 mm, which is within the range given by some manufacturers [30]. A similar approach was used for the rotational movement [31]. We expect that implementing smaller, more difficult-to-control movements would result in an even lower precision in the manual setup process. Such sizeable deviations in the setup model can lead to higher forces [26] or a retardation of tooth movement [32,33]. Excessive forces during orthodontic tooth movement may in turn induce external resorption [34–37].

According to our results, a manual setup can only guarantee a limited predictability of clinical tooth movement. Our study shows that it is difficult to manually move a tooth along one axis without simultaneously inducing movements along the other axes. The non-prescribed movements even exceeded a usual clinical staging step of 0.5 mm or 3° proposed for this technique [9,27,30]. A mean non-prescribed rotation of 3.32° was observed in the translational movement of tooth 11 and a mean non-prescribed translation of −0.88 mm in the rotational movement of tooth 23. This is in contrast to the fabrication of digital setups, where tooth movements can be performed with a high level of accuracy using a uniform coordinate system [24]. Additionally, the uniform coordinate system allows for a reliable superimposition and precise comparison of tooth movements without the necessity of coordinate transformation, regardless of whether it is applied to a scanned plaster model or an intraoral scan.

The extent to which aligner setups can be clinically realized remains to be investigated, especially with regard to the overall quality of the aligner setup and case-related staging.

5. Clinical Implications

Although various aligner manufacturers such as Invisalign® (Align Technology), CA® (Scheu-Dental), or Essix® (Dentsply) rely on the use of computer-aided technology and digital setups, the use of manual setups for the in-house fabrication of aligner models represents a cost-effective alternative method that does not require intraoral scanners and 3D printers [9,30,38,39].

In fact, to date, there are no available accuracy data to oppose the use of manual setups for aligner therapy. One available study even supported the clinical acceptability of manual setups, although only intra-arch and inter-arch measurements were considered [14]. In contrast, the results of the present study suggest that manual setups may not be suitable for the fabrication of aligners with respect to the high variability of results regarding individual tooth movements. Consequently, the manual approach for orthodontic aligner setups should be critically questioned.

6. Conclusions

In manual setups performed by dental technicians, tooth movements rarely achieved precise specifications and exhibited unwanted movements in all directions, for both translations and rotations. Based on the wide intra- and inter-technician variability and deviation from the measured values, the manual fabrication of setups should not be favored for aligner therapy.

Author Contributions: Conceptualization, A.W., T.S.; methodology, U.B., S.M.H. and H.S.; software, S.M.H., T.S.; validation, U.B. and T.S.; formal analysis, L.H.; investigation, S.M.H.; data curation, H.S. and L.H.; writing—original draft preparation, H.S. and L.H.; writing—review and editing, H.S. and L.H.; visualization, H.S. and L.H.; supervision, A.W.; All authors have read and agreed to the published version of the manuscript.

Funding: This research received no external funding.

Institutional Review Board Statement: Not applicable.

Informed Consent Statement: Not applicable.

Data Availability Statement: The original data set can be provided upon request.

Acknowledgments: The authors wish to thank the dental technicians for their participation in this study and for fabricating the setup models.

Conflicts of Interest: The authors declare no conflict of interest.

References

1. Buschang, P.H.; Shaw, S.G.; Ross, M.; Crosby, D.; Campbell, P.M. Comparative time efficiency of aligner therapy and conventional edgewise braces. *Angle Orthod.* **2014**, *84*, 391–396. [CrossRef] [PubMed]
2. Chisari, J.R.; McGorray, S.P.; Nair, M.; Wheeler, T.T. Variables affecting orthodontic tooth movement with clear aligners. *Am. J. Orthod. Dentofac. Orthop.* **2014**, *145*, S82–S91. [CrossRef] [PubMed]
3. Weir, T. Clear aligners in orthodontic treatment. *Aust. Dent. J.* **2017**, *62* (Suppl. 1), 58–62. [CrossRef]
4. Zheng, M.; Liu, R.; Ni, Z.; Yu, Z. Efficiency, effectiveness and treatment stability of clear aligners: A systematic review and meta-analysis. *Orthod. Craniofac. Res.* **2017**, *20*, 127–133. [CrossRef] [PubMed]
5. Rossini, G.; Parrini, S.; Castroflorio, T.; Deregibus, A.; Debernardi, C.L. Efficacy of clear aligners in controlling orthodontic tooth movement: A systematic review. *Angle Orthod.* **2015**, *85*, 881–889. [CrossRef] [PubMed]
6. Simon, M.; Keilig, L.; Schwarze, J.; Jung, B.A.; Bourauel, C. Treatment outcome and efficacy of an aligner technique–regarding incisor torque, premolar derotation and molar distalization. *BMC Oral Health* **2014**, *14*, 68. [CrossRef]
7. Kravitz, N.D.; Kusnoto, B.; BeGole, E.; Obrez, A.; Agran, B. How well does Invisalign work? A prospective clinical study evaluating the efficacy of tooth movement with Invisalign. *Am. J. Orthod. Dentofac. Orthop.* **2009**, *135*, 27–35. [CrossRef]
8. Sterental, R. Staging. In *The Invisalign System*; Tuncay, O.C., Ed.; Quintessence: New Malden, UK, 2006; pp. 105–113.
9. Kim, T.W.; Echarri, P. Clear aligner: An efficient, esthetic, and comfortable option for an adult patient. *World J. Orthod.* **2007**, *8*, 13–18.
10. Sheridan, J.J.; Ledoux, W.; McMinn, R. Essix appliance: Minor tooth movement with divots and windows. *J. Clin. Orthod.* **1994**, *28*, 659–663.
11. Barbagallo, L.J.; Shen, G.; Jones, A.S.; Swain, M.V.; Petocz, P.; Darendeliler, M.A. A novel pressure film approach for determining the force imparted by clear removable thermoplastic appliances. *Ann. Biomed. Eng.* **2008**, *36*, 335–341. [CrossRef]
12. Fleming, P.S.; Marinho, V.; Johal, A. Orthodontic measurements on digital study models compared with plaster models: A systematic review. *Orthod. Craniofac. Res.* **2011**, *14*, 1–16. [CrossRef] [PubMed]
13. Buschang, P.H.; Ross, M.; Shaw, S.G.; Crosby, D.; Campbell, P.M. Predicted and actual end-of-treatment occlusion produced with aligner therapy. *Angle Orthod.* **2015**, *85*, 723–727. [CrossRef] [PubMed]
14. Im, J.; Cha, J.Y.; Lee, K.J.; Yu, H.S.; Hwang, C.J. Comparison of virtual and manual tooth setups with digital and plaster models in extraction cases. *Am. J. Orthod. Dentofac. Orthop.* **2014**, *145*, 434–442. [CrossRef] [PubMed]
15. Cignoni, P.; Callieri, M.; Corsini, M.; Dellepiane, M.; Ganovelli, F.; Ranzuglia, G. MeshLab: An Open-Source Mesh Processing Tool. In *Eurographics Italian Chapter Conference*; Scarano, V., De Chiara, R., Erra, U., Eds.; The Eurographics Association: Geneva, Switzerland, 2008; pp. 129–136.
16. Faul, F.; Erdfelder, E.; Lang, A.G.; Buchner, A. G*Power 3: A flexible statistical power analysis program for the social, behavioral, and biomedical sciences. *Behav. Res. Methods* **2007**, *39*, 175–191. [CrossRef]
17. Palone, M.; Longo, M.; Arveda, N.; Nacucchi, M.; Pascalis, F.; Spedicato, G.A.; Siciliani, G.; Lombardo, L. Micro-computed tomography evaluation of general trends in aligner thickness and gap width after thermoforming procedures involving six commercial clear aligners: An in vitro study. *Korean J. Orthod.* **2021**, *51*, 135–141. [CrossRef]
18. Lombardo, L.; Arreghini, A.; Ramina, F.; Huanca Ghislanzoni, L.T.; Siciliani, G. Predictability of orthodontic movement with orthodontic aligners: A retrospective study. *Prog. Orthod.* **2017**, *18*, 35. [CrossRef] [PubMed]
19. Mantovani, E.; Castroflorio, E.; Rossini, G.; Garino, F.; Cugliari, G.; Deregibus, A.; Castroflorio, T. Scanning electron microscopy evaluation of aligner fit on teeth. *Angle Orthod.* **2018**, *88*, 596–601. [CrossRef]
20. Kim, S.Y.; Shin, Y.S.; Jung, H.D.; Hwang, C.J.; Baik, H.S.; Cha, J.Y. Precision and trueness of dental models manufactured with different 3-dimensional printing techniques. *Am. J. Orthod. Dentofac. Orthop.* **2018**, *153*, 144–153. [CrossRef]
21. Tomita, Y.; Uechi, J.; Konno, M.; Sasamoto, S.; Iijima, M.; Mizoguchi, I. Accuracy of digital models generated by conventional impression/plaster-model methods and intraoral scanning. *Dent. Mater. J.* **2018**, *37*, 628–633. [CrossRef]
22. Koenig, N.; Choi, J.Y.; McCray, J.; Hayes, A.; Schneider, P.; Kim, K.B. Comparison of dimensional accuracy between direct-printed and thermoformed aligners. *Korean J. Orthod.* **2022**, *online ahead of print*. [CrossRef]
23. Jaber, S.T.; Hajeer, M.Y.; Khattab, T.Z.; Mahaini, L. Evaluation of the fused deposition modeling and the digital light processing techniques in terms of dimensional accuracy of printing dental models used for the fabrication of clear aligners. *Clin. Exp. Dent. Res.* **2021**, *7*, 591–600. [CrossRef]
24. Abduo, J.; Elseyoufi, M. Accuracy of intraoral scanners: A systematic review of influencing factors. *Eur. J. Prosthodont. Restor. Dent.* **2018**, *26*, 101–121. [CrossRef] [PubMed]
25. Fabels, L.N.; Nijkamp, P.G. Interexaminer and intraexaminer reliabilities of 3-dimensional orthodontic digital setups. *Am. J. Orthod. Dentofac. Orthop.* **2014**, *146*, 806–811. [CrossRef] [PubMed]
26. Hahn, W.; Zapf, A.; Dathe, H.; Fialka-Fricke, J.; Fricke-Zech, S.; Gruber, R.; Kubein-Meesenburg, D.; Sadat-Khonsari, R. Torquing an upper central incisor with aligners–acting forces and biomechanical principles. *Eur. J. Orthod.* **2010**, *32*, 607–613. [CrossRef] [PubMed]
27. Gao, L.; Wichelhaus, A. Forces and moments delivered by the PET-G aligner to a maxillary central incisor for palatal tipping and intrusion. *Angle Orthod.* **2017**, *87*, 534–541. [CrossRef]
28. Paquette, D.E.; Colville, C.; Wheeler, T. Clear Aligner Treatment. In *Orthodontics—Current Principles and Techniques*, 6th ed.; Graber, L.W., Vanarsdall, R.L., Jr., Vig, K.W.L., Huang, G.J., Eds.; Elsevier: St. Louis, MO, USA, 2017; pp. 778–811.

29. Iwasaki, L.R.; Haack, J.E.; Nickel, J.C.; Morton, J. Human tooth movement in response to continuous stress of low magnitude. *Am. J. Orthod. Dentofac. Orthop.* **2000**, *117*, 175–183. [CrossRef]
30. Echarri, P. *Clear-Aligner*; Editoral Ripano S.A.: Madrid, Spain, 2013.
31. Elkholy, F.; Mikhaiel, B.; Schmidt, F.; Lapatki, B.G. Mechanical load exerted by PET-G aligners during mesial and distal derotation of a mandibular canine: An in vitro study. *J. Orofac. Orthop.* **2017**, *78*, 361–370. [CrossRef]
32. Alikhani, M.; Chou, M.Y.; Khoo, E.; Alansari, S.; Kwal, R.; Elfersi, T.; Almansour, A.; Sangsuwon, C.; Al Jearah, M.; Nervina, J.M.; et al. Age-dependent biologic response to orthodontic forces. *Am. J. Orthod. Dentofac. Orthop.* **2018**, *153*, 632–644. [CrossRef]
33. Tepedino, M.; Paoloni, V.; Cozza, P.; Chimenti, C. Movement of anterior teeth using clear aligners: A three-dimensional, retrospective evaluation. *Prog. Orthod.* **2018**, *19*, 9. [CrossRef]
34. Reitan, K. Initial tissue behavior during apical root resorption. *Angle Orthod.* **1974**, *44*, 68–82. [CrossRef]
35. Dudic, A.; Giannopoulou, C.; Meda, P.; Montet, X.; Kiliaridis, S. Orthodontically induced cervical root resorption in humans is associated with the amount of tooth movement. *Eur. J. Orthod.* **2017**, *39*, 534–540. [CrossRef]
36. Wishney, M. Potential risks of orthodontic therapy: A critical review and conceptual framework. *Aust. Dent. J.* **2017**, *62* (Suppl. 1), 86–96. [CrossRef] [PubMed]
37. Gandhi, V.; Mehta, S.; Gauthier, M.; Mu, J.; Kuo, C.L.; Nanda, R.; Yadav, S. Comparison of external apical root resorption with clear aligners and pre-adjusted edgewise appliances in non-extraction cases: A systematic review and meta-analysis. *Eur. J. Orthod.* **2021**, *43*, 15–24. [CrossRef] [PubMed]
38. Kim, T.W.; Wilhelmy, B.; Gaugel, H. CLEAR-ALIGNER—An Alternative Orthodontic Appliance. Available online: http://www.andersson-gaugel.de/pdf/SD_Clear-Aligner_klein.pdf (accessed on 21 April 2022).
39. Proffit, W.R.; Fields, H.W.; Larson, B.; Sarver, D.M. *Contemporary Orthodontics—E-Book*; Elsevier Health Sciences: Philadelphia, PA, USA, 2018.

Popova *et al. BMC Oral Health* (2023) 23:274
https://doi.org/10.1186/s12903-023-02984-2

BMC Oral Health

RESEARCH Open Access

Influence of growth structures and fixed appliances on automated cephalometric landmark recognition with a customized convolutional neural network

Teodora Popova[1], Thomas Stocker[1], Yeganeh Khazaei[2], Yoana Malenova[3], Andrea Wichelhaus[1] and Hisham Sabbagh[1*]

Abstract

Background One of the main uses of artificial intelligence in the field of orthodontics is automated cephalometric analysis. Aim of the present study was to evaluate whether developmental stages of a dentition, fixed orthodontic appliances or other dental appliances may affect detection of cephalometric landmarks.

Methods For the purposes of this study a Convolutional Neural Network (CNN) for automated detection of cephalometric landmarks was developed. The model was trained on 430 cephalometric radiographs and its performance was then tested on 460 new radiographs. The accuracy of landmark detection in patients with permanent dentition was compared with that in patients with mixed dentition. Furthermore, the influence of fixed orthodontic appliances and orthodontic brackets and/or bands was investigated only in patients with permanent dentition. A t-test was performed to evaluate the mean radial errors (MREs) against the corresponding SDs for each landmark in the two categories, of which the significance was set at $p < 0.05$.

Results The study showed significant differences in the recognition accuracy of the Ap-Inferior point and the Is-Superior point between patients with permanent dentition and mixed dentition, and no significant differences in the recognition process between patients without fixed orthodontic appliances and patients with orthodontic brackets and/or bands and other fixed orthodontic appliances.

Conclusions The results indicated that growth structures and developmental stages of a dentition had an impact on the performance of the customized CNN model by dental cephalometric landmarks. Fixed orthodontic appliances such as brackets, bands, and other fixed orthodontic appliances, had no significant effect on the performance of the CNN model.

Keywords Cephalometry, Convolutional neural network, Deep learning, Orthodontics, Cephalometric landmarks

*Correspondence:
Hisham Sabbagh
hisham.sabbagh@med.uni-muenchen.de
Full list of author information is available at the end of the article

© The Author(s) 2023. **Open Access** This article is licensed under a Creative Commons Attribution 4.0 International License, which permits use, sharing, adaptation, distribution and reproduction in any medium or format, as long as you give appropriate credit to the original author(s) and the source, provide a link to the Creative Commons licence, and indicate if changes were made. The images or other third party material in this article are included in the article's Creative Commons licence, unless indicated otherwise in a credit line to the material. If material is not included in the article's Creative Commons licence and your intended use is not permitted by statutory regulation or exceeds the permitted use, you will need to obtain permission directly from the copyright holder. To view a copy of this licence, visit http://creativecommons.org/licenses/by/4.0/. The Creative Commons Public Domain Dedication waiver (http://creativecommons.org/publicdomain/zero/1.0/) applies to the data made available in this article, unless otherwise stated in a credit line to the data.

Introduction

Cephalometric analysis involves identifying common landmarks, quantifying the various relationships between them, and diagnosing the correlations in a patient's craniofacial morphology. However, during the cephalometric tracing, sources of error or inter-observer variability may lead to low reproducibility of the observations [1–5]. Since the process of manually placing the landmarks in a cephalogram is also time consuming [6, 7], several studies have proposed frameworks using Deep Learning and Convolutional Neural Networks (CNN) for an automatic landmark recognition in lateral cephalometric radiographs [8–20]. One of the first publications about an automatic system for cephalometric landmark detection was published in 1986 [7], describing a knowledge-based line tracker guided by a reference map. Subsequently, an algorithm-based gray-scale mathematical morphology was presented [21]. In 2014-2015, several strategies for cephalometric landmark detection were introduced after a scientific challenge proposal by the International Symposium on Biomedical Imaging (ISBI). The game-theoretic landmark detection and random forest-based shape model [22] and the random forest regression-voting model [23] both performed favorably in the challenge. Recent studies focused on investigating the performance and reliability of different Convolutional Neural Network (CNN) models for cephalometric analysis [10, 15, 24–28]. As automated cephalometric software platforms are now available from different companies (e.g. OneCeph, Hyderabad, India; CellmatIQ, Hamburg, Germany; WebCeph, Republic of Korea; AudaxCeph, Ljubljana, Slovenia) more recent studies have focused on evaluating their accuracy [15, 29–33]. While the benefits of artificial intelligence in recognizing cephalometric landmarks have been acknowledged [34, 35], the need for further research regarding its accuracy in different clinical settings was recognized [36–38]. Previous studies tested the frameworks only on radiographs of patients with permanent dentition [24, 30, 33] or did not mention these characteristic of the datasets at all [15–17, 25, 26]. Despite the promising potential of automatic landmark recognition, conclusions and research regarding some clinical aspects are still lacking. Hence, this study aims to investigate the influence of growth structures, such as tooth germs in mixed dentitions, and fixed appliances on automated cephalometric landmark recognition.

In particular, the null hypothesis that developmental stages of a dentition, fixed orthodontic appliances or other dental appliances do not affect the accuracy of a customized artificial model for automatic detection of cephalometric landmarks shall be tested. For these purposes, a CNN model with commonly used architecture [39] was developed and the overall accuracy of the model and its validity was evaluated. Finally, the CNN was applied to investigate differences between the distinct patient groups.

Materials and methods

Study design

This retrospective diagnostic study was approved by the LMU Ethics Commitee (Ref. No 19–863). Cephalometric radiographs were obtained from the archives of the Department of Orthodontics and Dentofacial Orthopedics, University Hospital, LMU Munich. For this study, a Convolutional Neural Network (CNN) was developed for automatic recognition of cephalometric landmarks. The accuracy of landmark recognition in patients with permanent dentition was compared with that of patients with mixed dentition (both groups included radiographs without fixed orthodontic appliances). In addition, this study investigated the influence of fixed orthodontic appliances and orthodontic brackets and/or bands among patients with permanent dentition only. For reporting this study, the guidelines of the Checklist for Artificial Intelligence in Dentistry [40] and the Standards for Reporting of Diagnostic Accuracy Studies (STARD) [41] were followed.

Data, sampling and references standard

The patient sample was intended to be as comprehensive as possible, therefore exclusion criteria were limited to craniofacial anomalies and to images of poor quality and/or incorrect positioning of the skull, which might affect landmark recognition. Images of growing and adult patients with or without fixed orthodontic appliances, dental restorations and osteosynthesis plates were included. The distribution of data by age, sex and ethnicity are shown in Table 1. All included radiographs were obtained prior to the study from the same X-ray unit (Orthophos, Sirona, Germany) and had an image size of 2020×2012 pixels, where one pixel equals to a square

Table 1 Distribution of data by age, sex and ethnicity in the training and test dataset

	Train Dataset		Test Dataset	
	n		*n*	
age < 6	10	2%	3	1%
6 < age < 13	149	35%	233	51%
age > 13	271	63%	224	48%
female	203	47%	250	54%
male	227	53%	210	46%
caucasians	416	97%	452	98%
non-caucasians	14	3%	8	2%

with a length of 0.1 mm on each side and an area of 0.01 mm^2. Out of 1151 images, 251 images were excluded applying the exclusion criteria, 430 were included in the training dataset and 460 images were used as the test dataset.

Cephalometric analysis included 16 key landmarks for the orthodontic diagnosis of the skeletal and dental anatomy. Since soft tissue cephalometric landmarks are rarely located in the proximity of developing tooth germs or fixed orthodontic appliances, they were not considered in the present study. The positions of 16 cephalometric reference points (Table 2) were manually identified by two examiners (last year orthodontic residents), who traced a maximum of 10 lateral cephalograms a day. The annotated radiographs were revised by an orthodontic specialist (10 years of experience) who verified a maximum of 5 images daily, discrepancies were then resolved by consensus. The verified dataset was used as a reference for the training, testing and validation of the CNN model. The verified dataset was used as a reference for the training, testing and validation of the CNN model.

Training dataset

The training data set consisted of a total of 430 images including patients with both permanent dentition and mixed dentition, as well as radiographs with fixed orthodontic appliances, orthodontic brackets and/or bands, osteosynthesis plates, implants, dental prosthetic restorations and root canal treatments. The images were divided into training images (90%) and validation images (10%). The training images are used to adjust and optimize the model so that the CNN "learns" how to perform its task, while the validation images provide an objective evaluation of the model and its performance. Sets of input data were created which consisted of cephalometric radiographs and a corresponding pair of coordinates (X, horizontal; Y, vertical) indicating the exact location of each landmark.

Test dataset

A total of 460 cephalometric radiographs were used as the test dataset. The performance of the developed CNN was tested on a versatile data consisting of images with various radiographic features (such as fixed orthodontic appliances, osteosynthesis plates and others) and anatomical structures of patients at different stages of growth. The data were divided into independent subgroups to investigate the impact of the distinctive characteristics (Table 3). Radiographs of patients with mixed dentition and fixed orthodontic appliances were not included in the comparative analysis between the subgroups themselves. However, since they were part of the test data, they were included in the overall assessment of performance on the model. Similar to the training datasets, an input was created consisting of the cephalometric radiograph and a corresponding coordinate pair (X, Y) indicating the location of each landmark.

Data preparation and processing

For each case, one lateral cephalogram without annotations of reference points and one with identified

Table 2 Abbreviations and definitions of the cephalometric landmarks used in the study

Abbreviation	Landmark	Definition
A-Point	Subspinale	Most concave point on the anterior contour of the maxillary alveolar process in the midsagittal plane
Ap1	Apex superior	Furthest apical point of the upper central incisors
Ap$\bar{1}$	Apex inferior	Furthest apical point of the lower central incisors
ANS	Anterior nasal spine	The most anterior point of the anterior nasal spine in the median sagittal plane
Art	Articulare	The intersection of the inferior surface of the cranial base and the posterior border of the ascending rami of the mandible
B-Point	Supramentale	Most concave point on the anterior contour of the mandibular alveolar process in the midsagittal plane
Ba	Basion	Most anterior point on foramen magnum
Me	Menton	The lowest point on the mandibular symphysis in the midline
Is1	Incision Superior	The tip of the incisal edge of the most labially positioned upper central incisors
Is$\bar{1}$	Incision Inferior	The tip of the incisal edge of the most labially positioned lower central incisors
N	Nasion	The most anterior point on frontonasal suture
Pog	Pogonion	The most ventral point of the bony chin in the median sagittal plane
PNS	Posterior nasal spine	The intersection of a continuation of the anterior wall of the pterygopalatine fossa and the floor of the nose
S	Sella	Midpoint of Sella turcica
T1	Gonion superiorus	Most posterior point of posterior border of ramus ascendens
T2	Gonion inferius	Most inferior point of gonion area

Table 3 Detailed Summary and distribution of the dataset used for the training and testing of the CNN

Subgroup characteristics			Train Dataset		Test Dataset	
No fixed orthodontic appliances	Permanent Dentition	Group I/1	175	40%	141	31%
No fixed orthodontic appliances	Mixed Dentition	Group I/2	110	26%	164	36%
Orthodontic brackets and/or bands and other fixed orthodontic appliances	Permanent Dentition	Group II	134	31%	135	29%
Orthodontic brackets and/or bands and other fixed orthodontic appliances	Mixed Dentition	Not included in the comparative analysis	11	3%	20	4%
Total Number of images (n)			***430***		***460***	

as well as validated cephalometric landmarks were manually exported from the database. These were anonymised, labelled as a pair, and stored in two folders. For each case, the X and Y coordinates of all marked cephalometric reference points were automatically exported from the annotated X-ray image using a custom Python script and stored in a text file (.txt) labelled to match the corresponding case.

Subsequently, the text files were automatically filtered so that only a single pair of coordinates corresponding to a specific reference point was stored in a text file. Since the location of each reference point is distinct, a Python script was written for the extraction procedure for each of the 16 mentioned landmarks. Finally, the plain cephalograms and the text document (.txt) storing a pair of coordinates were used as input for the CNN models, dealing with each point independently.

The evaluation of the accuracy of the CNN model was also performed automatically using a Python script. By this means, the trained model was accessed and applied for the detection of the specific cephalometric point. The absolute difference between the predicted point (the point identified by the CNN) and the referenced point (the point positioned by the examiner) was determined. The Results were then imported into an Excel file (Microsoft Excel for Office 365, version 16.60, Microsoft Corporation, Redmond, WA, USA) where further statistical analysis was performed.

Model, model parameters, training and evaluation

A deep learning model, more specifically a CNN was constructed using the open-source deep learning frameworks Keras (Version 2.2.4, François Chollet) [42] and TensorFlow (Version 1.14.0, Google Brain Team) [43] accessed from a Python (Python Version 3.5.6, Python Software Foundation, Beaverton, USA) script running on NVIDIA GeForce RTX 2080 graphics card (NVIDIA, Santa Clara, CA, USA) for each of the previously mentioned landmarks (Table 2).

The model had a commonly used CNN Architecture for image classification [39], with some custom modification. In the following, the essential components and the architecture of the framework are described as shown in Fig. 1.

The input for the training of the proposed network involved a lateral cephalogram from the training dataset and a corresponding file containing the location for the cephalometric landmarks as pairs of X and Y coordinates. Consequently, the output of the CNN was a predicted pair of X, Y coordinates indicating the position of the landmark. For example, the Training Set for the Sella Point included 430 unmarked cephalograms and 430 corresponding text files containing the position of the landmark written as a pair of X and Y coordinates. This data was processed by a convolutional layer, which detects specific features and patterns. After a feature is detected, the information is compressed and passed to the next layers of the network. This process, which is responsible for pattern recognition, is called filtering and the filters used are adjusted throughout the learning process to benefit the performance of the machine learning model. The number of filters varies for each layer, with the first layer having 30 filters, the second 60 filters continuing in ascending order for each additional layer. The learning rate was set to 10^{-4}, batch size at 32 and as the number of layers was not consistent for each landmark. A detailed summary of the model for each point is provided in Supplementary file 1, code and data are available at Open Data LMU Platform under https://doi.org/10.5282/ubm/data.359. The performance in this model was measured with a mean squared error (MSE) cost function that quantifies the error between the real coordinates(input) of the landmark and the predicted ones(output).

In order to increase the capacity of the model, a non-linear activation function was applied after each convolutional layer (Fig. 1). To avoid the vanishing gradient problem [30] and accelerate the training speed of the neural network, a rectified linear activation function ReLU ($f(x)=\max(0,x)$) or Leaky ReLU ($f(x)=1(x<0)(\alpha x)+1(x>=0)(x)$) where $\alpha=0.5$, depending on the outcome, was chosen. Further, a maximum pooling

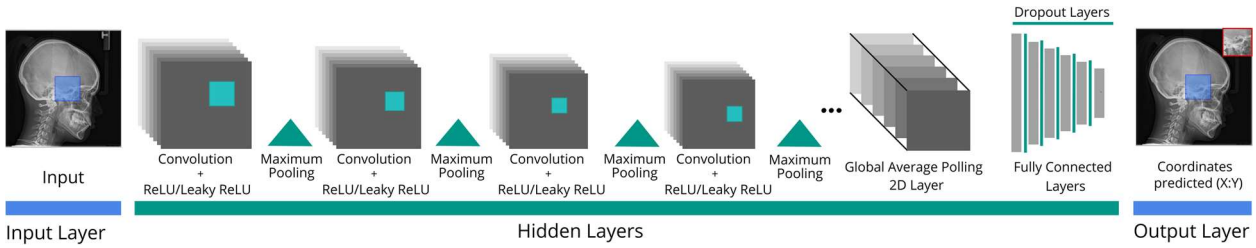

Fig. 1 The architecture of the CNN proposed for automated cephalometric landmark recognition

approach was used, which calculates the maximum value in each feature map and highlights the most frequently occurring feature in the pathway (Fig. 1).

Following the stack of convolutional layers, a global average polling 2D layer was added. This layer reduced the dimensionality of the learned feature maps by averaging over the special dimensions of the output and yielding a fixed-size vector representation, which can be processed with standard fully-connected layers.

Note, that the described composite neural architecture is comparatively large. A major problem in large neural networks is overfitting, that is, the danger of overspecialization to the training set and the resulting limited generalizability to new (upcoming) data. Regularization is a common technique to prevent overfitting and thus poor generalization performance of deep neural networks [44] To regularize the used model, dropout layers were added between the fully-connected layers of the neural network architecture (Fig. 1). Dropout is a commonly used regularization technique by which the system takes out a portion of the trainable parameters and temporarily removes them from the network, along with all incoming and outgoing connections [45].

Additionally, to optimize the performance of the model, each point was considered separately, and a modified CNN was created for each landmark. This made it possible to adapt the number of convolutional layers, filters, dropout layers, and activation functions for each landmark depending on the complexity and variety of the features, resulting in a different neural expert for each landmark. This study relied on a standard CNN architecture [39], which showed high accuracy after optimization. Therefore, an extensive hyperparameter search for neural network parameters was not conducted. However, a grid search was performed over a reasonable range of learning rates and optimizer sets without observing noticeable performance differences.

Validation

In order to quantify the utility of the model, the absolute difference between the predicted point (the point identified by the CNN) and the referenced point (the point positioned by the examiner) was determined along the X-axis (Δx_i) and correspondingly, along the Y-axis (Δy_i). This value was defined as Distance Error (DE) $D_i = \sqrt{\Delta x_i^2 + \Delta y_i^2}$ and it was measured across the entire dataset of test images. To be consistent with the evaluation metrics of previous studies [9, 10, 23, 37, 46], the mean radial error (MRE) along with Standard Deviation (SD) for each landmark was determined as follows:

$$MRE = \frac{\sum_{i=1}^{n} Di}{n}$$

and $SD = \sqrt{\frac{\sum_{i=1}^{n}\left(Di - \sqrt{\Delta x^2 - \Delta y^2}\right)^2}{n-1}}$ where n is the total amount of images.

The Successful Detection Rate (SDR), which indicates the percentage of correctly detected reference points in different precision ranges: $SDR_z = \frac{numberofaccuratedetection}{numberofdetection} \times 100\%$ was computed, specifying four types of accuracy ranges: $z =$ 2.0 mm, 2.5 mm, 3.0 mm, 4.0 mm.

It should be considered that the deviation of the distance error along a certain axis has greater importance for some points. For example, the accuracy of the B-Point along the X-axis is more significant as it marks the position of the mandible in the sagittal plane. Hence, the distribution of errors in the horizontal and vertical planes were considered separately.

Statistical analysis

Mean radial errors and standard deviations of the 16 used orthodontic cephalometric reference points were collected in an excel file (Microsoft Excel for Office 365, Version 16.60, Microsoft Corporation, Redmond, WA, USA). These numbers were categorized in two main comparing groups:

I No fixed orthodontic appliances—Permanent dentition XY – Error (Group I/1) versus No Fixed orthodontic appliances—Mixed dentition XY – Error (Group I/2)

II No fixed orthodontic appliances—Permanent dentition XY – Error (Group I/1) versus Orthodontic brackets and/or bands and other fixed orthodontic appliances—Permanent dentition XY – Error (Group II)

A t-test was applied to compare MREs with their corresponding SDs for each landmark in their two categories, to determine whether the means of these two groups are equal to each other. For this purpose, a t-test was run for both abovementioned categories (Table 4), separately for all the 16 points (an overall of 32 tests).

Table 4 Equation applied for statistical evaluation

$$t = \frac{\overline{x_1} - \overline{x_2}}{\sqrt{\frac{s_1^2}{n_1} + \frac{s_2^2}{n_2}}}$$

t: t-value

$\overline{x_1}$: Mean value of the first group

$\overline{x_2}$: Mean value of the second group

n_1 : Size of the first group

n_2: Size of the second group

s_1: Standard deviation of the first group

s_2: Standard deviation of the second group

All data were analyzed using R software (Version R-4.1.1, R Development Core Team, Vienna, Austria). Statistical significance was set at a p-value < 0.05.

Results

The results for the different groups are presented in Table 5. Statistically significant differences were observed in the recognition accuracy of the Ap-Inferior point and the Is-Superior point between patients with permanent dentition (I/1) and mixed dentition (I/2), both without fixed orthodontic appliances. No statistically significant differences were found in the recognition process between patients without fixed orthodontic appliances (I/1) and patients with orthodontic brackets and/or bands and/or other fixed orthodontic appliances (II), both examined in the permanent dentition only. The overall performance of the model showed higher MRE and SD in group I/2, suggesting lower accuracy in such conditions. The highest accuracy was obtained in group II, however without statistically significant differences from group I/1.

The descriptive statistics indicating the mean error in the X-axis and Y-axis, the mean radial error and standard deviation, and the SDR (accuracy ranges: z = 2.0 mm, 2.5 mm, 3.0 mm, 4.0 mm) for all studied groups of

Table 5 Comparison of model performance across different patient groups

	I. No fixed orthodontic appliances					**II. Orthodontic brackets and/or bands and other fixed orthodontic appliances**		
	I/1 Permanent Dentition		**I/2 Mixed Dentition**		**T-Test Between Groups I/1 and I/2**	**II Permanent Dentition**		**T-Test Between Groups I/1 and II**
N	**141**		**164**			**135**		
	MRE (mm)	**SD (mm)**	**MRE (mm)**	**SD (mm)**	***p value***	**MRE (mm)**	**SD (mm)**	***p value***
A-Point	1.21	0.71	1.31	0.76	0.25	1.31	0.84	0.30
Ap-Superior	1.90	1.21	2.15	1.52	0.12	1.72	1.07	0.19
Ap-Inferior	1.72	1.12	2.32	1.63	**< 0.01**	1.61	0.97	0.35
ANS	1.72	1.14	1.77	1.76	0.78	1.66	1.31	0.66
Art	1.24	1.00	1.25	0.72	0.93	1.20	0.79	0.72
B-Point	1.24	0.60	1.25	0.70	0.90	1.27	0.74	0.77
Ba	1.66	1.15	1.69	1.19	0.83	1.53	1.01	0.32
Me	1.37	0.89	1.46	0.92	0.40	1.25	0.95	0.28
Is-Superior	0.86	0.50	1.20	1.15	**< 0.01**	0.88	0.44	0.64
Is-Inferior	1.14	0.71	1.24	1.22	0.39	1.18	0.73	0.64
N	1.16	0.67	1.32	0.92	0.07	1.12	0.64	0.60
Pog	1.63	1.13	1.80	1.44	0.25	1.52	0.96	0.35
PNS	1.68	1.27	1.71	1.45	0.87	1.59	1.10	0.54
S	1.01	0.64	0.93	0.63	0.31	0.89	0.53	0.10
T1	1.71	1.29	1.60	1.20	0.45	1.54	1.14	0.27
T2	1.68	1.09	1.75	1.23	0.57	1.64	1.12	0.77
AVERAGE	**1.43**	**0.95**	**1.55**	**1.15**		**1.37**	**0.90**	

Table 6 Overall model performance for all observed patient groups

	Mean X -Error (mm)	Mean Y -Error (mm)	Mean Radial Error MRE (mm)	Standard Deviation SD (mm)	SDR (Successful detection rates) %			
					SDR % *2 mm*	SDR % *2.5 mm*	SDR % *3 mm*	SDR % *4 mm*
A-Point	0.74	0.90	1.29	0.77	89.57	93.91	96.09	99.13
Ap-Superior	1.08	1.38	1.93	1.30	66.74	75.43	84.57	93.48
Ap-Inferior	1.07	1.40	1.91	1.34	67.17	75.00	83.48	93.70
ANS	1.21	0.96	1.75	1.51	80.65	81.96	87.39	94.57
Art	0.79	0.79	1.25	0.85	89.57	92.39	95.87	98.48
B-Point	0.55	1.04	1.26	0.81	94.13	95.65	96.52	99.35
Ba	0.90	1.18	1.66	1.21	86.09	86.74	90.43	94.78
Me	1.00	0.75	1.38	0.93	85.87	89.57	93.91	97.39
Is-Superior	0.59	0.68	1.00	0.80	93.91	96.96	97.83	98.91
Is-Inferior	0.67	0.84	1.19	0.93	89.57	94.57	96.30	99.35
N	0.67	0.86	1.21	0.77	88.70	94.57	98.04	99.57
Pog	0.65	1.39	1.66	1.22	79.35	82.17	88.48	95.00
PNS	1.31	0.83	1.71	1.34	82.39	83.48	85.65	93.04
S	0.63	0.59	0.97	0.84	94.13	97.17	98.04	99.57
T1	1.00	1.02	1.61	1.21	83.26	85.00	89.35	94.57
T2	1.28	0.91	1.72	1.18	84.57	86.74	89.13	94.35
AVERAGE			**1.47**	**1.06**	**84.73**	**88.21**	**91.94**	**96.58**

patients are shown in Table 6. The proposed model exhibited an overall mean radial error (MRE) of 1.47 mm with a standard deviation of 1.06 mm. The results revealed a successful detection rate (SDR) of 84.73%, 88.21%, 91.94%, and 96.58% in the range of 2, 2.5, 3, and 4 mm, respectively. The Sella point demonstrated the lowest MRE and highest SDR values, whereas the Ap-Superior point had the highest MRE and lowest SDR values. The PNS point showed the smallest mean error on the Y-axis but the largest on the X-axis.

Discussion

The null hypothesis that developmental stages of a dentition, fixed orthodontic appliances or other dental appliances do not affect the accuracy of a customized artificial model for automatic detection of cephalometric landmarks was partially confirmed. The results of this study indicated that fixed orthodontic appliances had no significant impact on the recognition of cephalometric landmarks. However, growth structures such as tooth germs in the mixed dentition affected the performance of the studied model.

Images of patients with permanent dentition showed showed homogeneous anatomical patterns in the areas of the landmarks to be placed. In contrast, patients with mixed dentition were associated with complex growth structures, varying bone density and uniquely positioned permanent tooth germs. Consequently, the recognition process showed better accuracy for images of patients with permanent dentition, while the overall performance of the model was lower for cases with mixed dentition (Table 5). As the most common sequence of eruption is the lower central incisor, followed by the permanent molars, the upper central incisors and the lower lateral incisor, the radiographic appearance of the cephalometric landmarks marking the dental structures in this area may vary greatly depending on the stage of development of the permanent teeth as well as the extent of resorption of the roots of the deciduous teeth. In addition, a temporary stage of crowding of the incisors can be expected in the early mixed dentition [47], which may lead to the appearance of double contours, superimpositions, and density differences between adjacent regions. In this study, the impact of growth structures on the recognition process of the cephalometric landmarks marking dental structures in mixed dentition patients was found to be statistically significant ($p < 0.05$) observed in the MREs of Ap-Inferior Point and Is-Superior Point. A recent study also reported a lower accuracy rate of the detection of the root apices [25], however the tips of the incisal edges of the incisors were not associated with any recognition difficulties. The possible reason for this difference could be related to the stages of a mixed dentition. However, the data sample of adolescent patients in this study was categorized as mixed dentition, which included both early mixed dentition and late mixed dentition.

In order to eliminate the complexity of growth structures, the influence of fixed orthodontic appliances on the model's performance was studied only in patients with permanent dentition. Cephalometric radiographs with fixed orthodontic appliances are usually obtained at a later stage of treatment when initial objectives such as crowding, eruption problems, impacted teeth, and occlusal relationship problems have been resolved. Since at this stage of orthodontic treatment the teeth are usually well aligned, the overall detection of cephalometric points is less affected by double contours and superimpositions, but may be affected by metal artifacts. In this study, the overall detection of cephalometric points was more accurate for images of patients with fixed orthodontic appliances, and there was no significant difference in accuracy between cephalometric radiographs of patients with orthodontic brackets and/or bands and other fixed orthodontic appliances and cephalometric radiographs of patients without fixed orthodontic appliances. It should be noted that common fixed orthodontic appliances are made of stainless steel or other alloys and therefore have a different radiographic density than skeletal structures. A similar pattern of results may be seen in of radiographs with other factors associated with comparable density that may affect the performance of the framework, such as artifacts, osteosynthesis plates, implants, prosthetic restorations, and root canal fillings. Nevertheless, the present study did not investigate these aspects due to the limited study data.

The distribution of errors in the horizontal and vertical planes was considered independently of each other. By means of a common cephalometric appraisal, the anteroposterior or vertical position of the maxilla and mandible and their relationships to the cranial base and dental structures are evaluated. For this purpose, the image was considered as a coordinate system with its two axes: X and Y. Transferred to the lateral cephalogram, these mark the sagittal and vertical planes respectively. The results for cephalometric points marking important anteroposterior correlations, such as A point and B point, showed overall a smaller distance error on the X axis than on the Y axis (Table 6). It is at the reference points marking the positions of the skeletal structures in the sagittal plane that an error on the X-axis would be of greater clinical significance, as has been noted in a recent scoping review [37]. Equivalently, the results for cephalometric points, such as PNS and ANS, marking larger vertical correlations showed comparable results in terms of distance error on the Y-axis, which is more clinically relevant in this case.

Differences in landmark recognition in the X-axis or Y-axis can be explained by the fact that each landmark is located at a distinct anatomical site that is more accurate to locate in either the vertical or horizontal direction [4]. Especially bilateral landmarks might show higher deviations in the Y-axis due to double contours associated with motion artifacts or incorrect positioning [1]. Lastly, the annotation method used in the present study may be prone to error due to interrater and intrarater variability and may also have contributed to differences in recognition in one direction or the other.

Investigating the distinct characteristics and the exact position of the dentoskeletal landmarks is essential for the quality of the cephalometric appraisal. Therefore, the focus was set on developing an independent CNN type suitable for the unique characteristics of each reference point. This approach eliminated the expected decline in accuracy with increasing number of detection targets described in a previous study [48]. The number of convolutional layers, filters, dropout layers and activation functions were adjusted for each landmark depending on its anatomical complexity. The results of the present study in terms of MRE (1.47) and SD (1.06 mm) are generally consistent with those of previous studies [10, 14, 16, 18, 22, 49]. However, as both training and test data differ, an objective comparison is not possible. One limitation of the proposed CNN architecture is that it lacks uncertainty quantification [50]. Future research may distinguish between aleatoric (irreducible) and epistemic (reducible) uncertainty. The latter can be especially beneficial in the small to moderate data regime. Having established the feasibility of the method in cephalometric landmark detection of patients with fixed appliances and the underlying challenges in patients with mixed dentition, future research could focus on systematically comparing the performance of more advanced models, such as those based on ResNet or DenseNet [51–53] and improving network architectures (e.g., by applying Bayesian optimization techniques, [54]).

Although the performance of the developed CNN was tested on a versatile dataset consisting of images with a variety of radiological features, this study employed a relatively small dataset for images, particularly from Group III (Others (artifacts, osteosynthesis plates, implants, dental prosthetic restorations and root canal treatments)). Indeed, the challenge of limited training data in the health sector was also recognized in a recent review on deep learning [39]. Hence, following research based on larger and well-balanced datasets is needed to assess the specifics of these parameters.

Another limitation of this study is the annotation procedure used, as it is prone to error with regard to the examiner. In the absence of a gold standard, constructing a reliable reference test capable of reducing bias in the dataset remains a challenge [40].

Finally, since the reference points are used in a further step of the cephalometric analysis to perform angular measurements [52], a potential limitation of the proposed framework is that such measurements and index data were not obtained. Nevertheless, it should be noted that the cephalometric angles depend to a large extent on the correct positioning of the reference points. Future studies should address the aspect of the angular measurements to assess the suitability of automated cephalometric landmark recognition for clinical use.

Conclusions

The radiographic appearance of fixed orthodontic appliances such as brackets, bands, and other fixed orthodontic appliances on a lateral cephalometric radiograph did not significantly influence the performance of the model. Complex growth structures may affect the recognition accuracy of dental landmarks, thus detected references should be verified in growing patients and in the mixed dentition.

Abbreviations

CNN	Convolutional neural networks
MRE	Mean radial error
SDR	Successful detection rate
NNs	Neural networks
MSE	Mean squared error
SD	Standard Deviation
SDR	Successful Detection Rate

Supplementary Information

The online version contains supplementary material available at https://doi.org/10.1186/s12903-023-02984-2.

Additional file 1.

Acknowledgements

Not applicable.

Authors' contributions

TP programming, investigation and original draft preparation. TS conceptualization, programming and manuscript editing. YK statistical analysis and manuscript editing. YM validation, data interpretation and manuscript editing. AW supervision and project administration. HS image acquisition, investigation and original draft preparation. All authors read and approved the final version of the manuscript.

Funding

Open Access funding enabled and organized by Projekt DEAL. This study received no external funding.

Availability of data and materials

Data and material are available on Open Data LMU Platform under the following https://doi.org/10.5282/ubm/data.359.

Declarations

Ethics approval and consent to participate

All procedures performed were in accordance with the ethical standards of the institutional and/or national research commitee and with the 1975 Helsinki declaration and its later amendments or comparable ethical standards. The Institutional Review Board, the ethics commitee of the Ludwig-Maximilian-University of Munich authorised the study protocol and approved that informed patient consent was not required for this study according to national regulations (Ref. No 19–863). The cephalometric images used in this study were obtained from the database of the Department of Orthodontics and Dentofacial Orthopedics of the LMU University Hospital in accordance with the ethical approval and irreversibly anonymised before further processing.

Consent for publication

Not applicable.

Competing interests

The authors declare no competing interests.

Author details

[1]Department of Orthodontics and Dentofacial Orthopedics, University Hospital, LMU Munich, Goethestrasse 70, 80336 Munich, Germany. [2]Department of Statistics, Statistical Consultation Unit, StaBLab, LMU Munich, Akademiestr. 1, 80799 Munich, Germany. [3]Department of Oral and Maxillofacial Surgery, University Hospital, LMU Munich, Lindwurmstrasse 2a, 80337 Munich, Germany.

Received: 27 November 2022 Accepted: 20 April 2023
Published online: 10 May 2023

References

1. Ludlow JB, Gubler M, Cevidanes L, Mol A. Precision of cephalometric landmark identification: cone-beam computed tomography vs conventional cephalometric views. Am J Orthod Dentofacial Orthop. 2009;136(3):312 e1-10.
2. Houston WJ, Maher RE, McElroy D, Sherriff M. Sources of error in measurements from cephalometric radiographs. Eur J Orthod. 1986;8(3):149–51.
3. Houston WJ. The analysis of errors in orthodontic measurements. Am J Orthod. 1983;83(5):382–90.
4. Tng TTH, Chan TCK, Hägg U, Cooke MS. Validity of cephalometric landmarks. An experimental study on human skulls. Eur J Orthod. 1994;16(2):110–20.
5. Albarakati SF, Kula KS, Ghoneima AA. The reliability and reproducibility of cephalometric measurements: a comparison of conventional and digital methods. Dentomaxillofac Radiol. 2012;41(1):11–7.
6. Uysal T, Baysal A, Yagci A. Evaluation of speed, repeatability, and reproducibility of digital radiography with manual versus computer-assisted cephalometric analyses. Eur J Orthod. 2009;31(5):523–8.
7. Lévy-Mandel AD, Venetsanopoulos AN, Tsotsos JK. Knowledge-based landmarking of cephalograms. Comput Biomed Res. 1986;19(3):282–309.
8. Chen R, Ma Y, Chen N, Lee D, Wang W, editors. Cephalometric landmark detection by attentivefeature pyramid fusion and regression-voting. Shenzhen: Medical Image Computing and Computer Assisted Intervention – MICCAI 2019: 22nd International Conference, Shenzhen, China, October 13–17, 2019, Proceedings, Part III. 2019;873–881. https://doi.org/10.1007/978-3-030-32248-9_97.
9. Gilmour L, Ray N. Locating cephalometric x-ray landmarks with foveated pyramid attention. Computer Vision and Pattern Recognition (cs.CV). 2020. https://doi.org/10.48550/arXiv.2008.04428.
10. Lee JH, Yu HJ, Kim MJ, Kim JW, Choi J. Automated cephalometric landmark detection with confidence regions using Bayesian convolutional neural networks. BMC Oral Health. 2020;20(1):270.
11. Noothout JMH, De Vos BD, Wolterink JM, Postma EM, Smeets PAM, Takx RAP, et al. Deep learning-based regression and classification for automatic landmark localization in medical images. IEEE Trans Med Imaging. 2020;39(12):4011–22.
12. Qian J, Luo W, Cheng M, Tao Y, Lin J, Lin H. CephaNN: a multi-head attention network for cephalometric landmark detection. IEEE Access. 2020;8:112633–41.
13. Oh K, Oh IS, Le VNT, Lee DW. Deep anatomical context feature learning for cephalometric landmark detection. IEEE J Biomed Health Inform. 2021;25(3):806–17.

14. Lee C, Tanikawa C, Lim JY, Yamashiro T. Deep learning based cephalometric landmark identification using landmark-dependent multi-scale patches. 2019. https://doi.org/10.48550/arXiv.1906.02961.
15. Kunz F, Stellzig-Eisenhauer A, Zeman F, Boldt J. Artificial intelligence in orthodontics. J Orofac Orthop/ Fortschritte der Kieferorthopädie. 2020;81(1):52–68.
16. Park JH, Hwang HW, Moon JH, Yu Y, Kim H, Her SB, et al. Automated identification of cephalometric landmarks: Part 1-Comparisons between the latest deep-learning methods YOLOV3 and SSD. Angle Orthod. 2019;89(6):903–9.
17. Song Y, Qiao X, Iwamoto Y, Chen YW. Automatic cephalometric landmark detection on x-ray images using a deep-learning method. Appl Sci. 2020;10(7):2547.
18. Lindner C, Wang CW, Huang CT, Li CH, Chang SW, Cootes TF. Fully automatic system for accurate localisation and analysis of cephalometric landmarks in lateral cephalograms. Sci Rep. 2016;6:33581.
19. Kolsanov AV, Popov NV, Ayupova IO, Tsitsiashvili AM, Gaidel AV, Dobratulin KS. Cephalometric analysis of lateral skull X-ray images using soft computing components in the search for key points. Stomatologiia. 2021;100(4):63–7.
20. Yu HJ, Cho SR, Kim MJ, Kim WH, Kim JW, Choi J. Automated skeletal classification with lateral cephalometry based on artificial intelligence. J Dent Res. 2020;99(3):249–56.
21. Cardillo J, Sid-Ahmed MA. An image processing system for locating craniofacial landmarks. IEEE Trans Med Imaging. 1994;13(2):275–89.
22. Arik SO, Ibragimov B, Xing L. Fully automated quantitative cephalometry using convolutional neural networks. J Med Imaging (Bellingham, Wash). 2017;4(1):014501.
23. Lindner C, Cootes T. Fully automatic cephalometric evaluation using random forest regression-voting. ISBI 2015. 2015.
24. Li H, Xu Y, Lei Y, Wang Q, Gao X. Automatic classification for sagittal craniofacial patterns based on different convolutional neural networks. Diagnostics (Basel, Switzerland). 2022;12(6):1359.
25. Bulatova G, Kusnoto B, Grace V, Tsay TP, Avenetti DM, Sanchez FJC. Assessment of automatic cephalometric landmark identification using artificial intelligence. Orthod Craniofac Res. 2021;24(Suppl 2):37–42.
26. Hwang HW, Park JH, Moon JH, Yu Y, Kim H, Her SB, et al. Automated identification of cephalometric landmarks: Part 2- Might it be better than human? Angle Orthod. 2020;90(1):69–76.
27. Kim HJ, Kim KD, Kim DH. Deep convolutional neural network-based skeletal classification of cephalometric image compared with automated-tracing software. Sci Rep. 2022;12(1):11659.
28. Le VNT, Kang J, Oh IS, Kim JG, Yang YM, Lee DW. Effectiveness of Human-Artificial Intelligence Collaboration in Cephalometric Landmark Detection. J Pers Med. 2022;12(3):387.
29. Mahto RK, Kafle D, Giri A, Luintel S, Karki A. Evaluation of fully automated cephalometric measurements obtained from web-based artificial intelligence driven platform. BMC Oral Health. 2022;22(1):132.
30. Mohan A, Sivakumar A, Nalabothu P. Evaluation of accuracy and reliability of OneCeph digital cephalometric analysis in comparison with manual cephalometric analysis—a cross-sectional study. BDJ Open. 2021;7(1):22.
31. Ristau B, Coreil M, Chapple A, Armbruster P, Ballard R. Comparison of AudaxCeph®'s fully automated cephalometric tracing technology to a semi-automated approach by human examiners. Int Orthod. 2022;20:100691.
32. Kılınç DD, Kırcelli BH, Sadry S, Karaman A. Evaluation and comparison of smartphone application tracing, web based artificial intelligence tracing and conventional hand tracing methods. J Stomatol Oral Maxillofac Surg. 2022;123:e906–15.
33. Çoban G, Öztürk T, Hashimli N, Yağci A. Comparison between cephalometric measurements using digital manual and web-based artificial intelligence cephalometric tracing software. Dental Press J Orthod. 2022;27(4):e222112.
34. Subramanian AK, Chen Y, Almalki A, Sivamurthy G, Kafle D. Cephalometric analysis in orthodontics using artificial intelligence-a comprehensive review. Biomed Res Int. 2022;2022:1880113.
35. Khanagar SB, Al-Ehaideb A, Vishwanathaiah S, Maganur PC, Patil S, Naik S, et al. Scope and performance of artificial intelligence technology in orthodontic diagnosis, treatment planning, and clinical decision-making - a systematic review. J Dent Sci. 2021;16(1):482–92.
36. Huqh MZU, Abdullah JY, Wong LS, Jamayet NB, Alam MK, Rashid QF, et al. clinical applications of artificial intelligence and machine learning in children with cleft lip and palate-a systematic review. Int J Environ Res Public Health. 2022;19(17):10860.
37. Schwendicke F, Chaurasia A, Arsiwala L, Lee JH, Elhennawy K, Jost-Brinkmann PG, et al. Deep learning for cephalometric landmark detection: systematic review and meta-analysis. Clin Oral Invest. 2021;25(7):4299–309.
38. Leonardi R, Giordano D, Maiorana F, Spampinato C. Automatic cephalometric analysis. Angle Orthod. 2008;78(1):145–51.
39. Alzubaidi L, Zhang J, Humaidi AJ, Al-Dujaili A, Duan Y, Al-Shamma O, et al. Review of deep learning: concepts, CNN architectures, challenges, applications, future directions. J Big Data. 2021;8(1):53.
40. Schwendicke F, Singh T, Lee JH, Gaudin R, Chaurasia A, Wiegand T, et al. Artificial intelligence in dental research: checklist for authors, reviewers, readers. J Dent. 2021;107:103610.
41. Bossuyt PM, Reitsma JB, Bruns DE, Gatsonis CA, Glasziou PP, Irwig L, et al. STARD 2015: an updated list of essential items for reporting diagnostic accuracy studies. BMJ (Clin Res Ed). 2015;351:h5527.
42. Fao C. Keras. 2015.
43. Martín Abadi PB, Jianmin Chen, Zhifeng Chen, Andy Davis, Jeffrey Dean, Matthieu Devin, et al. Google Brain. TensorFlow: A System for Large-Scale Machine Learning. In 12th USENIX symposium on operating systems design and implementation (OSDI 16). November 2–4, 2016. Savannah, GA, USA; pp 265-283. ISBN: 978-1-931971-33-1.
44. Goodfellow I, Bengio Y, Courville A. Deep learning: MIT press; 2016; ISBN: 9780262035613.
45. Srivastava N, Hinton G, Krizhevsky A, Sutskever I, Salakhutdinov R. Dropout: a simple way to prevent neural networks from overfitting. J Mach Learn Res. 2014;15:1929–58.
46. Park WJ, Park JB. History and application of artificial neural networks in dentistry. Eur J Dent. 2018;12(4):594–601.
47. Proffit WR, Fields HW, Larson B, Sarver DM. Contemporary Orthodontics. 6th Edition ed: Elsevier Health Sciences, 2018; ISBN: 032354388X, 9780323543880.
48. Moon JH, Hwang HW, Yu Y, Kim MG, Donatelli RE, Lee SJ. How much deep learning is enough for automatic identification to be reliable? Angle Orthod. 2020;90(6):823–30.
49. Wang CW, Huang CT, Hsieh MC, Li CH, Chang SW, Li WC, et al. Evaluation and comparison of anatomical landmark detection methods for cephalometric x-ray images: a grand challenge. IEEE Trans Med Imaging. 2015;34(9):1890–900.
50. Kendall A, Gal Y, editors. What Uncertainties Do We Need in Bayesian Deep Learning for Computer Vision? NIPS'17: Proceedings of the 31st International Conference on Neural Information Processing Systems. 2017; 5580–5590.
51. Khazaei M, Mollabashi V, Khotanlou H, Farhadian M. Sex determination from lateral cephalometric radiographs using an automated deep learning convolutional neural network. Imaging Sci Dent. 2022;52(3):239–44. https://doi.org/10.5624/isd.20220016. Epub 2022 Jul 5. PMID: 36238705; PMCID: PMC9530293.
52. Bao H, Zhang K, Yu C, Li H, Cao D, Shu H, Liu L, Yan B. Evaluating the accuracy of automated cephalometric analysis based on artificial intelligence. BMC Oral Health. 2023;23(1):191. https://doi.org/10.1186/s12903-023-02881-8.PMID:37005593;PMCID:PMC10067288.
53. Seo H, Hwang J, Jeong T, Shin J. Comparison of deep learning models for cervical vertebral maturation stage classification on lateral cephalometric radiographs. J Clin Med. 2021;10(16):3591. https://doi.org/10.3390/jcm10163591. PMID:34441887;PMCID:PMC8397111.
54. Gelman A, Carlin JB, Stern HS, Dunson DB, Vehtari A, Rubin DB. Bayesian Data Analysis (3rd ed.). 2013. Chapman and Hall/CRC. https://doi.org/10.1201/b16018.

Publisher's Note

Springer Nature remains neutral with regard to jurisdictional claims in published maps and institutional affiliations.

Journal of
Clinical Medicine

MDPI

Systematic Review

Bracket Transfer Accuracy with the Indirect Bonding Technique—A Systematic Review and Meta-Analysis

Hisham Sabbagh [1,*,†], Yeganeh Khazaei [2,†], Uwe Baumert [1], Lea Hoffmann [1], Andrea Wichelhaus [1] and Mila Janjic Rankovic [1]

[1] Department of Orthodontics and Dentofacial Orthopedics, University Hospital, LMU Munich, Goethestrasse 70, 80336 Munich, Germany; uwe.baumert@med.uni-muenchen.de (U.B.); lea.hoffmann@med.uni-muenchen.de (L.H.); kfo.sekretariat@med.uni-muenchen.de (A.W.); mila.janjic@med.uni-muenchen.de (M.J.R.)
[2] Statistical Consultation Unit, StaBLab, Department of Statistics, LMU Munich, 80799 Munich, Germany; yeganekhazaei@gmail.com
* Correspondence: hisham.sabbagh@med.uni-muenchen.de; Tel.: +49-89-4400-53223
† These authors contributed equally to this work.

Abstract: Purpose: To investigate the bracket transfer accuracy of the indirect bonding technique (IDB). Methods: Systematic search of the literature was conducted in PubMed MEDLINE, Web of Science, Embase, and Scopus through November 2021. Selection Criteria: In vivo and ex vivo studies investigating bracket transfer accuracy by comparing the planned and achieved bracket positions using the IDB technique were considered. Information concerning patients, samples, and applied methodology was collected. Measured mean transfer errors (MTE) for angular and linear directions were extracted. Risk of bias (RoB) in the studies was assessed using a tailored RoB tool. Meta-analysis of ex vivo studies was performed for overall linear and angular bracket transfer accuracy and for subgroup analyses by type of tray, tooth groups, jaw-related, side-related, and by assessment method. Results: A total of 16 studies met the eligibility criteria for this systematic review. The overall linear mean transfer errors (MTE) in mesiodistal, vertical and buccolingual direction were 0.08 mm (95% CI 0.05; 0.10), 0.09 mm (0.06; 0.11), 0.14 mm (0.10; 0.17), respectively. The overall angular mean transfer errors (MTE) regarding angulation, rotation, torque were 1.13° (0.75; 1.52), 0.93° (0.49; 1.37), and 1.11° (0.68; 1.53), respectively. Silicone trays showed the highest accuracy, followed by vacuum-formed trays and 3D printed trays. Subgroup analyses between tooth groups, right and left sides, and upper and lower jaw showed minor differences. Conclusions and implications: The overall accuracy of the indirect bonding technique can be considered clinically acceptable. Future studies should address the validation of the accuracy assessment methods used.

Keywords: bracket bonding; indirect bonding; orthodontic brackets; transfer accuracy; bracket positioning; bonding accuracy; bonding tray

check for updates

Citation: Sabbagh, H.; Khazaei, Y.; Baumert, U.; Hoffmann, L.; Wichelhaus, A.; Janjic Rankovic, M. Bracket Transfer Accuracy with the Indirect Bonding Technique—A Systematic Review and Meta-Analysis. *J. Clin. Med.* **2022**, *11*, 2568. https://doi.org/10.3390/jcm11092568

Academic Editors: Joseph Nissan and Gavriel Chaushu

Received: 25 March 2022
Accepted: 30 April 2022
Published: 4 May 2022

Publisher's Note: MDPI stays neutral with regard to jurisdictional claims in published maps and institutional affiliations.

Copyright: © 2022 by the authors. Licensee MDPI, Basel, Switzerland. This article is an open access article distributed under the terms and conditions of the Creative Commons Attribution (CC BY) license (https://creativecommons.org/licenses/by/4.0/).

1. Introduction

The straight-wire technique derived from the works of Andrews [1,2] is the most commonly used technique in fixed orthodontic treatment [3]. In this technique, the ideal placement of the brackets is of utmost importance [4–7]. Positioning errors necessitate the repositioning of brackets or the insertion of additional compensatory bends [4,8–14] and increase the number of visits and the treatment duration [5], thus compromising treatment efficiency.

Clinically, brackets can be positioned directly with an instrument or indirectly with a transfer tray. Indirect bonding (IDB) was first proposed in 1972 [15] and has since been used mainly to improve accuracy through pre-planning the ideal bracket position [7]. Numerous studies have shown that IDB can increase the precision of bracket placement [8,16–20], but

neither the direct nor the indirect technique achieves ideal clinical results, and readjustments remain necessary [3,21–24].

More recently, with the introduction of software for virtual treatment planning and workflows for additive transfer tray manufacturing for IDB, another approach for ideal bracket placement was introduced [25]. By calculating and visualizing the tooth movements resulting from the application of the virtually positioned brackets, adjustments can be made to realize the treatment objectives in the digital setup [13]. Accurate clinical implementation of the planned bracket positions is crucial in this method to achieve the virtually simulated alignment [26].

A growing number of studies have addressed the topic of IDB accuracy [26–28]. There is, however, great variability in the reported results between studies, which might be due to underlying methodological or clinical heterogeneity. Thus, the aim of this study was to synthesize the findings and assess the accuracy of the IDB technique, focusing not only on the overall accuracy of the method or different types of indirect bonding trays but also taking into account methodological and clinical aspects such as the method used to evaluate accuracy, and tooth-type-specific and jaw-related differences.

2. Materials and Methods

This systematic review was conducted according to the "Preferred Reporting Items for a Systematic Review and Meta-analysis of Diagnostic Test Accuracy Studies" (PRISMA-DTA) statement [29] and registered at the PROSPERO platform (registration number: CRD42021243227). The PICO model (problem/patient, intervention, comparison, outcome) was followed to define the research question and eligibility criteria [30]. Detailed information on how this model influenced the study design, and the definition of each PICO element can be found in Supplementary Table S1.

2.1. Eligibility Criteria

Prospective and retrospective in vivo and ex vivo studies investigating bracket transfer accuracy by comparing the planned and achieved bracket positions for buccal bracket bonding were considered. The following eligibility criteria were applied. (1) At least one of the measurements in the linear (mesiodistal, buccolingual, vertical) and/or angular (angulation, rotation, torque) directions was reported. (2) Actual status of the bracket position was confirmed by comparing it to the planned bracket position. Studies assessing lingual bracket bonding accuracy were not considered for inclusion. Only studies published in English were considered, and the last update of the search according to the search strategy was performed on 1 November 2021.

2.2. Literature Search and Study Selection Process

Based on the research question and the aforementioned eligibility criteria, a search strategy was developed. Following the Cochrane recommendations for studies dealing with very specific topics, such as indirect bonding, we applied the following concept and broke it into three sub-concepts in order to create our search strategy [31] (Table 1).

Table 1. Concept of the search strategy.

Domain	Search Term
Field	orthodont*
	AND
Intervention	bonding
	AND
Outcome	positioning differences OR accuracy OR transfer accuracy OR ideal bracket placement OR accurate bracket positioning OR accurat*

This template was applied to four bibliographic databases (PubMed, Embase, Web of Science, and Scopus) with specific adaptations for each bibliographic database (Table 2). Sets of records from each database were downloaded to the bibliographic software package EndNote X9 (Clarivate Analytics, Philadelphia, PA, USA) and merged into one core database in order to remove duplicate records.

Table 2. List of adapted search strategies used for different databases and number of identified records.

Database	Search Strategies	Results
PubMed	orthodont* [All Fields] AND bonding [All Fields] AND ((positioning [All Fields] differences [All Fields]) OR accuracy [All Fields] OR (transfer [All Fields] accuracy [All Fields]) OR (ideal [All Fields] bracket [All Fields] placement [All Fields]) OR (accurate bracket [All Fields] positioning [All Fields]) [All Fields] OR accurat* [All Fields])	218
Embase	orthodont*.mp. AND bonding.mp. AND ((positioning differences).mp. OR accuracy.mp. OR (transfer accuracy).mp. OR (ideal bracket placement).mp. OR (accurate bracket positioning).mp. OR accurat*.mp.)	101
Web of Science	orthodont* AND bonding AND (positioning differences OR accuracy OR transfer accuracy OR ideal bracket placement OR accurate bracket positioning OR accurat*)	187
Scopus	TITLE-ABS-KEY (orthodont* AND bonding AND (“positioning differences” OR “positioning difference” OR accurac* OR “transfer accuracy” OR “ideal bracket placement” OR “ideal bracket placements” OR “accurate bracket positioning” OR accurat*))	125
	Total	312

All records identified by the searches were primarily checked on the basis of title and abstract. Full texts of the records identified as relevant were then downloaded and checked for meeting the eligibility criteria. The articles that did not meet the predefined inclusion criteria after the full-text assessment were excluded from further examination. The whole literature screening process was conducted independently in parallel by two of the authors (H.S, M.J.R). The Cohen’s K coefficient for agreement between the two reviewers was 0.89. Any doubts or disagreements were solved by discussion.

2.3. Data Extraction

Data from the included studies were extracted by both reviewers in specially prepared data extraction sheets. Any differences in extracted data were resolved through discussion until reaching a consensus.

Briefly, the following information was extracted from papers: author and year of publication, study design, number of assessed teeth (incisors, canines, premolars, molars); patient information in case of in vivo studies; IDB technique used (double polyvinyl siloxane (double-PVS); double vacuum-form (double-VF), polyvinyl siloxane vacuum-form (PVS-VF), polyvinyl siloxane putty (PVS-putty), and single vacuum-form (single-VF)); type of brackets used in the study; method for measuring transfer accuracy (digital photography, calipers, CBCT, 3D-scan and superimposition); mean transfer errors (MTE) in linear (mesiodistal, buccolingual, vertical) and angular (angulation, rotation, torque) directions expressed in millimeters (mm) and degrees (°). All corresponding authors of the included studies were contacted to provide the complete data sets or additional data if available. For included studies reporting data only graphically [10,32], data were collected using a data extraction software (WebPlotDigitzer, Version 4.4, Pacifica, CA, USA) as described and validated by Drevon et al. [33]. All data were later transferred to Excel spreadsheets (Excel 2010, Microsoft Corporation, Redmond, WA, USA). The data transfer was checked twice by both reviewers involved before further analysis.

2.4. Risk of Bias Assessment in Included Studies

In this review, an adapted risk of bias (RoB) assessment tool was used (Supplementary Table S3) [34,35]. The tool contained four domains (selection bias; reference test bias; verification bias; outcome bias), each of them included items that cover different sources of bias. One of the following three modalities was used to judge the RoB in the primary studies: high, low, or unclear risk of bias. The category "unclear RoB" was applied whenever incomplete details or no information could be found in the study. RoB assessment was performed independently by the two of the authors (H.S., M.J.R).

2.5. Meta-Analysis and Synthesis of Results

Meta-analysis was performed using R Statistical Software (Version 4.1.1, R Core Team, Vienna, Austria) according to published procedures [36,37]. To be included in the meta-analysis, the sample size and the mean and standard deviation (SD) of the bracket transfer error expressed in millimeters (mm) or degrees (°) were required.

The overall mean transfer errors (MTE) and further subgroup analyses in linear (mesiodistal, buccolingual, vertical) and angular (angulation, rotation, torque) directions were performed in the following categories: overall MTE; tooth group related MTE; jaw-related MTE (left vs. right/upper vs. lower); MTE in relation to accuracy assessment method; MTE in relation to the type of IDB tray.

Data wrangling and manipulation were performed using the statistical packages "tidyverse" [37], "dplyr" [38], and "ggplot2" [39]. Meta-analytic syntheses and further investigations were performed by "meta" and "dmetar" in RStudio (Rstudio Inc., Boston, MA, USA) [36,40]. Effect sizes of the overall MTE and subgroup analyses were calculated by the metamean function provided by "meta" and are reported in Table 2. Heterogeneity was assessed using Cochran's Q and I^2-statistics. A random-effects model was retained to pool effect sizes to better account for the differences in design amongst the included studies for both overall category and subgroups analysis. The restricted maximum likelihood estimator was used to calculate the heterogeneity variance τ^2 [41]. Knapp–Hartung adjustments were used to calculate the confidence interval around the pooled effect [42]. To investigate publication bias, funnel plots were prepared using the functionalities of the "meta" package. Additionally, drapery plots were produced based on *p*-value functions.

3. Results

3.1. Literature Search Results

The PRISMA workflow illustrating the whole study selection process is summarized in Figure 1. The electronic search resulted in 218 records from PubMed, 187 records from Web of Science, 101 records from EMBASE, and 125 records from Scopus.

After duplicate elimination, altogether, 312 studies were identified. Upon checking the titles and abstracts of the identified records, 35 studies were selected for full-text reading. Studies that did not meet the eligibility criteria (n = 19) were excluded from further assessment, and the reasoning is summarized in Supplementary Table S2. Additionally, one more study was selected for inclusion by cross-checking the reference lists of literature selected for inclusion, resulting in a total number of 16 included studies. For two publications [7,28], additional data that was not included in the original manuscripts were provided by the respective authors.

3.2. Results of the Risk of Bias Assessment

The overall risk of bias (RoB) of the different domains and items is given in Figure 2. Results of the RoB assessment of the individual studies are available in Supplementary Table S5. In eight studies, indirect bracket placement might have been affected by malocclusions, such as severe crowding or rotations, or no such information was provided [7,18,28,43–47]. Only seven studies provided information on sample size calculation [26–28,44,46–48]. Three studies considered only specific tooth groups in their investigations [44,45,48]. Nine studies did not report the experience and training of the bonding clinicians or indicated low

experience [7,10,26,32,43–45,47,48], and in three studies, the bonding clinicians' experience was unclear based on the provided information [27,46,49].

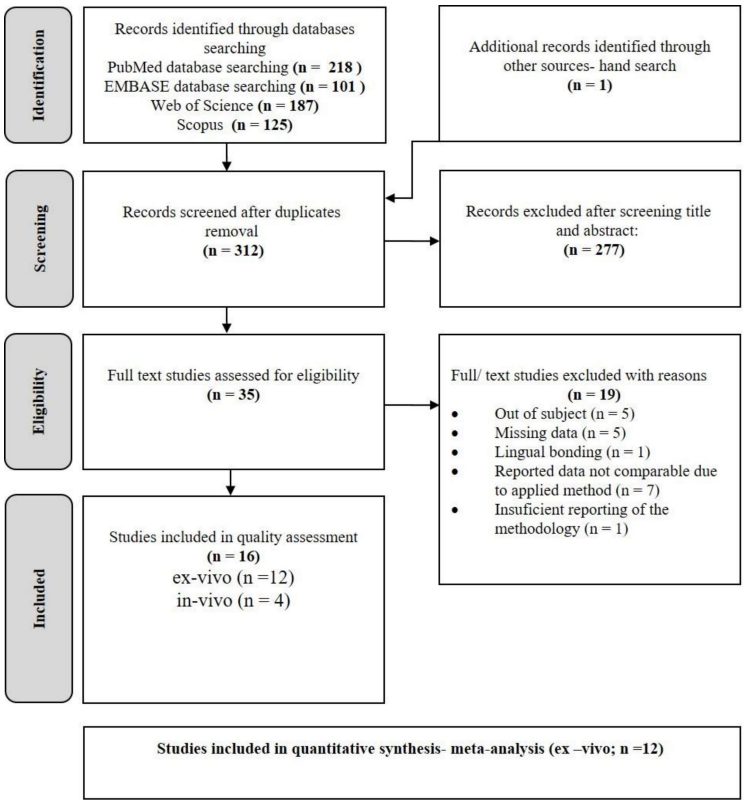

Figure 1. Flow diagram of information through the different phases of a systematic review according to Preferred Reporting Items for Systematic Reviews and Meta-Analyses (study selection process).

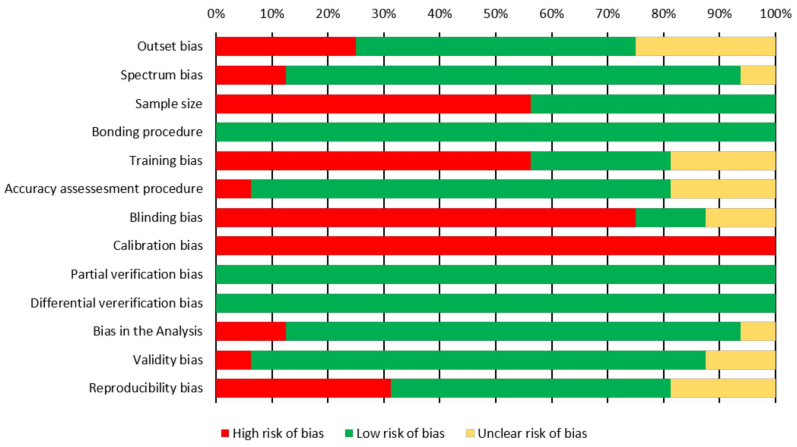

Figure 2. Overview of the overall RoB among different domains and items.

None of the included studies provided information on calibration, and only two studies provided information on blinding of the examiners [47,48]. Eight studies had a high or unclear risk of bias due to an insufficient method for reproducibility assessment or insufficient reporting [7,10,18,46–50].

3.3. Study Characteristics and Results of Individual Studies

The characteristics of the studies included for quality assessment are illustrated in Table 3.

Table 3. Study characteristics of the included studies.

Study Details		Sample Details			Bonding Procedure (Indirect)					Transfer Accuracy Assessment	
Author (Year)	Type of Study	Sample Size Calculation/Method	No. of Assessed Brackets Total/I/C/PM/M	No. of Bonding Clinicians	Type of IDB Tray	Bonded Subject (s)/Object (s)	Data for Reference Model(s)	Tray Construction	Type of Brackets	No. of Examiners	Measuring Method
Jungbauer et al. [28], 2021	ex vivo	Yes	280/80/40/80/80	NR	3D printed (soft)	bonding on plaster or printed model	impression	Virtual model, Rapid prototyping	conventional	NR	Scan + Software
			280/80/40/80/80		3D printed (hard)	bonding on plaster or printed model	impression	Virtual model, Rapid prototyping			
Park et al. [43], 2021	ex vivo	No	506/147/79/122/158	1	3D printed	bonding on plaster or printed model	model scan	Virtual model, Rapid prototyping	self-ligating	1	Scan + Software
Park et al. [44], 2021	ex vivo	Yes	225/NR	1	3D printed	bonding on plaster or printed model	model scan	Virtual model, Rapid prototyping	self-ligating	1	Scan + Software
Faus-Matoses et al. [50], 2021	ex vivo	No	335/NR	NR	3D printed	bonding on plaster or printed model	scan	Virtual model, Rapid prototyping	self-ligating	NR	Scan + Software
Niu et al. [32], 2021	ex vivo	Yes	108/37/10 19/32/20	NR	3D printed	bonding on plaster or printed model	intraoral scan	Virtual model, Rapid prototyping	conventional	NR	Scan + Software
		Yes	104/31/18/35/20	NR	Vacuum Form	bonding on plaster or printed model	intraoral scan	Virtual model, Rapid prototyping	conventional	NR	Scan + Software
Süpple et al. [49], 2021	ex vivo	No	729/210/107/207/205	NR	Vacuum Form (group H)	bonding on plaster or printed model	scan	Virtual model, Rapid prototyping	conventional	NR	Scan + Software
		No	724/209/106/206/203		Vacuum Form (group V)	bonding on plaster or printed model	scan	Model and laboratory process	conventional	NR	Scan + Software
Pottier et al. [27], 2020	ex vivo	Yes	97/38/20/39/-	1	Silicone	bonding on plaster or printed model	intraoral scan	Virtual model, Rapid prototyping	conventional	1	Scan + Software
		Yes	98/40/19/39/-		3D printed tray	bonding on plaster or printed model	intraoral scan	Virtual model, Rapid prototyping	conventional	1	Scan + Software
Kalra et al. [51], 2018	ex vivo	No	100/20/10/20/0	5	Vacuum Form	bonding on plaster or printed model	impression	Model cast and laboratory process	conventional	NR	Photography
Kim et al. [45], 2018	ex vivo	No	60/-/-/40/20	1	3D printed tray	bonding on plaster or printed model	model scan	Virtual model, Rapid prototyping	conventional	NR	Scan + Software
			30/-/-/20/10								
		No	60/-/-/40/20		3D printed tray	bonding on plaster or printed model	model scan	Virtual model, Rapid prototyping	conventional	NR	Scan + Software
			30/-/-/20/10								

Table 3. *Cont.*

Study Details		Sample Details			Bonding Procedure (Indirect)					Transfer Accuracy Assessment	
Author (Year)	Type of Study	Sample Size Calculation/Method	No. of Assessed Brackets Total/I/C/PM/M	No. of Bonding Clinicians	Type of IDB Tray	Bonded Subject (s)/Object (s)	Data for Reference Model(s)	Tray Construction	Type of Brackets	No. of Examiners	Measuring Method
Schmid et al. [46], 2018	ex vivo	Yes	132/54/24/54/-	1	Silicone	bonding on plaster or printed model	impression	Model cast and laboratory process	conventional	NR	Scan + Software
		Yes	134/52/29/53/-	1	Vacuum form	bonding on plaster or printed model	impression	Model cast and laboratory process	conventional	NR	Scan + Software
Castilla et al. [10], 2014	ex vivo	No	296/98/50/98/50 60/20/10/20/10	NR	Double PVS	bonding on plaster or printed model	impression	Model cast and laboratory process	conventional	NR	Photography, digital caliper
		No	296/98/50/98/50 60/20/10/20/1		PVS putty	bonding on plaster or printed model	impression	Model cast and laboratory process	conventional	NR	Photography, digital caliper
		No	296/98/50/98/50 60/20/10/20/10		PVS-VF	bonding on plaster or printed model	impression	Model cast and laboratory process	conventional	NR	Photography, digital caliper
		No	296/98/50/98/50 58/20/10/18/10		Double Vacuum Form	bonding on plaster or printed model	impression	Model cast and laboratory process	conventional	NR	Photography, digital caliper
		No	296/98/50/98/50 58/18/10/20/10		Single Vacuum Form	bonding on plaster or printed model	impression	Model cast and laboratory process	conventional	NR	Photography, digital caliper
Koo et al. [18], 1999	ex vivo	No	180/72/26/72/0	9	Silicone	bonding on plaster or printed model	impression	Model cast and laboratory process	conventional	NR	Photography
Chaudhary et al. [47], 2021	in vivo	Yes	300/120/60/120/0	NR	3D printed	bonding on patient	intraoral scan	Virtual model, Rapid prototyping	conventional	NR	Scan + Software
		Yes	300/120/60/120/0		PVS	bonding on patient	intraoral scan	Model cast and laboratory process	conventional	NR	Scan + Software
Xue et al. [26], 2020	in vivo	Yes	205/71/36/62/36	1	3D printed tray	digital or virtual bonding procedure	intraoral scan	Virtual model, Rapid prototyping	conventional	NR	Scan + Software
Grünheid et al. [7], 2016	in vivo	No	136/54/26/46/10	4	Silicone	Bonding on patient	impression	Model cast and laboratory process	conventional	1	CBCT + Software
Hodge et al. [48], 2004	in vivo	Yes	156/104/52/0/0	NR	Vacuum Form	Bonding on patient	impression	Model cast and laboratory process	conventional	NR	Photography, acetate copies

3.3.1. Study Characteristics and Results of the In Vivo Studies Not Included in the Quantitative Synthesis

Four in vivo studies were eligible for quality assessment after full-text reading [7,26,47,48]. Two of the studies investigated the bracket transfer accuracy of 3D printed trays [26,47], one of which compared 3D printed trays to silicone trays [47]. The other two studies investigated silicone trays [46] and vacuum-formed trays [48]. All included in vivo studies investigated the accuracy of bracket transfer with conventional brackets. In these studies, three different methods were used to evaluate accuracy: CBCT and software [7], photography [48], and scans and software [26,47]. Due to the small number of in vivo studies with different study characteristics, they were not included in the quantitative synthesis. The reported linear mean transfer errors ranged from 0.001 to 0.050 mm. The angular mean transfer errors ranged from 0.001 to 1.757°. The full extracted data is available in in Supplementary Tables S4.1–S4.6.

3.3.2. Study Characteristics of the Ex vivo Studies Included in the Quantitative Synthesis

A total of 12 ex vivo studies were eligible for quality assessment after full text reading [10,18,27,28,32,43–46,49–51]. Of these, 7 studies investigated 3D printed trays [27,28,32,43–45,50], while 5 investigated vacuum-formed trays [10,32,46,49,51], and 4 studies investigated silicone trays [10,18,27,46], with 4 of the 12 included studies comparing more than 1 material group [10,27,32,46]. Three studies used self-ligating brackets for indirect bonding [43,44,50]. The most common method of analysis was the use of scans and software (n = 9) [10,27,28,32,43–46,49,50], followed by methods using photography (n = 3) [10,18,51].

3.4. Results of the Meta-Analysis

The results of the meta-analysis are summarized in Table 4. The overall linear and angular mean bracket transfer errors are shown in forest plots in Figure 3. The full data sets, including forest plots, drapery plots, and funnel plots for different analysis groups, are available in Supplementary Tables S6.1–S8.12.

Table 4. Summary of the results of the meta-analysis. MTE, mean transfer errors.

Analyzed Parameters		Mesiodistal	Buccolingual	Vertical	Angulation	Rotation	Torque
Overall accuracy							
	n	23	21	23	20	10	10
	MTE (95% CI)	0.08 (0.05; 0.10)	0.09 (0.06; 0.11)	0.14 (0.10; 0.17)	1.13 (0.75; 1.52)	0.93 (0.49; 1.37)	1.11 (0.68; 1.53)
	Prediction interval	[−0.05; 0.20]	[−0.04; 0.21]	[−0.02; 0.30]	[−0.61; 2.87]	[−0.88; 2.74]	[−0.61; 2.83]
Tooth group comparison							
Incisors	n	14	12	14	14	8	12
	MTE (95% CI)	0.09 (0.05; 0.12)	0.14 (0.07; 0.21)	0.15 (0.10; 0.20)	1.43 (0.97; 1.89)	0.74 (0.43; 1.05)	1.63 (0.95; 2.32)
	Prediction interval	[−0.04; 0.22]	[−0.11; 0.40]	[−0.09; 0.39]	[−0.32; 3.18]	[−0.18; 1.66]	[−0.81; 4.08]
Canines	n	14	12	14	14	8	12
	MTE (95% CI)	0.09 (0.05; 0.13)	0.13 (0.07; 0.19)	0.15 (0.09; 0.24)	1.95 (1.15; 2.75)	0.90 (0.47; 1.32)	2.11 (1.13;3.09)
	Prediction interval	[−0.04; 0.22]	[−0.09; 0.34]	[−0.09; 0.40]	[−1.07; 4.97]	[−0.35; 2.15]	[−1.36; 5.58]
Premolars	n	16	14	16	16	16	10
	MTE (95% CI)	0.09 (0.05; 0.13)	0.10 (0.06; 0.14)	0.13 (0.10;0.17)	0.13 (0.10; 0.17)	1.46 (0.97;1.94)	0.95 (0.37; 1.53)
	Prediction interval	[−0.06; 0.24]	[−0.05; 0.24]	[−0.01; 0.27]	[−0.01; 0.27]	[−0.45; 3.36]	[−0.81; 2.71]
Molars	n	10	10	10	10	6	10
	MTE (95% CI)	0.06 (0.04; 0.08)	0.09 (−0.04; 0.13)	0.11 (0.04; 0.18)	1.47 (0.70; 2.23)	0.69 (0.32; 1.06)	2.29 (1.20; 3.38)
	Prediction interval	[0.01; 0.11]	[−0.04; 0.21]	[−0.08; 0.31]	[−0.99; 3.92]	[−0.26; 1.64]	[−1.24; 5.82]
Left vs. Right							
Left	n	5	3	5	2	-	-
	MTE (95% CI)	0.14 (0.04; 0.24)	0.11 (0.06; 0.17)	0.22 (0.10; 0.35)	2.91 (−1.59; 7.41)		
	Prediction interval	[−0.14; 0.42]	[−0.12; 0.35]	[−0.13; 0.57]	-		
Right	n	5	3	5	2	-	-
	MTE (95% CI)	0.14 (0.05; 0.22)	0.10 (0.02; 0.17)	0.23 (0.04; 0.42)	2.66 (2.59; 2.72)		
	Prediction interval	[−0.10: 0.37]	[−0.29; 0.48]	[−0.30; 0.76]			

Table 4. *Cont.*

Analyzed Parameters		Mesiodistal	Buccolingual	Vertical	Angulation	Rotation	Torque
Upper vs. Lower							
Upper	*n*	9	7	9	6	4	4
	MTE (95% CI)	0.10 (0.05; 0.16)	0.09 (0.02; 0.15)	0.18 (0.09; 0.26)	1.26 (0.00; 2.53)	0.59 (−0.49; 1.6)	0.73 (−0.50; 1.96)
	Prediction interval	[−0.08; 0.29]	[−0.10; 0.27]	[−0.10; 0.45]	[−2.34; 4.86]	[−2.67; 3.85]	[−2.97; 4.43]
Lower	*n*	4	2	4	4	2	2
	MTE (95% CI)	0.12 (−0.09; 0.33)	0.01 (−0.04; 0.05)	0.22 (−0.00; 0.44)	1.49 (−1.10; 4.08)	0.01 (−0.09;0.10)	0.18 (0.01; 0.35)
	Prediction interval	[−0.52; 0.76]		[−0.10; 0.45]-	[−6.32; 9.31]		
3D accuracy assessment vs. Photography							
3D	*n*	18	18	18	18	17	18
	MTE (95% CI)	0.06 (0.04; 0.08)	0.09 (0.05; 0.12)	0.11 (0.09; 0.13)	0.95 (0.63; 1.27)	0.93 (0.49; 1.37)	1.11 (0.68; 1.53)
	Prediction interval	[−0.03; 0.15]	[−0.05; 0.22]	[0.03; 0.18]	[−0.42; 2.32]	[−0.88; 2.74]	[−0.61; 2.83]
Photography	*n*	7	5	7	2		
	MTE (95% CI)	0.12 (0.06; 0.18)	0.09 (0.09; 0.10)	0.22 (0.12; 0.31)	2.74 (−1.50; 6.97)	-	-
	Prediction interval	[−0.05; 0.30]	[0.09; 0.10]	[−0.07; 0.50]	-		
Type of tray							
3D printed	*n*	13	13	4	13	11	13
	MTE (95% CI)	0.06 (0.03; 0.09)	0.10 (0.06; 0.13)	0.12 (0.09; 0.15)	1.14 (0.69; 1.60)	0.90 (0.36; 1.45)	1.42 (0.76; 2.09)
	Prediction interval	[−0.05; 0.16]	[−0.04; 0.24]	[0.02; 0.21]	[−0.57; 2.86]	[−0.94; 2.75]	[−1.01; 3.86]
Silicone	*n*	4	3	4	3	2	2
	MTE (95% CI)	0.10 (0.00; 0.19)	0.08 (−0.01; 0.18)	0.14 (−0.03; 0.32)	1.17 (−1.55; 3.88)	0.66 (−3.82; 5.13)	0.79 (−4.47; 6.05)
	Prediction interval	[−0.20; 0.39]	[−0.44; 0.61]	[−0.38; 0.67]	[−14.17; 17.12]		
Combined Silicone/Vacuum Form	*n*	1	1	1	-	-	-
	MTE (95% CI)	0.09 (0.07; 0.11)	0.09 (0.07; 0.11)	0.14 (0.11; 0.17)			
	Prediction interval	-	-	-			
Vacuum Form	*n*	6	5	6	5	4	4
	MTE (95% CI)	0.10 (0.02; 0.18)	0.08 (−0.03; 0.19)	0.16 (0.03; 0.29)	1.32 (−0.06; 2.71)	1.16 (−0.84; 3.16)	0.86 (0.26;1.46)
	Prediction interval	[−0.13; 0.33]	[−0.22; 0.39]	[−0.20; 0.52]	[−2.52; 5.17]	[−4.80; 7.13]	[−0.92; 2.63]

3.5. Linear Mean Transfer Errors

Overall linear mean transfer errors (MTE) in mesiodistal, buccolingual, and vertical directions were 0.08 mm, 0.09 mm, and 0.14 mm, respectively (Table 4). A comparison of linear MTE between different tooth groups revealed that IDB was less accurate in the incisor group, with an MTE of 0.14 mm in the buccolingual direction and 0.15 mm in the vertical direction. No significant differences could be observed in a comparison of IDB transfer accuracy between left and right sides in all three linear directions. The comparison between the upper and lower jaw showed slightly higher bracket transfer accuracy in the upper jaw in the mesiodistal and vertical directions (MTE 0.10 mm, 0.18 mm), whereas accuracy in the buccolingual direction was lower than in the lower jaw (MTE 0.09 mm). Among the different types of IDB trays, 3D printed trays showed the highest accuracy in the mesiodistal (MTE 0.06 mm) and vertical directions (MTE 0.12 mm) but the lowest accuracy in the buccolingual dimension (MTE 0.10 mm).

In studies that used photography as a method to assess accuracy, the MTE was higher in the mesiodistal and vertical directions (MTE 0.12, 0.22) than in studies that used 3D assessment methods (MTE 0.06, 0.11).

3.6. Angular Mean Transfer Errors

Overall angular mean transfer errors (MTE) regarding angulation, rotation, and torque were 1.13°, 0.93°, and 1.11°, respectively. Compared to the other tooth groups, molar tubes showed the highest transfer accuracy in rotation (MTE 0.69°) but the lowest in torque (MTE 2.29°). In the premolar group, the highest accuracy was observed for angulation (MTE 0.13°) and torque (0.95°), while rotation (MTE 1.46°) showed the lowest accuracy compared to the other tooth groups. The comparisons between the left and right sides, between upper and lower jaws, and between 3D accuracy assessment and photography could only be partially evaluated on the basis of the available data for angular values.

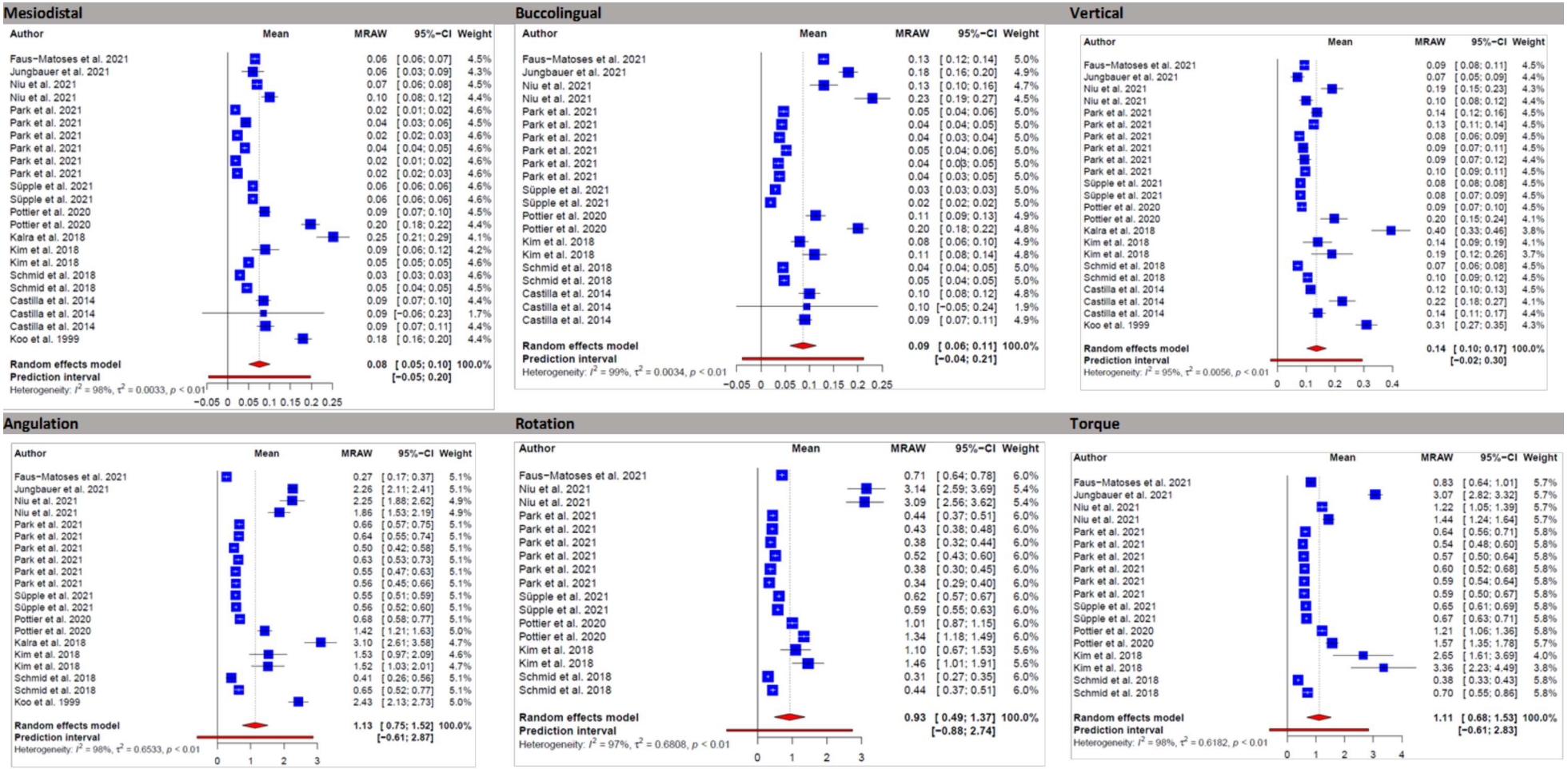

Figure 3. Forest plots showing overall linear and angular mean bracket transfer errors (MTE) [10,18,27,28,32,43–46,49–51].

Studies that used photography as a method showed a lower bracket transfer accuracy for angulation (MTE 2.74°) compared to studies that used 3D assessment (MTE 0.95°). IDB showed higher accuracy regarding angulation in the upper jaw (MTE 1.26°) but lower accuracy for rotation (MTE 0.59°) and torque (0.73°). For 3D printed trays, higher torque deviations were observed (MTE 1.42°) than for other types of IDB trays. For silicone trays, the highest accuracy was observed for angulation (MTE 0.66°) and torque (0.79°).

4. Discussion

4.1. Overall

In this study, the available literature on the indirect bonding technique was systematically reviewed regarding the accuracy of bracket transfer and differences among available methods to draw conclusions on methodological and clinical aspects.

The results of the meta-analysis showed an overall bracket transfer accuracy for the indirect bonding technique between 0.08 and 0.14 mm for linear and 0.93° and 1.13° for angular deviations, respectively. As there are no evidence-based limits for clinically acceptable bracket position deviations in the literature, most studies refer to the professional standards of the American Board of Orthodontics of 0.5 mm for linear and 2° for angular deviations [7,10,26,27,32,45,46,49,52]. However, these limits apply by definition to deviations of tooth positions. As full slot engagement with orthodontic archwires cannot be achieved in the straight-wire technique [27,53–55], exceeding these limits cannot be equated with malpositioning of the associated teeth. In view of these considerations and the limitations due to the current reference standard, the overall accuracy of the indirect bonding technique can be considered clinically acceptable.

Regarding linear deviations, a higher mean transfer error was observed for the vertical direction than for the mesiodistal and buccolingual directions, which is in line with previous studies [10,46,48,56] and mostly attributed by the authors to misfit phenomena of the indirect bonding trays. Therefore, it has been proposed to increase the distance between the dentition and the transfer tray by adapted designs to improve the fit and reduce vertical deviations [26]. Angular deviations (torque, rotation, and angulation), on the other hand, showed comparable values, although deviations for torque were reported to be highest in previous studies [26–28,32,57]. It is possible that the angular deviations are more dependent on the amount of adhesive, tray material, and tray design, and therefore different results are observed in the respective studies depending on the method used [28].

4.2. Tooth Groups

Subgroup analysis by tooth groups showed the lowest angular deviations in the premolar group for all directions but rotation, where transfer was most accurate for molar attachments. Interestingly, linear bracket transfer errors were higher for anterior teeth (incisors and canines) than for posterior teeth (premolars and molars), contrary to previous findings [7,32,57].

The high rotational accuracy of molar attachments could be explained by the larger mesio-distal extension compared to the attachments of other tooth groups. However, the overall differences between the tooth groups in the included ex vivo studies were small and likely to be clinically negligible.

4.3. Side Differences and Differences between Upper and Lower Jaw

It is considered that one of the advantages of the indirect bonding technique is that it allows for consistent accuracy in bracket placement, regardless of the practitioner's handedness or direction of viewing direction and sitting position [32]. However, only a few studies that met the inclusion criteria provided accuracy data separately for the right and left sides, and for the upper and lower jaws, so only limited conclusions can be drawn. Based on data from five studies included in the meta-analysis, no differences in bracket transfer accuracy were found between the right and left sides. In contrast, slightly higher bracket transfer accuracy was found for the upper jaw than for the lower jaw. This result

should be interpreted with caution, as it may be biased by the limited number of included studies providing accuracy data for the lower jaw.

4.4. Tray Materials

Regarding tray materials, silicone trays represent the reference in terms of accuracy [10,27,46,56]. In previous studies that compared 3D printed trays with other methods, 3D printed trays were found to have a higher bracket transfer accuracy than vacuum-formed trays [32] but lower than silicone trays [27,57]. Interestingly, in this study, 3D printed trays showed lower MTE in the mesiodistal and vertical directions and in angulation compared with the other tray material groups. The use of 3D-printed trays has been suggested to potentially increase treatment efficiency by improving treatment planning through digital setup, treatment simulation, implementation of 3D imaging data such as CBCT or MRI, and by simplifying the laboratory process [11,13,26]. However, further research is necessary to determine the influence of factors like tray design [26,32], material used [57], and manufacturing process.

4.5. Accuracy Assessment Method

Included studies using photography as a method for accuracy assessment showed a higher MTE in comparison to studies using 3D assessment. 3D assessment methods for bracket transfer accuracy using scanners or CBCT have been proposed to generally achieve higher accuracy [26,27]. However, most of the included studies did not adequately evaluate the accuracy of the assessment workflow or did not report all relevant reliability data. The sole use of Dahlberg's formula, intraclass correlation coefficient, or analysis using a paired *t*-test for reliability reporting in orthodontic research is not adequate [58]. Furthermore, Jungbauer et al. [28] questioned the suitability of intraoral scanners for accurately determining the bracket transfer accuracy because of significant artifacts on scanned brackets and low intra- and inter-rater reliability in their study. The use of photographic methods, on the other hand, has the disadvantage that not all deviation directions can be evaluated.

Accurate registration of achieved bracket positions is a technical challenge, which may partly explain why ex vivo studies are predominantly available on this topic. Despite the methodological limitations discussed, scans, photographs, and micro-Ct data appear to be suitable, in principle, for the assessment of IDB accuracy. However, adequate validation of the accuracy assessment method is required to reduce the risk of bias in future studies and to support more targeted research, in which the accuracy values obtained may be useful to practitioners with respect to the clinical protocols. Finally, all relevant data should be made available in future studies to allow for more comprehensive reviews.

5. Strengths and Limitations

To the authors' knowledge, to date, no systematic review has comprehensively addressed the assessment of bracket transfer accuracy, including methodological and clinical aspects of the IDB method. In addition, the number of available studies without standards on the methodological aspects of assessment, validation, and reporting is increasing, which limits the validity and generalizability of the results. However, it should not be neglected that conducting a meta-analysis with a small number of available studies is also subject to limitations.

As we anticipated considerable between-study heterogeneity, a random-effects model was used to pool effect sizes. The results of τ^2, I^2-statistics, and the corresponding *p*-values indicated that between-study heterogeneity existed in most of the categories and that the use of a random-effects model was appropriate. Nevertheless, the results of the subgroup analyses should be interpreted with caution. The statistical power of small subgroups is limited because the effects are smaller than in the meta-analysis performed for the overall group [36].

Moreover, a controversy around *p*-value and the sole use of forest plots to visualize results of meta-analyses is rising [59]. Forest plots can only display confidence intervals

with the assumption of a fixed significance threshold (p-value < 0.05). Therefore, in this study, we used drapery plots in addition to forest plots. Drapery plots that present the p-value function for all individual studies are suggested as being complementary figures to forest plots for presentation and interpretation of the results of a meta-analysis, specifically with a low number of studies, such as our study [60]. This prevents researchers from solely relying on the p-value < 0.05 significance threshold when interpreting the results. The resulting drapery plots are documented in Supplementary Tables S8.1–S8.12.

Due to the low number of in vivo studies (n = 4), with significant differences in the applied methodologies and an extensive and sometimes contradictory range of published results, a meta-analysis could only be carried out for ex vivo studies. The bracket transfer accuracy in in vivo settings could be lower due to limited accessibility of the oral cavity [46], moisture control and soft-tissue interference [32], patient management [45], malocclusion [10], and other factors. Therefore, further methodologically sound in vivo studies are necessary to evaluate the accuracy of the indirect bonding technique in clinical settings.

6. Clinical Implications

Accurate bracket placement is essential for effective and efficient treatment with fixed orthodontic appliances [1,7,10,26]. However, due to the complexity of the various clinical and technical aspects of bracket bonding and despite the large number of studies dealing with this topic, there is disagreement on the most appropriate techniques or methods [16]. Objective evidence from well-conducted, prospective, randomized clinical trials is still lacking [16,61].

The findings of this systematic review suggest that indirect bonding as a technique allows achieving planned bracket positions with high overall accuracy, even though the results addressed herein are not sufficient to reflect all of the various clinical aspects. It was shown that using indirect bonding, tooth-type-specific and jaw-related differences appear to have a rather negligible overall influence on accuracy. In contrast to previously published studies [27,47], indirect bracket positioning with 3D printed trays generally appears to be as accurate as silicone trays. Therefore, the selection of one of these techniques could be based on preferences or criteria such as fabrication cost, time, or cost-effectiveness, even though the reduced number of manufacturing steps and further advances in computer-aided technologies will likely favor 3D-printed trays [61].

Indirect bonding remains more time and cost-consuming overall than direct bonding due to the laboratory process required, although it has been shown to reduce clinical chair time [8,61,62]. Further research is needed to evaluate the correlation between the accuracy of bracket placement and the need for compensatory bends, bracket repositioning, and reduction in total treatment time, given the conflicting results to date [5,61,63,64].

7. Conclusions

The results of this meta-analysis indicate a generally precise implementation of planned bracket positions in the indirect bonding technique. Among tray materials, silicone trays and 3D printed trays showed higher accuracy compared to vacuum-formed trays. Subgroup analyses between tooth groups, right and left sides, and upper and lower jaw showed only minor differences. In addition to the main objectives, future studies should address the validation of the accuracy assessment methods and provide complete data sets, including adequate reliability data, to reduce the risk of bias.

Supplementary Materials: The following supporting information can be downloaded at: https://www.mdpi.com/article/10.3390/jcm11092568/s1, Supplementary Tables S1–S9. Additional references [65–79] are cited in the supplementary content.

Author Contributions: H.S. Reviewer 1, original draft preparation. M.J.R. Reviewer 2. Y.K. statistical analysis and meta-analysis. A.W. Conceptualisation. L.H. interpretation of the results. U.B. data

verification, review, and editing. All authors have read and agreed to the published version of the manuscript.

Funding: This research received no external funding.

Institutional Review Board Statement: Not applicable.

Informed Consent Statement: Not applicable.

Data Availability Statement: Not applicable.

Conflicts of Interest: The authors declare no conflict of interest.

References

1. Andrews, L.F. The straight-wire appliance, origin, controversy, commentary. *J. Clin. Orthod.* **1976**, *10*, 99–114. [PubMed]
2. Andrews, L.F. The straight-wire appliance, explained and compared. *J. Clin. Orthod.* **1976**, *10*, 174–195. [PubMed]
3. Fukuyo, K.; Nishii, Y.; Nojima, K.; Yamaguchi, H. A comparative study in three methods of bracket placement. *Orthod. Waves* **2004**, *63*, 63–70.
4. Birdsall, J.; Hunt, N.P.; Sabbah, W.; Moseley, H.C. Accuracy of positioning three types of self-ligating brackets compared with a conventionally ligating bracket. *J. Orthod.* **2012**, *39*, 34–42. [CrossRef] [PubMed]
5. Brown, M.W.; Koroluk, L.; Ko, C.C.; Zhang, K.; Chen, M.; Nguyen, T. Effectiveness and efficiency of a CAD/CAM orthodontic bracket system. *Am. J. Orthod. Dentofac. Orthop.* **2015**, *148*, 1067–1074. [CrossRef]
6. Garino, F.; Garino, G.B. Computer-aided interactive indirect bonding. *Prog. Orthod.* **2005**, *6*, 214–223.
7. Grunheid, T.; Lee, M.S.; Larson, B.E. Transfer accuracy of vinyl polysiloxane trays for indirect bonding. *Angle Orthod.* **2016**, *86*, 468–474. [CrossRef]
8. Aguirre, M.J.; King, G.J.; Waldron, J.M. Assessment of bracket placement and bond strength when comparing direct bonding to indirect bonding techniques. *Am. J. Orthod.* **1982**, *82*, 269–276. [CrossRef]
9. Carlson, S.K.; Johnson, E. Bracket positioning and resets: Five steps to align crowns and roots consistently. *Am. J. Orthod. Dentofac. Orthop.* **2001**, *119*, 76–80. [CrossRef]
10. Castilla, A.E.; Crowe, J.J.; Moses, J.R.; Wang, M.; Ferracane, J.L.; Covell, D.A.J. Measurement and comparison of bracket transfer accuracy of five indirect bonding techniques. *Angle Orthod.* **2014**, *84*, 607–614. [CrossRef]
11. El-Timamy, A.M.; El-Sharaby, F.A.; Eid, F.H.; Mostafa, Y.A. Three-dimensional imaging for indirect-direct bonding. *Am. J. Orthod. Dentofac. Orthop.* **2016**, *149*, 928–931. [CrossRef]
12. Guenthner, T.A.; Larson, B.E. Indirect bonding: A technique for precision and efficiency. *Semin. Orthod.* **2007**, *13*, 58–63. [CrossRef]
13. Suárez, C.; Vilar, T. The effect of constant height bracket placement on marginal ridge levelling using digitized models. *Eur. J. Orthod.* **2010**, *32*, 100–105. [CrossRef]
14. Israel, M.; Kusnoto, B.; Evans, C.A.; BeGole, E. A comparison of traditional and computer-aided bracket placement methods. *Angle Orthod.* **2011**, *81*, 828–835. [CrossRef]
15. Silverman, E.; Cohen, M.; Gianelly, A.A.; Dietz, V.S. A universal direct bonding system for both metal and plastic brackets. *Am. J. Orthod.* **1972**, *62*, 236–244. [CrossRef]
16. Yildirim, K.; Saglam-Aydinatay, B. Comparative assessment of treatment efficacy and adverse effects during nonextraction orthodontic treatment of class I malocclusion patients with direct and indirect bonding: A parallel randomized clinical trial. *Am. J. Orthod. Dentofac. Orthop.* **2018**, *154*, 26.e1–34.e1. [CrossRef]
17. Shpack, N.; Geron, S.; Floris, I.; Davidovitch, M.; Brosh, T.; Vardimon, A.D. Bracket placement in lingual vs. labial systems and direct vs. indirect bonding. *Angle Orthod.* **2007**, *77*, 509–517. [CrossRef]
18. Koo, B.C.; Chung, C.-H.; Vanarsdall, R.L. Comparison of the accuracy of bracket placement between direct and indirect bonding techniques. *Am. J. Orthod. Dentofac. Orthop.* **1999**, *116*, 346–351. [CrossRef]
19. Bousema, E.J.; Koops, E.A.; van Dijk, P.; Dijkstra, P.U. Association Between Subjective Tinnitus and Cervical Spine or Temporomandibular Disorders: A Systematic Review. *Trends Heart* **2018**, *22*, 2331216518800640. [CrossRef]
20. Nichols, D.A.; Gardner, G.; Carballeyra, A.D. Reproducibility of bracket positioning in the indirect bonding technique. *Am. J. Orthod. Dentofac. Orthop.* **2013**, *144*, 770–776. [CrossRef]
21. Dellinger, E.L. A scientific assessment of the straight-wire appliance. *Am. J. Orthod.* **1978**, *73*, 290–299. [CrossRef]
22. Miethke, R.R.; Melsen, B. Effect of variation in tooth morphology and bracket position on first and third order correction with preadjusted appliances. *Am. J. Orthod. Dentofac. Orthop.* **1999**, *116*, 329–335. [CrossRef]
23. Germane, N.; Bentley, B.E.J.; Isaacson, R.J. Three biologic variables modifying faciolingual tooth angulation by straight-wire appliances. *Am. J. Orthod. Dentofac. Orthop.* **1989**, *96*, 312–319. [CrossRef]
24. Li, Y.; Mei, L.; Wei, J.; Yan, X.; Zhang, X.; Zheng, W.; Li, Y. Effectiveness, efficiency and adverse effects of using direct or indirect bonding technique in orthodontic patients: A systematic review and meta-analysis. *BMC Oral Health* **2019**, *19*, 137. [CrossRef] [PubMed]
25. Duarte, M.E.A.; Gribel, B.F.; Spitz, A.; Artese, F.; Miguel, J.A.M. Reproducibility of digital indirect bonding technique using three-dimensional (3D) models and 3D-printed transfer trays. *Angle Orthod.* **2019**, *90*, 92–99. [CrossRef] [PubMed]

26. Xue, C.; Xu, H.; Guo, Y.; Xu, L.; Dhami, Y.; Wang, H.; Liu, Z.; Ma, J.; Bai, D. Accurate bracket placement using a computer-aided design and computer-aided manufacturing–guided bonding device: An in vivo study. *Am. J. Orthod. Dentofac. Orthop.* **2020**, *157*, 269–277. [CrossRef] [PubMed]
27. Pottier, T.; Brient, A.; Turpin, Y.L.; Chauvel, B.; Meuric, V.; Sorel, O.; Brezulier, D. Accuracy evaluation of bracket repositioning by indirect bonding: Hard acrylic CAD/CAM versus soft one-layer silicone trays, an in vitro study. *Clin. Oral Investig.* **2020**, *24*, 3889–3897. [CrossRef]
28. Jungbauer, R.; Breunig, J.; Schmid, A.; Hüfner, M.; Kerberger, R.; Rauch, N.; Proff, P.; Drescher, D.; Becker, K. Transfer accuracy of two 3D printed trays for indirect bracket bonding—An in vitro pilot study. *Appl. Sci.* **2021**, *11*, 6013. [CrossRef]
29. Liberati, A.; Altman, D.G.; Tetzlaff, J.; Mulrow, C.; Gøtzsche, P.C.; Ioannidis, J.P.; Clarke, M.; Devereaux, P.J.; Kleijnen, J.; Moher, D. The PRISMA statement for reporting systematic reviews and meta-analyses of studies that evaluate health care interventions: Explanation and elaboration. *PLoS Med.* **2009**, *6*, e1000100. [CrossRef]
30. Richardson, W.S.; Wilson, M.C.; Nishikawa, J.; Hayward, R.S. The well-built clinical question: A key to evidence-based decisions. *ACP J. Club* **1995**, *123*, A12–A13. [CrossRef]
31. Lefebvre, C.; Glanville, J.; Briscoe, S.; Featherstone, R.; Littlewood, A.; Marshall, C.; Metzendorf, M.-I.; Noel-Storr, A.; Paynter, R.; Rader, T.; et al. Chapter 4: Searching for and selecting studies. In *Cochrane Handbook for Systematic Reviews of Interventions version 6.3*; Updated February 2022; Higgins, J.P.T., Thomas, J., Chandler, J., Cumpston, M., Li, T., Page, M.J., Welch, V.A., Eds.; Cochrane: London, UK, 2022.
32. Niu, Y.; Zeng, Y.; Zhang, Z.; Xu, W.; Xiao, L. Comparison of the transfer accuracy of two digital indirect bonding trays for labial bracket bonding. *Angle Orthod.* **2021**, *91*, 67–73. [CrossRef]
33. Drevon, D.; Fursa, S.R.; Malcolm, A.L. Intercoder reliability and validity of webplotdigitizer in extracting graphed data. *Behav. Modif.* **2017**, *41*, 323–339. [CrossRef]
34. Kühnisch, J.; Janjic Rankovic, M.; Kapor, S.; Schüler, I.; Krause, F.; Michou, S.; Ekstrand, K.; Eggmann, F.; Neuhaus, K.W.; Lussi, A.; et al. Identifying and avoiding risk of bias in caries diagnostic studies. *J. Clin. Med.* **2021**, *10*, 3223. [CrossRef]
35. Whiting, P.F.; Rutjes, A.W.; Westwood, M.E.; Mallett, S.; Deeks, J.J.; Reitsma, J.B.; Leeflang, M.M.; Sterne, J.A.; Bossuyt, P.M.; QUADAS-2 Group. QUADAS-2: A revised tool for the quality assessment of diagnostic accuracy studies. *Ann. Intern. Med.* **2011**, *155*, 529–536. [CrossRef]
36. Harrer, M.; Cuijpers, P.; Furukawa, T.A.; Ebert, D.D. *Doing Meta-Analysis with R: A Hands-on Guide*; CRC Press: Boca Raton, FL, USA, 2021.
37. Wickham, H.; Averick, M.; Bryan, J.; Chang, W.; McGowan, L.D.A.; François, R.; Grolemund, G.; Hayes, A.; Henry, L.; Hester, J.; et al. Welcome to the Tidyverse. *J. Open Source Softw.* **2019**, *4*, 1686. [CrossRef]
38. Wickham, H.; François, R.; Henry, L.; Müller, K. *A Grammar of Data Manipulation [R package dplyr Version 1.0.2]*, 2020.
39. Wilkinson, L. ggplot2: Elegant Graphics for Data Analysis by WICKHAM, H. *Biometrics* **2011**, *67*, 678–679. [CrossRef]
40. Balduzzi, S.; Rücker, G.; Schwarzer, G. How to perform a meta-analysis with R: A practical tutorial. *Évid. Based Ment. Health* **2019**, *22*, 153–160. [CrossRef]
41. Veroniki, A.A.; Jackson, D.; Viechtbauer, W.; Bender, R.; Bowden, J.; Knapp, G.; Kuss, O.; Higgins, J.P.T.; Langan, D.; Salanti, G. Methods to estimate the between-study variance and its uncertainty in meta-analysis. *Res. Synth. Methods* **2016**, *7*, 55–79. [CrossRef]
42. Knapp, G.; Hartung, J. Improved tests for a random effects meta-regression with a single covariate. *Stat. Med.* **2003**, *22*, 2693–2710. [CrossRef]
43. Park, J.-H.; Choi, J.-Y.; Oh, S.H.; Kim, S.-H. Three-dimensional digital superimposition of orthodontic bracket position by using a computer-aided transfer jig system: An accuracy analysis. *Sensors* **2021**, *21*, 5911. [CrossRef]
44. Park, J.H.; Choi, J.Y.; Kim, S.H.; Kim, S.J.; Lee, K.J.; Nelson, G. Three-dimensional evaluation of the transfer accuracy of a bracket jig fabricated using computer-aided design and manufacturing to the anterior dentition: An in vitro study. *Korean J. Orthod.* **2021**, *51*, 375–386. [CrossRef] [PubMed]
45. Kim, J.; Chun, Y.S.; Kim, M. Accuracy of bracket positions with a CAD/CAM indirect bonding system in posterior teeth with different cusp heights. *Am. J. Orthod. Dentofac. Orthop.* **2018**, *153*, 298–307. [CrossRef] [PubMed]
46. Schmid, J.; Brenner, D.; Recheis, W.; Hofer-Picout, P.; Brenner, M.; Crismani, A.G. Transfer accuracy of two indirect bonding techniques-an in vitro study with 3D scanned models. *Eur. J. Orthod.* **2018**, *40*, 549–555. [CrossRef] [PubMed]
47. Chaudhary, V.; Batra, P.; Sharma, K.; Raghavan, S.; Gandhi, V.; Srivastava, A. A comparative assessment of transfer accuracy of two indirect bonding techniques in patients undergoing fixed mechanotherapy: A randomised clinical trial. *J. Orthod.* **2021**, *48*, 13–23. [CrossRef]
48. Hodge, T.M.; Dhopatkar, A.A.; Rock, W.P.; Spary, D.J. A randomized clinical trial comparing the accuracy of direct versus indirect bracket placement. *J. Orthod.* **2004**, *31*, 132–137. [CrossRef]
49. Süpple, J.; von Glasenapp, J.; Hofmann, E.; Jost-Brinkmann, P.G.; Koch, P.J. Accurate bracket placement with an indirect bonding method using digitally designed transfer models printed in different orientations-an in vitro study. *J. Clin. Med.* **2021**, *10*, 2002. [CrossRef]
50. Faus-Matoses, I.; Guinot Barona, C.; Zubizarreta-Macho, Á.; Paredes-Gallardo, V.; Faus-Matoses, V. A novel digital technique for measuring the accuracy of an indirect bonding technique using fixed buccal multibracket appliances. *J. Pers. Med.* **2021**, *11*, 932. [CrossRef]

51. Kalra, R.K.; Mittal, S.; Gandikota, C.; Sehgal, V.; Gupta, R.; Bali, Z. Comparison of accuracy of bracket placement by direct and indirect bonding techniques using digital processing—An in-vitro study. *J. Clin. Diagn. Res.* **2018**, *12*, 7–11. [CrossRef]
52. Armstrong, D.; Shen, G.; Petocz, P.; Darendeliler, M.A. A comparison of accuracy in bracket positioning between two techniques—Localizing the centre of the clinical crown and measuring the distance from the incisal edge. *Eur. J. Orthod.* **2007**, *29*, 430–436. [CrossRef]
53. Archambault, A.; Lacoursiere, R.; Badawi, H.; Major, P.W.; Carey, J.; Flores-Mir, C. Torque expression in stainless steel orthodontic brackets. A systematic review. *Angle Orthod.* **2010**, *80*, 201–210. [CrossRef]
54. Dalstra, M.; Eriksen, H.; Bergamini, C.; Melsen, B. Actual versus theoretical torsional play in conventional and self-ligating bracket systems. *J. Orthod.* **2015**, *42*, 103–113. [CrossRef]
55. Arreghini, A.; Lombardo, L.; Mollica, F.; Siciliani, G. Torque expression capacity of 0.018 and 0.022 bracket slots by changing archwire material and cross section. *Prog. Orthod.* **2014**, *15*, 53. [CrossRef]
56. Dörfer, S.; König, M.; Jost-Brinkmann, P.G. Übertragungsgenauigeit beim indirekten Platzieren von Brackets. *Kieferorthoädie* **2006**, *20*, 91–103.
57. Hoffmann, L.; Sabbagh, H.; Wichelhaus, A.; Kessler, A. Bracket transfer accuracy with two different three-dimensional printed transfer trays vs. silicone transfer trays. *Angle Orthod.* **2022**, *92*, 364–371. [CrossRef]
58. Donatelli, R.E.; Lee, S.J. How to report reliability in orthodontic research: Part 1. *Am. J. Orthod. Dentofac. Orthop.* **2013**, *144*, 156–161. [CrossRef]
59. Wellek, S. A critical evaluation of the current "*p*-value controversy". *Biom. J.* **2017**, *59*, 854–872. [CrossRef]
60. Rücker, G.; Schwarzer, G. Beyond the forest plot: The drapery plot. *Res. Synth. Methods* **2021**, *12*, 13–19. [CrossRef]
61. Czolgosz, I.; Cattaneo, P.M.; Cornelis, M.A. Computer-aided indirect bonding versus traditional direct bonding of orthodontic brackets: Bonding time, immediate bonding failures, and cost-minimization. A randomized controlled trial. *Eur. J. Orthod.* **2021**, *43*, 144–151. [CrossRef]
62. Bozelli, J.V.; Bigliazzi, R.; Barbosa, H.A.; Ortolani, C.L.; Bertoz, F.A.; Faltin Junior, K. Comparative study on direct and indirect bracket bonding techniques regarding time length and bracket detachment. *Dental Press. J. Orthod.* **2013**, *18*, 51–57. [CrossRef]
63. Weber, D.J., II.; Koroluk, L.D.; Phillips, C.; Nguyen, T.; Proffit, W.R. Clinical effectiveness and efficiency of customized vs. Conventional preadjusted bracket systems. *J. Clin. Orthod.* **2013**, *47*, 261–266.
64. Deahl, S.T.; Salome, N.; Hatch, J.P.; Rugh, J.D. Practice-based comparison of direct and indirect bonding. *Am. J. Orthod. Dentofac. Orthop.* **2007**, *132*, 738–742. [CrossRef]
65. Brignardello-Petersen, R. There may be no difference in failure and orthodontic bracket placement accuracy when using a direct or indirect bonding technique. *J. Am. Dent. Assoc.* **2020**, *151*, e7. [CrossRef]
66. De Oliveira, N.S.; Rossouw, E.; Lages, E.M.B.; Macari, S.; Pretti, H. Influence of clinical experience on accuracy of virtual orthodontic attachment bonding in comparison with the direct procedure. *Angle Orthod.* **2019**, *89*, 734–741. [CrossRef]
67. El Nigoumi, A. Assessing the Accuracy of Indirect Bonding with 3D Scanning Technology. *J. Clin. Orthod.* **2016**, *50*, 613–619.
68. Gayake, P.V.; Chitko, S.S.; Sutrave, N.; Gaikwad, P.M. The direct way of indirect bonding—the combined effect. *Int. J. Orthod. Milwaukee* **2013**, *24*, 15–17.
69. Hiro, T.; Iglesia, F.; Andreu, P. Indirect bonding technique in lingual orthodontics: The HIRO system. *Prog. Orthod.* **2008**, *9*, 34–45.
70. Mazzeo, F.; Marchese, E.; Assumma, V.; Sepe, J.; Perillo, L. A new device (FAQ.FIX®) for orthodontic bracket placement in straight wire technique. *Prog. Orthod.* **2013**, *14*, 23. [CrossRef]
71. Mohlhenrich, S.C.; Alexandridis, C.; Peters, F.; Kniha, K.; Modabber, A.; Danesh, G.; Fritz, U. Three-dimensional evaluation of bracket placement accuracy and excess bonding adhesive depending on indirect bonding technique and bracket geometry: An in-vitro study. *Head Face Med.* **2020**, *16*, 17. [CrossRef] [PubMed]
72. Mota Júnior, S.L.; de Andrade Vitral, J.; Schmitberger, C.A.; Machado, D.B.; Avelar, J.C.; Fraga, M.R.; da Silva Campos, M.J.; Vitral, R.W. Evaluation of the vertical accuracy of bracket placement with the Boone gauge. *Am. J. Orthod. Dentofacial Orthop.* **2015**, *148*, 821–826. [CrossRef] [PubMed]
73. Mota Júnior, S.L.; Campos, M.; Schmitberger, C.A.; Vitral, J.A.; Fraga, M.R.; Vitral, R.W.F. Evaluation of the prototype of a new bracket-positioning gauge. *Dental Press J. Orthod.* **2018**, *23*, 68–74. [CrossRef] [PubMed]
74. Nojima, L.I.; Araújo, A.S.; Alves Júnior, M. Indirect orthodontic bonding—A modified technique for improved efficiency and precision. *Dental Press J. Orthod.* **2015**, *20*, 109–117. [CrossRef]
75. Oliveira, N.S.; Gribel, B.F.; Neves, L.S.; Lages, E.M.B.; Macari, S.; Pretti, H. Comparison of the accuracy of virtual and direct bonding of orthodontic accessories. *Dental Press J. Orthod.* **2019**, *24*, 46–53. [CrossRef]
76. Schubert, K.; Halbich, T.; Jost-Brinkmann, P.G.; Müller-Hartwich, R. Precision of indirect bonding of lingual brackets using the Quick Modul System (QMS)®. *J. Orofac. Orthop.* **2013**, *74*, 6–17. [CrossRef]
77. Shin, S.H.; Lee, K.J.; Kim, S.J.; Yu, H.S.; Kim, K.M.; Hwang, C.J.; Cha, J.Y. Accuracy of bracket position using thermoplastic and 3D-printed indirect bonding trays. *Int. J. Comput. Dent.* **2021**, *24*, 133–145.
78. Wendl, B.; Droschl, H.; Muchitsch, P. Indirect bonding–a new transfer method. *Eur. J. Orthod.* **2008**, *30*, 100–107. [CrossRef]
79. Zhang, Y.; Yang, C.; Li, Y.; Xia, D.; Shi, T.; Li, C. Comparison of three-dimensional printing guides and double-layer guide plates in accurate bracket placement. *BMC Oral Health* **2020**, *20*, 127. [CrossRef]

Original Article

Bracket transfer accuracy with two different three-dimensional printed transfer trays vs silicone transfer trays

Lea Hoffmann[a]; Hisham Sabbagh[a]; Andera Wichelhaus[b]; Andreas Kessler[c]

ABSTRACT

Objectives: To compare the transfer accuracy of two different three-dimensional printed trays (Dreve FotoDent ITB [Dreve Dentamid, Unna, Germany] and NextDent Ortho ITB [NextDent, Soesterberg, the Netherlands]) to polyvinyl siloxane (PVS) trays for indirect bonding.

Materials and Methods: A total of 10 dental models were constructed for each investigated material. Virtual bracket placement was performed on a scanned dental model using OnyxCeph (OnyxCeph 3D Lab, Chemnitz, Germany). Three-dimensional printed transfer trays using a digital light processing system three-dimensional printer and silicone transfer trays were produced. Bracket positions were scanned after the indirect bonding procedure. Linear and angular transfer errors were measured. Significant differences between mean transfer errors and frequency of clinically acceptable errors ($<$0.25 mm/1°) were analyzed using the Kruskal–Wallis and χ^2 tests, respectively.

Results: All trays showed comparable accuracy of bracket placement. NextDent exhibited a significantly higher frequency of rotational error within the limit of 1° ($P = .01$) compared with the PVS tray. Although PVS showed significant differences between the tooth groups in all linear dimensions, Dreve exhibited a significant difference in the buccolingual direction only. All groups showed a similar distribution of directional bias.

Conclusions: Three-dimensional printed trays achieved comparable results with the PVS trays in terms of bracket positioning accuracy. NextDent appears to be inferior compared with PVS regarding the frequency of clinically acceptable errors, whereas Dreve was found to be equal. The influence of tooth groups on the accuracy of bracket positioning may be reduced by using an appropriate three-dimensional printed transfer tray (Dreve). (*Angle Orthod.* 2022;92:364–371.)

KEY WORDS: Indirect bonding; Virtual bracket placement; Transfer accuracy; 3D printing

INTRODUCTION

In fixed orthodontic therapy, brackets, bands, and buccal tubes are used to transfer force and torque to teeth, thereby inducing tooth movement. The accurate positioning of orthodontic brackets plays a crucial role because deviations from the correct bracket positions can lead to undesirable tooth movement, poor treatment results, and prolonged treatment time. Brackets and buccal tubes can be positioned on the teeth either directly or indirectly via a transfer aid (transfer tray). Advantages of indirect bonding compared with the direct bonding technique have been described in the literature and include, in particular, a higher accuracy of bracket position, reduced chair time, and a higher patient comfort.[1–7] In addition, computer-aided planning and manufacturing technology enables virtual planning of bracket positions. As a result of additive manufacturing (three-dimensional printing), cost-effective and easy manufacturing of bracket transfer splints is possible.[8] This new digital workflow has the potential to minimize positioning errors and increase treatment efficiency.

Accuracy of the final bracket position is defined as the deviation between the planned and actual position

[a] Assistant Physician, Department of Orthodontics and Dentofacial Orthopedics, University Hospital, Munich, Germany.

[b] Professor and Chair, Department of Orthodontics and Dentofacial Orthopedics, University Hospital, Munich, Germany.

[c] Assistant Physician, Department of Conservative Dentistry and Periodontology, University Hospital, Munich, Germany.

Corresponding author: Dr Lea Hoffmann, Ludwig-Maximilians-University of Munich, Department of Orthodontics and Dentofacial Orthopedics, Goethestraße 70, Munich 80336, Germany
(e-mail: lea.hoffmann@med.uni-muenchen.de)

Accepted: November 2021. Submitted: April 2021.
Published Online: January 4, 2022

© 2022 by The EH Angle Education and Research Foundation, Inc.

Downloaded from http://meridian.allenpress.com/angle-orthodontist/article-pdf/92/3/364/3045270/i1945-7103-92-3-364.pdf by guest on 08 September 2023

of the bracket. Error during data acquisition, transfer, processing, splint design, and the printing process as well as the material properties might influence the accuracy. To date, there are only a few studies available comparing the accuracy of bracket position using different indirect bonding three-dimensional printed trays.[9–14]

The primary objective of this study was to investigate the bracket transfer accuracy (bracket offset of bonded bracket position to designed bracket position in millimeters and degrees) of three-dimensional printed transfer trays in comparison with a PVS tray. As a secondary objective, the effect of different tooth groups (incisors, canines, premolars, molars) on the bracket transfer accuracy in comparison with PVS trays was analyzed.

MATERIALS AND METHODS

A manikin head was chosen to simulate an in vivo situation as accurately as possible. An upper jaw model with 16 plastic teeth (World Dental Federation [FDI] tooth notation) was digitized with a model scanner (S300 ARTI; Zirkonzahn, Gais, Italy) and imported into the software OnyxCeph (OnyxCeph 3D Lab, Germany). This scanned model provided the basis for the digital bracket construction and tray preparation. The following materials already approved for dental use were selected for the three-dimensional printed trays: Dreve FotoDent ITB (Dreve Dentamid, Unna, Germany) and NextDent Ortho ITB (NextDent, Soesterberg, the Netherlands).

Preparation of the Models and Transfer Trays

For construction of the dental models for the manikin head, the initially scanned maxillary model was duplicated using a silicone impression and plaster, resulting in 10 models for each material group (Dreve, NextDent, PVS). Duplicate models were conically trimmed and extended with an adapter for the manikin head (Figure 1).

Virtual bracket placement was performed on teeth 16–26 with data sets of self-ligating straight-wire brackets (0.022 × 0.028) and buccal tubes (BioQuick; Forestadent, Pforzheim, Germany). All brackets and buccal tubes were manually readjusted and aligned in all three dimensions according to the straight-wire concept. The final bracket design represented the reference data set.

The design of the three-dimensional printed bracket transfer trays was carried out using the OnyxCeph3TM (OnyxCeph 3D Lab, Chemnitz, Germany) software module “Bonding Trays 3D." The trays were configured with 0.05-mm distance to the tooth crowns, a material thickness of 1.3 mm, and a 1.5-mm slot overlap in the bracket region. A flat design in the occlusal region was chosen to allow three-dimensional printing without support structures directly on the printer’s platform. The designed bracket transfer trays were exported as a Standard Triangle Language (STL) file and aligned flat on the building platform using Autodesk Netfabb Premium software (version 2019.0; Autodesk, Mill Valley, Calif). Product-specific print parameters for the three-dimensional printing materials were applied according to the manufacturer’s specifications. Slicing was performed according to the manufacturer’s settings with a corresponding layer thickness of 50 μm. A total of 10 transfer trays with each material (Dreve, NextDent) were printed with a digital light processing (DLP) system three-dimensional printer (D20 II; Rapidshape, Heimsheim, Germany). Postprocessing was carried out according to manufacturer’s specifications, including cleaning of the trays for 6 minutes in isopropanol (96%) activated with ultrasound followed by drying. Trays were postcured using the Otoflash G171 (NK-Optik, Baierbrunn, Germany) with 2 × 2000 flashes under a nitrogen atmosphere.

To produce the 10 silicone trays, physical models (Grey Resin; Formlabs, Berlin, Germany) were necessary. Virtually planned bracket positions were mapped on a physical model. Positioning aids were calculated using Kylix 3D (OnyxCeph3TM). The digital model data set with positioning aids was printed using a stereolithography (SLA) printer (Form2; Formlabs; Figure 1). Based on these tooth models, the silicone transfer trays were made using PVS putty (Tresident 2000K; Schütz Dental, Rosbach, Germany) according to previously described recommendations.[15–17]

Bonding and Scanning of the Bonded Models

The bonding process was likewise performed for all material groups. A thin layer of composite luting cement was applied on the base of each bracket and buccal tube (RelyX Unicem 2 Automix; 3M, Seefeld, Germany). Transfer trays were positioned on the maxilla attached to the phantom patient, and the optimal fit of the tray was verified with a mirror. The composite luting cement was cured for 10 seconds at each tooth before the transfer splint was removed and postcured for another 10 seconds.

After the bonding process, the brackets were scanned with an industrial three-dimensional scanner ATOS 5 (GOM, Braunschweig, Germany) with a resolution of 10 μm. Scans and the reference data set were aligned (OnyxCeph 3D Lab software) over 10 visually identifiable anatomical points in a radius of 1.0 mm using a best-fit algorithm. Linear (mesiodistal, vertical, buccolingual) and angular offset (angulation,

Downloaded from http://meridian.allenpress.com/angle-orthodontist/article-pdf/92/3/364/3045270/i1945-7103-92-3-364.pdf by guest on 08 September 2023

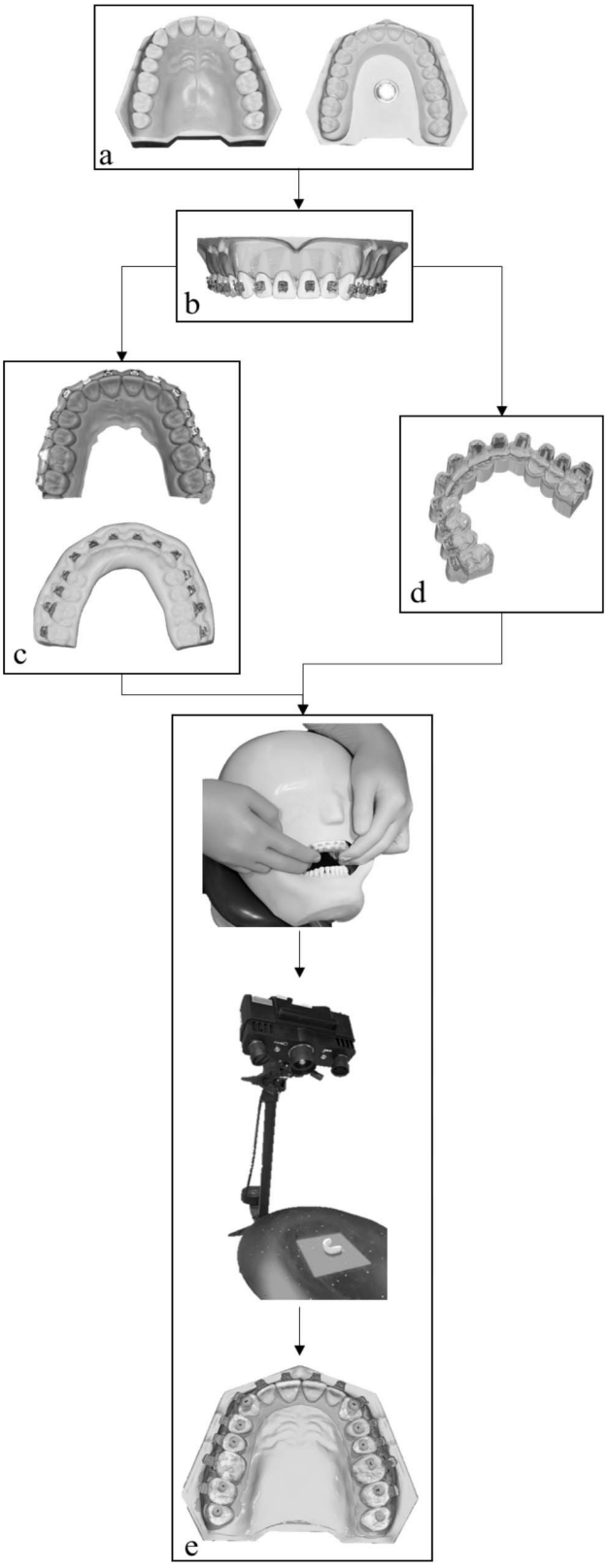

Figure 1. Workflow for the different material trays. (a) Dental models. (b) Virtual bracket placement. (c) Silicone trays. (d) Three-dimensional printed transfer trays of each material. (e) Bonding, scanning of the brackets, and overlay with the reference data set.

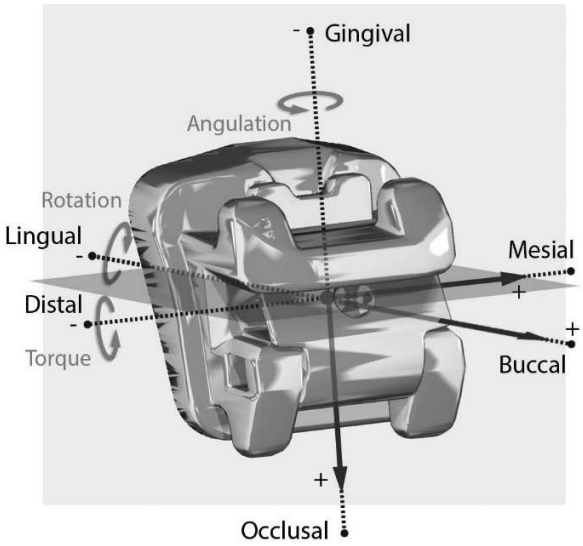

Figure 2. Defined coordinate system for analyzing the offset of the overlay of the scan and the reference data set. Mesiodistal: Mesial(+), Distal(–). Vertical: Occlusal(+), Gingival(–). Buccolingual: Buccal(+), Lingual(–). Angulation: mesial root tip(+), distal root tip(–). Torque: buccal crown torque(+), lingual crown torque(–). Rotation: mesiobuccal(+), mesiolingual(–).

rotation, torque) between the scanned and reference data set were calculated (Figure 2).

Clinically acceptable limit values were analyzed based on the American Board of Orthodontics (ABO) objective grading system for dental casts. Deviations of $\leq$0.5 mm and 2° were defined as clinically acceptable.[9,11] To account for the possibility of two adjacent brackets deviating in opposite directions, the limit of clinical acceptability in the present study was set at 0.25 mm and 1°.

For the calculation of linear and angular offsets, as well for calculating the frequency of exceeding clinically acceptable limit values, all values were set to the amount. Therefore, we have included that various directional deviations (+/–) have no influence on the actual deviation. This accounted for the possibility that some brackets have a positive offset of, for example, +1 mm, and others a negative offset of –1 mm, resulting in a higher distance of 2 mm comparing these two bracket positions. In addition, the directional bias of the offset was analyzed.

A power of 0.99 was analyzed using G*Power1 (version 3.1; Düsseldorf, Germany). Statistical analysis was carried out with IBM SPSS Statistics version 26 (IBM, Armonk, N.Y.). Metric data were tested for normal distribution using the Shapiro-Wilk test. Significant differences in metric data were analyzed using the Kruskal-Wallis test and a post hoc Dunn-Bonferroni test. Nominal data were tested for significant differences using the Pearson χ^2 test. A P value $<$.05 was considered significant.

Downloaded from http://meridian.allenpress.com/angle-orthodontist/article-pdf/92/3/364/3045270/i1945-7103-92-3-364.pdf by guest on 08 September 2023

Table 1. Mean (±SD) Difference in mm and Degrees Between the Simulated Bracket Position and the Postoperatively Scanned Bracket Position. Significant differences are represented by homogenous subgroups (α=0.05). Numbers with the same letters do not differ significantly. Numbers with different letters differ significantly. PVS and Dreve exhibited significant differences in the buccolingual and vertical direction.

		Material						
		NextDent		PVS		Dreve		
Dimension		Mean	±SD	Mean	±SD	Mean	±SD	*P*-Value
Linear error (mm)	Mesiodistal	0.07[a]	0.05	0.08 [a]	0.06	0.07 [a]	0.04	.49
	Vertical	0.10 [ab]	0.07	0.07[b]	0.06	0.11 [a]	0.06	**.001**
	Buccolingual	0.09 [ab]	0.06	0.10[a]	0.05	0.08[b]	0.06	**.02**
Angular error (°)	Angulation	0.51 [a]	0.47	0.43 [a]	0.32	0.48 [a]	0.36	.43
	Torque	0.62 [a]	0.38	0.59 [a]	0.46	0.69 [a]	0.43	.08
	Rotation	0.43 [a]	0.31	0.40 [a]	0.26	0.38 [a]	0.27	.63

Bold signifies significant difference.

RESULTS

In total, 360 brackets were bonded using the three different material trays investigated (120 brackets each on 10 upper jaw models, teeth 16–26). No bracket loss occurred during the entire study. Table 1 shows the mean deviation of the bracket position of the different tray materials between the digital design and the scanned bracket position after bonding. All bonding trays provided accurate bracket placement. The mean deviations of the bracket positions of all materials investigated were in a similar range (0.07–0.11 mm/ 0.38–0.69°). Significant differences were observed between the PVS and Dreve in the vertical ($P = .01$) and buccolingual ($P = .02$) directions.

The mean deviations of the bracket positions of the different tooth types are summarized in Table 2. Molars almost always exhibited the highest mean values regardless of the tray used. Significant differences between the tooth groups were only observed in the linear values. Although PVS tray values showed significant differences between the tooth groups in all linear dimensions, Dreve tray values exhibited a significant difference in the buccolingual direction only.

Clinically acceptable limits were more frequently exceeded by angular compared with linear values. PVS tray values were most often within the range of clinically acceptable limits followed by Dreve and NextDent (Figure 3). Compared with the PVS tray, NextDent significantly exceeded the critical limit of 1° more frequently regarding the rotation criterion.

Molars exceeded the range of clinically acceptable transfer errors more frequently, followed by canines, incisors, and premolars. However, a significant difference between the tooth groups was not observed (Figure 4).

Table 2. Mean (±SD) Difference in mm and Degrees Between the Simulated Bracket Position and the Postoperative Scanned Bracket Position of the Different Tooth Types Subdivided by the Tray Materials Investigated. Significant differences are represented by homogenous subgroups (α=0.05). Numbers with the same letters do not differ significantly. Numbers with different letters differ significantly. Significant differences could be observed in the linear directions between the different tooth types.

			Molars		Premolars		Canines		Incisors		
Material			Mean	±SD	Mean	±SD	Mean	±SD	Mean	±SD	*P*-Value
NextDent	Linear error (mm)	Mesiodistal	0.14[a]	0.06	0.07[b]	0.04	0.06[b]	0.04	0.05[b]	0.04	**.001**
		Vertical	0.11[a]	0.11	0.10 [a]	0.05	0.09 [a]	0.07	0.09 [a]	0.05	.79
		Buccolingual	0.15[a]	0.04	0.10[b]	0.05	0.03[c]	0.03	0.08[b]	0.05	**.001**
	Angular error (°)	Angulation	0.55 [a]	0.32	0.47 [a]	0.34	0.50 [a]	0.35	0.48 [a]	0.27	.81
		Torque	0.66 [a]	0.39	0.53 [a]	0.34	0.75 [a]	0.44	0.62 [a]	0.36	.29
		Rotation	0.55 [a]	0.35	0.40 [a]	0.30	0.40 [a]	0.27	0.40 [a]	0.31	.39
PVS	Linear error (mm)	Mesiodistal	0.11[a]	0.06	0.09[a]	0.06	0.08[ab]	0.06	0.05[b]	0.04	**.003**
		Vertical	0.10[a]	0.05	0.07[ab]	0.04	0.06[b]	0.06	0.07[ab]	0.05	**.04**
		Buccolingual	0.12[a]	0.06	0.12[a]	0.06	0.05[b]	0.04	0.10[a]	0.05	**.001**
	Angular error (°)	Angulation	0.39 [a]	0.32	0.37 [a]	0.28	0.45 [a]	0.24	0.49 [a]	0.28	.20
		Torque	0.75 [a]	0.51	0.50 [a]	0.38	0.66 [a]	0.47	0.57 [a]	0.42	.21
		Rotation	0.46 [a]	0.27	0.38 [a]	0.26	0.48 [a]	0.30	0.34 [a]	0.30	.17
Dreve	Linear error (mm)	Mesiodistal	0.08 [a]	0.07	0.06 [a]	0.04	0.06 [a]	0.04	0.07 [a]	0.03	.37
		Vertical	0.13 [a]	0.05	0.10 [a]	0.06	0.13 [a]	0.05	0.10 [a]	0.06	.05
		Buccolingual	0.17[a]	0.04	0.06[bc]	0.03	0.03[c]	0.02	0.08[b]	0.04	**.001**
	Angular error (°)	Angulation	0.53 [a]	0.30	0.42 [a]	0.32	0.39 [a]	0.42	0.57 [a]	0.38	.08
		Torque	0.57 [a]	0.26	0.68 [a]	0.46	0.65 [a]	0.32	0.80 [a]	0.50	.46
		Rotation	0.42 [a]	0.26	0.39 [a]	0.28	0.44 [a]	0.28	0.33 [a]	0.26	.43

Bold signifies significant difference.

Downloaded from http://meridian.allenpress.com/angle-orthodontist/article-pdf/92/3/364/3045270/i1945-7103-92-3-364.pdf by guest on 08 September 2023

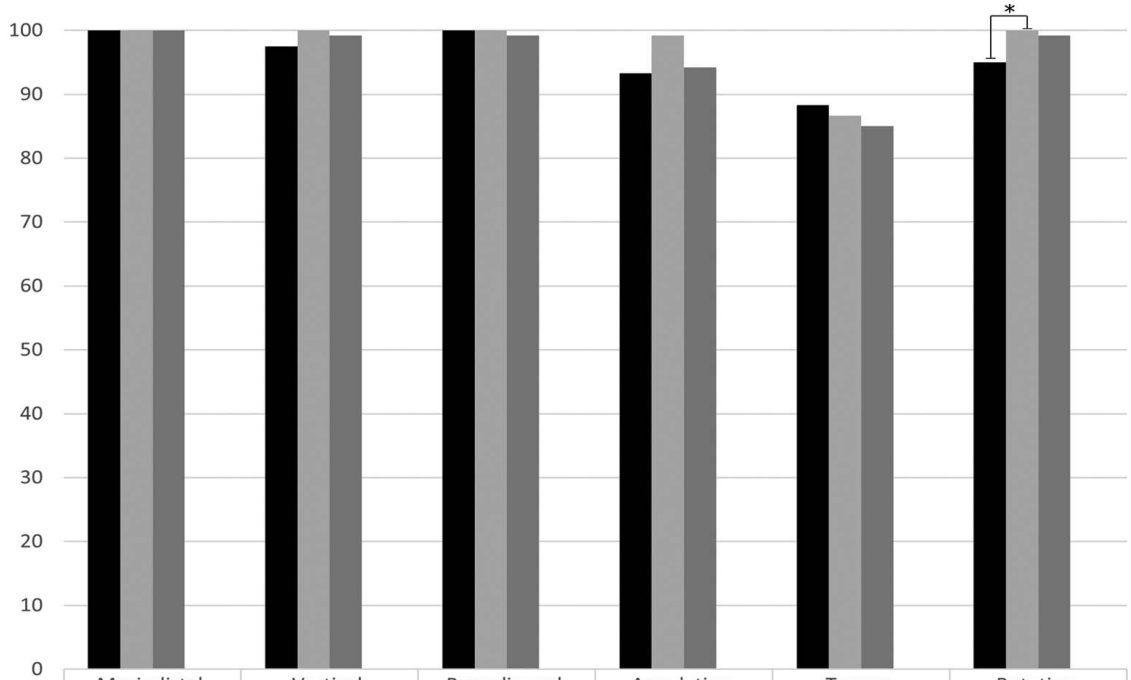

	Mesiodistal	Vertical	Buccolingual	Angulation	Torque	Rotation
NextDent (n=120) in %	100	97.5	100	93.3	88.3	95.0
PVS (n=120) in %	100	100	100	99.2	86.7	100
Dreve (n=120) in %	100	99.2	99.2	94.2	85.0	99.2
p- value	–	0.17	0.37	0.06	0.75	0.01

Figure 3. Prevalence of the clinically acceptable transfer errors of the different tray materials. NextDent significantly exceeded the critical limit of 1° more frequently compared with PVS. *$P = .01$.

Table 3 summarizes the directional bias of transfer errors in percent. All materials exhibited a comparable negative or positive deviation. A maximum bias of 98.3% was observed with Dreve regarding the torque criterion.

DISCUSSION

All transfer trays showed accurate bracket placement. Significant differences were observed for the mean vertical and buccolingual errors between the PVS tray and Dreve tray, once for the benefit of the PVS tray and once for the benefit of the Dreve tray. Mean values for NextDent were in between and showed no significant differences compared with the other materials investigated. Thus, in general, all materials were found to have comparable accuracy, with advantages in certain sections.

To date, only a few publications on this topic are available, reporting inconsistent results.[9–13] Using a study design similar to that of the current study, Pottier et al. investigated three-dimensional printed trays vs PVS trays.[11] They showed that PVS trays were more precise than three-dimensional printed trays as they observed significantly lower values for PVS trays.[11] However, comparing results of the mean bracket placement error to the current study, all values of the three-dimensional printed trays reported by Pottier et al. were up to twice as high. Based on these findings, it may be assumed that the three-dimensional transfer tray used in the present study achieved a higher accuracy in bracket placement compared with Pottier et al.

Niu et al. examined the bracket accuracy of three-dimensional printed vs double vacuum-formed trays.[10] They reported that the three-dimensional printed trays had higher transfer accuracy than the double vacuum-formed trays.[10] Unlike in the current study, they used double vacuum trays as a reference, which have been proven to be less accurate than PVS trays.[15] The transfer accuracy of the three-dimensional printed material trays in terms of the linear errors observed in the current study were comparable with those reported by Niu et al.[10] However, lower mean angular errors were observed, indicating better angular control during bracket placement. Compared with this study, similar results regarding the rate of exceeding clinically relevant limits (ABO limits of 1°/2.5 mm) were observed by Niu et al. Although the frequency in the linear dimensions was comparable (Niu et al., 97.5%–100%;

Downloaded from http://meridian.allenpress.com/angle-orthodontist/article-pdf/92/3/364/3045270/i1945-7103-92-3-364.pdf by guest on 08 September 2023

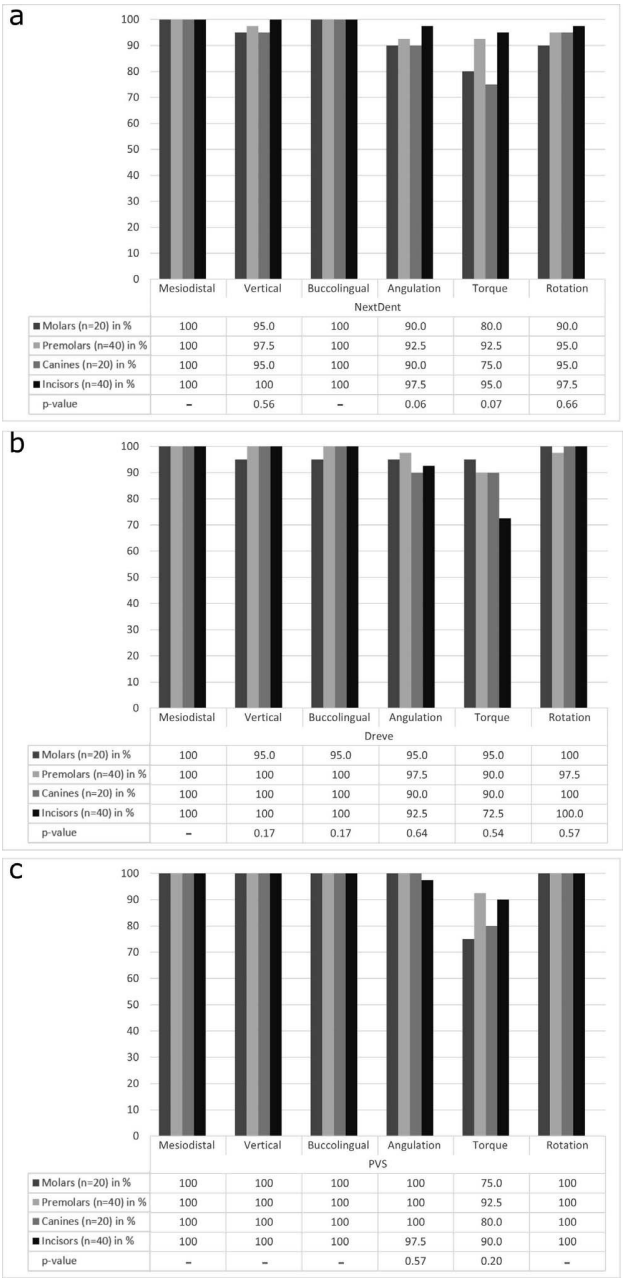

Figure 4. Prevalence of the clinically acceptable transfer errors of the tooth types and tray materials investigated. (a) NextDent. (b) Dreve. (c) PVS.

present study, 95.4%–100%), it was substantially lower in the angular dimension (Niu et al., 50.9%–85.2%; present study, 85.9%–99.2%).[10,11]

The higher accuracy of bracket placement observed in the present study compared with Pottier et al., as well as the better angular control compared with Niu et al., may be attributed to numerous factors: bracket transfer skills, tray design, scanners, different tray materials, software settings, or the three-dimensional

Table 3. Frequencies of Directional Bias of the Different Tray Materials Investigated

	Materials		
Dimension[a]	NextDent	PVS	Dreve
Mesiodistal (%)			
Mesial (+)	65.0	68.3	55.0
Distal (−)	30.0	27.5	41.7
Vertical (%)			
Occlusal (+)	20.8	26.7	11.7
Gingival (−)	75.8	69.2	85.0
Buccolingual (%)			
Buccal (+)	14.2	15.0	13.3
Lingual (−)	83.3	79.2	84.2
Angulation (%)			
MRT (+)	17.5	42.5	25.0
DRT (−)	80.0	52.5	69.2
Torque (%)			
BCT (+)	96.7	83.3	98.3
LCT (−)	1.7	15.8	0
Rotation (%)			
m-b (+)	38.3	41.7	43.3
m-l (−)	50.0	54.2	44.2

[a] BCT indicates buccal crown torque; DRT, distal root tip; LCT, lingual crown torque; m-b, mesiobuccal; m-l, mesiolingual; and MRT, mesial root tip.

printers used. To eliminate potential operator-dependent variability, bracket placement was performed by only one operator in the current study.

In contrast to the present study, Niu et al. used a semi-enclosed design that covered the two sides and the occlusal surface of the bracket, but not the gingival and undercut surfaces. They concluded that their design might have lowered the accuracy of bracket positioning in three dimensions, particularly in the angular control. As a fully covered tray design was used, this may explain the lower angular errors observed in the present study.

To minimize errors in the scanning process, an industrial ATOS 5 three-dimensional scanner with a high resolution was used. By contrast, Pottier et al. and Niu et al. used the intraoral scanner Trios2 Color (3Shape Dental Systems, Copenhagen, Denmark). In general, industrial scanners provide a higher resolution than intraoral scanners. Although more accurate scans may be achieved and thus better results with the industrial scanner, it is important to establish a reliable scanning process that is practically applicable in a clinical patient setting.

Comparisons with data from Niu et al. and Pottier et al. on further possible influencing factors, such as slicing process or material or printers used, are limited as precise information is not available in the publications.[10,11]

Because additive manufacturing is layer by layer, the printer software has to break down the tray design into individual layers before printing. In this so-called slicing

Downloaded from http://meridian.allenpress.com/angle-orthodontist/article-pdf/92/3/364/3045270/i1945-7103-92-3-364.pdf by guest on 08 September 2023

process, a layer thickness of 25–100 μm is usually selected. A smaller layer thickness provides a high-resolution object surface, which may enable a more exact setting of the bracket in the tray and thus improve the accuracy of bracket placement.[18] In the current study, a layer thickness of 50 μm was chosen. Pottier et al. and Niu et al., however, did not report on layer thickness for printing, on the material used for the three-dimensional printed trays, or on the type of DLP printer. However, as shown in the current study (Dreve vs NextDent), layer thickness and choice of the three-dimensional printed material had an influence on the accuracy of bracket placement (Figure 3), making a comparison of this study to results reported by Niu et al. and Pottier et al. difficult.

In the current study, PVS trays exceeded clinically acceptable limits the least frequently, followed by Dreve and NextDent (Figure 3). Regarding the rotation dimension, NextDent exceeded a clinically acceptable limit value of 1° significantly more often compared with PVS. Although this affected only one section of six dimensions investigated, NextDent appeared to be inferior to PVS. By contrast, Dreve exhibited similar results compared with PVS. Most likely, differences in the rate of exceeding the limit values were related to the material properties, as tray design and processes were identical. Underlining this assumption, it was noticed that the NextDent material had a much higher elasticity compared with Dreve and PVS. However, because the materials are new to the dental market and the manufacturer does not provide any information about the modulus of elasticity of the different materials, it was not possible to further substantiate that hypothesis.

The additional aim of the present study was to analyze the influence of the tooth groups on bracket transfer accuracy. Molars almost always exhibited the highest mean values of the transfer error regardless of the tray used (Table 2). However, Dreve only showed significantly higher values for molars in the buccolingual direction, whereas PVS trays exhibited significantly higher values for molars in all linear dimensions. A common explanation for higher transfer inaccuracies of molars is the difficulty in maintaining the same pressure on the entire tray during transfer, especially in the hard-to-reach posterior regions.[15,16] Following this argument, the same errors would be expected in all three trays. However, the transfer accuracy of Dreve trays were less influenced by the tooth groups. Based on this finding and in line with Niu et al., it may be assumed that the transfer error attributed to the influence of the different tooth groups may be reduced by an accurate three-dimensional printed tray (Dreve).

In general, the directional bias of the transfer error was evenly distributed for the different material groups (Table 3). However, an angular directional bias of up to 98.3% was observed for Dreve. In contrast to previous publications, an increased gingival shift was seen in this current study, probably attributed to excessive pressure on the tray during transfer. In addition, a lingual shift was found, probably caused by insufficient application of the luting material.

The high angular directional bias of up to 98.3% may be explained by the tray design. However, a similar bias was observed with the PVS trays, manufactured according to a standardized procedure independent of the three-dimensional printed trays. Therefore, it is more likely that angular directional bias was also caused by the transfer process.

CONCLUSIONS

- Three-dimensional printed trays achieved comparable results with the PVS trays in terms of bracket positioning accuracy.
- NextDent appears to be inferior compared with PVS regarding the frequency of clinically acceptable errors, whereas Dreve was found to be equal.
- The influence of tooth groups on the accuracy of bracket positioning may be reduced by using an appropriate three-dimensional printed transfer tray.

REFERENCES

1. Dalessandri D, Dalessandri M, Bonetti S, Visconti L, Paganelli C. Effectiveness of an indirect bonding technique in reducing plaque accumulation around braces. *Angle Orthod*. 2012;82(2):313–318.
2. Gange P. The evolution of bonding in orthodontics. *Am J Orthod Dentofacial Orthop*. 2015;147(4):56–63.
3. Guenthner TA, Larson BE. Indirect bonding: a technique for precision and efficiency. *Semin Orthod*. 2007;13(1):58–63.
4. Kalange JT. Indirect bonding: a comprehensive review of the advantages. *World J Orthod*. 2004;5(4):301–307.
5. Keim RG, Gottlieb EL, Vogels DS, Vogels PB. 2014 JCO study of orthodontic diagnosis and treatment procedures, part 1: results and trends. *J Clin Orthod*. 2014;48(10):607–630.
6. Thomas RG. Indirect bonding: simplicity in action. *J Clin Orthod*. 1979;13(2):93–106.
7. White LW. A new and improved indirect bonding technique. *J Clin Orthod*. 1999;33(1):17–23.
8. Tack P, Victor J, Gemmel P, Annemans L. 3D-printing techniques in a medical setting: a systematic literature review. *Biomed Eng Online*. 2016;15(1):1–21.
9. Kim J, Chun Y-S, Kim M. Accuracy of bracket positions with a CAD/CAM indirect bonding system in posterior teeth with different cusp heights. *Am J Orthod Dentofacial Orthop*. 2018;153(2):298–307.
10. Niu Y, Zeng Y, Zhang Z, Xu W, Xiao L. Comparison of the transfer accuracy of two digital indirect bonding trays for labial bracket bonding. *Angle Orthod*. 2021;91(1):67–73.
11. Pottier T, Brient A, Turpin YL, et al. Accuracy evaluation of bracket repositioning by indirect bonding: hard acrylic CAD/

Downloaded from http://meridian.allenpress.com/angle-orthodontist/article-pdf/92/3/364/3045270/i1945-7103-92-3-364.pdf by guest on 08 September 2023

CAM versus soft one-layer silicone trays, an in vitro study. *Clin Oral Investig*. 2020;24(11):3889–3897.
12. Schmid J, Brenner D, Recheis W, Hofer-Picout P, Brenner M, Crismani AG. Transfer accuracy of two indirect bonding techniques-an in vitro study with 3D scanned models. *Eur J Orthod*. 2018;40(5):549–555.
13. Xue C, Xu H, Guo Y, et al. Accurate bracket placement using a computer-aided design and computer-aided manufacturing-guided bonding device: an in vivo study. *Am J Orthod Dentofacial Orthop*. 2020;157(2):269–277.
14. Zhang Y, Yang C, Li Y, Xia D, Shi T, Li C. Comparison of three-dimensional printing guides and double-layer guide plates in accurate bracket placement. *BMC Oral Health*. 2020;20(1):1–8.
15. Castilla AE, Crowe JJ, Moses JR, Wang M, Ferracane JL, Covell DA. Measurement and comparison of bracket transfer accuracy of five indirect bonding techniques. *Angle Orthod*. 2014;84(4):607–614.
16. Grünheid T, Lee MS, Larson BE. Transfer accuracy of vinyl polysiloxane trays for indirect bonding. *Angle Orthod*. 2016; 86(3):468–474.
17. Kalange JT. Prescription-based precision full arch indirect bonding. *Semin Orthod*. 2007;13(1):19–42.
18. Favero CS, English JD, Cozad BE, Wirthlin JO, Short MM, Kasper FK. Effect of print layer height and printer type on the accuracy of 3-dimensional printed orthodontic models. *Am J Orthod Dentofacial Orthop*. 2017;152(4):557–565.

Downloaded from http://meridian.allenpress.com/angle-orthodontist/article-pdf/92/3/364/3045270/i1945-7103-92-3-364.pdf by guest on 08 September 2023

Hegele *et al. Prog Orthod.* (2021) 22:40
https://doi.org/10.1186/s40510-021-00386-0

RESEARCH

Open Access

Clinical effects with customized brackets and CAD/CAM technology: a prospective controlled study

Julia Hegele, Lena Seitz, Cora Claussen, Uwe Baumert, Hisham Sabbagh and Andrea Wichelhaus*

Abstract

Objective: Nowadays, CAD/CAM technologies enrich orthodontics in several ways. While they are commonly used for diagnoses and treatment planning, they can also be applied to create individualized bracket systems. The purpose of this prospective quasi-randomized study was to evaluate the clinical efficiency of a customized bracket system and its comparison with directly bonded conventional self-ligating bracket treatment.

Materials and methods: Altogether 38 patients were separated into two groups, treated either with direct bonded self-ligating brackets (Damon, Ormco, USA) or with indirect bonded customized CAD/CAM brackets (Insignia™, Ormco, USA). Overall treatment time, number of treatment appointments, number of lost or repositioned brackets, number of arch wires and wire bends, Little Irregularity Index, cephalometric analyses and ABO scores were compared. Superimpositions of the virtual set-ups and the treatment results of the CAD/CAM group were performed to evaluate the clinical realization of the treatment planning.

Results: No differences between both treatment groups were found concerning overall treatment time, number of appointments and number of archwire bends. Bonding failures occurred more often using the CAD/CAM system. Indirectly bonded brackets did not have to be repositioned as often as directly bonded brackets. Treatment results with both systems were similar concerning their effects on the reduction of ABO scores. The number of used archwires was higher in the CAD/CAM group. Treatment with both systems led to further proclination of the incisors. Proclination in the lower jaw was greater than proclination in the upper jaw, and there was a statistically significant difference between the two treatment systems. Comparing the treatment results with the virtual set-ups, mesial positions were met best, followed by vertical positions. Transversal positions showed the greatest discrepancies. Concerning angles, values of angulation showed greatest accordance to the virtual set-up, while values of inclinations showed greatest discrepancies.

Conclusion: In comparison with a direct bonded self-ligating bracket system the use of indirect bonded customized CAD/CAM brackets showed only minor influence on treatment efficiency and treatment outcomes. Transversal expansion, deep bite correction, expression of torque and anchorage loss remain challenges in the treatment with straight-wire appliances.

Trial registration DRKS, DRKS00024350. Registered 15 February 2021, https://www.drks.de/drks_web/navigate.do?navigationId=trial.HTML&TRIAL_ID=DRKS00024350.

Keywords: CAD/CAM, Customized brackets, Orthodontic treatment, 3D treatment planning

*Correspondence: kfo.sekretariat@med.uni-muenchen.de
Department of Orthodontics and Dentofacial Orthopedics, University Hospital, LMU Munich, Goethestrasse 70, 80336 Munich, Germany

Springer Open

© The Author(s) 2021. **Open Access** This article is licensed under a Creative Commons Attribution 4.0 International License, which permits use, sharing, adaptation, distribution and reproduction in any medium or format, as long as you give appropriate credit to the original author(s) and the source, provide a link to the Creative Commons licence, and indicate if changes were made. The images or other third party material in this article are included in the article's Creative Commons licence, unless indicated otherwise in a credit line to the material. If material is not included in the article's Creative Commons licence and your intended use is not permitted by statutory regulation or exceeds the permitted use, you will need to obtain permission directly from the copyright holder. To view a copy of this licence, visit http://creativecommons.org/licenses/by/4.0/.

Background

The introduction of intraoral scanners and CAD/CAM technology in dentistry has provided numerous innovations and possibilities. At the beginning, it was only possible to scan single teeth, and manufacturing was limited to smaller prosthetic restorations. Nowadays, the improvements in this field allow scans of larger areas, and huge amounts of data can be processed [1]. This is why these procedures are applied in almost every field of dentistry to improve the effectiveness and efficiency of dental treatments.

In orthodontics, CAD/CAM technologies are used as tools for diagnosis and treatment planning as well as for the manufacturing of aligners and fixed custom labial and lingual systems [2]. Concerning fixed appliances, this technology may facilitate the accuracy of bracket placement [3], as the position of brackets has great influence on treatment results. However, other findings show that there is no statistically significant difference in the accuracy of bracket placement between direct and indirect bonding, and neither direct nor indirect bonding can achieve ideal bracket placement [4]. To decrease errors occurring by human failure, manufacturers offer indirect bonding jigs not only to ease the bonding process, but also to evaluate the optimal bracket positions. This way, the bracket position is generated by algorithms and is no longer influenced by subjective factors like visual estimation. However, new technologies offer even more possibilities. The Insignia™ system (Ormco, Orange, USA) is a fully individualized bracket system and includes virtual set-ups to simulate the treatment results, individually manufactured bracket bases regarding tooth surface and tooth morphology with individual bracket prescriptions, individual transfer jigs and archwires.

Patients treated with a customized CAD/CAM orthodontic system showed fewer archwire appointments, shorter overall treatment time and lower American Board of Orthodontics (ABO) scores [5]. However, it is not clear whether these effects occur due to indirect bonding or due to customized brackets [6]. Additionally, current literature reports clinical outcomes only by comparing ABO scores of pre- and post-treatment records. There are no reports concerning the explicit achievement of predefined treatment goals being set by the virtual set-ups made during treatment planning. Since the advertisement of systems like Insignia™ promises a high-quality treatment by using virtual treatment planning and customized brackets, the predictability of the treatment results needed to be examined.

Therefore, the primary aim of this study was to evaluate the clinical efficiency of a directly bonded self-ligating brackets (Damon™) with an indirect bonded customized CAD/CAM bracket system (Insignia™) by comparing several clinical measurements including but not limited to ABO scores, Little Irregularity Index, treatment time, and bracket loss. In addition, the clinical realization of the treatment planning was registered by matching post-treatment scans with the virtual set-ups of patients that were treated with the Insignia™ bracket system.

Methods

Patient recruitment

To assess the clinical efficiency of customized brackets and CAD/CAM technology, a prospective quasi-randomized controlled study design [7] was chosen, which was approved by the local ethics committee (LMU Munich; reference 312-15) and registered (German Register of Clinical Studies; DRKS00024350). Continuous patient recruitment took place at the Orthodontic Department of the Ludwig Maximilians University, Munich, between July 2015 and June 2017. The treatment of the last patient was completed in August 2019, which also determined the end of the trial. All patients and their parental guidance gave informed consent beforehand. CONSORT 2010 flow diagram and CONSORT 2010 checklist [8] are included as Additional files 1 and 2: files 1 and 2.

To ensure good collaboration and to minimize longer waiting periods, patients suitable for inclusion were continuously enrolled following a quasi-random protocol, in which patients were alternatingly assigned to one of the study arms by the treating clinician. In the first group, treatment was done with the Insignia™ system (Ormco, Orange, USA). In the second group, patients were treated with Damon™ brackets (Ormco), which were directly bonded. Based on previous studies [5, 9], 40 patients were included. Inclusion criteria for both groups were as follows: (1) no extractions needed for treatment; (2) no orthognathic surgery necessary; (3) all permanent teeth erupted (except third molars); (4) class I malocclusion. Before the start of the treatment, initial documentation including model casts and cephalometric X-rays was done. Both groups were treated by the same orthodontist. In both groups, regular control intervals of six weeks were applied.

Group 1 Intraoral scans of the initial situation were generated with the Lythos scanner (Ormco) and virtual set-ups were created by Insignia™. After review, modification and final approval of the virtual set-ups and the treatment plan, self-ligating brackets with individual bases, bonding jigs for indirect bonding and archwires were manufactured by Ormco and used as specified by the Insignia™ system. The archwire sequence included 0.014″ NiTi, 0.018″ NiTi, 0.016″ × 0.025″ CuNiTi, 0.016″ × 0.022″ ss, 0.019″ × 0.025″ ss and 0.019″ × 0.025″ TMA (maxilla) / 0.017″ × 0.025″ TMA (mandible) wires

and was individually adjusted for each patient in form, lengths, and wire bends if needed. These individual features were given by the virtual set-ups.

Originally, this group consisted of 20 patients. Two of them withdrew their consent during treatment. Therefore, group 1 consisted of 18 patients (male: 8/18, 44.4%; female: 10/18, 55.5%) between 13.1 and 18.5 years of age.

Group 2 Patients of the second group were treated with Damon™ brackets (Ormco), which were directly bonded. Damon standard brackets with MBT prescription and a predefined archwire sequence including 0.014″ NiTi, 0.016″ NiTi, 0.016″ × 0.022″ NiTi, 0.016″ × 0.022″ ss, 0.018″ × 0.025″ ss, and 0.019″ × 0.025″ ss were used. This group included 20 patients (male: 7/20, 35%; female: 13/20, 65%) between 12.4 and 22.2 years of age.

Clinical measurements

At the foreseeable end of the treatment, cephalometric X-rays were repeated in both groups in order to compare the inclination of the incisors. The Little Irregularity Index [10] was determined to evaluate the amount of crowding at treatment start. The time of debonding was defined by the treating orthodontist based on the six keys of occlusion [11], overjet and overbite correction. After debonding, alginate impressions were taken. This way, ABO scores of all patients before and after the treatment were evaluated and compared by the same person. Patients' records from both groups were analysed with respect to overall treatment time, number of treatment appointments (including emergency appointments, for example, for rebonding brackets), number of rebonded brackets (e.g. due to bracket loss or repositioning), number of arch wires, and number of wire bends additionally applied. Each of the steps "treatment", "measurement", and "statistics" was performed by a different author of this study independent of each other.

Achievement of three-dimensional alignment (as planned in set-ups)

For the Insignia™ system, the achievement of the three-dimensional alignment was analysed additionally by an overlay of the virtual set-ups with the post-treatment intraoral scans for each of the patients from group 1. Virtual set-up models were exported from the Insignia™ software. Both, post-treatment scans and virtual set-ups were imported into OnyxCeph^{3}™ 3D Pro (Image Instruments, Chemnitz, Germany) using the CAD exchange format STL. The post-treatment models were then superimposed onto the virtual set-up models. For the superimposition, soft tissue landmarks visible in both models were used as references, which were not affected by changes in tooth positions during treatment. Since no reliable recognizable landmarks in the soft tissue of the lower jaw (e.g. transverse folds of the mucous membrane of the palate in the upper jaw) exist, superimposition was only applied to the maxilla scans. Differences between the post-treatment tooth positions and tooth positions in the virtual set-ups were analysed for each tooth in the following dimensions: inclination, angulation, rotation, mesial (sagittal) position, buccal (transversal) position, and occlusal (vertical) position. The direction of the discrepancy was given using digit signs "+" and "−". Absolute values (without digit signs) were used to examine how precisely the teeth met their set-up position regardless of the direction. The results were compared to the definitions of clinical acceptable ranges in all three angles and planes [9].

Statistics

Descriptive and inferential statistical analysis was done using IBM SPSS Statistics for Mac, version 26 (IBM Corp, Armonk, NY, USA). All numerical data including cephalometric, angular and planar measurements were presented with median and range, i.e. minimum and maximum. To assess potential differences between groups, nonparametric inferential methods were applied, as most of the measurements showed deviation from the assumption of normality and due to the sample size. The Mann–Whitney U test was used to test for differences between both treatment groups and for differences between anterior and posterior teeth regarding the achievement of the 3-D alignment between virtual set-ups and post-treatment intraoral scans. To test for differences between pre- and post-treatment (U1-NL, L1-ML), the Wilcoxon signed-rank test was used. Fisher's exact test was applied to test for a difference in proportion of gender between both treatment groups. The level of significance was set at $\alpha < 0.05$. Post hoc power analysis was applied using G*Power (version 3.1.9.6, Mac) [12] for two-tailed tests assuming $\alpha = 0.05$ and a power of 0.8. Additionally, based on this assumptions a sensitivity analysis was carried out based on the anticipated sample size ($N = 40$; $N_1 = N_2 = 20$), resulting in a minimum detectable effect size of $d = 0.931$. Due to the drop-outs in group 1 ($N = 38$; $N_1 = 18$, $N_2 = 20$), the minimum detectable effect size increased to $d = 0.958$. The results of the power analysis were reported (Cohen's d, power and correlation if appropriate) and considered in the interpretation.

Results

The first patient group was treated with the Insignia™ system and consisted of 18 patients (male: 8/18, 44.4%; female: 10/18, 55.5%) between 13.1 and 18.5 years of age (Table 1). The second group, treated with Damon™ brackets, included 20 patients (male: 7/20, 35%; female: 13/20, 65%) between 12.4 and 22.2 years

Table 1 Descriptive statistics of conditions during therapy including ABO scores

	Total	Group 1	Group 2	*p* Values (1–2)	Effect size
Patients [*n* (%)]	38 (100)	18 (47.4)	20 (52.6)		
Sex [*n* (% of total)]					
Male	15 (39.5)	8 (21.1)	7 (18.4)	0.741[a]	0.097[c]
Female	23 (60.5)	10 (26.3)	13 (34.2)		
Age at the start of treatment (years)	14.3 [12.4; 22.2]	14.3 [13.1; 18.5]	14.3 [12.4; 22.2]	0.696[b]	0.044[d]
Little Irregularity Index	3.6 [0.5; 13.0]	4.7 [0.5; 8.0]	2.7 [1.6; 13.0]	0.051[b]	0.438[d]
Treatment time (months)	16.7 [10.1; 35.2]	16.7 [13.0; 30.1]	16.8 [10.1; 35.26]	0.654[b]	0.084[d]
Number of brackets lost	1.0 [0; 19]	2.0 [0; 19]	1 [0; 3]	0.035[b]	0.813[d]
Number of brackets repositioned	0 [0; 10]	0 [0; 5]	0.5 [0; 10]	0.024[b]	0.611[d]
Number of archwires	4.5 [3; 6]	6 [3; 6]	4 [3; 6]	< 0.001[b]	1.3[d]
Number of archwire bends	2.5 [0; 14]	2 [0; 5]	5 [0; 14]	0.093[b]	0.789[d]
Number of appointments	15.0 [8; 28]	16.5 [10; 28]	14 [8; 25]	0.082[b]	0.494[d]
ABO scores before treatment	46 [30; 62]	46 [30; 62]	48 [32; 62]	0.874[b]	0.105[d]
ABO scores after treatment	13 [3; 24]	12 [3; 23]	16 [7; 24]	0.133[b]	0.442[d]
ABO score change within treatment	32 [16; 53]	32 [20; 53]	32 [16; 48]	0.806[b]	0.248[d]

If not otherwise stated, median and range [minimum; maximum] were reported including effect sizes. The Mann–Whitney U test was applied to compare both groups: group 1 (individualized CAD/CAM system) and group 2 (conventional self-ligating system)

[a] Fisher's exact test, [b]exact significance Mann–Whitney U test, [c]Cohen's *w*, [d]Cohen's *d*

of age (Table 1). Both groups did not differ in the proportion of male and female patients (Fisher's exact test; $p = 0.741$).

The median overall treatment time of the patient cohort was 16.7 months (range 10.1–35.2; group 1: median 16.7 months; group 2: median 16.8 months; Table 1). This difference was statistically not significant ($p = 0.654$) (Table 1, Fig. 1a).

Little Irregularity Index

Little Irregularity Indices of both groups before the treatment showed no statistically significant difference ($p = 0.051$; Table 1), indicating a similar amount of crowding in both groups.

Effectiveness

The number of appointments did not differ statistically significant between both groups ($p = 0.082$) (Table 1, Fig. 1f). Archwires were changed significantly more frequently in group 1 than in group 2 ($p < 0.001$) ($d = 1.3$, power = 0.967) (Table 1, Fig. 1d); the number of wire bends showed no statistically significant difference ($p = 0.093$) (Table 1, Fig. 1e). In addition, bracketloss was observed more often in group 1 than in group 2 ($p = 0.035$; $d = 0.813$, power = 0.661) (Table 1, Fig. 1b), whereas brackets were replaced more frequently in group 2 than in group 1 ($p = 0.024$; $d = 0.611$, power = 0.432) (Table 1, Fig. 1c).

ABO scores

The ABO scores before treatment did not differ significantly between both study groups ($p = 0.874$). After treatment, the ABO scores in both groups were reduced, but did not significantly differ between both groups ($p = 0.806$) (Table 1).

Cephalometric analyses

Concerning cephalometric analyses, especially the values of the inclination of the incisors and their development during the treatment, seemed particularly interesting.

In both groups, upper incisors (U1-NL) already showed protrusion before the treatment (group 1: median 111.4°; group 2: median 113.3°; Table 2). The protrusion of the upper incisors increased statistically

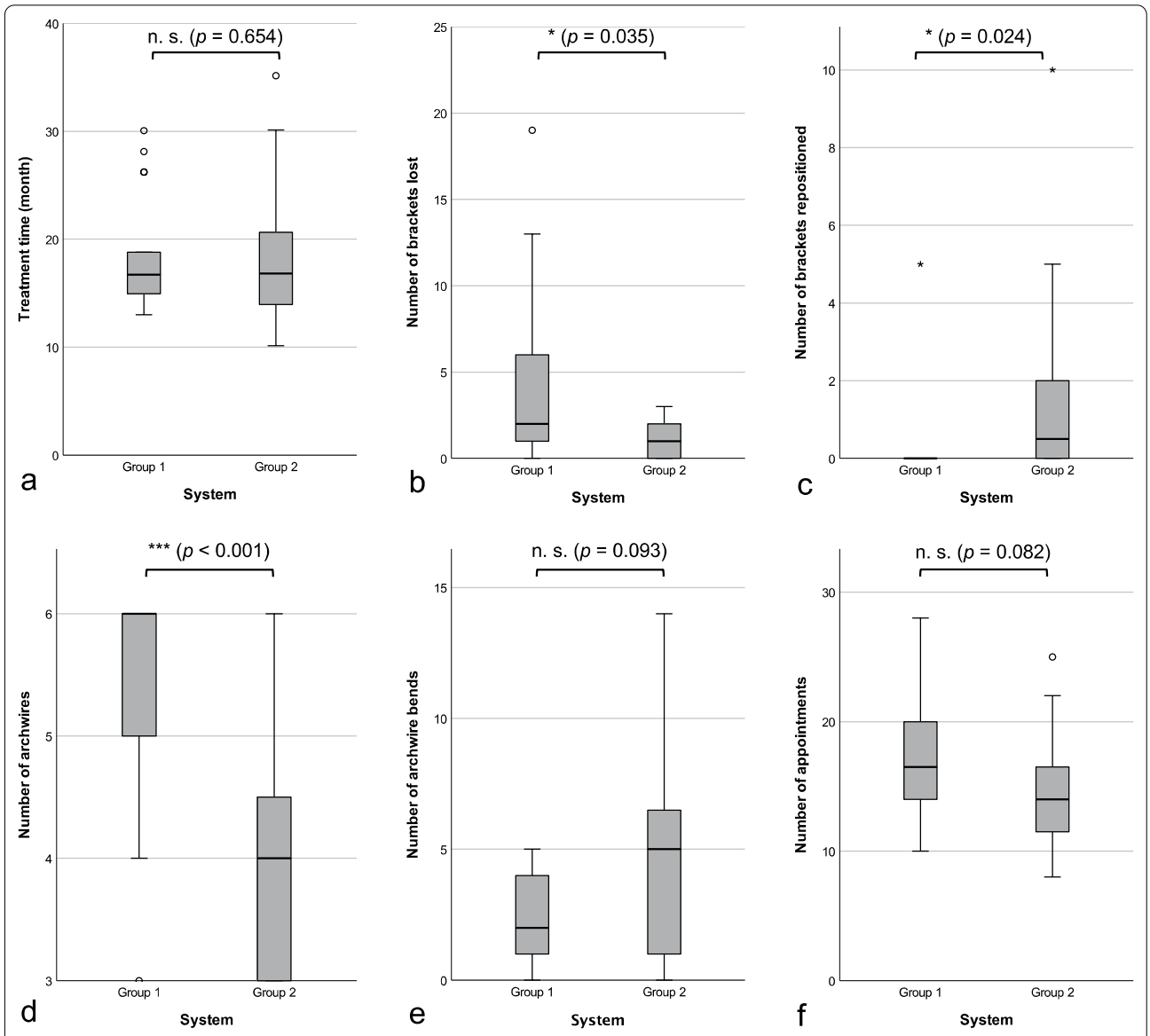

Fig. 1 Distribution of treatment time (**a**), and the number of brackets lost (**b**), brackets repositioned (**c**), archwires used (**d**), archwire bends (**e**), and appointments (**f**) in groups 1 and 2. Pairwise comparisons were done using the Mann–Whitney U test and their test statistics (n.s., not significant; *, $p < 0.05$; ***, $p < 0.001$)

Table 2 Descriptive statistics of U1-NL and L1-ML values before and after the treatment for both groups, group 1 (individualized CAD/CAM system) and group 2 (conventional self-ligating system)

Measurement	Group	Before treatment (Median [range])	After treatment (Median [range])	*P* values Wilcoxon test (effect size)	Absolute difference (Median [range])	*p* Values U test (effect size)
U1-NL (°)	Group 1	111.4 [98.0; 126.6]	115.2 [101.6; 125.2]	0.008[a] (0.654)	3.2 [0.7; 10.8]	0.206[b] (0.085)
	Group 2	114.5 [97.3; 129.3]	114.7 [98.8; 127.2]	0.191[a] (0.654)	5.5 [0.3; 16.5]	
L1-ML (°)	Group 1	96.4 [87.7; 105.8]	99.4 [87.8; 107.3]	0.006[a] (0.721)	4.4 [0.3; 13.9]	0.016[b] (0.866)
	Group 2	94.5 [82.5; 106.8]	101.5 [90.7; 116.7]	< 0.001[a] (1.584)	8.5 [2.1; 18.7]	

Matched pairs (before vs. after treatment, B-A) were compared with the Wilcoxon signed-rank test, and pairwise comparisons of the measurements between group 1 and group 2 were analysed using Mann–Whitney U test, and *p* values and effect sizes (Cohen's *d*) reported

[a] Asymptotic significance, [b]exact significance

significant in group 1 after treatment (median: 114.0; $p = 0.008$; $d = 0.654$, $r = 0.857$, power = 0.970). In group 2, the inclination of the upper incisors did not change significantly during treatment ($p = 0.191$). However, these changes were not statistically significant different between both groups ($p = 0.206$) (Table 2).

In both groups, the lower incisors (L1-ML) showed protrusion before treatment (group 1: median 96.4°; group 2: median 94.5°). In both groups, treatment led to statistically significant changes of inclination in terms of further protrusion (group 1: $p = 0.006$, $d = 0.721$, $r = 0.653$, power = 0.983; group 2: $p < 0.001$, $d = 1.584$, $r = 0.776$, power > 0.999). Lower incisors of group 2 were statistically significant more protruded than lower incisors of group 1 ($d = 0.866$, power = 0.717; Table 2).

Achievement of teeth positions (as planned in set-ups)

Concerning achieving the predefined teeth positions, the results of this study showed that sagittal positions were met best, while transversal positions showed the greatest discrepancies to the virtual set-up positions (Table 3).

Regarding vestibular/transversal positions, the anterior teeth showed smaller discrepancies than posterior teeth (Table 3). Only the positions of the lateral incisors and the canines were achieved within a clinically acceptable range of 0.5 mm, whereas other teeth showed larger discrepancies. Both tooth segments (anterior tooth segment and posterior tooth segment) differed statistically significant from the median of the allowed range of 0–0.5 mm (anterior teeth $p < 0.001$, posterior teeth $p < 0.001$). Furthermore, the results showed poorest positions for the molars. Concerning the direction of the discrepancies, the transversal position of the posterior teeth was too palatal, while the transversal position of the anterior teeth was too buccal/anterior (Fig. 2).

The planned sagittal/mesial movements in our study were attainable with discrepancies lower than 0.5 mm for all teeth except upper left canines and performed better for anterior teeth than for posterior teeth (Table 3). Concerning the direction of discrepancies, all teeth showed the tendency to be positioned too far anterior, except upper right second molars that were positioned too far posterior (Fig. 2).

In the vertical/occlusal plane, discrepancies for anterior teeth in our study were lower than for posterior teeth (Table 3). They were most precise for second premolars, whereas the vertical position for the second molars showed worst results with discrepancies higher than 0.5 mm. Considering the directions, anterior teeth tended to show suprapositions compared to the set-ups. Upper posterior right and left teeth (15–17, 25–27) were not extruded enough (Fig. 2).

Achievement of three-dimensional alignment (as planned in set-ups)

The results of our study showed in terms of reaching all three predefined angles, that the values for angulation showed greatest accordance with the virtual set-up, while values of inclinations showed greatest discrepancies (Table 3).

The inclination of the virtual set-up positions was met more precisely by posterior teeth than by anterior teeth. In our study, the planned movement in this dimension was achieved in a clinically acceptable range of 2° by second premolars. Worst results were shown in the movement of second molars and upper left central incisors. In comparison with the virtual set-up, inclination values of upper frontal teeth including the first premolars (14–24) were too high, whereas for the upper posterior right and left teeth (15–17, 25–27) these were too low (Fig. 2).

Table 3 CAD/CAM group analysis with reference to the achievement of teeth positions and their three-dimensional alignment as planned in the set-ups for the maxilla

	All teeth ($n = 252$)	Anterior teeth ($n = 108$)	Posterior teeth ($n = 144$)	Effect size (Cohen's *d*)	U test (A-P)	
					p Values	Sig. level[a]
Absolute inclination (°)	4.30 [0; 18.40]	4.30 [0; 17.30]	4.25 [0; 18.40]	0.002	0.420	N.s
Absolute angulation (°)	2.80 [0; 42.00]	2.20 [0; 42.00]	3.20 [0.10; 31.00]	0.143	0.020	*
Absolute rotation (°)	3.75 [0; 32.70]	4.65 [0; 23.60]	3.20 [0.20; 32.70]	0.271	0.017	*
Absolute mesial movement (mm)	0.51 [0; 7.34]	0.50 [0; 2.09]	0.51 [0; 7.34]	0.193	0.357	N.s
Absolute vestibular movement (mm)	0.84 [0; 5.07]	0.70 [0.01; 2.23]	1.02 [0; 5.07]	0.544	0.001	***
Absolute occlusal movement (mm)	0.63 [0.01; 5.19]	0.57 [0.01; 5.19]	0.68 [0.01; 3.21]	0.153	0.065	N.s

Absolute values of discrepancies (median [min; max]) of the dental arch for all teeth and for both frontal and posterior teeth separately and their effect size (Cohen's *d*) were reported. Given are inclination, angulation, rotation, mesial (sagittal) position, vestibular (transversal) position and occlusal (vertical) position. Mann–Whitney U test was applied to compare anterior and posterior teeth

[a] *, $p < 0.05$; ***, $p \leq 0.001$; *n.s.* not significant

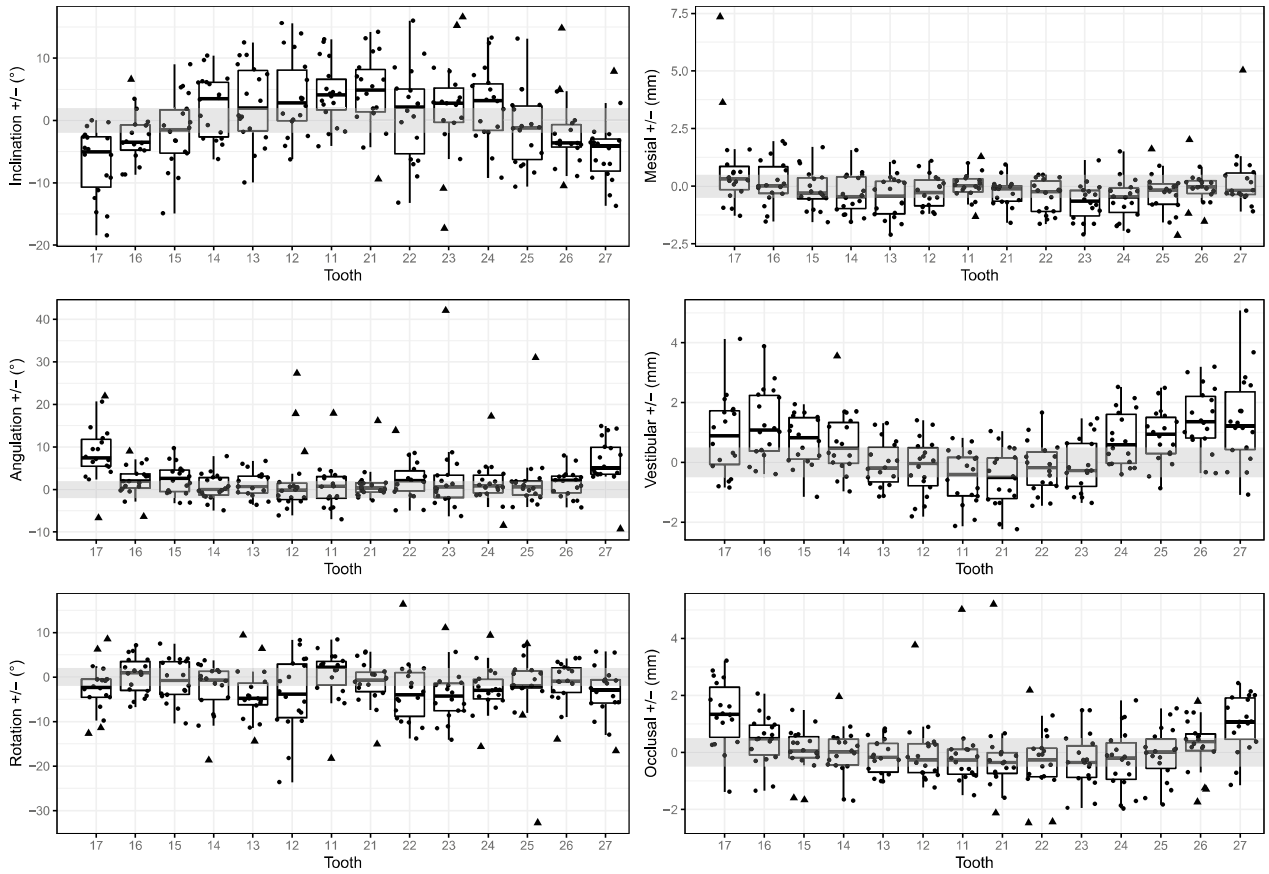

Fig. 2 Values of discrepancies of each tooth in the all three angles (inclination, angulation, rotation) and all three planes (mesial [sagittal], vestibular [transversal], occlusal [vertical]) between set-up and the situation after treatment. The grey rectangles define the "allowed" or "tolerable" areas according to Larson et al. [9]: ± 2.0° for angular and ± 0.5 mm for linear measurements

Regarding the values for angulation, posterior teeth showed greater discrepancies than anterior teeth (Table 3). Only molars showed discrepancies greater than 2° as well as the greatest range of values. Lowest discrepancies could be shown by canines and first premolars. Except of the upper right lateral incisors, the angulation of all teeth was too mesial (Fig. 2).

The results of our study showed that derotation tends to be performed better by posterior teeth than by anterior teeth ($d = 0.271$, power = 0.543; Table 3). Upper left central incisors, right first premolars, second premolars on both sides and first molars on both sides showed discrepancies lower than 2°, whereas the position of the canines after the treatment showed the greatest discrepancies to their position in the virtual set-up. Except upper right central incisors, right second premolars and right first molars, the rotation of all teeth was too distal in the end of the treatment (Fig. 2).

Discussion

Since new CAD/CAM technologies offer new possibilities concerning fixed appliances in orthodontics, their clinical effectiveness and efficiency needed to be evaluated. Our study compared various treatment variables of directly bonded customized brackets with individualized CAD/CAM brackets from the same manufacturer that were indirectly bonded. Furthermore, the treatment results of the latter system were evaluated by superimposing these with the virtual set-ups.

Inclusion criteria of our study kept the sample size relatively small and recruited patients with rather simple cases. This way, the treatment was completed in a measurable period of time and consistent material application for each patient could be guaranteed. Additionally, both treatment modalities were applied by the same orthodontist. Thus, differences in both, the concept of the ideal virtual set-up and the debonding criteria, were avoided if applied by different orthodontists.

In comparison with earlier studies, we did not find a statistical significant difference in treatment time between both study groups [5, 6]. However, our study was different in terms of design, order and inclusion criteria. While earlier data were collected in retrospective trials with different timing and several orthodontists involved in treatment, our study was performed as a prospective trial and in a defined chronological order. In addition, there were no standardized intervals between the appointments in earlier studies, whereas the patients in our study were scheduled with appointments ~ 6 weeks to avoid an impact of variable appointment intervals on total treatment time [5]. Although emergency appointments were recorded as well, this might explain the similar numbers of appointments of both groups in our study.

We observed that brackets were lost more often in group 1, which included indirectly bonded CAD/CAM brackets. However, though this was a large-sized effect ($d = 0.813$), it was missing the necessary power (power = 0.661). Therefore, these findings should be considered with caution, especially, since earlier reports showed that there were no differences in terms of bonding failure rates between directly and indirectly bonded custom brackets [4]. This leads to the assumption that clinicians might need to develop some routine in the process of indirect bonding. Since rebonding of previously lost brackets sometimes requires to return to the previous wire dimension, the number of wires used in our study was subsequently higher in group 1 than in group 2. Nevertheless, the use of bonding jigs by Insignia™ might lead to a reduction in bracket reposition. Being a medium-sized effect ($d = 0.611$), the necessary power was missing (power = 0.432). Even though this fact implies that bracket placement was more accurate for indirectly bonded brackets, this assumption needs to be viewed with caution, because additional wire bends for accurate levelling were needed equally often in both groups. An orthodontist with little experience would benefit in the initial phase of treatment from the computer-assisted method: digital placement and indirect bonding as well as prefabricated archwires do not require higher manual skills. Nevertheless, because of the individual biological reaction of each patient, good manual skills and clinical experience are necessary to finish the case.

Concerning ABO scores, our study confirmed earlier findings that showed no differences between directly bonded custom brackets, indirectly bonded custom brackets, and indirectly bonded CAD/CAM brackets [6]. Furthermore, both patient groups showed similar scores before the treatment emphasizing that the degree of severity of both groups was equivalent and reaffirms the comparability of the treatment groups. The ABO score does not take into account the sagittal position change of the incisors of the respective jaws. Any compensatory movements of the front therefore could not be evaluated this way. This is why also cephalometric analyses were necessary.

Cephalometric analyses showed that incisors were protruded in both groups before treatment and that during treatment incisors proclined even more. Using a fixed buccal bracket system, load application cannot be placed in the centre of resistance. Biomechanically, treatment with straight-wire systems leads to further protrusion of frontal teeth. Our results confirm earlier findings that showed proclination of mandibular incisors using brackets of the Damon system [13]. Even though the amount of crowding in the beginning of the treatment was similar in both groups, mandibular incisors in group 1 showed less protrusion during the treatment than in group 2. Though being a large-sized effect ($d = 0.886$), its statistical power of 0.717 was just below the limit. Nevertheless, this could be an effect of individual bracket bases and individual torque values of the brackets in group 1. To verify this finding, a superimposition of the lower jaws would have been beneficial. For superimposition of virtual set-ups with the corresponding scans of the treatment results, only data of the maxilla were used leading to a smaller data set. However, the method of superimposing landmarks of the palate was used in several studies before and is considered the most accurate superimposition approach applied to teeth of the maxilla [14]. So far, no valid method for superimposition of intraoral scans exists. Usage of CBCT data might have been a more accurate way, since this allows the registration of mandibular tooth movements. But generating CBCTs for patients that fit our inclusion criteria would have been ethically not acceptable [14].

Our superimposition data described the differences between virtual set-up and treatment results averaged over anterior and posterior teeth, respectively. Discrepancies between the virtual set-up and the clinical result of the treatment do not necessarily mean that the clinical result itself is not acceptable. It only shows that the planned tooth movement could not be performed as it was supposed. Our superimposition results showed that positions of anterior teeth were met better than the planned positions of posterior teeth. This might be caused by the smaller root surface and therefore less anchorage of anterior teeth.

In our study, tooth positions showed greatest discrepancies in the vestibular/transversal plane. The results showed that the posterior teeth have not reached their planned transversal positions and remained too palatal. Dental crowding in non-extraction cases is normally dissolved by transverse expansion and proclination of the incisors [15]. Instead of performing physical movements to widen the dental arches, posterior teeth were rather tipped buccally. This effect can be explained by the mechanical limitation

of a fixed bracket appliance. It was shown that transversal expansion of the arch by tipping of teeth will lead to relapse [16], especially in the upper molar region [17].

Since transversal tooth movement could not be performed as planned, space gain was created by anterior positioning of the frontal teeth. The dental arch of the maxilla can best be compared with the geometrical figure of an ellipse. The perimeter "*P*" of the ellipsoid is calculated by the Ramanujan approximation for the circumference of an ellipse and is given by the formula [18]:

$$P = \pi(a+b)\left\{1 + \frac{3h}{10 + \sqrt{(4-3h)}}\right\},$$
$$\text{where } h = \frac{(a-b)^2}{(a+b)^2}.$$

This formula shows that a reduction of the ellipse's width "*a*" while the perimeter of the arch "*P*" remains constant will lead to an expansion of the height "*b*" of that ellipse. Knowing that transversal movements cannot be performed as planned, alternative strategies for the creation of space must be developed before the treatment. One possibility might be an overcorrection in the virtual set-up. However, this might lead to even more buccal tipping of the molars as presented in our results. Another possibility would be to create space by precisely planned slicing in stages.

Our inclination data showed that upper incisors have not reached the required torque levels simulated in the virtual set-up. This was an expected effect, since even with arch dimensions of $0.018'' \times 0.025''$ and $0.019'' \times 0.025''$ stainless steel, no effective torque can be transmitted with a right angular slot geometry [19–24]. Clinical studies also confirm that even different prescriptions and torque angles do not result in different axis positions [25]. In addition, especially with passive self-ligating brackets, the play between slot and archwire is larger in comparison with conventional brackets due to a larger slot dimension [23]. Variations in the fabrication accuracies of the slot and the archwire dimension as well as biological factors lead to insufficient torque transmission [26].

Concerning the achieved tooth positions, mesial/sagittal positions were met best and discrepancies were in a clinical acceptable range of less than 0.5 mm. Regarding the direction of the discrepancies, our results showed that teeth were positioned too mesially. The cause of this might have been the use of low frictional brackets without auxiliary devices or selectively placed ligatures to prevent mesial drifts of the teeth and to keep anchorage levels high. It has been shown that lower incisors of patients treated with the Damon system were significantly advanced and proclined [13]. However, this effect was also shown in the control group that was treated with edgewise brackets [13]. This leads to the assumption that the straight-wire appliance itself might be responsible for the observed proclination due to biomechanical side effects. Therefore, the proclination and advancement of the incisors should be considered in treatment planning with a straight-wire appliance regardless of the used system and even if individual CAD/CAM brackets are used. This was confirmed by the angulation values that showed mesial-tipping of teeth, which can be seen as another indication of anchorage loss. In summary, the application of a CAD/CAM system requires an exact staging and selectively placed ligatures.

Values of rotation angles showed that canine positions differed the most, which can be related to their larger root surface. The clinically relevant deviation of more than 2° in ~ 50% of the teeth showed that the application of passive self-ligating brackets and archwires of small dimensions not necessarily result in an accurate derotation even if individual bracket bases were used. Passive self-ligating brackets show worse results concerning rotational control than active self-ligating brackets [27], and the used ligation technique has great influence on rotational control [28]. Taken together, we concluded that additional ligatures were needed even with individual bracket bases.

Besides accurate levelling, another main task of fixed buccal appliances is the correction of deep bite including levelling of the curve of Spee. In the upper jaw, this would lead to a relative intrusion of incisors and a relative extrusion of posterior teeth. According to the literature, levelling the curve of Spee with straight-wire appliances predominantly leads to molar extrusion and only slight intrusion of incisors occurs [29] since biological and biomechanical factors limit the intrusion movement [30]. As such, the Insignia™ bracket system is unlikely to perform incisor intrusion as planned in the virtual set-ups in the first place when straight-wire techniques are used. This is also shown by the vertical discrepancies of incisor positions between the virtual set-ups and the treatment results. Furthermore, the results of our study showed that posterior teeth failed to perform extrusion as planned. As a result, deep bite correction could not be performed as planned in the virtual set-ups, and the use of individual bracket bases cannot correct this type of malocclusion on its own.

Randomized clinical trials (RCTs) are considered being of highest evidence. Nevertheless, it should be mentioned that even RCT studies are not necessarily bias-free [31]. Herein, a single-centre study was described applying a quasi-randomized protocol for patient allocation. As such waiting times for patients were limited, and all patients were treated in a reasonable period of

time. As discussed by Bondemark and Ruf [31], complete blinding in a clinical study like this is almost impossible, since patient and caregiver exactly know which treatment modality was applied. However, treatment, measurements, and statistics were performed by different persons, which also reduced the risk of bias. Therefore, when weighting and interpreting the results, these points should be taken into account.

Conclusions

1. Virtual treatment planning and individualized bracket bases and bracket positioning seemed to have no influence on overall treatment time, number of appointments, number of archwire bends, and the reduction of ABO-scores.
2. Treatment with both systems leads to further proclination of incisors.
3. Comparing the treatment results with the virtual set-ups, mesial positions were met best, followed by vertical positions. Transversal positions showed the greatest discrepancies. Concerning angles, values for angulation showed greatest accordance to the virtual set-up, while values of inclinations showed greatest discrepancies.
4. The use of individualized bracket systems and the development of virtual set-ups does require well-considered space management as well as exact planning of anchorage devices and selectively placed ligatures.
5. Transversal expansion, deep bite correction, expression of torque, and anchorage loss remain challenges in the treatment with straight-wire appliances.

Abbreviations
ABO: American Board of Orthodontics; CAD/CAM: Computer-aided design/computer-aided manufacturing; SD: Standard deviation.

Supplementary Information

The online version contains supplementary material available at https://doi.org/10.1186/s40510-021-00386-0.

Additional file 1. CONSORT 2010 flow diagram.

Additional file 2. CONSORT 2010 checklist.

Acknowledgements
Not applicable.

Authors' contributions
JH drafted the manuscript and carried out the measurements. LS designed the study, treated the patients, and collected the data. CC assisted in data analysis and contributed to manuscript finalization. UB drafted the manuscript and carried out the statistical analysis. HS contributed to the analysis and revised the manuscript. AW supervised study, measurements and analysis and drafted the manuscript. All authors read and approved the final manuscript.

Funding
During the initial phase of this study, L.S. received funding from Ormco. Ormco also provided the materials. Ormco had no influence on study design, analysis and reporting.

Availability of data and materials
The datasets used and/or analysed during the current study are available from the corresponding author upon reasonable request.

Declarations

Ethics approval and consent to participate
The study protocol was approved by the local ethics committee and registered at the German Register of Clinical Studies (DRKS00024350).

Consent for publication
Not applicable.

Competing interests
None.

Received: 19 April 2021 Accepted: 20 September 2021
Published online: 06 December 2021

References

1. Miyazaki T, Hotta Y, Kunii J, Kuriyama S, Tamaki Y. A review of dental CAD/CAM: current status and future perspectives from 20 years of experience. Dent Mater J. 2009;28(1):44–56.
2. Al Mortadi N, Eggbeer D, Lewis J, Williams RJ. CAD/CAM/AM applications in the manufacture of dental appliances. Am J Orthod Dentofac Orthop. 2012;142(5):727–33.
3. Koo BC, Chung CH, Vanarsdall RL. Comparison of the accuracy of bracket placement between direct and indirect bonding techniques. Am J Orthod Dentofac Orthop. 1999;116(3):346–51.
4. Li Y, Mei L, Wei J, Yan X, Zhang X, Zheng W, et al. Effectiveness, efficiency and adverse effects of using direct or indirect bonding technique in orthodontic patients: a systematic review and meta-analysis. BMC Oral Health. 2019;19(1):137.
5. Weber DJ 2nd, Koroluk LD, Phillips C, Nguyen T, Proffit WR. Clinical effectiveness and efficiency of customized vs. conventional preadjusted bracket systems. J Clin Orthod. 2013;47(4):261–6 (**quiz 8**).
6. Brown MW, Koroluk L, Ko CC, Zhang K, Chen M, Nguyen T. Effectiveness and efficiency of a CAD/CAM orthodontic bracket system. Am J Orthod Dentofac Orthop. 2015;148(6):1067–74.
7. Lefebvre C, Glanville J, Briscoe S, Littlewood A, Marshall C, Metzendorf M-I, et al. Technical Supplement to Chapter 4: Searching for and selecting studies. . In: Higgins JPT, Thomas J, Chandler J, Cumpston MS, Li T, Page MJ, et al., editors. Cochrane Handbook for Systematic Reviews of Interventions Version 62 (updated February 2021): Cochrane; 2021.
8. Schulz KF, Altman DG, Moher D, Group C. CONSORT 2010 statement: updated guidelines for reporting parallel group randomised trials. BMJ. 2010;340:c332.
9. Larson BE, Vaubel CJ, Grunheid T. Effectiveness of computer-assisted orthodontic treatment technology to achieve predicted outcomes. Angle Orthod. 2013;83(4):557–62.
10. Little RM. The irregularity index: a quantitative score of mandibular anterior alignment. Am J Orthod. 1975;68(5):554–63.
11. Andrews LF. Straight wire—the concept and appliance. San Diego: LA Wells Co.; 1989.
12. Faul F, Erdfelder E, Lang AG, Buchner A. G*Power 3: a flexible statistical power analysis program for the social, behavioral, and biomedical sciences. Behav Res Methods. 2007;39(2):175–91.

13. Vajaria R, BeGole E, Kusnoto B, Galang MT, Obrez A. Evaluation of incisor position and dental transverse dimensional changes using the Damon system. Angle Orthod. 2011;81(4):647–52.
14. Klaus K, Xirouchaki F, Ruf S. 3D-analysis of unwanted tooth movements despite bonded orthodontic retainers: a pilot study. BMC Oral Health. 2020;20(1):308.
15. Fleming PS, Lee RT, McDonald T, Pandis N, Johal A. The timing of significant arch dimensional changes with fixed orthodontic appliances: data from a multicenter randomised controlled trial. J Dent. 2014;42(1):1–6.
16. Reitan K. Principles of retention and avoidance of posttreatment relapse. Am J Orthod. 1969;55(6):776–90.
17. Kahl-Nieke B, Fischbach H, Schwarze CW. Treatment and postretention changes in dental arch width dimensions—a long-term evaluation of influencing cofactors. Am J Orthod Dentofac Orthop. 1996;109(4):368–78.
18. Singaraju GS, Js YP, Mandava P, Ganugapanta VR, Teja NR, Jn PR. Data set for computation of maxillary arch perimeter with ramanujan's equation for ellipse in different skeletal malocclusions. Data Brief. 2020;32:106079.
19. Wichelhaus A. A new elastic slot system and V-wire mechanics. Angle Orthod. 2017;87(5):774–81.
20. Major TW, Carey JP, Nobes DS, Major PW. Orthodontic bracket manufacturing tolerances and dimensional differences between select self-ligating brackets. J Dent Biomech. 2010;2010:781321.
21. Kusy RP, Whitley JQ. Assessment of second-order clearances between orthodontic archwires and bracket slots via the critical contact angle for binding. Angle Orthod. 1999;69(1):71–80.
22. Cash AC, Good SA, Curtis RV, McDonald F. An evaluation of slot size in orthodontic brackets—are standards as expected? Angle Orthod. 2004;74(4):450–3.
23. Brauchli LM, Senn C, Wichelhaus A. Active and passive self-ligation-a myth? Angle Orthod. 2011;81(2):312–8.
24. Fattori L, Brangeli LAM, Capelozza FL. Assessment of tooth inclination in the compensatory treatment of pattern II using computed tomography. Dental Press J Orthod. 2010;15(5):118–29.
25. Mittal M, Thiruvenkatachari B, Sandler PJ, Benson PE. A three-dimensional comparison of torque achieved with a preadjusted edgewise appliance using a Roth or MBT prescription. Angle Orthod. 2015;85(2):292–7.
26. Pandis N, Strigou S, Eliades T. Maxillary incisor torque with conventional and self-ligating brackets: a prospective clinical trial. Orthod Craniofac Res. 2006;9(4):193–8.
27. Pesce RE, Uribe F, Janakiraman N, Neace WP, Peterson DR, Nanda R. Evaluation of rotational control and forces generated during first-order archwire deflections: a comparison of self-ligating and conventional brackets. Eur J Orthod. 2014;36(3):245–54.
28. Bednar JR, Gruendeman GW. The influence of bracket design on moment production during axial rotation. Am J Orthod Dentofac Orthop. 1993;104(3):254–61.
29. Weiland F, Bantleon HP, Droschl H. The orthodontic treatment of deep bite in adults—a comparison of the straight-wire appliance and the segmented arch technic. Fortschr Kieferorthop. 1992;53(3):153–60.
30. Preston CB, Maggard MB, Lampasso J, Chalabi O. Long-term effectiveness of the continuous and the sectional archwire techniques in leveling the curve of Spee. Am J Orthod Dentofac Orthop. 2008;133(4):550–5.
31. Bondemark L, Ruf S. Randomized controlled trial: the gold standard or an unobtainable fallacy? Eur J Orthod. 2015;37(5):457–61.

Publisher's Note

Springer Nature remains neutral with regard to jurisdictional claims in published maps and institutional affiliations.

Submit your manuscript to a SpringerOpen journal and benefit from:

► Convenient online submission
► Rigorous peer review
► Open access: articles freely available online
► High visibility within the field
► Retaining the copyright to your article

Submit your next manuscript at ► springeropen.com

Clinical Oral Investigations
https://doi.org/10.1007/s00784-023-05125-9

RESEARCH

Accuracy of maxillary positioning using computer-designed and manufactured occlusal splints or patient-specific implants in orthognathic surgery

Yoana Malenova[1] · Florian Ortner[1] · Paris Liokatis[1] · Selgai Haidari[1] · Matthias Tröltzsch[1,2] · Florian Fegg[1] · Katharina T. Obermeier[1] · Jens T. Hartung[1] · Tamara K. Kakoschke[1] · Egon Burian[3] · Sven Otto[1] · Hisham Sabbagh[4] · Florian A. Probst[1]

Received: 19 February 2023 / Accepted: 20 June 2023
© The Author(s) 2023

Abstract

Objective To determine the accuracy of maxillary positioning using computer-designed and manufactured occlusal splints or patient-specific implants in orthognathic surgery.

Material and Methods A retrospective analysis of 28 patients that underwent virtually planned orthognathic surgery with maxillary Le Fort I osteotomy either using VSP-generated splints ($n = 13$) or patient-specific implants (PSI) ($n = 15$) was conducted. The accuracy and surgical outcome of both techniques were compared by superimposing preoperative surgical planning with postoperative CT scans and measurement of translational and rotational deviation for each patient.

Results The 3D global geometric deviation between the planned position and the postoperative outcome was 0.60 mm (95%-CI 0.46–0.74, range 0.32–1.11 mm) for patients with PSI and 0.86 mm (95%-CI 0.44–1.28, range 0.09–2.60 mm) for patients with surgical splints.

Postoperative differences for absolute and signed single linear deviations between planned and postoperative position were a little higher regarding the x-axis and pitch but lower regarding the y- and z-axis as well as yaw and roll for PSI compared to surgical splints.

There were no significant differences regarding global geometric deviation, absolute and signed linear deviations in the x-, y-, and z-axis, and rotations (yaw, pitch, and roll) between both groups.

Conclusions Regarding accuracy for positioning of maxillary segments after Le Fort I osteotomy in orthognathic surgery patient-specific implants and surgical splints provide equivalent high accuracy.

Clinical relevance Patient-specific implants for maxillary positioning and fixation facilitate the concept of splintless orthognathic surgery and can be reliably used in clinical routines.

Keywords PSI · Patient-specific implants · Occlusal splint · Orthognathic Surgery · CAD/CAM

Introduction

In orthognathic surgery, preoperative clinical findings, 2D radiographs, plaster models, and consecutive manual model surgery have been the basis of treatment planning for many years. Model surgery in semi-adjustable articulators has been transferred into the operating theatre using interocclusal splints [1, 2]. However, conventional techniques are limited due to lack of control in the third dimension, inaccuracy of face-bow transfer or interocclusal splints [3, 4], and autorotation of the temporomandibular joint in the supine and anesthetized patient [5]. Especially in patients with strong occlusal tilt and asymmetric

✉ Yoana Malenova
yoanamalenova@gmail.com

1 Department of Oral and Maxillofacial Surgery and Facial Plastic Surgery, University Hospital LMU Munich, Munich, Germany

2 Center for Oral, Maxillofacial, and Facial Reconstructive Surgery, Ansbach, Germany

3 Institute of Diagnostic and Interventional Radiology, Technical University of Munich, School of Medicine, Munich, Germany

4 Department of Orthodontics and Dentofacial Orthopedics, University Hospital LMU Munich, Munich, Germany

Published online: 29 June 2023

deformities positioning of the maxilla has been demanding [6]. Another difficulty in conventional treatment planning is the impact on soft tissue and smile line.

To improve accuracy, computer-aided design (CAD) and computer-aided manufacturing (CAM) have been applied increasingly within the past decade. Furthermore, virtual treatment planning offers the possibility to simulate postoperative soft tissue prediction using preoperative computed tomography (CT) scans [7, 8]. Initial approaches such as computer designed and manufactured splints were the first promising techniques using virtual 3D planning [9–12]. Other techniques use locating guides accompanied with pre-bent titanium plates on the basis of a resin model manufactured using laser sintering rapid prototyping that depicts the planned outcome [13]. Another method to improve positioning is intraoperative simulation-guided navigation [14]. Newer waferless techniques use cutting guides and patient-specific implants (PSI) without interocclusal reference [15–17].

In general, virtual treatment planning regarding CAD/CAM surgical splints, navigation, and soft tissue planning appear to be accurate and reproducible methods for orthognathic surgery [18]. Few studies indicate that positioning using customized cutting guides and PSI leads to higher clinical accuracy in orthognathic surgery [19–21].

Yet, the best and most accurate transfer of virtual planning into surgery is necessary so that the advantages of CAD/CAM in orthognathic surgery come into use. Therefore, the aim of this study was to determine the accuracy of maxillary positioning in relation to virtual treatment planning using CAD/CAM patient-specific implants compared with VSP-generated surgical splints.

Material and methods

Study design

The presented survey is a retrospective single-center cohort study. The institutional review board authorized the study, and informed consent was waived (Ethics Committee, Ludwig-Maximilians-University, Munich, Germany: Ref.-No. 21-0164). Study participants were selected from an electronic database at our hospital. The database consecutively included all patients who received orthognathic surgery in the Department of Oral and Maxillofacial Surgery and Facial Plastic Surgery, University Hospital, Munich, Germany between January 2015 and December 2020. The study follows the standards for reporting observational studies (STROBE guidelines) [22].

Study population

The study population consisted of patients who underwent virtually planned orthognathic surgery with maxillary Le Fort I osteotomy using computer designed and either manufactured surgical splints or PSIs. The decision on virtually planned surgical intervention and manufacturing of a VSP-generated splint or PSI was made in the context of an individual case decision of the treating surgeons each with more than 10 years of experience in this subject. Only primary maxillary or bimaxillary osteotomies were included in the study (uniformly as maxilla-first surgery). A further inclusion criterion was the availability of a post-interventional high-resolution computed tomography (CT, isotropic resolution ≤ 1 mm) in the Department of Radiology, University Hospital, Munich, Germany within 2 weeks after surgery. The CT scans in all cases were performed before the postoperative orthodontic readjustment. Patients with underlying syndromic disease, cleft lip, palate, or secondary orthognathic surgery as well as patients younger than 18 years were excluded from the study.

Clinical workflow

Patients with indications for combined orthodontic orthognathic surgical treatment first received orthodontic pretreatment. After completion of pretreatment preoperative preparation for each patient included clinical examination by maxillofacial surgeons, high-resolution CT scans (isotropic resolution 0.625 mm), production of plaster models, and occlusal scans of the corresponding dental arch. Resulting DICOM data from CT scans and STL data from occlusal scans were transferred to an industrial partner for subsequent virtual surgical planning (VSP) using ProPlan CMF software (Materialise®, Leuven, Belgium). At first, the preoperatively collected high-resolution CT scans (DICOM data) were imported and lined up in the natural head position with respect to the Frankfurt horizontal plane, facial midline, and bibupillary line [23]. Subsequently, the occlusal scans (STL data) were imported and combined with the CT scan using a semiautomatic fusing algorithm resulting in a model with high-resolution of the dental arch.

The following steps including cephalometric analysis, virtual Le Fort I, and BSS (Bilateral Sagittal Split) osteotomies for maxillary and mandibular movement respectively were performed with the corresponding analysis tools provided by the software. Based on the clinical findings and the virtual models, the segments of the upper and lower jaw were merged in final occlusion and the monoblock of the osteotomized maxilla and mandible then shifted into the final position in relation to the cranial base

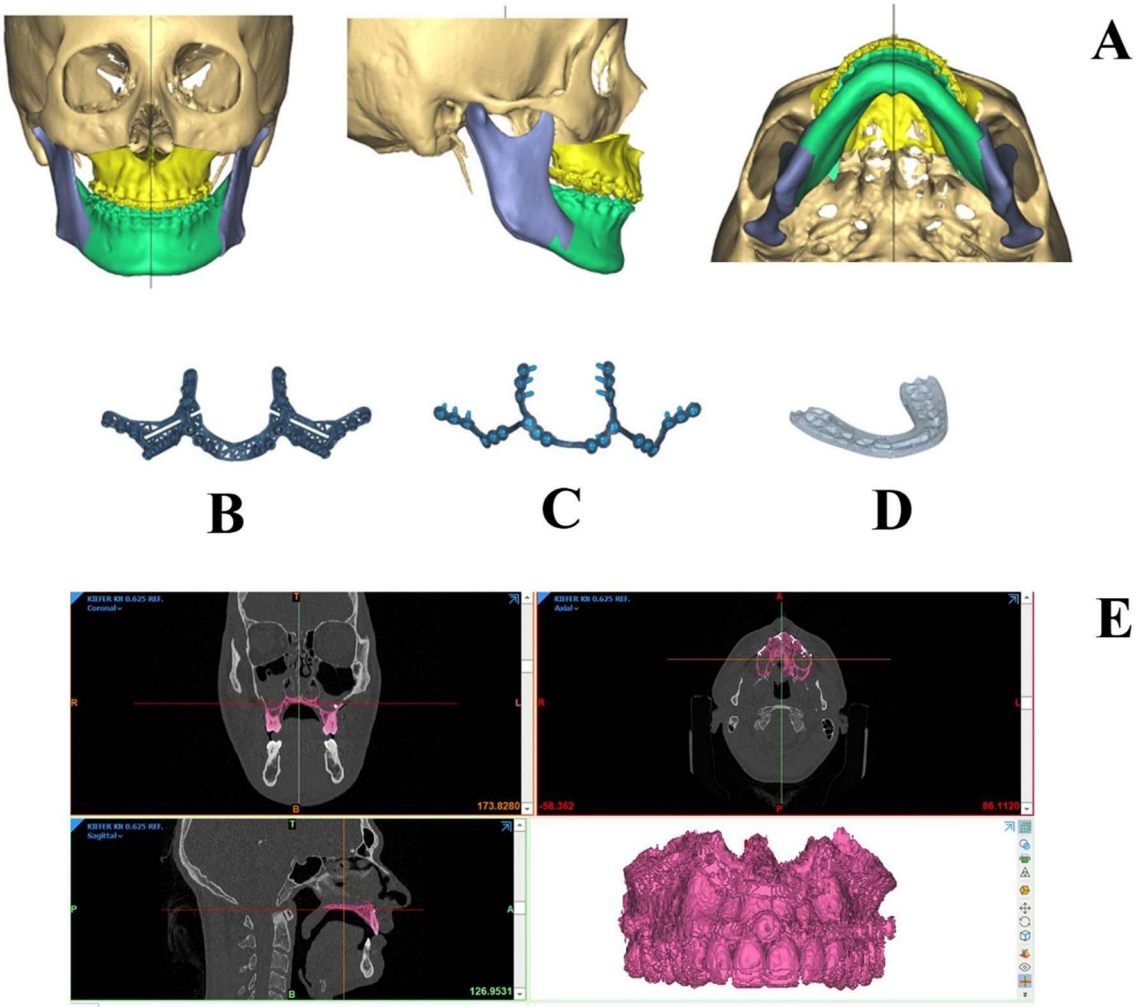

Fig. 1 Planned postoperative position before bimaxillary orthognathic surgery with maxillary advancement and retropositioning of the lower jaw. Maxilla in yellow, mandibular body in green, and rami in blue (**A**), CAD/CAM cutting guide (**B**), patient-specific implants (PSI, **C**), and VSP generated surgical splints (**D**), segmentation of postoperative CT-scan using Mimics software (Materialise, Leuven, Belgium). The maxillary segment in purple (**E**)*

or the two articulated rami respectively (Fig. 1). Finally, an automated soft tissue simulation was performed using the same software (ProPlan CMF software, Materialise, Leuven, Belgium).

Positioning was checked regarding the position of the osteotomized maxilla and mandible (including the dental arches) in relation to the midface, skull base, center line, occlusal plane, and soft tissue.

This way, movement in all three dimensions of the osteotomized maxilla and mandible was encoded into the design and shape of either surgical splints or PSIs (Fig. 1B, C, and D).

After finishing the planning process and final approval by the surgeon the cutting guides, surgical splints as well as the PSIs went into computer-aided manufacturing (CAM) using resin based or selective laser melting (SLM), respectively. After sterilization, the operations were performed under general anesthesia by certified specialists for oral and maxillofacial surgery.

All cutting guides, as well as surgical splints or PSIs, were placed freehand, without the use of navigational systems or physical positioning guides. In bimaxillary surgery, maxillary repositioning was performed as the first step.

Postoperatively, high-resolution CT scans (isotropic resolution 0.625 mm) and routine ophthalmologic and follow-up clinical examinations were performed. Postoperative CT scans were performed as part of the clinical routine and before the start of any post-operative elastic treatment or otherwise orthodontic treatment.

Data acquisition

The primary outcome variable was defined as the global geometric deviation between the virtually planned and the finally position of the maxilla determined by computed tomography in both groups.

First, postoperative CT scans were segmented using Mimics software (Materialise, Leuven, Belgium) differentiating soft tissue (HU < 300), bone tissue (HU 300–1500), and titanium (HU > 2000) (Fig. 1E).

Data were exported as STL files (.stl) into 3-matic (Materialise, Leuven, Belgium), a dedicated CAD analyzing software. The corresponding STL files of the virtual treatment planning were provided by the industrial partner (Materialise, Leuven, Belgium) and imported into 3-matic as well. The non-osteotomized upper midfaces of the pre and postoperative datasets were aligned employing a semiautomatic superimposition algorithm. A 3-point alignment procedure (first alignment, Fig. 2A) followed by a semiautomatic superimposition algorithm (with 10 iterations) led to a matching of both datasets with an accuracy of approximately 30 µm (final alignment).

Subsequently, five measurement points were marked for each patient in the virtually planned and actual postoperative positions. For the best possible reproducible and precise measurement, five points with the greatest possible distance on the dental at the cusp tips of the maxillary teeth were chosen (the mesiobuccal cusps of the second molars, the tips of the canines, and the mesial contact point of the incisors) (Fig. 2B).

The geometric deviation between the virtually planned and the finally resulting position was compared by assessing differences in the entire bone surface and direct distances between the corresponding 5 selected reference points in spatial planes representing the primary outcome variables.

First 3D global geometric deviations were calculated. Therefore, the entire bone surface points of the virtually planned position were assigned to the respective closest points of the corresponding bone surface in the postoperative data set, and the respective Euclidean distances were measured.

Thereafter, direct distances between the respective five reference points of the maxillary teeth were measured and single linear deviations according to the spatial axes (x-, y-, z-axis) were evaluated with regard to absolute and signed linear deviations (Fig. 2C).

The x-axis is corresponding to transversal (lateral/medial), the y-axis is corresponding to sagittal (anterior/posterior), and the z-axis is corresponding to axial (cranial/caudal) movement. The planning model represented the starting point, and accordingly, the deviations of the postoperative position of the maxillary segment in the x-axis are defined as right/left. Differences to the right were defined as positive and those to the left as negative deviations.

For the assessment of rotational movements, angles in the corresponding planes were measured. Thus, for yaw angles in the x-y-plane, for pitch in the y–z-plane, and for a roll in the x-z-plane were evaluated.

Finally, color-coded heatmaps were generated to visualize areas with high or low deviation and therefore the distribution of geometric deviations (Fig. 2D).

Statistics

Statistical analysis was performed using Excel (Microsoft, Redmond, USA) and SPSS 26 (SPSS Inc., Chicago, USA). Descriptive statistics were carried out for each study variable. Thus, means and standard deviations were calculated for global deviations between the bone segments, Euclidean distances, and absolute or signed distances in spatial axes for each measurement point in both groups as well as rotation angles.

For normally distributed data means were statistically compared by performing a student's t-test. Normally distributed data was presented using mean ± standard deviation (SD).

Non-normally distributed data (according to Kolmogorov-Smirnov-Test und Shapiro-Wilk-Test) were statistically compared using the nonparametric Mann-Whitney U test. Non-normally distributed data were illustrated by depicting median and interquartile ranges.

Statistical significance was defined as $p \leq 0.05$.

Intraclass correlation (ICC) assessed inter-rater agreement with respect to global deviations, Euclidean distances, and single linear deviations in the x-, y-, and z-axis of five corresponding measurement points as well as rotation angles.

Results

The study included 28 patients that underwent virtually planned orthognathic surgery with maxillary Le Fort I osteotomy. In 15 patients (6 female, 9 male; average age: 27.6 years), maxillary positioning was conducted using PSI. In 13 patients (6 female, 7 male; average age: 27.5 years), surgical splints were used. In each group, there is one patient who only required correction of the upper jaw whereas the other patients underwent a bimaxillary osteotomy. In all cases, maxillary retrognathia was observed, and the choice of therapy in favor of the maxillary advancement was made accordingly.

Intraclass correlation (ICC) assessing inter-observer reliability of single linear deviations was 0.977 (PSI) and 0.918 (surgical splint).

3D global geometric deviation (in mm)

The 3D global geometric deviation between planned position and postoperative outcome referred to as "mean surface distance" was 0.60 mm (95%-CI 0.46–0.74, range 0.32–1.11 mm)

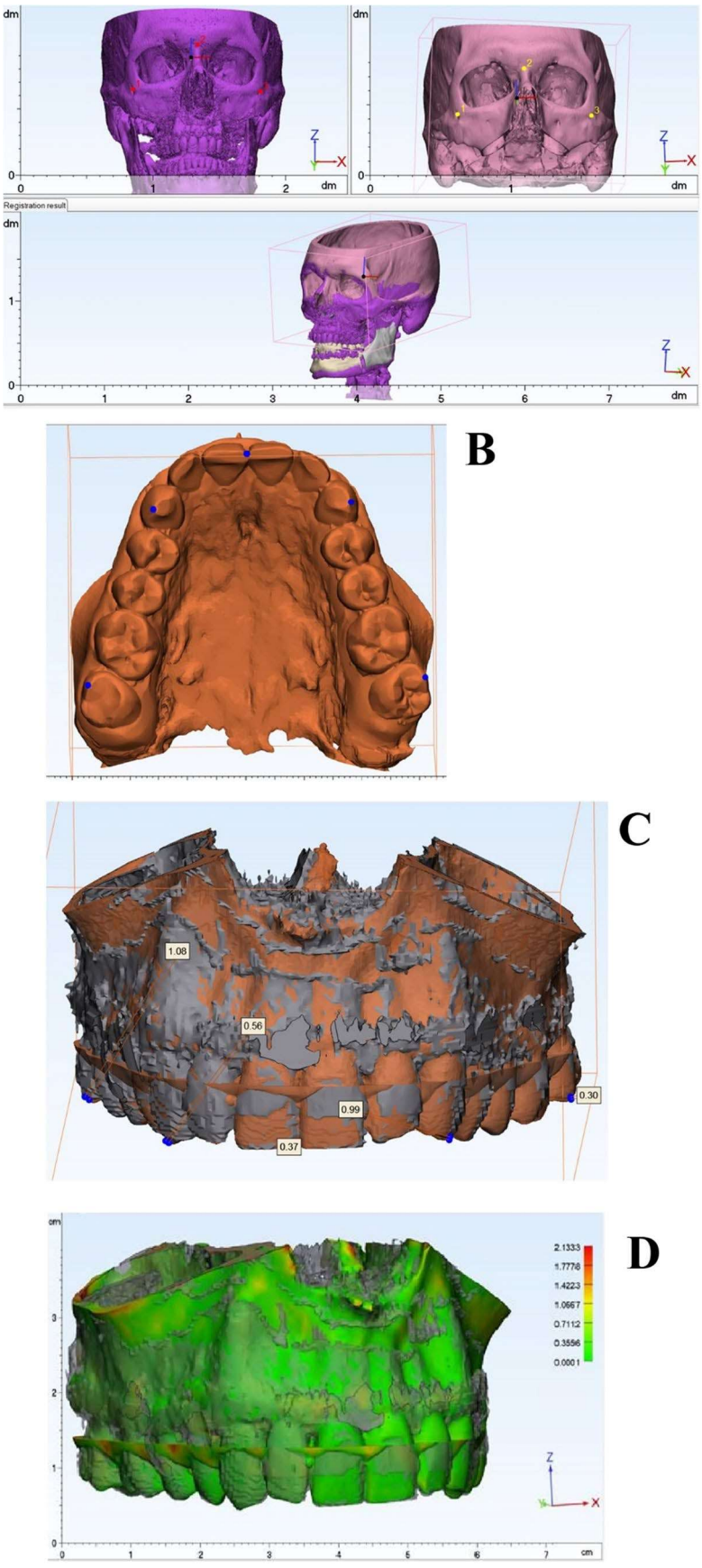

Fig. 2 First alignment of planned (pink) and postoperative (purple) dataset using 3-matic software (Materialise, Leuven, Belgium) (**A**), selection of five measurement points: mesiobuccal cusps of the second molars, tips of the canines and mesial contact point of the incisors (**B**), measurement of direct distances between the respective five reference points of the maxillary teeth and subsequent evaluation of discrepancies in the spatial axes (**C**), color-coded heatmap visualizing areas with high (red) or low deviation (green) (**D**)

for patients with PSI and 0.86 mm (95%-CI 0.44–1.28, range 0.09–2.60 mm) for patients with surgical splints. This difference was not statistically significant (level of significance $p < 0.05$). Compare Fig. 3A.

Absolute linear deviations of five corresponding reference points according to the spatial axes (in mm)

Absolute linear deviations in the x-, y-, and z-axis for five corresponding reference points between the planned and the postoperative position were slightly higher regarding the x-axis but lower regarding the y- and z-axis for PSIs compared to surgical splints. The highest deviation was found in the y-axis for surgical splints. There were no statistically significant differences between the x-, y-, and z-axis comparing both groups (level of significance $p < 0.05$, Friedman test). Compare Table 1 and Fig. 3B.

Signed linear deviations for five corresponding reference points (in mm):

Signed linear deviations in the x-, y-, and z-axis for five corresponding reference points between the planned and the postoperative position were higher regarding the x-axis (to the right) but lower regarding the y- and z-axis for PSIs compared to surgical splints. The highest deviation (posterior) was found in the y-axis for surgical splints. For patients with PSI maxillary segments by trend were positioned to the right. There were no statistically significant differences between the x-, y-, and z-axis comparing both groups (level of significance $p < 0.05$, Friedman test). Compare Table 2 and Fig. 3C.

Rotations yaw, pitch, and roll (in degree)

With respect to rotations pitch (transversal axis), yaw (longitudinal axis), and roll (sagittal axis) the planned and the postoperative position were a little higher regarding pitch but lower regarding yaw and roll for PSIs compared to surgical splints. There were no statistically significant differences between rotations comparing both groups ($p < 0.05$, Friedman test). Compare Table 3 and Fig. 4.

Discussion

Particularly over the past decades, a lot of research groups and medical device manufacturers have made great efforts to improve 3D treatment planning and technical devices in order to improve accuracy and predictability in orthognathic surgery.

The first promising approaches included VSP-generated surgical splints, locating guides with pre-bent titanium plates on the basis of a resin model as well as intraoperative simulation-guided navigation [9–14].

Newer waferless techniques use cutting guides and patient-specific implants (PSI) without interocclusal reference [15–17], and some studies indicate that positioning using this technique leads to higher clinical accuracy in orthognathic surgery [19–21]. Therefore, the aim of this study was to determine the accuracy of maxillary positioning in relation to virtual treatment planning using either VSP-generated surgical splints or PSI.

Our results show comparable high accuracy of maxillary positioning using PSI or VSP-generated surgical splints with discrepancies less than 1 mm. In this study, there was no significant difference regarding any examined parameter for postoperative outcome after surgery between both techniques. Yet, deviations between the planned and postoperative position of the maxilla were lower with respect to 3D global geometric deviation, the y- and z-axis regarding for absolute and signed linear deviations in spatial axes as well as yaw and roll regarding rotations for PSIs compared to surgical splints.

Various studies have tried to analyze the accuracy of 3D virtually treatment planning of orthognathic surgery by different evaluating methods. Yet, there is no uniform measurement and statistical method available. The methods include measurement of linear and angular deviations between manually set landmarks, calculation of translational and rotational deviations with or without manually set reference points, color-coded heatmaps as well as intraclass coefficients [5, 9, 19–21, 24–34]. To achieve reliable results, this study combined these so far known evaluation methods. Besides artifacts in CT scans, every single method has its inaccuracy, such as imprecise manually set reference points or software-related inaccuracies. However, the different evaluation methods yielded comparable results in this study.

The main benefit of wafer-less surgery with CAD/CAM cutting guides and PSI is that positioning is conducted without interocclusal reference and therefore independent of the temporomandibular joint which should theoretically be more accurate for transferring the virtual plan into orthognathic surgery with maxillary Le Fort I osteotomy [19–21]. In our study, discrepancies tend to be a little lower for PSIs compared to surgical splints. Yet, VSP-generated surgical splints were a little more accurate regarding absolute and signed linear deviations in the x-axis as well as pitch in terms of rotational movements. For patients with PSI maxillary segments by trend were positioned to the right which might be caused by the operational perspective of the surgeon who is usually standing on the patient's right side. The highest alterations were found for absolute and signed linear (posterior) deviations

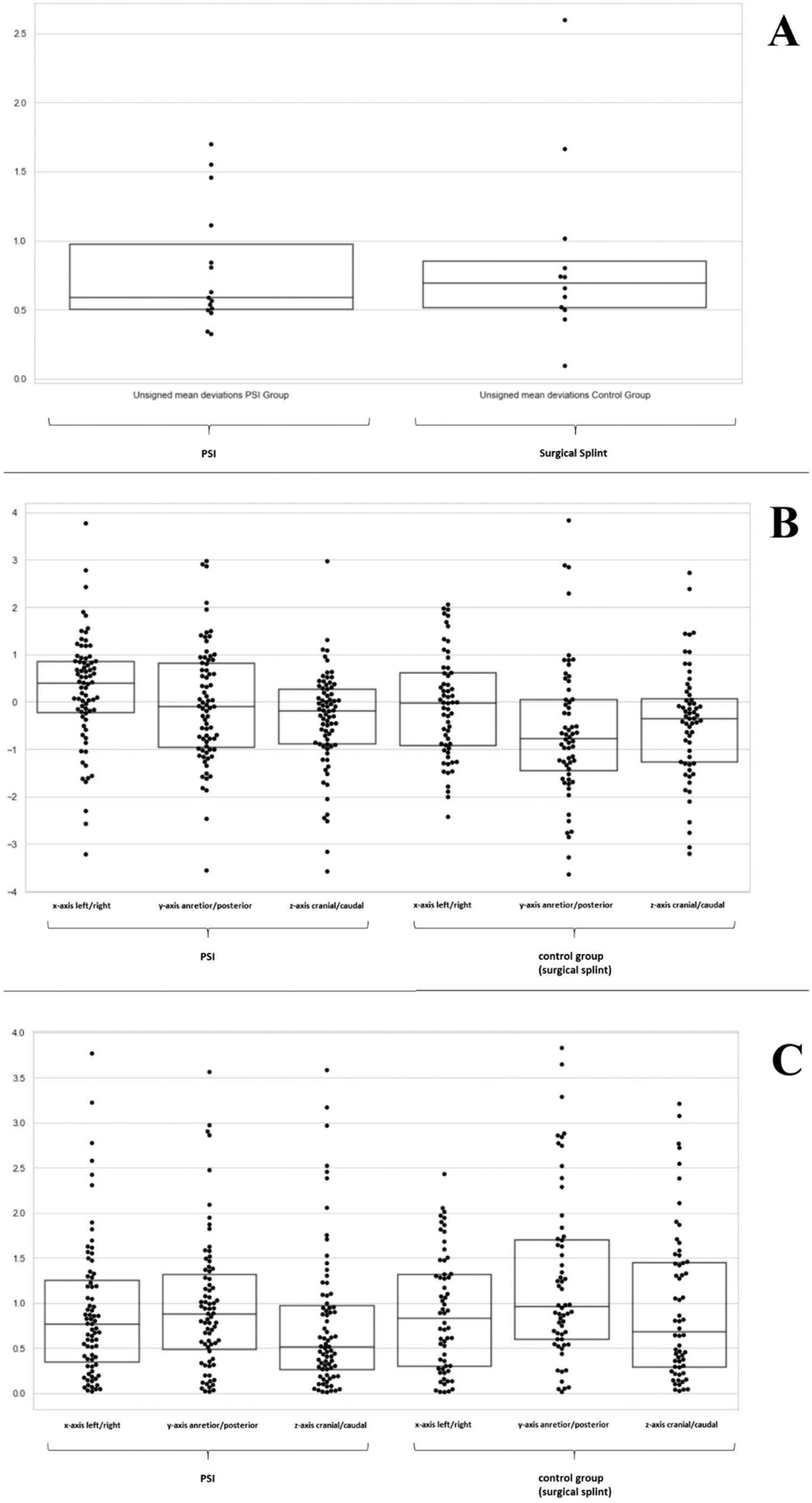

Fig. 3 3D global geometric deviation ("mean surface distance") between the planned position and the postoperative outcome was a little lower for patients with PSI (**A**), absolute linear deviations in the x-, y-, and z-axis for five corresponding reference points between the planned and the postoperative position for PSI group (on the left) and patients with VSP generated surgical splint (on the right) (**B**), signed linear deviations in the x-, y-, and z-axis for five corresponding reference points between the planned and the postoperative position for PSI group (on the left) and patients with VSP generated surgical splint (on the right) (**C**)

Table 1 Absolute linear deviations in the x-, y-, and z-axis for five corresponding reference points between the planned and the postoperative position for PSI compared to surgical splints

	PSI	Surgical splint	*p*
x-axis (left/right)	0.90 mm (95%-CI 0.73–1.08, range 0.02–3.77 mm)	0.89 mm (95%-CI 0.72–1.06, range 0.01–2.43 mm)	1.00
y-axis (anterior/posterior)	0.97 mm (95%-CI 0.80–1.14, range 0.02–3.56 mm)	1.26 mm (95%-CI 1.01–1.50, range 0.01–3.83 mm)	1.00
z-axis (cranial/caudal)	0.77 mm (95%-CI 0.59–0.95, range 0.01–3.58 mm)	0.96 mm (95%-CI 0.74–1.18, range 0.02–3.21 mm)	0.25

Table 2 Signed linear deviations in the x-, y-, and z-axis for five corresponding reference points between the planned and the postoperative position for PSI compared to surgical splints

	PSI	Surgical splint	*p*
x-axis (right/left)	0.24 mm (95%-CI − 0.02–0.51, range 3.22–3.77 mm)	− 0.09 mm (95%-CI (− 0.38)–0.19, range (− 2.43)–2.05 mm)	0.42
y-axis (anterior/posterior)	− 0.06 mm (95%-CI (− 0.34)–0.23, range (-3.56)–2.97 mm)	− 0.63 mm (95%-CI (− 1.00)–(− 0.26), range (− 3.65)–3.83 mm)	0.22
z-axis (cranial/caudal)	− 0.37 mm (95%-CI (− 0.61)–(− 0.13), range (− 3.58)–2.97 mm)	− 0.44 mm (95%-CI (− 0.75)–(− 0.13), range (− 3.21)–2.72 mm)	1.00

Table 3 Rotations yaw (longitudinal axis), pitch (transversal axis), and roll (sagittal axis) between the planned and the postoperative position for PSI compared to surgical splints

	PSI	Surgical splint	*p*
Yaw (longitudinal axis)	2.19 (95%-CI 1.71–2.67, range 0.05–7.90)	2.64 (95%-CI 1.90–3.38, range 0.04–11.64)	0.77
Pitch (transversal axis))	2.17 (95%-CI 1.64–2.70, range 0.15–8.36)	2.10 (95%-CI 1.62–2.57, range 0.05–7.12)	0.25
Roll (sagittal axis)	2.96 (95%-CI 2.22–3.71, range 0.05–11.15)	3.19 (95%-CI 2.34–4.04, range 0.03–10.86)	0.25

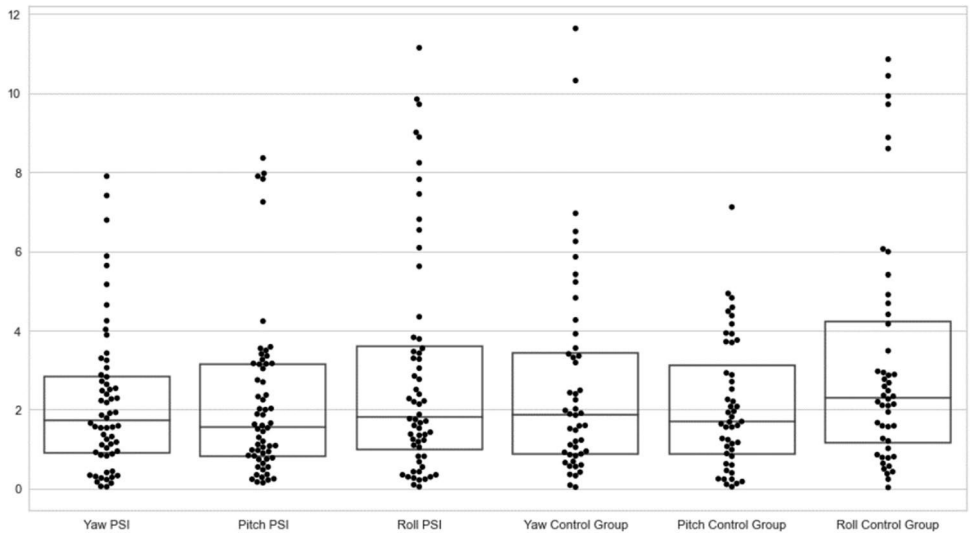

Fig. 4 Differences in rotations pitch (transversal axis), yaw (longitudinal axis), and roll (sagittal axis) between the planned and the postoperative position for the PSI group (on the left) and patients with a surgical splint (on the right)

in the y-axis for surgical splints, which indicate an undercorrection in maxillary advancement.

Given the small sample size of our study, missing significance in this analysis should not be interpreted as the definite absence of a real effect. By trend positioning of the maxillary segment was more accurate using PSI compared to VSP-generated splints.

Prospective randomized and controlled trials are necessary to finally assess which method is more accurate. However, our results show that both methods provide

high clinical accuracy. The simultaneous use of PSI with VSP-generated surgical splints for maxillary positioning in orthognathic surgery might have a complementary effect.

Conclusion

There were no statistically significant differences in the positioning of maxillary segments after Le Fort I osteotomy between patient-specific implants and surgical splints regarding 3D global geometric deviation, absolute and signed linear deviations in the x-, y-, and z-axis, and rotations (yaw, pitch, and roll) comparing both groups. Therefore, patient-specific implants and VSP-generated surgical splints provide comparable high accuracy for maxillary positioning in orthognathic surgery.

Author contribution FO, YM, and FAP contributed to the study conception and design, to data acquisition, to data analysis and interpretation, and to the writing and revision of the manuscript; HS contributed to the study design, data interpretation, and the writing and revision of the manuscript; PL, MT, and SH contributed to data acquisition, to data analysis and interpretation and to the revision of the manuscript; FF, KO, and JH contributed to data acquisition, to data analysis and to the revision of the manuscript; EB contributed to data analysis and interpretation and to the revision of the manuscript; SO contributed to the study conception and revision of the manuscript.

Funding Open Access funding enabled and organized by Projekt DEAL.

Data availability The data that support the findings of this study are not publicly available due to confidentiality reasons. The anonymized statistical data is available from the corresponding author (YM) upon reasonable request.

Declarations

Ethics approval The institutional review board authorized the retrospective study and informed consent was waived (Ethics Committee, Ludwig-Maximilians-University, Munich, Germany: Ref.-No. 21-0164). No other ethical approval or consent to participate was necessary.

Competing interests The authors declare no competing interests.

Open Access This article is licensed under a Creative Commons Attribution 4.0 International License, which permits use, sharing, adaptation, distribution and reproduction in any medium or format, as long as you give appropriate credit to the original author(s) and the source, provide a link to the Creative Commons licence, and indicate if changes were made. The images or other third party material in this article are included in the article's Creative Commons licence, unless indicated otherwise in a credit line to the material. If material is not included in the article's Creative Commons licence and your intended use is not permitted by statutory regulation or exceeds the permitted use, you will need to obtain permission directly from the copyright holder. To view a copy of this licence, visit http://creativecommons.org/licenses/by/4.0/.

References

1. Ellis E (1990) Accuracy of model surgery: evaluation of an old technique and introduction of a new one. J Oral Maxillofac Surg 48:1161–1167. https://doi.org/10.1016/0278-2391(90)90532-7
2. Ritto FG, Schmitt ARM, Pimentel T, Canellas JV, Medeiros PJ (2018) Comparison of the accuracy of maxillary position between conventional model surgery and virtual surgical planning. Int J Oral Maxillofac Surg 47:160–166. https://doi.org/10.1016/j.ijom.2017.08.012
3. Ellis E, Tharanon W, Gambrell K (1992) Accuracy of face-bow transfer: effect on surgical prediction and postsurgical result. J Oral Maxillofac Surg 50:562–567. https://doi.org/10.1016/0278-2391(92)90434-2
4. Zizelmann C, Hammer B, Gellrich N-C, Schwestka-Polly R, Rana M, Bucher P (2012) An evaluation of face-bow transfer for the planning of orthognathic surgery. J Oral Maxillofac Surg 70:1944–1950. https://doi.org/10.1016/j.joms.2011.08.025
5. Sharifi A, Jones R, Ayoub A, Moos K, Walker F, Khambay B, McHugh S (2008) How accurate is model planning for orthognathic surgery? Int J Oral Maxillofac Surg 37:1089–1093. https://doi.org/10.1016/j.ijom.2008.06.011
6. Gateno J, Forrest KK, Camp B (2001) A comparison of 3 methods of face-bow transfer recording: implications for orthognathic surgery. J Oral Maxillofac Surg 59:635–40. discussion 640–1. https://doi.org/10.1053/joms.2001.23374
7. Xia J, Ip HH, Samman N, Wong HT, Gateno J, Wang D et al (2001) Three-dimensional virtual-reality surgical planning and soft-tissue prediction for orthognathic surgery. IEEE Trans Inf Technol Biomed 5:97–107. https://doi.org/10.1109/4233.924800
8. Chabanas M, Marécaux C, Chouly F, Boutault F, Payan Y (2004) Evaluating soft tissue simulation in maxillofacial surgery using preoperative and postoperative CT scans. Int Congr Ser 1268:419–424. https://doi.org/10.1016/j.ics.2004.03.165
9. Metzger MC, Hohlweg-Majert B, Schwarz U, Teschner M, Hammer B, Schmelzeisen R (2008) Manufacturing splints for orthognathic surgery using a three-dimensional printer. Oral Surg Oral Med Oral Pathol Oral Radiol Endod 105:e1-7. https://doi.org/10.1016/j.tripleo.2007.07.040
10. Song K-G, Baek S-H (2009) Comparison of the accuracy of the three-dimensional virtual method and the conventional manual method for model surgery and intermediate wafer fabrication. Oral Surg Oral Med Oral Pathol Oral Radiol Endod 107:13–21. https://doi.org/10.1016/j.tripleo.2008.06.002
11. Hsu SS-P, Gateno J, Bell RB, Hirsch DL, Markiewicz MR, Teichgraeber JF et al (2013) Accuracy of a computer-aided surgical simulation protocol for orthognathic surgery: a prospective multicenter study. J Oral Maxillofac Surg 71:128–42. https://doi.org/10.1016/j.joms.2012.03.027
12. Schouman T, Rouch P, Imholz B, Fasel J, Courvoisier D, Scolozzi P (2015) Accuracy evaluation of CAD/CAM generated splints in orthognathic surgery: a cadaveric study. Head Face Med 11:24. https://doi.org/10.1186/s13005-015-0082-9
13. Bai S, Shang H, Liu Y, Zhao J, Zhao Y (2012) Computer-aided design and computer-aided manufacturing locating guides accompanied with prebent titanium plates in orthognathic surgery. J Oral Maxillofac Surg 70:2419–2426. https://doi.org/10.1016/j.joms.2011.12.017
14. Mazzoni S, Badiali G, Lancellotti L, Babbi L, Bianchi A, Marchetti C (2010) Simulation-guided navigation: a new approach to improve intraoperative three-dimensional reproducibility during orthognathic surgery. J Craniofac Surg 21:1698–1705. https://doi.org/10.1097/SCS.0b013e3181f3c6a8
15. Gander T, Bredell M, Eliades T, Rücker M, Essig H (2015) Splintless orthognathic surgery: a novel technique using patient-specific

implants (PSI). J Craniomaxillofac Surg 43:319–322. https://doi.org/10.1016/j.jcms.2014.12.003
16. Kraeima J, Jansma J, Schepers RH (2016) Splintless surgery: does patient-specific CAD-CAM osteosynthesis improve accuracy of Le Fort I osteotomy? Br J Oral Maxillofac Surg 54:1085–1089. https://doi.org/10.1016/j.bjoms.2016.07.007
17. Suojanen J, Leikola J, Stoor P (2016) The use of patient-specific implants in orthognathic surgery: a series of 32 maxillary osteotomy patients. J Craniomaxillofac Surg 44:1913–1916. https://doi.org/10.1016/j.jcms.2016.09.008
18. Stokbro K, Aagaard E, Torkov P, Bell RB, Thygesen T (2014) Virtual planning in orthognathic surgery. Int J Oral Maxillofac Surg 43:957–965. https://doi.org/10.1016/j.ijom.2014.03.011
19. Heufelder M, Wilde F, Pietzka S, Mascha F, Winter K, Schramm A, Rana M (2017) Clinical accuracy of waferless maxillary positioning using customized surgical guides and patient-specific osteosynthesis in bimaxillary orthognathic surgery. J Craniomaxillofac Surg 45:1578–1585. https://doi.org/10.1016/j.jcms.2017.06.027
20. Rückschloß T, Ristow O, Müller M, Kühle R, Zingler S, Engel M et al (2019) Accuracy of patient-specific implants and additive-manufactured surgical splints in orthognathic surgery - a three-dimensional retrospective study. J Craniomaxillofac Surg 47:847–853. https://doi.org/10.1016/j.jcms.2019.02.011
21. Rückschloß T, Ristow O, Kühle R, Weichel F, Roser C, Aurin K et al (2020) Accuracy of laser-melted patient-specific implants in genioplasty - a three-dimensional retrospective study. J Craniomaxillofac Surg 48:653–660. https://doi.org/10.1016/j.jcms.2020.05.003
22. von Elm E, Altman DG, Egger M, Pocock SJ, Gøtzsche PC, Vandenbroucke JP (2007) Strengthening the reporting of observational studies in epidemiology (STROBE) statement: guidelines for reporting observational studies. BMJ 335:806–808. https://doi.org/10.1136/bmj.39335.541782.AD
23. Meiyappan N, Tamizharasi S, Senthilkumar KP, Janardhanan K (2015) Natural head position: an overview. J Pharm Bioallied Sci 7:S424–S427. https://doi.org/10.4103/0975-7406.163488
24. Aboul-Hosn Centenero S, Hernández-Alfaro F (2012) 3D planning in orthognathic surgery: CAD/CAM surgical splints and prediction of the soft and hard tissues results - our experience in 16 cases. J Craniomaxillofac Surg 40:162–168. https://doi.org/10.1016/j.jcms.2011.03.014
25. Badiali G, Ferrari V, Cutolo F, Freschi C, Caramella D, Bianchi A, Marchetti C (2014) Augmented reality as an aid in maxillofacial surgery: validation of a wearable system allowing maxillary repositioning. J Craniomaxillofac Surg 42:1970–1976. https://doi.org/10.1016/j.jcms.2014.09.001
26. de Riu G, Meloni SM, Baj A, Corda A, Soma D, Tullio A (2014) Computer-assisted orthognathic surgery for correction of facial asymmetry: results of a randomised controlled clinical trial. Br J Oral Maxillofac Surg 52:251–257. https://doi.org/10.1016/j.bjoms.2013.12.010
27. Li B, Zhang L, Sun H, Yuan J, Shen SGF, Wang X (2013) A novel method of computer aided orthognathic surgery using individual CAD/CAM templates: a combination of osteotomy and repositioning guides. Br J Oral Maxillofac Surg 51:e239–e244. https://doi.org/10.1016/j.bjoms.2013.03.007
28. Shehab MF, Barakat AA, AbdElghany K, Mostafa Y, Baur DA (2013) A novel design of a computer-generated splint for vertical repositioning of the maxilla after Le Fort I osteotomy. Oral Surg Oral Med Oral Pathol Oral Radiol 115:e16-25. https://doi.org/10.1016/j.oooo.2011.09.035
29. Sun Y, Luebbers H-T, Agbaje JO, Schepers S, Vrielinck L, Lambrichts I, Politis C (2013) Accuracy of upper jaw positioning with intermediate splint fabrication after virtual planning in bimaxillary orthognathic surgery. J Craniofac Surg 24:1871–1876. https://doi.org/10.1097/SCS.0b013e31829a80d9
30. Xia JJ, Gateno J, Teichgraeber JF, Christensen AM, Lasky RE, Lemoine JJ, Liebschner MAK (2007) Accuracy of the computer-aided surgical simulation (CASS) system in the treatment of patients with complex craniomaxillofacial deformity: a pilot study. J Oral Maxillofac Surg 65:248–254. https://doi.org/10.1016/j.joms.2006.10.005
31. Zinser MJ, Mischkowski RA, Sailer HF, Zöller JE (2012) Computer-assisted orthognathic surgery: feasibility study using multiple CAD/CAM surgical splints. Oral Surg Oral Med Oral Pathol Oral Radiol 113:673–687. https://doi.org/10.1016/j.oooo.2011.11.009
32. Marchetti C, Bianchi A, Bassi M, Gori R, Lamberti C, Sarti A (2006) Mathematical modeling and numerical simulation in maxillo-facial virtual surgery (VISU). J Craniofac Surg 17:661–7. discussion 668. https://doi.org/10.1097/00001665-200607000-00009
33. Hernández-Alfaro F, Guijarro-Martínez R (2013) New protocol for three-dimensional surgical planning and CAD/CAM splint generation in orthognathic surgery: an in vitro and in vivo study. Int J Oral Maxillofac Surg 42:1547–1556. https://doi.org/10.1016/j.ijom.2013.03.025
34. Baan F, Liebregts J, Xi T, Schreurs R, de Koning M, Bergé S, Maal T (2016) A new 3D tool for assessing the accuracy of bimaxillary surgery: the orthognathic analyser. PLoS One 11:e0149625. https://doi.org/10.1371/journal.pone.0149625

Publisher's note Springer Nature remains neutral with regard to jurisdictional claims in published maps and institutional affiliations.

journal of the mechanical behavior of biomedical materials 144 (2023) 105960

Contents lists available at ScienceDirect

Journal of the Mechanical Behavior of Biomedical Materials

journal homepage: www.elsevier.com/locate/jmbbm

Biomechanical simulation of forces and moments of initial orthodontic tooth movement in dependence on the used archwire system by ROSS (Robot Orthodontic Measurement & Simulation System)

Benedikt Dotzer [a], Thomas Stocker [a], Andrea Wichelhaus [a], Mila Janjic Rankovic [a], Hisham Sabbagh [a,*]

[a] Department of Orthodontics and Dentofacial Orthopedics, University Hospital, LMU Munich, Goethestrasse 70, Munich 80336, Germany

ARTICLE INFO

Keywords:
Biomechanics
Robotics
Orthodontic simulation
Orthodontic tooth movement
Force control
Leveling archwire

ABSTRACT

Objectives: Aim of this study was to determine the forces and moments during simulated initial orthodontic tooth movements using a novel biomechanical test setup.
Methods: The test setup consisted of an industrial precision robot with a force-torque sensor, a maxillary model and a control computer and software. Forces and moments acting on the corresponding experimental tooth during the motion simulations were dynamically measured for two 0.016" NiTi round archwires (Sentalloy Light/Sentalloy Medium). Intrusive (#1), rotational (#2) and angular (#3) tooth movements were simulated by a control program based on the principle of force control and executed by the robot. The results were statistically analysed using K–S-test and Mann-Whitney *U* test with a significance level of $\alpha = 5\%$.
Results: Sentalloy Medium archwires generated higher forces and moments than the Sentalloy Light archwires in all simulations. In simulation #1 the mean initial forces/moments reached 1.442 N/6.781 Nmm for the Light archwires and 1.637 N/9.609 Nmm for the Medium archwires. In movement #2 Light archwires generated mean initial forces/moments of 0.302 N/−8.271 Nmm whereas Medium archwires generated 0.432 N/−9.653 Nmm. Simulation #3 showed mean initial forces/moments of −0.122 N/8.477 Nmm from the Light archwires compared to −0.300 N/11.486 Nmm for the Medium archwires.
Significance: The measured forces and moments were suitable for initial orthodontic tooth movement in simulations #2 and #3, however inadequate in simulation #1. Reduced archwire dimensions (<0.016″) should be selected for initial leveling of vertical malocclusions.

1. Introduction

Orthodontic multibracket appliances are widely used for the treatment of malocclusions (Graber et al., 2022; Proffit et al., 2007). In these systems, archwires can be used to apply forces and moments to the teeth to induce tooth movements (Burstone and Koenig, 1974). Orthodontic tooth movement is achieved by a biological reaction in terms of bone remodeling, as a result of a complex interaction between the cells of the periodontal ligament, the bone matrix, hormones, cytokines, and growth factors (Xu et al., 2022; Zhang et al., 2022; Jeon et al., 2021). For a clinically efficient tooth movement with minimal hyalinization and pain, as well as a reduced risk of apical root resorption (ARR), the application of suitable force and moment magnitudes is required (Reitan, 1957, 1960, 1967, 1985; Wichelhaus, 2013; Wichelhaus et al., 2021).

However, in clinical practice, it is often difficult for the practitioner to accurately estimate the magnitude and direction of the forces and moments that will develop within an orthodontic appliance (Koenig et al., 1980). Since intraoral measurements are limited, in-vitro studies have been conducted in the field of biomechanics to investigate orthodontic appliances, mostly applying biomechanical test stands or finite element (FE) simulations (Friedrich et al., 1999; Mascarenhas et al., 2018; Rajgopal, 2022; Adel et al., 2021).

Numerical methods such as the finite element method (FEM) are increasingly being applied due to advances in computer technology, as they allow the simulation of complex and adaptive models of biological systems and processes (Cicciu, 2020; Cervino et al., 2020; Singh et al., 2016; Ahuja et al., 2018; de Brito et al., 2019). These digital simulations

* Corresponding author.
E-mail address: hisham.sabbagh@med.uni-muenchen.de (H. Sabbagh).

https://doi.org/10.1016/j.jmbbm.2023.105960
Received 21 April 2023; Received in revised form 5 June 2023; Accepted 6 June 2023
Available online 19 June 2023
1751-6161/© 2023 The Authors. Published by Elsevier Ltd. This is an open access article under the CC BY-NC-ND license (http://creativecommons.org/licenses/by-nc-nd/4.0/).

are usually performed based on experimentally determined parameters, but also on simplified assumptions (Hayashi et al., 2007; Romanyk et al., 2020; Wanjun et al., 2015; Ammar et al., 2011). Biomechanical test stands, on the other hand, are less adaptable than computer models, but allow the investigation of the actual underlying physical properties of materials, specimens and appliances without the influence of subjectively determined parameters. One difficulty, however, is the biomechanical simulation of dynamic processes as they occur during orthodontic treatment, since the resulting force-moment systems are constantly changing due to the continuous tooth movements. To overcome these limitations, more complex, computerized and robotic biomechanical test stands have been developed. (Bourauel et al., 1992; Fuck and Drescher, 2006; Fansa et al., 2009; Pandis et al., 2009; Badawi et al., 2009; Chen et al., 2007, 2010). In 1992, the "OMSS – Orthodontic Measurement and Simulation System" was introduced to conduct computer-assisted examinations of tooth movements in relation to the forces and moments acting on them (Bourauel et al., 1992). In 2006 the "Robotic Measurement System" (RMS) was introduced, using a robot in the experimental setup to investigate the initial force systems generated by different leveling archwires (Fuck and Drescher, 2006). However, due to the static experimental setup, it was not possible to track the dynamic changes of the archwire forces and moments. By programming feedback between measured force-moment values and movements executed automatically by robots, dynamic motion sequences can be simulated. The conduct of such biomechanical investigations is complex, thus only few test stands have been validated and employed to date (Badawi et al., 2009; Liu et al., 2014).

Aim of this study is to determine the forces and moments of a fixed multibracket appliance dynamically during simulated initial tooth movements using a novel biomechanical test setup.

2. Materials and methods

2.1. Development of the test stand

The test setup used was developed in the Biomechanics Laboratory of the Department of Orthodontics and Dentofacial Orthopedics of the LMU University Hospital. The core component of the setup was an industrial precision robot KUKA KR 5-sixx R650 (KUKA Roboter GmbH, Germany) with six degrees of freedom. At the top of the robot, a FTS Nano 17 SI-12-0.12 force-torque sensor (ATI Industrial Automation, USA), which can detect forces along the three spatial axes with a resolution of 0.0031 N and moments with 0.0156 Nmm, was attached via an aluminium flange. The experimental tooth on which the acting forces and moments were to be measured, a central upper incisor (11), was attached to the sensor via an adapter plate with a threaded rod. In order to investigate the force systems at a physiological oral or application temperature, the whole experimental setup including the associated Kavo Typodont model, which was attached to an aluminium profile via SAM® Axiosplit® mounting plates (SAM Präzisionstechnik GmbH, Germany), was surrounded by a thermal chamber (Fig. 1A).

By employing a temperature sensor close to the experimental tooth and a corresponding temperature controller REX-C100 PID (RKC Instrument Inc., Japan), a constant experimental temperature of 37.0 ± 0.5 °C was maintained throughout the experiment. Active self-ligating 0.022″ slot straightwire brackets with MBT prescription (Bioquick, Forestadent GmbH, Germany) were placed on the Kavo Typodont model and the experimental tooth. The brackets were positioned using a passive pre-bent 0.021″ × 0.025″ steel wire and then fixed with a two-component epoxy adhesive.

2.2. Biomechanical measurements and simulation

Forces and moments during orthodontic tooth movement were simulated for three different scenarios: an extruded tooth, a rotated tooth, and an angulated tooth. For the simulation of the intrusion, the tooth was extruded from its idealized position in the dental arch by 1.6 mm. In the rotational movement, the starting position of the experiment corresponded to a mesial rotation of the tooth by 6°. In the final series of experiments, the starting position was defined by angulating the tooth by 10° mesially. The respective misalignments were programmed into the robot's control software, allowing them to be driven to the same starting position for all experiments. Forces and moments were determined for two 0.016″ Nickel–Titanium (NiTi) leveling archwires Sentalloy Light and Sentalloy Medium (GC Corporation, Japan). Five wires of each type were examined in independent measurement cycles. The sensor's coordinate system was configured such that its x-axis corresponds to the mesiodistal axis, the y-axis corresponds to the orovestibular axis, and the z-axis corresponds to the vertical axis of the orthogonally aligned bracket slot (Fig. 1B). Consequently, a measured moment about the x-axis corresponds to a root moment, in the case of the y-axis to an angulation moment, and for the z-axis to a rotation moment. Furthermore, a positive F_z corresponds to an intrusive force, and a positive M_x corresponds to a protrusive moment.

Before engaging the archwire into the brackets, no forces or moments were acting on the test tooth or the corresponding sensor. Mathematical

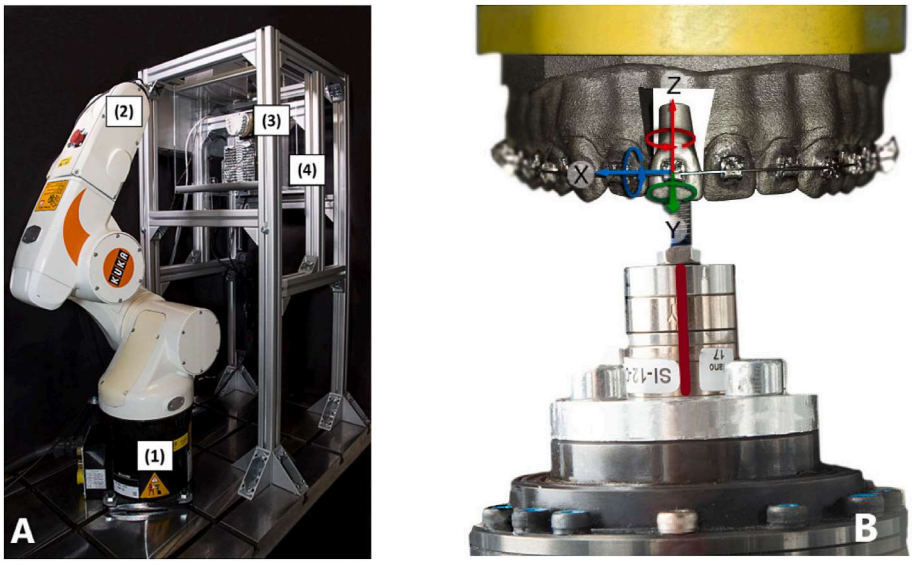

Fig. 1. A: ROSS: KUKA KR 5-sixx R650 Industrial robot (1), robot end effector with force-torque sensor and test tooth (2), KAVO Typodont model (3) within the reference frame constructed for the experiment including the thermocamber (4). B: Close-up of the experimental setup: KAVO Typodont model made of high-strength titanium alloy, force-torque sensor (indicated by a red vertical line), robot end effector and test tooth 11 with a schematic representation of the spatial coordinate system of the sensor. The direction of the measurement components along the x- (mesiodistal), y- (orovestibular), and z- (vertical) axis are shown by the arrows.

corrections within the robot program also ensured that distortions of the measurement data due to gravity or the robot's own weight or movement could be excluded. The measured force and moment values were transformed to the bracket slot or the center of force (CoF) and the center of resistance (CoR) of the tooth. This transformation was performed by geometrically measuring the distances and angles between the plane of the force/torque sensor and those of the center of force/resistance using the 3D CAD program Autodesk Inventor (Autodesk GmbH, Germany). The transformation matrix used, based on the x–y′–z″ convention, describes the coordinate transformations from the original coordinate system of the force/torque sensor to that of the center of force/resistance. The data was transmitted to the connected measurement computer through the robot control. After the start of the experiment, the control program calculated position corrections and the robot moved the attached tooth according to the calculated specifications, intending to cyclically reduce the forces and moments. No additional forces or moments, other than those of the archwire, were produced by the position adjustments since the robot only moved in the direction of the applied force vectors in order to reduce the forces and moments acting on it. This principle of adaptive compliance is also called force control and is an effective method that enables a robot to adapt to changing forces and moments during a task. Feedback parameters programmed into the force control determined the robot's movement sensitivity by assigning movement amplitudes to the respective force systems. The data exchange within the experiment took place until a termination condition was reached, which was defined by an asymptotic course of the forces and moments. In addition, a time limit of 10 min for communication between the robot and computer or control program was defined. The described test stand was named – "3-D Robot Orthodontic Measurement & Simulation System" (ROSS).

2.3. Statistical analysis

The Kolmogorov-Smirnov test was used to verify normal distribution, which was true for the majority of the calculated values. Therefore, the Mann-Whitney *U* test was applied as a non-parametric test for independent samples. Calculations were performed using IBM SPSS 27 (IBM Corp., Armonk, NY, USA), with a significance level of $\alpha = 5\%$.

3. Results

3.1. Intrusion

The simulated intrusion of the experimental tooth showed that, in addition to the intrusive force F_z, a protruding moment M_x around the mesio-distal x-axis occurred. The evaluation of the results showed correspondingly higher initial forces and moments for the Sentalloy Medium archwires with $F_z = 1.637$ N and $M_x = 9.609$ Nmm compared to the Light archwire measurement series with $F_z = 1.442$ N and $M_x = 6.781$ Nmm. These initial moments of the tested archwires differed significantly ($p = 0.008$). The course of the individual graphs showed that forces and moments decreased in relatively equal extent for both archwires. The scaling of the x-axis was set to a reference distance of 0.8 mm to eliminate retreats towards the end of the experiment to facilitate a comparable interpretation (Fig. 2). The realized intrusion distances only slightly differed from an average of $z = 1.089$ mm to $z = 1.139$ mm ($p = 0.690$). An intrusion over the full distance of 1.6 mm from the extruded position to the idealized physiological position was not achieved in any of the test series. The maximum intrusion was 1.346 mm (Table 1).

Additional movements in the other spatial planes occurred during the simulated intrusion. From the start of the experiment, the tooth was continuously moved mesially along the x-axis until a maximum deflection of $x = -0.101$ mm (Fig. 3A). In addition, there was a vestibular directed shift of the tooth along the oro-vestibular y-axis. The tooth was moved vestibularly by up to $y = 0.169$ mm (Sentalloy Light archwires) or within a range of $y = \pm 0.044$ mm (Sentalloy Medium archwires) (Fig. 3B).

3.2. Rotation

The simulated rotations showed significant differences between the Sentalloy Light and Medium archwires regarding the acting forces ($p = 0.008$) and moments ($p = 0.008$). Values of rotational moment M_z and the force in the oro-vestibular direction F_y, corresponding to a rotational movement, are presented relative to the rotation R_z of the tooth about its longitudinal z-axis for illustration (Fig. 4). Forces in the oro-vestibular direction (F_y) showed initial forces of $F_y = 0.432$ N (Sentalloy Medium), compared to $F_y = 0.302$ N (Sentalloy Light) (Table 2).

Sentalloy Light archwires showed lower initial values of $M_z = -8.271$ Nmm compared to the Sentalloy Medium archwires with $M_z = -9.653$ Nmm. Additionally, the experimental tooth was derotated about 0.4° further by the Sentalloy Medium archwires compared to the simulations with the Sentalloy Light archwires ($p = 0.008$). However, a complete rotation of $R_z = 6°$ was not achieved.

Additionally, movements in the mesio-distal (x) and vestibulo-oral (y) direction were observed (Fig. 5). When moving along the x-axis, the tooth was initially deflected mesially by up to $x = -0.119$ mm before moving distally by up to $x = 0.339$ mm in the further course of the experiment (Fig. 5A and B). The deflection of the tooth in the vestibular direction reached its peak with up to $y = 0.371$ mm after a rotation of $Rz = 1.5–2.0°$. Subsequently, the tooth moved back towards the starting position but did not fully reach it by the end of the simulation, resulting in a slightly vestibular position of the tooth in all cases (Fig. 6B).

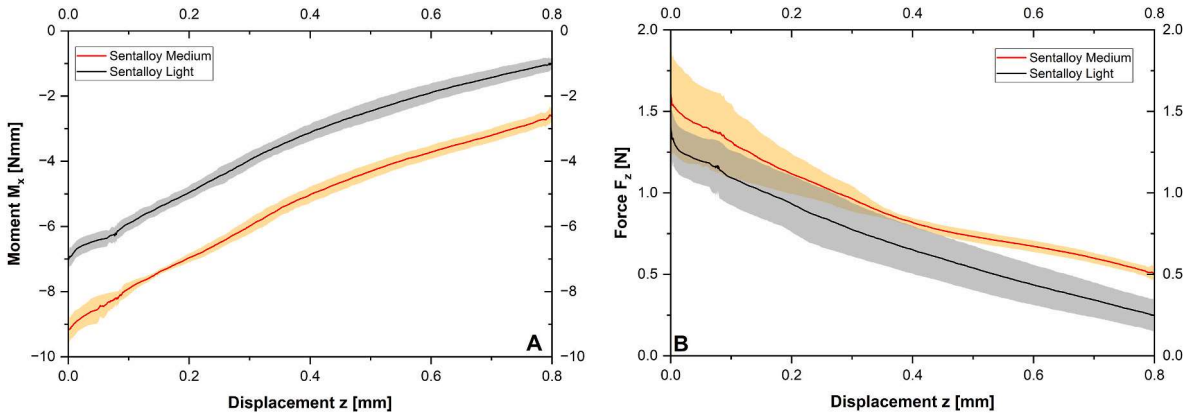

Fig. 2. A: Correlation between protrusion moment [M_x] and intrusion distance [z] B: Correlation between intrusion force [F_z] and intrusion distance [z] – Shown are the averaged curves of each archwire system with a graphically visualized standard deviation range.

Table 1
Means, maximum values (Max.), and respective standard deviations (SD) of the initial intrusion forces F_z [N], the initial protrusion moments M_x [Nmm], and realized intrusion distances z [mm] for Sentalloy Light and Medium 0.016″ archwires.

Archwire [Inch]	F_z [N]			M_x [Nmm]			z [mm]		
	Mean	SD	Max.	Mean	SD	Max.	Mean	SD	Max.
Sentalloy .016 Light	1.442	±0.127	1.545	6.781	±0.937	8.152	1.139	±0.173	1.346
Sentalloy .016 Medium	1.637	±0.328	2.163	9.609	±0.871	10.790	1.089	±0.016	1.113
p-Value*	0.222			0.008†			0.690		

*Mann-Whitney *U* test.
†Statistically significant difference.

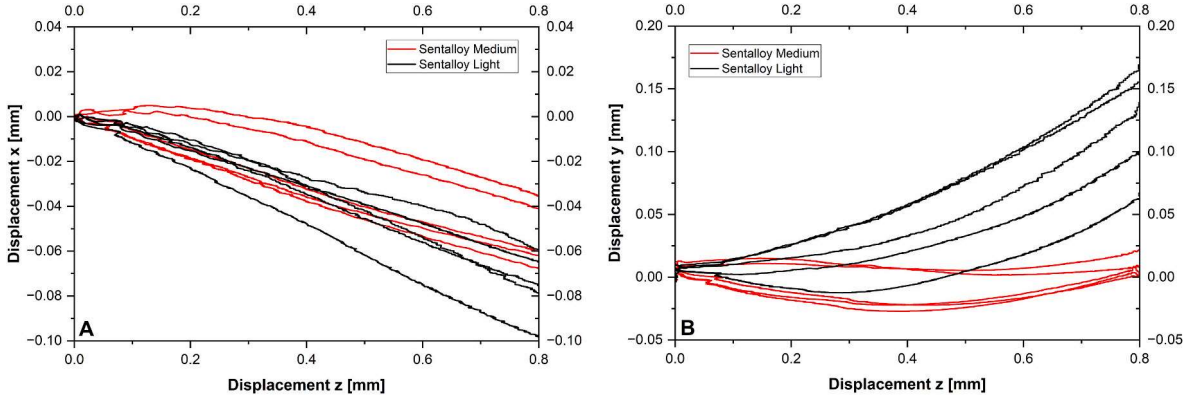

Fig. 3. A: Correlation between displacement along the mesio-distal axis [x] and the intrusion [z]. B: Correlation between displacement along the vestibulo-oral axis [y] and the intrusion [z] - Shown are the individual curves of the ten measured archwires.

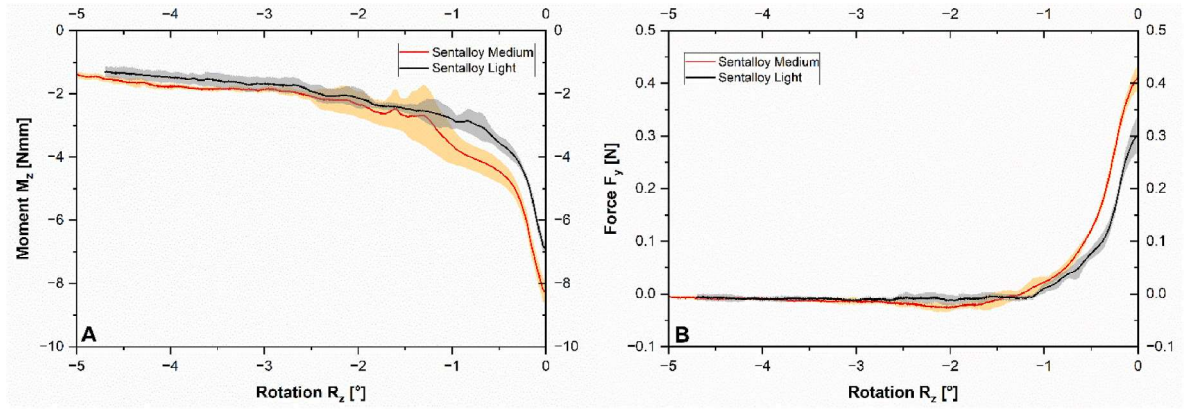

Fig. 4. A: Correlation between the de-rotational moment [M_z] and the rotation around the tooth axis [R_z] B: Correlation between the oro-vestibular force [F_y] and the rotation around the tooth axis [R_z] - Shown are the averaged curves of each archwire system with a graphically visualized standard deviation range.

Table 2
Means, maximum values (Max.), and respective standard deviations (SD) of the initial oro-vestibular forces F_y [N], the initial rotational moments M_z [Nmm] and realized rotations R_z [°] for Sentalloy Light and Medium 0.016″ archwires.

Archwire [Inch]	F_y [N]			M_z [Nmm]			R_z [°]		
	Mean	SD	Max.	Mean	SD	Max.	Mean	SD	Max.
Sentalloy .016 Light	0.302	±0.036	0.349	−8.271	±0.243	−8.477	−4.853	±0.154	−5.056
Sentalloy .016 Medium	0.432	±0.049	0.509	−9.653	±0.512	−10.076	−5.316	±0.098	−5.452
p-Value*	0.008†			0.008†			0.008†		

*Mann-Whitney *U* test.
†Statistically significant difference.

Movements along the tooth axis (z) also occurred in two phases or directions. At the beginning of the rotation, the front tooth was intruded by up to z = 0.122 mm, before it extruded in the further course of the experiment (Fig. 5C). After the end of the experiment, the tooth was therefore on average in a position extruded by z = −0.081 mm (Table 2).

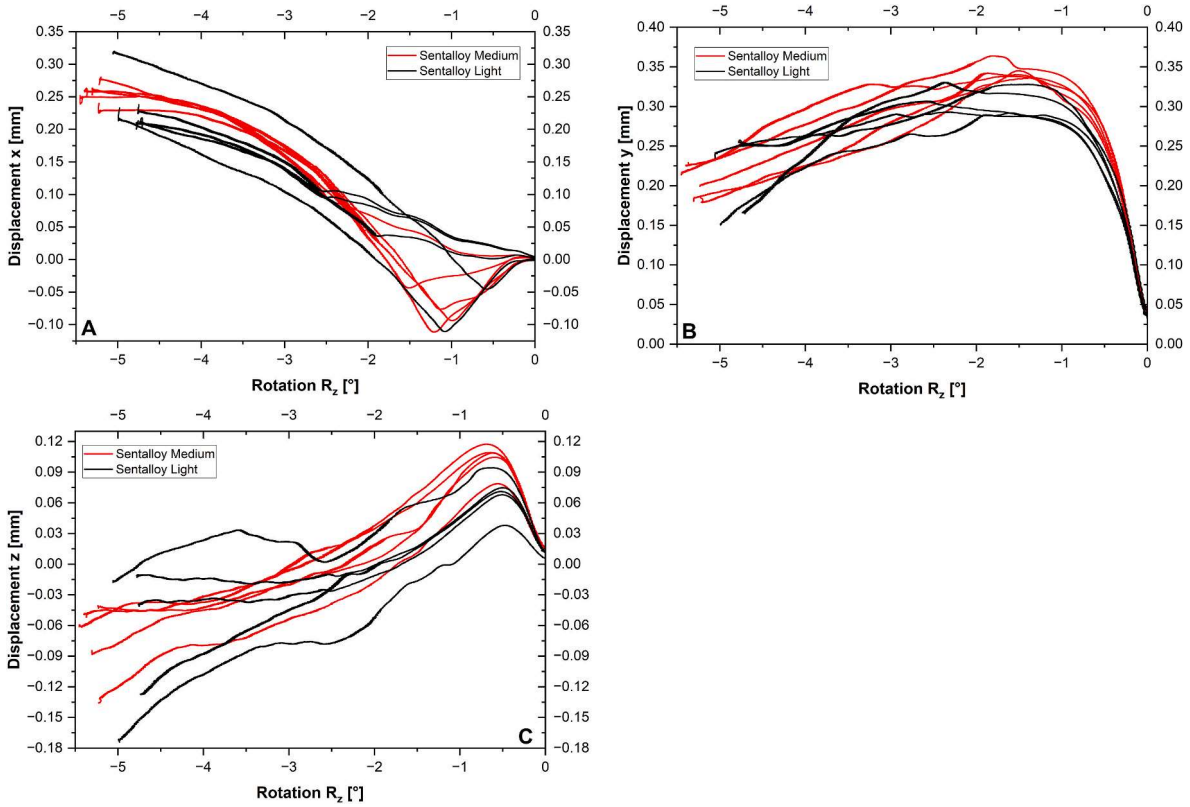

Fig. 5. A: Correlation between the displacement along the mesio-distal axis [x] and the rotation around the tooth axis [R_z]. B: Correlation between the displacement along the oro-vestibular axis [y] and the rotation around the tooth axis [R_z]. C: Correlation between the displacement along the tooth's longitudinal axis [z] and the rotation around the tooth axis [R_z]. – Shown are the individual curves of the ten measured archwires.

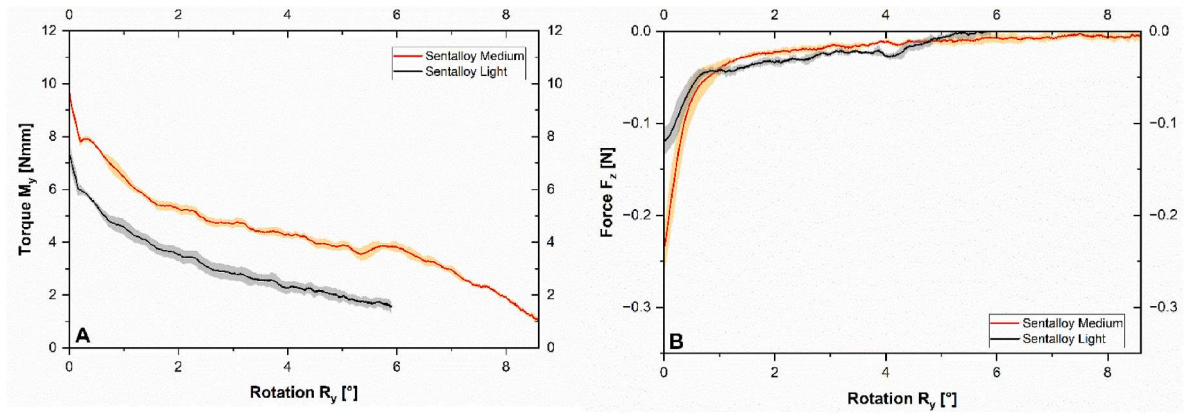

Fig. 6. A: Correlation between the up-righting moment [M_y] and the angulation or rotation around the oro-vestibular axis [R_y]. B: Correlation between the up-righting force [F_z] and the angulation or rotation around the oro-vestibular axis [R_y]. – Shown are the averaged curves of each archwire system with a graphically visualized standard deviation range.

3.3. Angulation

The simulated angulation movements showed significant differences regarding the measured forces ($p = 0.008$) and moments ($p = 0.008$) between the Light and Medium archwires respectively. The main parameters of this simulation were moments around the oro-vestibular y-axis (M_y) and the force along the tooth or z-axis (F_z), corresponding to an uprighting of the experimental tooth.

Sentalloy Medium archwires produced higher moments and forces compared to the Sentalloy Light archwires (Fig. 6). Regarding the moment around the oro-vestibular y-axis, the initial values of the Sentalloy Medium archwires, with an average of $M_y = 11.486$ Nmm, were about 3 Nmm above the values of the Sentalloy Light archwires, with $M_y = 8.477$ Nmm. Regarding the initial force F_z, which acts in the direction of the tooth axis, the Sentalloy Medium archwires ($F_z = -0.300$ N) produced forces nearly three times as high as the Sentalloy Light archwires ($F_z = -0.122$ N). Furthermore, the Sentalloy Medium archwires were able to upright the experimental tooth further, with an average of $R_y = 8.636°$, compared to the Sentalloy Light archwires with $R_y = 6.383°$. Despite a maximum root angulation of up to $R_y = 8.710°$, complete up-righting of the tooth was not achieved (Table 3).

In Fig. 7 the displacements of the tooth along the three spatial axes during the simulation of the movement are represented. With approximately $x = 1.466$ mm and $x = 1.936$ mm, mainly a distally directed

Table 3
Means, maximum values (Max.), and respective standard deviations (SD) of the initial up-righting forces along the tooth axis F_z [N], the initial angulation moments M_y [Nmm] and realized angulations R_y [°] for Sentalloy Light and Medium .016″ archwires.

Archwire [Inch]	F_z [N]			M_y [Nmm]			R_y [°]		
	Mean	SD	Max.	Mean	SD	Max.	Mean	SD	Max.
Sentalloy .016 Light	−0.122	±0.014	−0.138	8.477	±0.447	8.984	6.383	±0.303	6.773
Sentalloy .016 Medium	−0.300	±0.036	−0.331	11.486	±0.161	11.655	8.636	±0.045	8.710
p-Value*	0.008†			0.008†			0.008†		

*Mann-Whitney *U* test.
†Statistically significant difference.

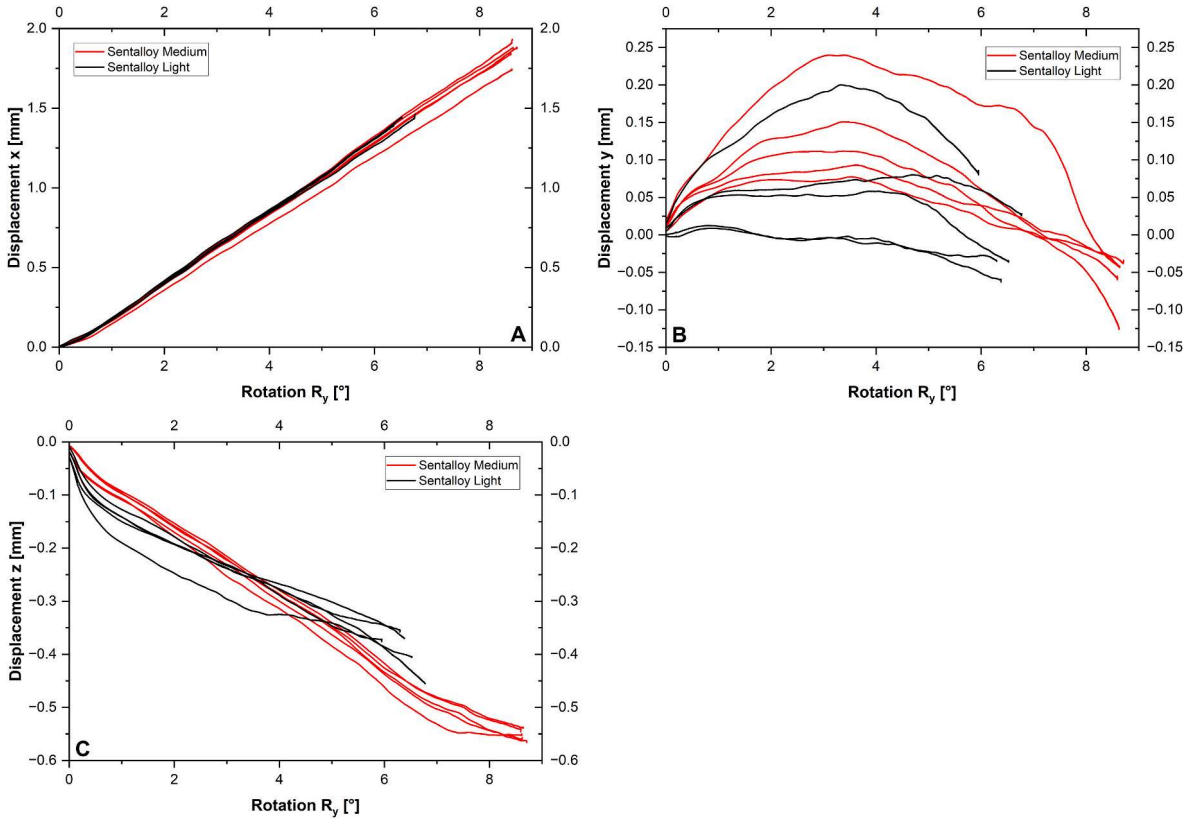

Fig. 7. A: Correlation between the displacement along the mesio-distal axis [x] and the angulation around the oro-vestibular axis [R_y] B: Correlation between the displacement along the oro-vestibular axis [y] and the angulation around the same axis [R_y] C: Correlation between the displacement along the longitudinal axis of the tooth [z] and the angulation around the oro-vestibular axis [R_y] – Shown are the individual curves of the ten measured archwires.

movement along the x-axis occurred (Fig. 7A). Additionally, the tooth was often initially deflected towards the buccal side by up to y = 0.247 mm after the start of the simulation before the movement direction reversed and turned back towards the point of origin. At the end of the simulation, the tooth had almost reached its starting position or slightly exceeded it (Fig. 7B). Furthermore, an extrusion movement of up to z = −0.458 mm or z = −0.570 mm along the z- or tooth-axis took place (Fig. 7C).

4. Discussion

Employing the newly developed biomechanical test stand ROSS, forces and moments were dynamically measured for three different typical scenarios of orthodontic tooth movement with a multibracket appliance during the leveling phase: rotation, angulation and intrusion.

The investigation of the force systems generated by the archwires showed that in all the experiments performed, the resulting forces and moments of the Sentalloy Medium archwires were higher than those of the Sentalloy Light. This can be explained by the fact that, due to their material properties, the Medium archwires apply a greater force at comparable deflection than the Light versions. Furthermore, for each of the three motion simulations conducted, it was shown that the tooth did not fully return to its starting position after the completion of the trial. This is primarily attributable to the mismatch of the used archwire dimensions and the slot size of the brackets used. The angle (θ_c) by which the wire can move maximally in the slot can be calculated from the mathematical relationship between the slot width (slot), the diameter of the wire used (size), and the length of the bracket slot in mesio-distal extent (width) (Kusy and Whitley, 1999). In the conducted experiments, two round archwires with a dimension of 0.016″ were used, which resulted in a maximum loss- or critical contact angle of approximately $\theta_c = 3°$, taking into account the 0.022″ slot width and a measured mesio-distal slot length of 0.112". In the simulated rotation and angulation movements, the physiological ideal positions were missed by 0.586–3.92°, which was close to the calculated value. In the investigated intrusion, a play of 0.006″ resulted from the mismatch between the slot width (0.022″) and archwires (0.016″), due to the vertical movement pattern. However, the remaining intrusion distance was

partially up to 0.021″. This can be attributed to the fact that the tooth and bracket were tilted vestibularly from their neutral position due to the observed protruding moment M_x, resulting in an increased mismatch between the slot size and archwire dimension in the protruded state.

The force systems of the three different motion simulations must be evaluated separately. For rotational and angular movements with tooth misalignments of 6° and 10° as starting positions, the applied forces and moments averaged at 0.432 N and 0.3 N and 9.653 Nmm and 11.486 Nmm, which is within the physiologically acceptable range for the corresponding tooth movements (Proffit et al., 2007; Ricketts, 1976; Reitan et al., 1989). In a comparable biomechanical study, derotation movements were simulated using aligners with rotational moments of up to 71.8 Nmm, exceeding the suitable load of approximately 20 Nmm by a factor of 3.6 (Proffit et al., 2007; Hahn et al., 2010). In another study investigating thinner aligners with a thickness of only 0.3 mm, which are clinically considered inadequate due to their insufficient dimensional stability, acceptable rotational moments of 17.48 Nmm were measured, however with an intrusive force of 3.58 N as a side effect (Elkholy et al., 2017). Such high forces and moments would be expected to cause significant overloading of periodontal structures and apical root resorption (Barbagallo et al., 2008). As described in the literature, orthodontic tooth derotation with superelastic NiTi leveling archwires is more effective, biomechanically favorable and shows a lower risk of adverse effects compared to tooth derotations with aligners (Simon et al., 2014; Rossini et al., 2015; Charalampakis et al., 2018; Grünheid et al., 2017; Papadimitriou et al., 2018). Although the results of different biomechanical studies are not directly comparable, this view is supported by the results of Elkholy et al. and the results of this study in terms of the forces and moments that occur (Elkholy et al., 2017). With regard to angulation movements, no comparable biomechanical studies are available to the authors' knowledge.

In contrast to the simulation of rotation and angulation movements with suitable force and moment ranges, inadequate forces up to 1.5 N were measured for the simulated intrusion movements starting with an initial extrusion of 1.6 mm. Since the force during an axial or vertical tooth movement is only distributed over approximately 10% of the total root surface, even forces of 0.3–0.5 N may already cause increased root resorptions (Wichelhaus, 2013; Sander et al., 2011; Kurol and Owman-Moll, 1998). Consequently, the 0.016″ NiTi archwires tested do not appear to be suitable for leveling a tooth extruded by 1.6 mm. One way to reduce the magnitude of the acting forces and moments while keeping the archwire dimensions constant is to use different alloys with lower force levels. However, in the case of intrusion simulation, even the Light archwires applied averaging initial forces of 1.442 N, which were significantly higher than the recommended values. Therefore, archwires with smaller diameters can be used to reduce the forces (Reddy et al., 2016; Gabersek, 2007). Reducing the archwire diameter by 0.002″ was found to decrease the deflection force plateau of about 50%, and reducing the diameter by 0.004″, from 0.016″ to 0.012″, by about 150% (Lombardo et al., 2012).

Even though the simulations with the newly developed test stand ROSS allow the investigation of the dynamic course of forces and moments of orthodontic multibracket appliances, the results of in vitro studies can only reflect the clinical situation to a limited extent (Sifakakis and Eliades, 2017). The measurements in this study refer to data transformed to the idealized center of resistance of the experimental tooth, since the forces and moments present at that point are decisive for the resulting tooth movement. Relevant clinical parameters such as the individual tooth anatomy, the dynamic shift of the center during tooth movement or the damping effect of the periodontal ligament during the initial deflection of the tooth could not be considered (Wichelhaus, 2013). Furthermore, it should be noted that the described experimental approach represents a simplification of orthodontic tooth movements, as the constant values used as feedback parameters for the robot's movement do not capture the complexity of the individual movement phases, where the velocity of tooth movement may vary (Reitan, 1957, 1960). The archwire diameter and starting positions for the experiments were selected based on the available literature (Elkholy et al., 2017; Sander et al., 2011; Perrey et al., 2015; Jain et al., 2021; Mandall et al., 2006; Ong et al., 2011; Wang et al., 2010). However, three simplified misalignments of an experimental tooth in combination with two archwires were simulated, which does not represent the multitude of possible force systems for individual more complex malocclusions and different archwire and bracket systems.

Despite the limitations of in vitro studies, they present a valid method to investigate the behaviour of orthodontic appliances and to derive conclusions for their clinical application. The results of the present investigation show that 0.016″ NiTi archwires produced forces beyond the recommended ranges for orthodontic tooth movement during simulated intrusion movements for the complete motion sequence (Wichelhaus, 2013; Ricketts, 1976; Reitan et al., 1989; Sander et al., 2011; Faltin et al., 1998). Although super-elastic 0.016″ NiTi archwires have been proposed for initial leveling (Jain et al., 2021; Mandall et al., 2006; Ong et al., 2011; Wang et al., 2010), practitioners should consider using reduced archwire diameters (<0.016″) when vertical deviations are present.

5. Conclusions

A novel biomechanical test stand was developed to measure the dynamic course of forces and moments during simulated orthodontic tooth movement with multibracket appliances. Within the limits of the study, 0.016″ NiTi archwires generated suitable forces and moments for a derotation of 6° and an angulation of 10° of the experimental tooth, whereas forces were inadequate for a simulated intrusion of 1.6 mm.

Funding

This research did not receive any specific grant from funding agencies in the public, commercial, or not-for-profit sector.

CRediT authorship contribution statement

Benedikt Dotzer: Writing – original draft, Investigation. **Thomas Stocker:** Writing – review & editing, Methodology, Conceptualization. **Andrea Wichelhaus:** Writing – review & editing, Supervision, Project administration. **Mila Janjic Rankovic:** Writing – review & editing, Formal analysis. **Hisham Sabbagh:** Writing – original draft, Validation, Formal analysis.

Declaration of competing interest

The authors declare that they have no known competing financial interests or personal relationships that could have appeared to influence the work reported in this paper.

Data availability

Data will be made available on request.

Acknowledgements

Not applicable.

References

Adel, S., Zaher, A., El Harouni, N., Venugopal, A., Premjani, P., Vaid, N., 2021. Robotic applications in orthodontics: changing the face of contemporary clinical care. BioMed Res. Int. 2021, 1–16.

Ahuja, S., Gupta, S., Bhambri, E., Ahuja, V., Jaura, B.S., 2018. Comparison of conventional methods of simultaneous intrusion and retraction of maxillary anterior: a finite element analysis. J. Orthod. 45, 243–249.

Ammar, H.H., Ngan, P., Crout, R.J., Mucino, V.H., Mukdadi, O.M., 2011. Three-dimensional modeling and finite element analysis in treatment planning for orthodontic tooth movement. Am. J. Orthod. Dentofacial Orthop. 139, e59–e71.
Badawi, H.M., Toogood, R.W., Carey, J.P., Heo, G., Major, P.W., 2009. Three-dimensional orthodontic force measurements. Am. J. Orthod. Dentofacial Orthop. 136, 518–528.
Barbagallo, L.J., Jones, A.S., Petocz, P., Darendeliler, M.A., 2008. Physical properties of root cementum: Part 10. Comparison of the effects of invisible removable thermoplastic appliances with light and heavy orthodontic forces on premolar cementum. A microcomputed-tomography study. Am. J. Orthod. Dentofacial Orthop. 133, 218–227.
Bourauel, C., Drescher, D., Thier, M., 1992. An experimental apparatus for the simulation of three-dimensional movements in orthodontics. J. Biomed. Eng. 14, 371–378.
Burstone, C.J., Koenig, H.A., 1974. Force systems from an ideal arch. Am. J. Orthod. 65, 270–289.
Cervino, G., Fiorillo, L., Arzukanyan, A.V., Spagnuolo, G., Campagna, P., Cicciu, M., 2020. Application of bioengineering devices for stress evaluation in dentistry: the last 10 years FEM parametric analysis of outcomes and current trends. Minerva Stomatol. 69, 55–62.
Charalampakis, O., Iliadi, A., Ueno, H., Oliver, D.R., Kim, K.B., 2018. Accuracy of clear aligners: a retrospective study of patients who needed refinement. Am. J. Orthod. Dentofacial Orthop. 154, 47–54.
Chen, J., Bulucea, I., Katona, T.R., Ofner, S., 2007. Complete orthodontic load systems on teeth in a continuous full archwire: the role of triangular loop position. Am. J. Orthod. Dentofacial Orthop. 132, 143 e1–e8.
Chen, J., Isikbay, S.C., Brizendine, E.J., 2010. Quantification of three-dimensional orthodontic force systems of T-loop archwires. Angle Orthod. 80, 566–570.
Cicciu, M., 2020. Bioengineering methods of analysis and medical devices: a current trends and state of the art. Materials 13.
de Brito, G.M., Brito, H.H.A., Marra, G.G.M., Freitas, L.R.P., Hargreaves, B.O., Magalhaes Jr., P.A.A., et al., 2019. Pure mandibular incisor intrusion: a finite element study to evaluate the segmented arch technique. Materials 12.
Elkholy, F., Schmidt, F., Jager, R., Lapatki, B.G., 2017. Forces and moments applied during derotation of a maxillary central incisor with thinner aligners: an in-vitro study. Am. J. Orthod. Dentofacial Orthop. 151, 407–415.
Faltin, R.M., Arana-Chavez, V.E., Faltin, K., Sander, F.G., Wichelhaus, A., 1998. Root resorptions in upper first premolars after application of continuous intrusive forces. Intra-individual study. J. Orofac. Orthop. 59, 208–219.
Fansa, M., Keilig, L., Reimann, S., Jager, A., Bourauel, C., 2009. The leveling effectiveness of self-ligating and conventional brackets for complex tooth malalignments. J. Orofac. Orthop. 70, 285–296.
Friedrich, D., Rosarius, N., Rau, G., Diedrich, P., 1999. Measuring system for in vivo recording of force systems in orthodontic treatment-concept and analysis of accuracy. J. Biomech. 32, 81–85.
Fuck, L.M., Drescher, D., 2006. Force systems in the initial phase of orthodontic treatment – a comparison of different leveling arch wires. J. Orofac. Orthop. 67, 6–18.
Gabersek, G., 2007. Kraftsysteme in Abhängigkeit von der Zahnfehlstellung: Nivellierungsbögen im Vergleich: Düsseldorf, 2007. Univ., Diss.
Graber, L.W., Vig, K.W., Huang, G.J., Fleming, P., 2022. Orthodontics-e-book: Current Principles and Techniques. Elsevier Health Sciences.
Grünheid, T., Loh, C., Larson, B.E., 2017. How accurate is Invisalign in nonextraction cases? Are predicted tooth positions achieved? Angle Orthod. 87, 809–815.
Hahn, W., Engelke, B., Jung, K., Dathe, H., Fialka-Fricke, J., Kubein-Meesenburg, D., et al., 2010. Initial forces and moments delivered by removable thermoplastic appliances during rotation of an upper central incisor. Angle Orthod. 80, 239–246.
Hayashi, K., Uechi, J., Lee, S.P., Mizoguchi, I., 2007. Three-dimensional analysis of orthodontic tooth movement based on XYZ and finite helical axis systems. Eur. J. Orthod. 29, 589–595.
Jain, S., Sharma, P., Shetty, D., 2021. Comparison of two different initial archwires for tooth alignment during fixed orthodontic treatment-A randomized clinical trial. J. Orthod. Sci. 10, 13.
Jeon, H.H., Teixeira, H., Tsai, A., 2021. Mechanistic insight into orthodontic tooth movement based on animal studies: a critical review. J. Clin. Med. 10.
Koenig, H.A., Vanderby, R., Solonche, D.J., Burstone, C.J., 1980. Force systems from orthodontic appliances: an analytical and experimental comparison. J. Biomech. Eng. 102, 294–300.
Kurol, J., Owman-Moll, P., 1998. Hyalinization and root resorption during early orthodontic tooth movement in adolescents. Angle Orthod. 68, 161–166.
Kusy, R.P., Whitley, J.Q., 1999. Influence of archwire and bracket dimensions on sliding mechanics: derivations and determinations of the critical contact angles for binding. Eur. J. Orthod. 21, 199–208.
Liu, Y.F., Zhang, P.Y., Zhang, Q.F., Zhang, J.X., Chen, J., 2014. Digital design and fabrication of simulation model for measuring orthodontic force. Bio Med. Mater. Eng. 24, 2265–2271.
Lombardo, L., Marafioti, M., Stefanoni, F., Mollica, F., Siciliani, G., 2012. Load deflection characteristics and force level of nickel titanium initial archwires. Angle Orthod. 82, 507–521.
Mandall, N., Lowe, C., Worthington, H., Sandler, J., Derwent, S., Abdi-Oskouei, M., et al., 2006. Which orthodontic archwire sequence? A randomized clinical trial. Eur. J. Orthod. 28, 561–566.
Mascarenhas, R., Parveen, S., Shenoy, B.S., Kumar, G.S.S., Ramaiah, V.V., 2018. Infinite applications of finite element method. J. Indian Orthod. Soc. 52, 142–150.
Ong, E., Ho, C., Miles, P., 2011. Alignment efficiency and discomfort of three orthodontic archwire sequences: a randomized clinical trial. J. Orthod. 38, 32–39.
Pandis, N., Eliades, T., Bourauel, C., 2009. Comparative assessment of forces generated during simulated alignment with self-ligating and conventional brackets. Eur. J. Orthod. 31, 590–595.
Papadimitriou, A., Mousoulea, S., Gkantidis, N., Kloukos, D., 2018. Clinical effectiveness of Invisalign® orthodontic treatment: a systematic review. Prog. Orthod. 19, 1–24.
Perrey, W., Konermann, A., Keilig, L., Reimann, S., Jager, A., Bourauel, C., 2015. Effect of archwire qualities and bracket designs on the force systems during leveling of malaligned teeth. J. Orofac. Orthop. 76 (129–38), 40–42.
Proffit, W.R., Fields Jr., H.W., Sarver, D.M., 2007. Contemporary Orthodontics, fourth ed. ed. Elsevier Health Sciences, St. Louis.
Rajgopal, N., 2022. Finite element analysis in orthodontics. Curr. Trends Orthodont. 79.
Reddy, R.K., Katari, P.K., Bypureddy, T.T., Anumolu, V.N., Kartheek, Y., Sairam, N.R., 2016. Forces in initial archwires during leveling and aligning: an in-vitro study. J. Int. Soc. Prev. Community Dent. 6, 410–416.
Reitan, K., 1957. Some factors determining the evaluation of forces in orthodontics. Am. J. Orthod. 43, 32–45.
Reitan, K., 1960. Tissue behavior during orthodontic tooth movement. Am. J. Orthod. 46, 881–900.
Reitan, K., 1967. Clinical and histologic observations on tooth movement during and after orthodontic treatment. Am. J. Orthod. 53, 721–745.
Reitan, K., 1985. Biological principles and reactions. Orthodont., Curr. Orthodont. Concepts Techn. 141–142.
Reitan, K., Graber, T., Swain, B., 1989. Biomechanische Prinzipien der Gewebsreaktion. Grundlagen und moderne Techniken der Kieferorthopädie, pp. 149–270.
Ricketts, R.M., 1976. Bioprogressive therapy as an answer to orthodontic needs. Part II. Am. J. Orthod. 70, 359–397.
Romanyk, D.L., Vafaeian, B., Addison, O., Adeeb, S., 2020. The use of finite element analysis in dentistry and orthodontics: critical points for model development and interpreting results. Semin. Orthod. 162–173. Elsevier.
Rossini, G., Parrini, S., Castroflorio, T., Deregibus, A., Debernardi, C.L., 2015. Efficacy of clear aligners in controlling orthodontic tooth movement: a systematic review. Angle Orthod. 85, 881–889.
Sander, F.G., Ehrenfeld, M., Schwenzer, N., 2011. Zahn-Mund-Kiefer-Heilkunde Kieferorthopädie. Georg Thieme Verlag KG, Stuttgart.
Sifakakis, I., Eliades, T., 2017. Laboratory Evaluation of Orthodontic Biomechanics: the Clinical Applications Revisited. Elsevier, Semin Orthod, pp. 382–389.
Simon, M., Keilig, L., Schwarze, J., Jung, B.A., Bourauel, C., 2014. Treatment outcome and efficacy of an aligner technique–regarding incisor torque, premolar derotation and molar distalization. BMC Oral Health 14, 1–7.
Singh, J.R., Kambalyal, P., Jain, M., Khandelwal, P., 2016. Revolution in orthodontics: finite element analysis. J. Int. Soc. Prev. Community Dent. 6, 110–114.
Wang, Y., Jian, F., Lai, W., Zhao, Z., Yang, Z., Liao, Z., et al., 2010. Initial arch wires for alignment of crooked teeth with fixed orthodontic braces. Cochrane Database Syst. Rev. CD007859.
Wanjun, Z., Jinyuan, L., Yongping, M., Linqing, G., 2015. The development of orthodontics in the three dimensional finite element method. J. Hebei Med. Coll. Continuing Educ. 32, 75.
Wichelhaus, A., 2013. Kieferorthopädie - Therapie Band 1: Farbatlanten der Zahnmedizin. Stuttgart Georg Thieme Verlag.
Wichelhaus, A., Dulla, M., Sabbagh, H., Baumert, U., Stocker, T., 2021. Stainless steel and NiTi torque archwires and apical root resorption. J. Orofac. Orthop. 82, 1–12.
Xu, H., Zhang, S., Sathe, A.A., Jin, Z., Guan, J., Sun, W., et al., 2022. CCR2(+) macrophages promote orthodontic tooth movement and alveolar bone remodeling. Front. Immunol. 13, 835986.
Zhang, M., Yu, Y., He, D., Liu, D., Zhou, Y., 2022. Neural regulation of alveolar bone remodeling and periodontal ligament metabolism during orthodontic tooth movement in response to therapeutic loading. J. World Fed. Orthod. 11, 139–145.

bioengineering

MDPI

Article

Force-Controlled Biomechanical Simulation of Orthodontic Tooth Movement with Torque Archwires Using HOSEA (Hexapod for Orthodontic Simulation, Evaluation and Analysis)

Ellen Haas, Andreas Schmid, Thomas Stocker, Andrea Wichelhaus and Hisham Sabbagh *

Department of Orthodontics and Dentofacial Orthopedics, LMU University Hospital, LMU Munich, Goethestraße 70, 80336 Munich, Germany; ellen.haas@med.uni-muenchen.de (E.H.); schmid.92@gmx.de (A.S.); th.stocker@med.uni-muenchen.de (T.S.); kfo.sekretariat@med.uni-muenchen.de (A.W.)

* Correspondence: hisham.sabbagh@med.uni-muenchen.de; Tel.: +49-89-4400-53223

Abstract: This study aimed to investigate the dynamic behavior of different torque archwires for fixed orthodontic treatment using an automated, force-controlled biomechanical simulation system. A novel biomechanical simulation system (HOSEA) was used to simulate dynamic tooth movements and measure torque expression of four different archwire groups: 0.017″ x 0.025″ torque segmented archwires (TSA) with 30° torque bending, 0.018″ x 0.025″ TSA with 45° torque bending, 0.017″ x 0.025″ stainless steel (SS) archwires with 30° torque bending and 0.018″ x 0.025″ SS with 30° torque bending (n = 10/group) used with 0.022″ self-ligating brackets. The Kruskal–Wallis test was used for statistical analysis ($p < 0.050$). The 0.018″ x 0.025″ SS archwires produced the highest initial rotational torque moment (M_y) of −9.835 Nmm. The reduction in rotational moment per degree (M_y/R_y) was significantly lower for TSA compared to SS archwires ($p < 0.001$). TSA 0.018″ x 0.025″ was the only group in which all archwires induced a min. 10° rotation in the simulation. Collateral forces and moments, especially F_x, F_z and M_x, occurred during torque application. The measured forces and moments were within a suitable range for the application of palatal root torque to incisors for the 0.018″ x 0.025″ archwires. The 0.018″ x 0.025″ TSA reliably achieved at least 10° incisal rotation without reactivation.

Keywords: orthodontics; 3D measurement; force control; biomechanics; hexapod

check for updates

Citation: Haas, E.; Schmid, A.; Stocker, T.; Wichelhaus, A.; Sabbagh, H. Force-Controlled Biomechanical Simulation of Orthodontic Tooth Movement with Torque Archwires Using HOSEA (Hexapod for Orthodontic Simulation, Evaluation and Analysis). *Bioengineering* **2023**, *10*, 1055. https://doi.org/10.3390/bioengineering10091055

Academic Editor: Yanqi Yang

Received: 4 August 2023
Revised: 4 September 2023
Accepted: 6 September 2023
Published: 7 September 2023

Copyright: © 2023 by the authors. Licensee MDPI, Basel, Switzerland. This article is an open access article distributed under the terms and conditions of the Creative Commons Attribution (CC BY) license (https://creativecommons.org/licenses/by/4.0/).

1. Introduction

In orthodontic therapy with fixed appliances, biological tooth movement is achieved by applying forces and moments to the teeth and further to the surrounding structures involved—the periodontal ligament and alveolar bone [1–3]. For efficient tooth movement and avoidance of adverse effects such as pain, extensive hyalinization and root resorption, knowledge and control of orthodontically applied forces and moment magnitudes is required [4,5].

While force magnitudes can be accurately determined for some components used with fixed appliances, such as elastic chains, nickel–titanium springs, cantilevers, and intermaxillary elastics, the resulting forces of more complex archwire bends are difficult to determine or even estimate in vivo [6]. However, this knowledge is particularly important for critical orthodontic tooth movements frequently leading to apical root resorption, such as orthodontic torque application [7]. Clinically, the application of palatal root torque is indicated for orthodontically correct incisor inclination or to maintain it, e.g., during incisor retraction [7]. To obtain information about forces, moments, movements or similar, two methods of in vitro investigations are established in orthodontic science: digital, finite element (FE) simulation and biomechanical experiments [8–10].

FE simulations are based on computer-aided numerical methods and can perform analyses on a virtual model [11,12]. However, FE simulations have limitations implement-

ing complex structures consisting of multiple components and reflect dynamic material interactions [13]. Simplifications are necessary during the modeling process, thus the clinical implications of FE simulations are to be interpreted carefully and may require experimental verification in more complex cases [14].

Biomechanical experiments, on the other hand, can serve to investigate material characteristics, such as geometrical accuracy, Young's modulus, surface properties and frictional behavior, among others [15–17]. Biomechanical simulation systems can additionally address complex dynamic physical behaviors and material interactions during simulated clinical procedures. Most biomechanical simulation systems focus mainly on specific individual tooth movements, such as distalization or mesialization [18] or static torque expression and rotating movements [15,19]. Only a few experimental setups are designed to simulate complex motion sequences, such as dynamic torque expression [20,21].

HOSEA is a novel biomechanical simulation system based on a hexapod platform with a parallel kinematics positioning system that allows coordinated multi-axis motion in all six degrees of freedom. Controlled by a force–moment-dependent algorithm, this platform can move autonomously with respect to defined points such as the center of force or center of resistance to simulate the dynamic behavior of orthodontic mechanics.

The aim of this study was to investigate the dynamic torque expression of different orthodontic torque archwires during tooth movement using an automated, force-controlled biomechanical simulation system.

2. Materials and Methods

2.1. Biomechanical Simulation System

A hexapod or Stewart platform HP-550 (PI GmbH, Karlsruhe, Germany) was used as central motion element of HOSEA. The integrated six linear actuators are able to move a platform in six degrees of freedom (three translational and three rotational) with the highest precision and almost play-free. A computer and a control unit (Geobrink LV 8-axis, Delta Tau Data Systems Inc., Chatsworth, LA, USA) were used to control the Stewart platform. The control software was developed using LabView 12 (NI, Austin, TX, USA). As the main part of the software, an algorithm was implemented to allow force-controlled movement. This enables the platform to move autonomously, depending on the continuously measured forces and moments. A six-axis force-torque sensor was integrated into HOSEA to measure forces and moments (Nano17 SI-50-0.5, ATI Industrial Automation, New York, NY, USA). It is able to measure a force range of 70 N in the axial direction and 50 N for the two space vectors at a resolution of 1/80 N. The measuring range for the torsional moment is 500 Nmm in all spatial planes at a resolution of 1/16 Nmm (Figure 1a).

All experiments were conducted at $\vartheta = (36 \pm 1)$ °C in a temperature chamber with a temperature controller (TOHO TM-105, TOHO electronics, Sagamihara, Japan), because of the temperature-dependent material characteristics of the nickel–titanium component of the investigated archwires. HOSEA as a whole was housed in this chamber.

An experimental plaster model was made based on a typodont (Frasaco GmbH, Tettnang, Germany). Simulating an extraction therapy case, the first premolars were removed and replaced by canines. The model was divided into two segments, an anterior (teeth 12, 11, 21, 22) and one posterior segment (teeth 13–17, 23–27). The anterior segment was attached to the sensor and the posterior segment to the Stewart platform by a SAM articulator plate and base (SAM Praezisionstechnik GmbH, Munich, Germany) (Figure 1). The sensor and the anterior segment are fixed onto a strut of the housing, while the posterior segment is moved by the hexapod. The interbracket distance between the first molar and the lateral incisor was set at 28 mm on both sides.

Subsequently, the experimental model and four plastic incisors (ANA-4 ZP, Frasaco GmbH, Tettnang, Germany) were digitized using a desktop 3D scanner (Everest Scan, KaVo Dental GmbH, Biberach an der Riß, Germany). The scans of the incisors were post-processed with modeling software (Autodesk Meshmixer Version 3.5, Autodesk Inc., San

Rafael, CA, USA). The length of the incisors' roots were set according to average length values [22].

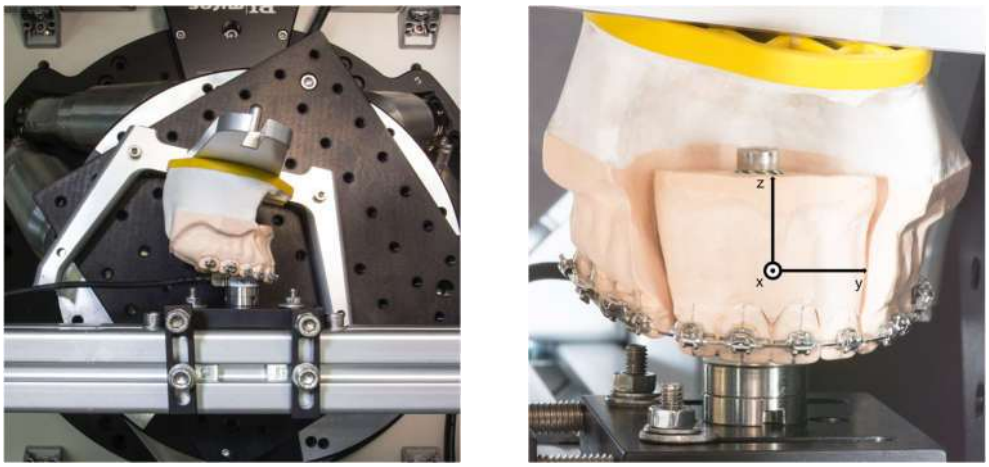

(**a**) (**b**)

Figure 1. (**a**) Plaster model in the examination chamber of HOSEA; the force-torque sensor is attached to the anterior segment, while the posterior segment is connected to the moving Stewart platform. (**b**) Plaster model in the starting position, with superimposed coordinate system used for the measurements.

The model scan and the tooth scans were matched with MeshLab [23] using an iterative closest point algorithm. Afterwards, MeshLab was utilized to determine the root surface barycenter which was identified as the center of resistance of the anterior segment of the four incisors. This center of resistance was set as the pivot point of HOSEA. Additionally, root surfaces were used to calculate the coefficients of a transformational matrix to specify the movement for each spatial direction. To describe directions of forces and moments, a coordinate system was defined on the anterior segment of the teeth (Figure 1b). It is aligned in such a way that its origin matches the center of the sensor. The position has been designed to coincide with the position of the calculated center of resistance. The sensor has a coordinate system determined by the manufacturer. The manufacturer's coordinate system was adapted to the anterior tooth coordinate system by employing mathematical transformation. As a result, the data measured by the sensor can be described in anterior segment system coordinates. Vertical movements are defined in the coordinate system along the *z*-axis, while anteroposterior movements are defined along the *x*-axis. The distance between the sensor center and the center of force of the anterior tooth segment was considered mathematically.

Self-ligating orthodontic brackets (0.022″, In-Ovation R, Dentsply Sirona, New York, NY, USA) were passively bonded to the plaster model using a 0.021″ x 0.025″ stainless steel archwire aligned along the marked FACC points [24].

The starting position of the mounted model in the experimental setup was determined with the help of the previously utilized 0.021″ x 0.025″ stainless steel archwire to obtain a fully passive fit. It is important to point out that in the given experimental setup, the position of the anterior segment is fixed while the posterior jaw segment is moved by the HOSEA system.

2.2. Measurements and Biomechanical Simulation of Tooth Movement

For the measurements and biomechanical simulations, pre-torqued archwires were ligated to the jaw model after passive alignment and initial calibration with supplementary steel ligatures (Forestadent GmbH, Pforzheim, Germany) in the starting position of the experimental setup of HOSEA.

In total, 40 torque archwires were examined. Four groups of ten samples were bent and adapted to the model by the same experienced clinician (Table 1). The measurement cycle was finished as soon as the anterior segment stopped rotating. All experiments were conducted at the lowest velocity to reduce the effect of the movements on the measurements.

Table 1. Sample groups used for the investigations, their material composition, the archwire dimensions and the amount of applied torque bends.

Archwire Material	Material Identification	Applied Torque	Sample Size	Archwire Size
Stainless steel	X10CrNi 18-8	30°	10	0.017″ x 0.025″
Stainless steel	X10CrNi 18-8	30°	10	0.018″ x 0.025″
Torque-segmented archwire	X5CrNi 18-10 Nickel Titanium	30°	10	0.017″ x 0.025″
Torque-segmented archwire	X5CrNi 18-10 Nickel Titanium	45°	10	0.018″ x 0.025″

2.3. Statistical Analysis

Graphs were generated using OriginPro 2020b (OriginLab Corporation, Northampton, MA, USA), and tables were prepared using Microsoft Excel 2016 (Microsoft Corporation, Redmond, WA, USA).

For statistical analysis, Kruskal–Wallis test with a significant value of $\alpha = 0.050$ was conducted in IBM SPSS Statistics 26 (International Business Machines Corporation, Armonk, NY, USA).

3. Results

Figure 2 illustrates the rotational moment M_y in relation to the rotation of the anterior segment R_y. Each of the four graphs represents a single archwire category, in which the 10 archwires are individually identified by different colors. The results of the measurements are presented according to the implemented Tweed coordinate system for the anterior tooth segment (Figure 1b). Since forces and moments were calculated at the center of resistance of the segment, the resulting force and moment values' direction indicate specific tooth movements. Negative values of M_y resemble the rotational moment resulting in a palatal root torque expression. Initial moments and forces were measured at 0.1° of rotation to reduce initial irregularities. Figure 2 and Table 2 show that larger wire dimensions account for higher rotational moments, initially and throughout the rotation, compared to smaller dimensions. The SS archwires have a tendency towards higher rotational moments. The highest rotational moment was observed in the SS 0.018″ x 0.025″ group, measuring −9.835 Nmm at 1° rotation on average.

The four graphs (Figure 2) also illustrate a difference in rotation achievable through archwires within each group. To investigate this further, Table 2 differentiates between certain degrees of rotation (2.5°, 5° and 10°), the according rotational moment My and the number of archwires successfully achieving rotation to the respective degree. Within a group, some samples failed to rotate to a certain degree. All investigated 0.018″ x 0.025″ TSA archwires successfully managed to rotate the segment for 10°. In contrast, in the 0.018″ x 0.025″ SS group, only four archwires reached this amount of rotation. The 0.017″ x 0.025″ SS and TSA archwires failed to reach this mark. Only a reduced number of 0.017″ x 0.025″ archwires caused a 5° rotation. Within the TSA 0.017″ x 0.025″ group, eight archwires achieved a 2.5° rotation (Table 2).

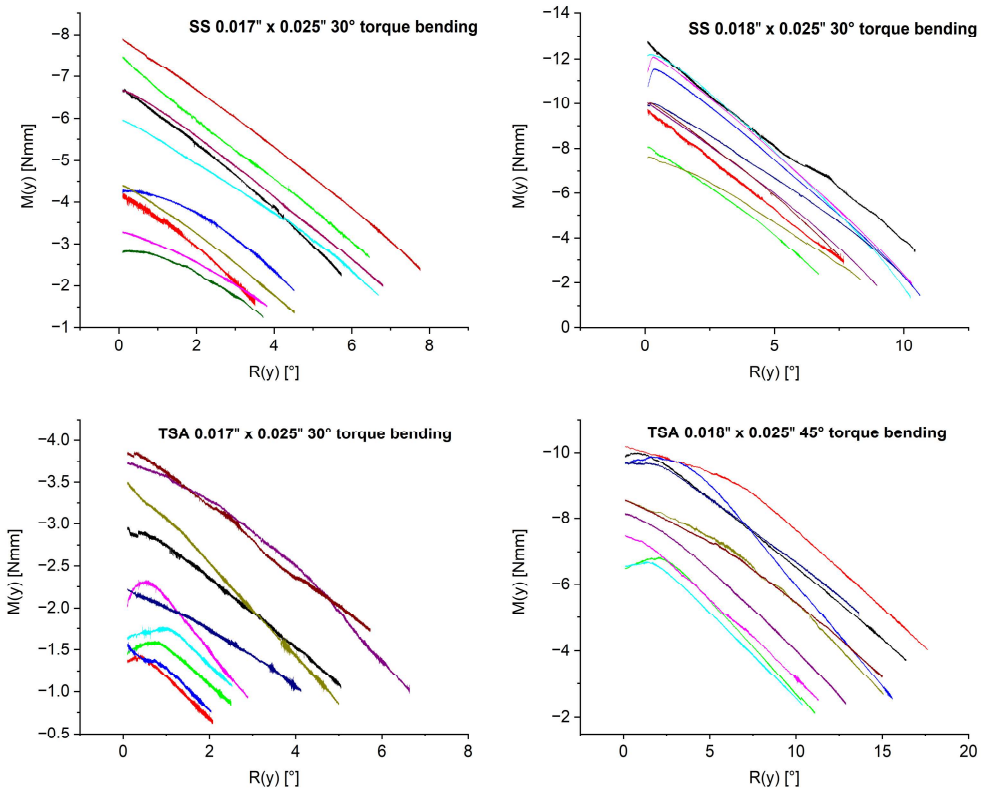

Figure 2. Graphs depicting rotational moments (Nmm) at the center of force in relation to the rotation of the segment (°). All measurements started at a rotational angle of 0° with an initial moment M_y (R_y = 0.1°). HOSEA rotates the posterior segment until My has come to an equilibrium position and rotation has stopped. Every colored curve corresponds to the measurement of one archwire. Each graph represents the archwires within a sample group.

Table 2. Mean rotational moments at the center of force at different stages of rotation for the different archwires investigated. Each archwire category consisted of 10 archwires. The number of archwire samples per group succeeding to rotate the anterior segment by a certain degree (1°, 2.5°, 5°, 10°) are shown in the line "No. of samples". Only the successful samples were included in the calculation at the defined rotational position of the anterior segment. If the amount of rotation was not been reached by any of the archwire samples in the respective group this is indicated by "-".

Archwire Category	Torque Bending	M_y (Nmm) (SD)	M_y (Nmm) (SD)	M_y (Nmm) (SD)	M_y (Nmm) (SD)
		R_y = 1°	R_y = 2.5°	R_y = 5°	R_y = 10°
0.018″ x 0.025″ TSA No. of samples	45°	8.468 (1.330) 10	−8.207 (1.372) 10	−7.297 (1.576) 10	−3.927 (3.753) 10
0.018″ x 0.025″ SS No. of samples	30°	−9.835 (1.701) 10	−8.604 (1.563) 10	−6.393 (1.414) 10	−2.579 (0.916) 4
0.017″ x 0.025″ SS No. of samples	30°	−4.914 (1.648) 10	−4.004 (1.547) 10	−3.571 (0.664) 5	-
0.017″ x 0.025″ TSA No. of samples	30°	−2.284 (0.906) 10	−1.903 (0.879) 8	0.022 (0.022) 3	-

In general, all four types of archwires had a reduction in the rotational moment as soon as the anterior segment rotates (Figure 2). However, the rate of rotational moment decrease varied depending on the archwire group. SS archwires showed a significantly higher moment reduction per degree (M_y/R_y) than TSA archwires (Table 3). Statistical analysis revealed a difference between the two material classifications but not between the

archwire sizes ($p = 0.006$ for 0.017″ x 0.025″ wire dimensions, $p < 0.001$ for 0.018″ x 0.025″). Furthermore, the rotational moment depletion rate of the TSA groups showed a smaller standard deviation than the SS groups (Table 3).

Table 3. Rotational moment depletion rate for the different archwire categories. The sample size for each archwire category was $n = 10$.

Archwire Category	Torque Bending	M_y/R_y (Nmm/°)	SD	*p*
0.018″ x 0.025″ TSA	45°	−0.405	0.045	<0.001
0.018″ x 0.025″ SS	30°	−0.898	0.108	
0.017″ x 0.025″ TSA	30°	−0.396	0.083	0.006
0.017″ x 0.025″ SS	30°	−0.717	0.136	

During rotation, collateral forces and moments were observed. The initial values of these forces and moments at 1° rotation are reported in Table 4. The 0.018″ x 0.025″ SS group showed the highest values for the collateral force F_y of −0.788 N. Statistical analysis showed that the two SS archwire groups differed significantly ($p = 0.042$) (Table 4). They were also both different from the 0.017″ x 0.025″ (30° torque) TSA group ($p = 0.037$ for 0.017″ x 0.025″, $p = 0.000$ for 0.018″ x 0.025″). A significant difference ($p = 0.010$) could also be observed among the TSA groups. There was no significant difference between the SS 0.018″ x 0.025″ (30° torque) and TSA 0.018″ x 0.025″ (45° torque) groups ($p = 0.137$). Focusing on the extrusive force F_z, larger values could be observed in the 0.018″ x 0.025″ archwire groups (Table 4). A significant difference was observed between the 0.017″ x 0.025″ and 0.018″ x 0.025″ archwire dimensions in each material group ($p = 0.003$ for SS, $p = 0.001$ for TSA). The SS group showed higher mean values and standard deviations compared to the two TSA groups (Table 4). M_x corresponds to a rotational movement that leads to extrusion on one side of the incisal segment and intrusion on the other.

Table 4. Average initial forces and moments for the different archwire categories in and around the three spatial dimensions (x, y, z). The superscripts correspond to a significant difference between the measured variable and the examined sample of the corresponding archwire categories titled variables ($^{a, b, c, d}$) according to the Kruskal–Wallis test with $\alpha = 0.050$. The sample size of each archwire category was $n = 10$.

	Archwire Category	Torque Bending	F_x (N) (SD)	F_y (N) (SD)	F_z (N) (SD)	M_x (Nmm) (SD)	M_y (Nmm) (SD)	M_z (Nmm) (SD)
a	0.017″ x 0.025″ SS	30°	−0.399 (0.133) ^{bc}	−0.195 (0.189) ^{cd}	−0.083 (0.092) ^{bd}	2.099 (2.037) ^{c}	−4.914 (1.648) ^{b}	0.018 (0.086) ^{d}
b	0.018″ x 0.025″ SS	30°	−0.788 (0.159) ^{ac}	−0.193 (0.260)	−0.300 (0.089) ^{a}	2.104 (2.723)	−9.835 (1.701) ^{ac}	−0.079 (0.173)
c	0.017″ x 0.025″ TSA	30°	−0.150 (0.055) ^{abd}	0.070 (0.100) ^{ad}	−0.113 (0.069) ^{abd}	−0.586 (1.189) ^{a}	−2.284 (0.906) ^{bd}	−0.070 (0.194)
d	0.018″ x 0.025″ TSA	45°	−0.457 (0.160) ^{c}	0.078 (0.156) ^{ac}	−0.325 (0.081) ^{ac}	0.051 (1.664)	−8.468 (1.330) ^{c}	−0.886 (0.881) ^{a}

Figure 3 depicts the measured collateral forces F_x, representing a retractive force, and F_z, corresponding to an extrusive force. Focusing on F_x, both SS groups showed a linear force reduction during the rotation of the anterior segment. In contrast, in the TSA groups, the extrusive force increased at the beginning of the rotation, peaked during the course of movement and then decreased. The measured retractive Force F_x ranged from a minimum of 0 N to a maximum of −1.0 N and was lowest in the TSA 0.017″ x 0.025″ group.

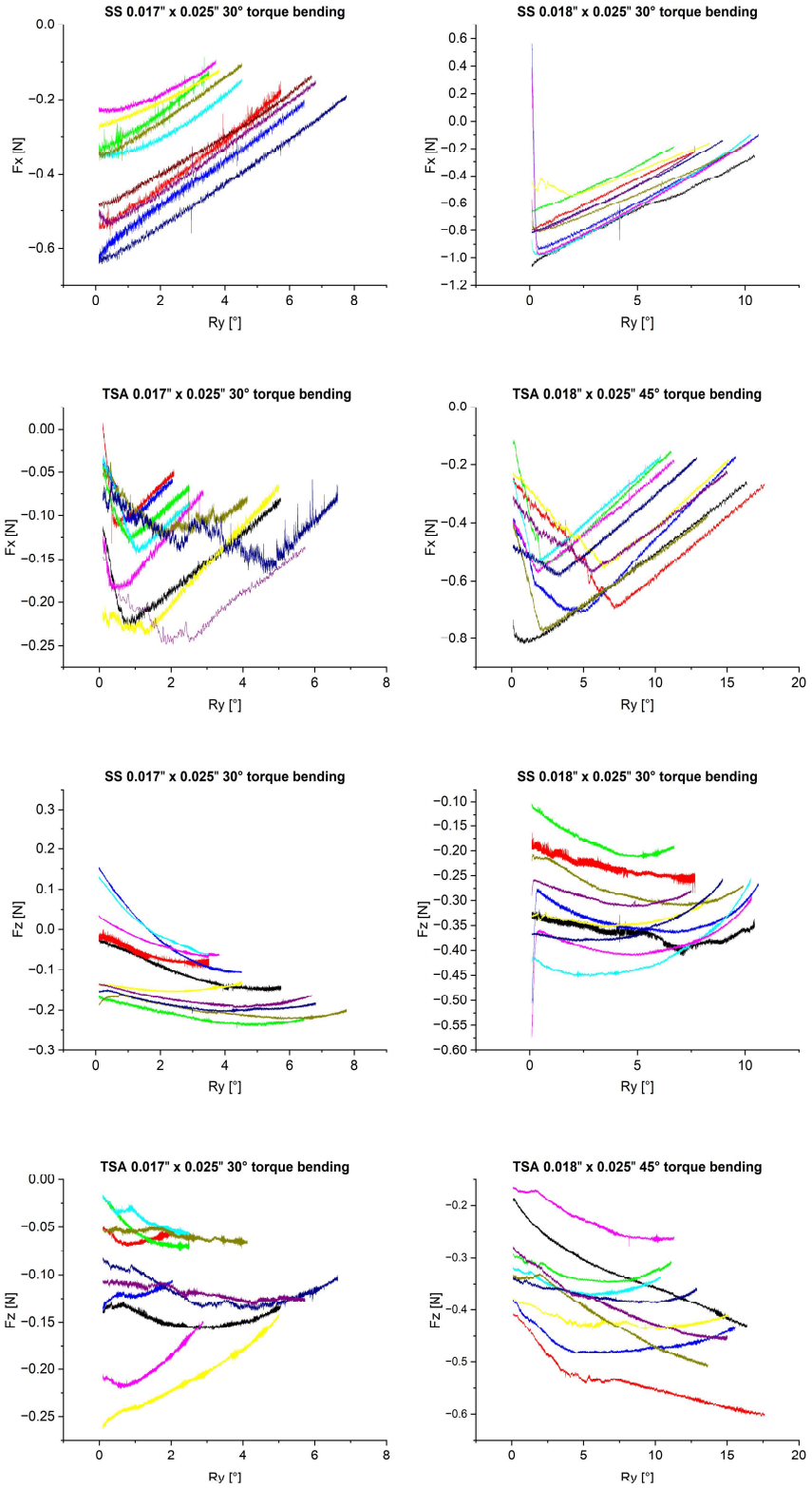

Figure 3. Graphs depicting collateral forces F_x and F_z at the center of force in relation to the rotation of the segment (°). All measurements started at a rotational angle of 0° with an initial moment My (R_y = 0.1°). Every colored curve corresponds to the measurement of one archwire. Each graph represents the archwires within a sample group.

The measured extrusive force F_z was generally larger in the 0.018″ x 0.025″ archwire groups. For SS 0.018″ x 0.025″ archwires, extrusive force F_z values ranged between −0.1 N and −0.45 N. For TSA 0.018″ x 0.025″ archwires, F_z values ranged between −0.15 N and

−0.6 N. In comparison, measured forces for the SS 0.017″ x 0.025″ archwire group ranged between 0.1 N and −0.2 N, while the extrusive force of TSA remained in the negative section between 0 N and −0.3 N.

In general, large variations in F_x and F_z between archwires within all groups were evident.

4. Discussion

The dynamic course of torque expression of different orthodontic torque archwires was investigated using the fully automated and force-controlled biomechanical simulation system HOSEA.

Clinically, the application of rotational moments between 5 and 20 Nmm has been recommended to achieve adequate torque on the incisors [25,26]. In this study, mean values for rotational moments (M_y) ranged between 2.284 Nmm and 9.835 Nmm, where none of the samples exceeded the upper limit of 20 Nmm. This is in line with the lower range of comparable torque measurements in the literature [15,21,27]. Based on the archwire–bracket configurations used, higher values would have been expected. Theoretically, the torsional play between bracket and archwire can be calculated through geometric considerations [28]. However, the manufacturer's specifications for the dimensions of both, bracket as well as archwire, often do not correspond to the actual sizes due to manufacturing tolerances. Studies have shown that bracket slots may be oversized by up to 24% in some areas [29]. Additionally, archwire examinations have shown that archwire sizes are outside lower tolerance limits given by the relevant normative standards [30]. In this context, the results of the present study suggest that more torsional play effectively occurs than theoretically anticipated [31,32], leading to a significant loss of rotational moment.

As can be seen in Figure 2, the torsional moments from the TSA samples with the smaller dimensions are very low, leading to the conclusion that the chosen configuration of 0.017″ x 0.025″ with 30° of torque in combination with a 0.022″ slot is not suitable to perform incisor torque movements. Therefore, the sample group based on this combination will not be considered further in this discussion.

In addition to the magnitude of the applied rotational moments, the rotational moment reduction rate (M_y/R_y) is of particular clinical importance. In this regard, significant differences were found between the groups investigated. The present study compared SS with TSA archwires, in which the posterior segment was made of stainless steel and the anterior segment was made of a superelastic nickel–titanium alloy. Compared to stainless steel alloys, nickel–titanium alloys exhibit a low Young's Modulus and show constant force-deflection plateaus over rather long deflection ranges [33,34]. This was also reflected in the results of this study, as the TSA groups showed a lower rotational moment depletion rate (around 0.4 Nmm/°) compared to the SS groups (between 0.7 and 0.9 Nmm/°).

Furthermore, the need for reactivations of treatment mechanics is clinically relevant. Reactivation becomes necessary when suitable moments are no longer exerted by the orthodontic appliance. In this study, some specimens failed to achieve a reasonable amount of rotation during the simulations, while the 0.018″ x 0.025″ TSA was the most reliable in achieving a rotation of at least 10°. On the other side, depending on the magnitude of initial starting moment M_y, the achievable rotational angle may also range up to 17.5° under the same experimental conditions. It was shown that the final rotational angle depends on the initial rotational moment M_y and the moment depletion rate. Clinically, this fact may be of concern, especially because a similar wide spread of final rotational angles was also found in all sample groups. One possible explanation for the wide range of initial rotational moments M_y can be found in the manual torque bending and measuring procedure, which is performed through a visual template comparison. Even though all archwires were bent by the same experienced clinician, visual inspection cannot exclude slight variations in torque bends and bends to adjust the archwire shape to the template. Although the anterior segments in the TSA group were pre-torqued, these archwires were also adapted to the shape of the template and a comparable pattern was found here as well. This probably also explains the wide variation in the measured extrusive and retractive collateral forces in all

archwire groups investigated. A calibrated measuring device for the effectively applied torque angle is under development and will be validated for further research.

In addition to the measured rotational moment M_y resulting in palatal torque movement of the incisors, significant collateral forces and moments were observed in F_z, F_x and M_x. This corresponds to an extrusion, as well as a mesio-distal movement and a rotation around the *y*-axis. Extrusion and retraction of the anterior segment must generally be anticipated biomechanically during torque application [7,35]. The sideways movement and rotation are more likely to result from asymmetrical adjustment of the archwires. This effect may be more pronounced in contrast to the clinical situation, as contacts between bracket and archwire cannot be released by chewing forces and, in absence of lubricating saliva, more pronounced frictional phenomena may occur. The measured collateral moment M_x was higher for the SS groups with values of 2.099 Nmm and 2.104 Nmm compared to the TSA groups with values ranging between −0.586 Nmm and 0.051 Nmm. The difference between the groups supports the assumptions, since TSAs are prefabricated in the anterior segment and thus show lower asymmetry In comparison with the manually bent SS archwires.

In vitro investigations with biomechanical test devices such as HOSEA are limited to purely mechanical simulations and cannot reproduce orthodontic tooth movements as a biological process. In addition to the absence of a periodontal ligament (PDL) and saliva, simplifying assumptions were made in the simulations by using a standardized model and in defining a static center of resistance of the anterior segment. Although the setup used cannot simulate a PDL, the software allows the integration of previously calculated characteristics, such as the center of resistance and the root resistance, into the simulated movement. Despite the fact that, at present, it is recognized that each tooth has a unique center of resistance, in this study, in order to simulate the movement of the anterior block of teeth, a joint center of resistance was calculated as proposed in previous studies [36,37]. It was determined on the basis of indications in the literature at 10.324 mm apically of the combined center of force of the four incisors [2,37,38].

Compared to in silico FE analysis, HOSEA allows the observation and analysis of the biomechanical properties of physical orthodontic appliances, whereas FE analyses are solely based on calculative models [3,39]. FE simulations calculate forces and moments generated by mechanically idealized orthodontic appliances or archwires. The present investigations can thus be perceived as an addition and validation to FE studies by providing values for respective computations and allowing comparisons between investigation methods. The presented setup can perform force-controlled simulations of different tooth movements in terms of dynamic three-dimensional measurements, which is rare in orthodontic research to date [10,20,40]. Furthermore, it is possible to conduct these measurements on real patient's dental casts in order to validate treatment plans in highly complex cases.

Considering the results and limitations of this study, the following clinical implications can be derived:

- The 0.017″ x 0.025″ archwires in combination with 0.022″ slot brackets produced forces and moments that were too low to achieve adequate palatal incisor root torque, regardless of material group. Therefore, the use of 0.018″ x 0.025″ archwires with 30° torque bends (SS) or 45° torque bends (TSA) are recommended for clinical use.
- Although higher initial moments (M_y) were measured for the 0.018″ x 0.025″ SS archwires, the 0.018″ x 0.025″ TSA archwires exhibited a lower moment reduction rate, indicating a reduced need for reactivation and appearing to be more suitable for applying more constant rotational moments. Due to collateral effects such as extrusive forces occurring during torque expression, the application of compensatory vertical bends should be considered.

5. Conclusions

The dynamic course of torque expression of SS and TSA archwires during force-controlled simulation of orthodontic tooth movement was investigated using the novel

biomechanical test stand HOSEA. Both SS and TSA archwires produced suitable moment magnitudes for palatal root movements at 0.018″ x 0.025″ dimensions in combination with 0.022″ slot brackets. In contrast, 0.017″ x 0.025″ archwires did not produce sufficient moment magnitudes and thus did not achieve adequate palatal root torque regardless of the material. TSA archwires showed significantly lower rotational moment reduction rate over time in comparison with SS archwires.

Author Contributions: E.H.: writing—original draft, visualization, data curation; A.S.: investigation, software; A.W.: supervision, project administration; T.S.: formal analysis, writing—review and editing; H.S.: writing—original draft. All authors have read and agreed to the published version of the manuscript.

Funding: This research received no external funding.

Institutional Review Board Statement: Not applicable.

Informed Consent Statement: Not applicable.

Data Availability Statement: Data are available on request from the corresponding author.

Conflicts of Interest: The authors declare no conflict of interest.

References

1. Burstone, C.J.; Pryputniewicz, R.J. Holographic determination of centers of rotation produced by orthodontic forces. *Am. J. Orthod.* **1980**, *77*, 396–409. [CrossRef] [PubMed]
2. Pedersen, E.; Isidor, F.; Gjessing, P.; Andersen, K. Location of centres of resistance for maxillary anterior teeth measured on human autopsy material. *Eur. J. Orthod.* **1991**, *13*, 452–458. [CrossRef] [PubMed]
3. Kojima, Y.; Fukui, H. Numerical simulations of canine retraction with T-loop springs based on the updated moment-to-force ratio. *Eur. J. Orthod.* **2010**, *34*, 10–18. [CrossRef] [PubMed]
4. Zhang, X.; Zhou, H.; Liao, X.; Liu, Y. The influence of bracket torque on external apical root resorption in bimaxillary protrusion patients: A retrospective study. *BMC Oral. Health* **2022**, *22*, 7. [CrossRef]
5. Nakano, T.; Hotokezaka, H.; Hashimoto, M.; Sirisoontorn, I.; Arita, K.; Kurohama, T.; Darendeliler, M.A.; Yoshida, N. Effects of different types of tooth movement and force magnitudes on the amount of tooth movement and root resorption in rats. *Angle Orthod.* **2014**, *84*, 1079–1085. [CrossRef] [PubMed]
6. Pandis, N.; Walsh, T.; Polychronopoulou, A.; Katsaros, C.; Eliades, T. Factorial designs: An overview with applications to orthodontic clinical trials. *Eur. J. Orthod.* **2014**, *36*, 314–320. [CrossRef] [PubMed]
7. Wichelhaus, A.; Dulla, M.; Sabbagh, H.; Baumert, U.; Stocker, T. Stainless steel and NiTi torque archwires and apical root resorption. *J. Orofac. Orthop. = Fortschritte Kieferorthopadie Organ/Off. J. Dtsch. Ges. Kieferorthopadie* **2021**, *82*, 1–12. [CrossRef] [PubMed]
8. Cai, Y. Finite element analysis of archwire parameters and activation forces on the M/F ratio of vertical, L- and T-loops. *BMC Oral Health* **2020**, *20*, 70. [CrossRef] [PubMed]
9. Burstone, C.J.; Koenig, H.A. Optimizing anterior and canine retraction. *Am. J. Orthod.* **1976**, *70*, 1–19. [CrossRef] [PubMed]
10. Badawi, H.M.; Toogood, R.W.; Carey, J.P.; Heo, G.; Major, P.W. Three-dimensional orthodontic force measurements. *Am. J. Orthod. Dentofac. Orthop.* **2009**, *136*, 518–528. [CrossRef] [PubMed]
11. Tominaga, J.Y.; Tanaka, M.; Koga, Y.; Gonzales, C.; Kobayashi, M.; Yoshida, N. Optimal loading conditions for controlled movement of anterior teeth in sliding mechanics. *Angle Orthod.* **2009**, *79*, 1102–1107. [CrossRef] [PubMed]
12. Kojima, Y.; Fukui, H. Numeric simulations of en-masse space closure with sliding mechanics. *Am. J. Orthod. Dentofac. Orthop.* **2010**, *138*, e701–e706. [CrossRef] [PubMed]
13. Stokes, I.A.; Chegini, S.; Ferguson, S.J.; Gardner-Morse, M.G.; Iatridis, J.C.; Laible, J.P. Limitation of finite element analysis of poroelastic behavior of biological tissues undergoing rapid loading. *Ann. Biomed. Eng.* **2010**, *38*, 1780–1788. [CrossRef] [PubMed]
14. Singh, J.R.; Kambalyal, P.; Jain, M.; Khandelwal, P. Revolution in Orthodontics: Finite element analysis. *J. Int. Soc. Prev. Community Dent.* **2016**, *6*, 110–114. [CrossRef] [PubMed]
15. Arreghini, A.; Lombardo, L.; Mollica, F.; Siciliani, G. Torque expression capacity of 0.018 and 0.022 bracket slots by changing archwire material and cross section. *Prog. Orthod.* **2014**, *15*, 53. [CrossRef] [PubMed]
16. Hodecker, L.; Bourauel, C.; Braumann, B.; Kruse, T.; Christ, H.; Scharf, S. Sliding behaviour and surface quality after static air polishing of conventional and modern bracket materials: In vitro analysis. *J. Orofac. Orthop.* **2023**, *84*, 110–124. [CrossRef] [PubMed]
17. Stocker, T.; Li, H.; Bamidis, E.P.; Baumert, U.; Hoffmann, L.; Wichelhaus, A.; Sabbagh, H. Influence of normal forces on the frictional behavior in tribological systems made of different bracket types and wire dimensions. *Dent. Mater. J.* **2022**, *41*, 402–413. [CrossRef]

18. Chen, J.; Isikbay, S.C.; Brizendine, E.J. Quantification of three-dimensional orthodontic force systems of T-loop archwires. *Angle Orthod.* **2010**, *80*, 566–570. [CrossRef]
19. McKnight, M.M.; Jones, S.P.; Davies, E.H. A study to compare the effects of simulated torquing forces on pre-adjusted orthodontic brackets. *Br. J. Orthod.* **1994**, *21*, 359–365. [CrossRef] [PubMed]
20. Drescher, D.; Bourauel, C.; Thier, M. Application of the orthodontic measurement and simulation system (OMSS) in orthodontics. *Eur. J. Orthod.* **1991**, *13*, 169–178. [CrossRef]
21. Morina, E.; Eliades, T.; Pandis, N.; Jäger, A.; Bourauel, C. Torque expression of self-ligating brackets compared with conventional metallic, ceramic, and plastic brackets. *Eur. J. Orthod.* **2008**, *30*, 233–238. [CrossRef] [PubMed]
22. Hülsmann, M. *Endodontie*; Georg Thieme: New York, NY, USA, 2008.
23. Cignoni, P.; Callieri, M.; Corsini, M.; Dellepiane, M.; Ganovelli, F.; Ranzuglia, G. Meshlab: An open-source mesh processing tool. In Proceedings of the Eurographics Italian Chapter Conference 2008, Salerno, Italy, 2–4 July 2008; pp. 129–136.
24. Andrews, L.F. The straight-wire appliance. *Br. J. Orthod.* **1979**, *6*, 125–143. [CrossRef]
25. Bantleon, H.P.; Droschl, H. Front torque using a partial arch technic. *Fortschr. Kieferorthop.* **1988**, *49*, 203–212. [CrossRef]
26. Gmyrek, H.; Bourauel, C.; Richter, G.; Harzer, W. Torque capacity of metal and plastic brackets with reference to materials, application, technology and biomechanics. *J. Orofac. Orthop./Fortschritte Kieferorthopädie* **2002**, *63*, 113–128. [CrossRef] [PubMed]
27. Hirai, M.; Nakajima, A.; Kawai, N.; Tanaka, E.; Igarashi, Y.; Sakaguchi, M.; Sameshima, G.T.; Shimizu, N. Measurements of the torque moment in various archwire-bracket-ligation combinations. *Eur. J. Orthod.* **2012**, *34*, 374–380. [CrossRef] [PubMed]
28. Kusy, R.P.; Whitley, J.Q. Influence of archwire and bracket dimensions on sliding mechanics: Derivations and determinations of the critical contact angles for binding. *Eur. J. Orthod.* **1999**, *21*, 199–208. [CrossRef]
29. Cash, A.; Good, S.; Curtis, R.; McDonald, F. An evaluation of slot size in orthodontic brackets—Are standards as expected? *Angle Orthod.* **2004**, *74*, 450–453.
30. Joch, A.; Pichelmayer, M.; Weiland, F. Bracket slot and archwire dimensions: Manufacturing precision and third order clearance. *J. Orthod.* **2010**, *37*, 241–249. [CrossRef] [PubMed]
31. Dalstra, M.; Eriksen, H.; Bergamini, C.; Melsen, B. Actual versus theoretical torsional play in conventional and self-ligating bracket systems. *J. Orthod.* **2015**, *42*, 103–113. [CrossRef] [PubMed]
32. Archambault, A.; Lacoursiere, R.; Badawi, H.; Major, P.W.; Carey, J.; Flores-Mir, C. Torque expression in stainless steel orthodontic brackets. A systematic review. *Angle Orthod.* **2010**, *80*, 201–210. [CrossRef] [PubMed]
33. Garrec, P.; Jordan, L. Stiffness in bending of a superelastic Ni-Ti orthodontic wire as a function of cross-sectional dimension. *Angle Orthod.* **2004**, *74*, 691–696. [CrossRef] [PubMed]
34. Miura, F.; Mogi, M.; Ohura, Y.; Hamanaka, H. The super-elastic property of the Japanese NiTi alloy wire for use in orthodontics. *Am. J. Orthod. Dentofac. Orthop.* **1986**, *90*, 1–10. [CrossRef] [PubMed]
35. Wichelhaus, A.; Sander, F.G. [Biomechanical testing of the new torque-segmented arch (TSA)]. *Fortschr. Kieferorthop.* **1995**, *56*, 224–235. [CrossRef] [PubMed]
36. Schmidt, F.; Geiger, M.E.; Jäger, R.; Lapatki, B.G. Comparison of methods to determine the centre of resistance of teeth. *Comput. Methods Biomech. Biomed. Eng.* **2016**, *19*, 1673–1682. [CrossRef] [PubMed]
37. Reimann, S.; Keilig, L.; Jager, A.; Bourauel, C. Biomechanical finite-element investigation of the position of the centre of resistance of the upper incisors. *Eur. J. Orthod.* **2007**, *29*, 219–224. [CrossRef] [PubMed]
38. Vanden Bulcke, M.M.; Burstone, C.J.; Sachdeva, R.C.; Dermaut, L.R. Location of the centers of resistance for anterior teeth during retraction using the laser reflection technique. *Am. J. Orthod. Dentofac. Orthop.* **1987**, *91*, 375–384. [CrossRef] [PubMed]
39. George, S.S.; Reddy, T.R.J.; Kv, S.K.; Chaudhary, G.; Farooq, U.; Cherukuri, V.; Likitha, C. The Influence of Heights of Power Arm for Controlled Anterior Teeth Movement in Sliding Mechanics: A 3D FEM Study. *Cureus* **2022**, *14*, e25976. [CrossRef] [PubMed]
40. Liu, Y.F.; Zhang, P.Y.; Zhang, Q.F.; Zhang, J.X.; Chen, J. Digital design and fabrication of simulation model for measuring orthodontic force. *Biomed. Mater. Eng.* **2014**, *24*, 2265–2271. [CrossRef] [PubMed]

Disclaimer/Publisher's Note: The statements, opinions and data contained in all publications are solely those of the individual author(s) and contributor(s) and not of MDPI and/or the editor(s). MDPI and/or the editor(s) disclaim responsibility for any injury to people or property resulting from any ideas, methods, instructions or products referred to in the content.

7. Vollständiges Schriftenverzeichnis

7.1 Originalarbeiten als Erst- oder Letztautor (10)

1. Dotzer, B.; Stocker, T.; Wichelhaus, A.; Janjic Rankovic, M.; **Sabbagh, H.**
Biomechanical simulation of forces and moments of initial orthodontic tooth movement in dependence on the used archwire system by ROSS (Robot Orthodontic Measurement & Simulation System).
J Mech Behav Biomed Mater 2023, 144, 105960, doi:10.1016/j.jmbbm.2023.105960.

2. Haas, E.; Schmid, A.; Stocker, T.; Wichelhaus, A.; **Sabbagh, H.**
Force-Controlled Biomechanical Simulation of Orthodontic Tooth Movement with Torque Archwires Using HOSEA (Hexapod for Orthodontic Simulation, Evaluation and Analysis).
Bioengineering 2023, 10, 1055.

3. Popova, T.; Stocker, T.; Khazaei, Y.; Malenova, Y.; Wichelhaus, A.; **Sabbagh, H.**
Influence of growth structures and fixed appliances on automated cephalometric landmark recognition with a customized convolutional neural network.
BMC Oral Health 2023, 23, 274, doi:10.1186/s12903-023-02984-2.

4. **Sabbagh, H.**; Bamidis,E.; Keller, A.; Stocker, T.; Baumert, U.; Hoffmann, L.; Wichelhaus, A.
Force behaviour of elastic chains during a simulated gap closure in extraction therapy cases.
Orthod Craniofac Res 2022, doi:10.1111/ocr.12626.

5. **Sabbagh, H.**; Heger, S.M.; Stocker, T.; Baumert, U.; Wichelhaus, A.; Hoffmann, L.
Accuracy of 3D Tooth Movements in the Fabrication of Manual Setup Models for Aligner Therapy.
Materials 2022, 15, 3853.

6. **Sabbagh, H.**; Khazaei, Y.; Baumert, U.; Hoffmann, L.; Wichelhaus, A.; Janjic Rankovic, M.
Bracket Transfer Accuracy with the Indirect Bonding Technique: A Systematic Review and Meta-Analysis.
Journal of Clinical Medicine 2022, 11, 2568.

7. **Sabbagh, H.**; Nikolova, T.; Kakoschke, S.C.; Wichelhaus, A.; Kakoschke, T.K.
Functional Orthodontic Treatment of Mandibular Condyle Fractures in Children and Adolescent Patients: An MRI Follow-Up.

Life (Basel) 2022, 12, doi:10.3390/life12101596.

8. **Sabbagh, H.**; Sabbagh, A.; Heppner, A.; Auer, C.; Wichelhaus, A.; Hoffmann, L.
Patients' perceptions on temporomandibular disorder treatment with hydrostatic oral splints - a pilot study.
BDJ Open 2022, 8, 4, doi:10.1038/s41405-022-00096-7.

9. **Sabbagh, H.**; Sabbagh, A.; Rankovic, M.J.; Huber, C.; Wichelhaus, A.; Hoffmann, L.
Influence of the force magnitude of fixed functional appliances for class II subdivision 1 treatment—a cephalometric study.
Journal of Orofacial Orthopedics / Fortschritte der Kieferorthopädie 2023, doi:10.1007/s00056-023-00455-5.

10. Stocker, T.; Li, H.; Bamidis, E.P.; Baumert, U.; Hoffmann, L.; Wichelhaus, A.; **Sabbagh, H.**
Influence of normal forces on the frictional behavior in tribological systems made of different bracket types and wire dimensions.
Dental Materials Journal 2022, 41, 402-413, doi:10.4012/dmj.2021-112.

7.2 Originalarbeiten als Co-Autor (7)

1. Hegele, J.; Seitz, L.; Claussen, C.; Baumert, U.; **Sabbagh, H.**; Wichelhaus, A.
Clinical effects with customized brackets and CAD/CAM technology: a prospective controlled study.
Progress in Orthodontics 2021, 22, 40, doi:10.1186/s40510-021-00386-0.

2. Hoffmann, L.; Marschner, S.N.; Kakoschke, T.K.; Hickel, R.; **Sabbagh, H.**; Wölfle, U.C.
Dental management before radiotherapy of the head and neck region: 4-year single-center experience.
Clin Exp Dent Res 2022, 8, 1478-1486, doi:10.1002/cre2.662.

3. Hoffmann, L.; **Sabbagh, H.**; Wichelhaus, A.; Kessler, A.
Bracket transfer accuracy with two different three-dimensional printed transfer trays vs silicone transfer trays.
The Angle Orthodontist 2022, 92, 364-371, doi:10.2319/040821-283.1.

4. Li, H.; Stocker, T.; Bamidis, E.P.; **Sabbagh, H.**; Baumert, U.; Mertmann, M.; Wichelhaus, A.
Effect of different media on frictional forces between tribological systems made from self-ligating brackets in combination with different stainless steel wire dimensions.
Dental Materials Journal 2021, 40, 1250-1256, doi:10.4012/dmj.2020-424.

5. Malenova, Y.; Ortner, F.; Liokatis, P.; Haidari, S.; Tröltzsch, M.; Fegg, F.; Obermeier, K.T.; Hartung, J.T.; Kakoschke, T.K.; Burian, E.; Otto, S.; **Sabbagh, H.**; Probst, F.
Accuracy of maxillary positioning using computer-designed and manufactured occlusal splints or patient-specific implants in orthognathic surgery.
Clin Oral Investig 2023, doi:10.1007/s00784-023-05125-9.

6. Wichelhaus, A.; Dulla, M.; **Sabbagh, H.**; Baumert, U.; Stocker, T.
Stainless steel and NiTi torque archwires and apical root resorption.
Journal of Orofacial Orthopedics / Fortschritte der Kieferorthopädie 2021, 82, 1-12, doi:10.1007/s00056-020-00244-4.

7. Wichelhaus, A.; Mehnert, A.; Stocker, T.; Baumert, U.; Mertmann, M.; **Sabbagh, H.**; Seidel, C.L.
Thermal Programming of Commercially Available Orthodontic NiTi Archwires.
Materials (Basel) 2023, 16, doi:10.3390/ma16103683.

8. Danksagung

Zunächst möchte ich Frau Prof. Dr. Andrea Wichelhaus, der Klinikdirektorin der Poliklinik für Kieferorthopädie, meiner Chefin und geschäftsführenden Fachmentorin, meinen herzlichen Dank aussprechen. Ihre fortwährende Unterstützung, ihr Vertrauen und ihre wertvollen Ratschläge haben maßgeblich zu meiner fachlichen und wissenschaftlichen Entwicklung und dem Abschluss dieser Habilitationsschrift beigetragen.

Ebenso möchte ich meinen geschätzten Fachmentoren Herrn Prof. Dr. Edelhoff und Herrn Prof. Dr. Dr. Sven Otto für die Betreuung und Unterstützung dieser Arbeit danken.

Besonders Dank gilt auch meinen wissenschaftlich aktiven Kolleginnen und Kollegen am LMU Klinikum, die mich in verschiedenen Konstellationen bei den einzelnen Projekten begleitet haben. Hier seien stellvertretend genannt Herr Privatdozent Dr. Uwe Baumert, Herr Dr. Thomas Stocker, Herr Dr. Matthias Mertmann, Herr Privatdozent Dr. Andreas Keßler, Herr Prof. Dr. Dr. Florian Probst, Frau Dr. Mila Janjic Rankovic, Frau Dr. Tamara Kakoschke, Frau Dr. Corinna Seidel, Herr Dr. Elias Bamidis, Herr Vinzenz Le, Frau Yoana Malenova, Frau Yeganeh Khazaei, Herr Dr. Elias Walter und Frau Dr. Lea Hoffmann. Weiterhin meinen Doktorandinnen und Doktoranden Frau Ellen Haas, Frau Teodora Popova, Herr Benedikt Dotzer, Frau Christine Huber und Herr Christian Nikolov, denen ich an dieser Stelle zu Ihren Leistungen gratulieren und für ihnen die produktive Zusammenarbeit danken will. Zudem möchte ich Frau Anja Günter und Frau Jacqueline Hettmann für die Unterstützung bei der Erstellung von Grafiken und Abbildungen danken.

Dem gesamten Team der Poliklinik für Kieferorthopädie sei für die tolle Zusammenarbeit in den letzten Jahren vom Beginn meiner kieferorthopädischen Weiterbildung bis zur Habilitation gedankt.

Mein tiefster Dank gilt meiner geliebten Familie, meinen Eltern Dr. Aladin Sabbagh und Dr. Reem Sabbagh sowie meinen Brüdern Kinan Sabbagh und Samy Sabbagh.